Supporting Information

for

Synthesis of hybrid phosphinoferrocene ligands bearing amine pendants and catalytic evaluation of their gold(I) complexes

David Rezazgui, Ivana Císařová, Petr Štěpnička and Jiří Schulz*

Department of Inorganic Chemistry, Faculty of Science,

Charles University, Prague, Czech Republic. E-mail: jiri.schulz@natur.cuni.cz

Contents

Experimental

Materials and methods

NMR spectra were recorded at 25 °C (unless noted otherwise) on a Varian UNITY Inova 400 (^{1}H, 399.95 MHz; ^{13}C{^{1}H}, 100.58 MHz; ^{31}P{^{1}H}, 161.90 MHz), a Bruker Avance III HD 400 (^{1}H, 400.13 MHz; ^{13}C{^{1}H}, 100.61 MHz; ^{31}P{^{1}H}, 161.90 MHz), or a Bruker AVANCE III 600 (^{1}H, 600.17 MHz; ^{13}C{^{1}H}, 150.93 MHz; ^{31}P{^{1}H}, 242.96 MHz) spectrometer. Chemical shifts (δ in ppm) are given relative to internal tetramethylsilane (^{1}H and ^{13}C NMR) and to external 85% aqueous H_4PO_4 (^{31}P NMR). The signals are denoted as s (singlet), d (doublet), t (triplet), q (quartet), and m (multiplet). The prefix v is added for virtual multiplets arising from the magnetically nonequivalent hydrogen atoms at the substituted cyclopentadienyl rings (C_5H_4; fc = ferrocene-1,1′-diyl). Mass spectra were recorded on an Esquire 3000 or a Compact QTOF-MS (ESI MS, both Bruker Daltonics) spectrometer. The identities of the observed ionic species were corroborated by comparison of the theoretical and experimentally determined isotopic patterns. Elemental analyses were performed using a Perkin-Elmer PE 2400 CHN analyzer. The amount of residual solvent (if applicable) was verified by NMR analysis.

Anhydrous tetrahydrofuran, dichloromethane, diethyl ether, and acetonitrile were obtained from an in-house PureSolv MD5 Solvent Purification System (Innovative Technology, Inc., USA). Anhydrous *N,N*-dimethylformamide stored over molecular sieves was purchased from Sigma–Aldrich. 1-Bromo-1'-(diphenylthiophosphoryl)ferrocene,[1] 4-toluenesulfonyl azide (TsN_3),[2] *O*-benzoyl-*N*-hydroxylamines,[3] and *N*-(prop-2-yn-1-yl)benzamide[4] were prepared according to the literature procedures. Other chemicals were purchased from commercial suppliers and used as received (Alfa–Aesar, TCI, and Sigma–Aldrich). Copper(II) chloride dihydrate (Lach-Ner) was dehydrated by heating to 150 °C under vacuum for 2 h before use.

Syntheses

Preparation of 8. In an oven-dried, three-necked flask flushed with argon and sealed with a rubber septum, 1-bromo-1′-(diphenylthiophosphoryl)ferrocene (2.41 g, 5.0 mmol) was dissolved in anhydrous tetrahydrofuran (80 mL). The resulting solution was cooled to −78 °C using a dry ice/ethanol bath, and *n*-butyllithium (2.0 mL of a 2.5 M solution in pentane, 5.0 mmol) was added dropwise while stirring and cooling for 30 min. An orange precipitate separated during this time. Neat TsN_3 (0.77 mL, 5.0 mmol) was introduced, and the mixture was allowed to react for 2 h at room temperature, during which time the precipitate dissolved. The reaction mixture was transferred *via* a cannula into a suspension of $Li[AlH_4]$ (0.38 g, 10.0 mmol) in anhydrous tetrahydrofuran (10 mL), cooled in an ice bath. The resulting mixture was stirred at room temperature overnight and then quenched by adding 0.5 mL of a 10% aqueous sodium hydroxide. The mixture was stirred for an additional 15 min, whereupon it turned black and deposited a

precipitate. Anhydrous magnesium sulfate was added to the mixture, and the suspension was filtered through a Celite layer on a glass frit. The clear orange filtrate was evaporated under vacuum, and the residue was purified by silica gel column chromatography using ethyl acetate-hexane (1:1) as the eluent. The third dark brown band containing the amine was collected and evaporated to dryness under vacuum. The solid residue was dissolved in a small amount of dichloromethane and precipitated by a slow addition to pentane (25 mL). The separated solid was isolated by decantation and dried under a vacuum. Yield of **8**: (0.44 g, 32%), orange powder.

^{1}H NMR ($CDCl_3$, 399.95 MHz): δ 2.87 (s, 2 H, NH_2), 3.72 (vt, *J′* = 1.9 Hz, 2 H, CH of fc), 4.05 (vt, *J′* = 1.9 Hz, 2 H, CH of fc), 4.29 (vq, *J′* = 2.0 Hz, 2 H, CH of fc), 4.47 (vq, *J′* = 1.7 Hz, 2 H, CH of fc), 7.39–7.50 (m, 6 H, PPh_2), 7.70–7.78 (m, 4 H, PPh_2). ^{13}C{^{1}H} NMR ($CDCl_3$, 100.58 MHz): δ 60.30 (CH of fc), 64.72 (CH of fc), 72.18 (d, J_{PC} = 10 Hz, CH of fc), 73.84 (d, J_{PC} = 13 Hz, CH of fc), 74.55 (d, $^{1}J_{PC}$ = 99 Hz, C^{ipso}–P of fc), 107.47 (C^{ipso}–N of fc), 128.19 (d, J_{PC} = 13 Hz, CH of PPh_2), 131.17 (d, $^{4}J_{PC}$ = 3 Hz, CH^{para} of PPh_2), 131.60 (d, J_{PC} = 11 Hz, CH of PPh_2), 134.66 (d, $^{1}J_{PC}$ = 86 Hz, C^{ipso} of PPh_2). ^{31}P{^{1}H} NMR ($CDCl_3$, 161.90 MHz): δ 42.5 (s). HR MS ESI+, *m/z* calc. for $C_{22}H_{21}FeNPS$ ($[M + H]^+$): 418.0476, found 418.0483. Anal. Calc. for $C_{22}H_{20}FeNPS$ (417.0): C 63.32, H 4.83, N 3.36%. Found: C 62.96, H 4.73, N 3.11%.

Preparation of 1aS. A two-necked flask was charged with **8** (200 mg, 0.48 mmol), potassium carbonate (138 mg, 1.0 mmol), sodium iodide (150 mg, 1.0 mmol), flushed with argon, and sealed with a septum. The solid educts were dissolved in anhydrous *N,N*-dimethylformamide (10 mL), and bis(2-chloroethyl)ether (60 mL, 0.48 mmol) was added to the solution by a syringe. The reaction mixture was heated at 100 °C overnight. Then, it was allowed to cool to room temperature and evaporated to dryness under vacuum. The solid residue was dissolved in a small amount of dichloromethane and filtered through a PTFE syringe filter (0.45 μm porosity). The crude product was purified by column chromatography on silica gel, eluting with dichloromethane-methanol (50:1). The first dark orange band was collected and evaporated, leaving **1aS** as a brown solid. Yield: 0.19 g (80%), brown powder. The crystal suitable for structure determination was obtained by slowly cooling a saturated solution of the substance in boiling heptane.

^{1}H NMR ($CDCl_3$, 399.95 MHz): δ 2.57–2.63 (m, 4 H, CH_2N), 3.69–3.73 (m, 4 H, CH_2O), 3.81 (vt, *J′* = 2.0 Hz, 2 H, CH of fc), 3.96 (vt, *J′* = 1.9 Hz, 2 H, CH of fc), 4.59-4.62 (m, 2 H, CH of fc), 4.63-4.65 (m, 2 H, CH of fc), 7.38–7.50 (m, 6 H, PPh_2), 7.69–7.76 (m, 4 H, PPh_2). ^{13}C{^{1}H} NMR ($CDCl_3$, 100.58 MHz): δ 49.62 (CH_2N), 55.71 (CH of fc), 66.04 (CH of fc), 66.34 (CH_2O), 70.72 (d, J_{PC} = 10 Hz, CH of fc), 72.18 (d, J_{PC} = 13 Hz, CH of fc), 73.59 (d, $^{1}J_{PC}$ = 99 Hz, C^{ipso}–P of fc), 115.14 (C^{ipso}–N of fc), 128.15 (d, J_{PC} = 12 Hz, CH of PPh_2), 131.06 (d, $^{4}J_{PC}$ = 3 Hz, CH^{para} of PPh_2), 131.62 (d, J_{PC} = 11 Hz, CH of PPh_2), 134.89 (d, $^{1}J_{PC}$ = 86 Hz, C^{ipso} of PPh_2). ^{31}P{^{1}H} NMR ($CDCl_3$, 161.90 MHz): δ 42.3 (s). HR MS ESI+,

m/z calc. for $C_{26}H_{27}FeNOPS$ ([M + H]$^+$): 488.0895, found 488.0889. Anal. Calc. for $C_{26}H_{26}FeNOPS$ (487.4): C 64.07, H 5.38, N 2.87%. Found: C 64.06, H 5.28, N 2.85%.

Preparation of 1a by desulfurization of 1aS. An aqueous slurry of active Raney nickel (ca. 3.0 g; Raney 2400 from Sigma–Aldrich) was decanted under an argon atmosphere using a cannula and washed carefully with anhydrous acetonitrile (5× 20 mL). The obtained powder was suspended in anhydrous acetonitrile (20 mL) and mixed with a solution of **1aS** (0.53 g, 1.1 mmol) in the same solvent (100 mL). The reaction mixture was stirred at 50 °C for two days. After cooling to room temperature, the mixture was filtered, and the filtrate was evaporated under vacuum. During the evaporation, a white solid separated on the walls of the flask, especially at the neck, while an orange powder deposited at the bottom. The orange powder was dissolved in dichloromethane and carefully pipetted off. This solution was concentrated under vacuum and purified by chromatography over a silica gel column using dichloromethane as the eluent. The product was collected in the first orange band. Yield of **1a**: 0.38 g (75%), orange powder. Single crystals suitable for X-ray analysis were grown by dissolving the substance in boiling heptane and allowing the solution to cool slowly to room temperature.

^{1}H NMR ($CDCl_3$, 399.95 MHz): δ 2.63–2.67 (m, 4 H, CH_2N), 3.72 (vt, *J*′ = 2.0 Hz, 2 H, CH of fc), 3.72–3.76 (m, 4 H, CH_2O), 3.84 (vt, *J*′ = 2.0 Hz, 2 H, CH of fc), 4.26 (vq, *J*′ = 1.9 Hz, 2 H, CH of fc), 4.52 (vt, *J*′ = 1.7 Hz, 2 H, CH of fc), 7.28–7.32 (m, 6 H, PPh_2), 7.34–7.40 (m, 4 H, PPh_2). ^{13}C{^{1}H} NMR ($CDCl_3$, 100.58 MHz): δ 49.94 (CH_2N), 55.45 (CH of fc), 64.87 (CH of fc), 66.43 (CH_2O), 69.47 (d, J_{PC} = 4 Hz, CH of fc), 72.13 (d, J_{PC} = 15 Hz, CH of fc), 74.86 (d, $^1J_{PC}$ = 5 Hz, C^{ipso}–P of fc), 114.26 (C^{ipso}–N of fc), 128.09 (d, J_{PC} = 7 Hz, CH of PPh_2), 128.37 (CH^{para} of PPh_2), 133.50 (d, J_{PC} = 20 Hz, CH of PPh_2), 139.42 (d, $^1J_{PC}$ = 10 Hz, C^{ipso} of PPh_2). ^{31}P{^{1}H} NMR ($CDCl_3$, 161.90 MHz): δ −15.8 (s). ESI+ MS: *m/z* 456.0 ([M + H]$^+$). Anal. Calc. for $C_{26}H_{26}FeNOP$ (455.3): C 68.58, H 5.76, N 3.08%. Found: C 68.60, H 5.60, N 2.97%.

Preparation of 10. Bromoferrocene (2.65 g, 10.0 mmol) was dissolved in anhydrous tetrahydrofuran (20 mL) in a flame-dried Schlenk flask flushed with nitrogen. The solution was cooled with a dry ice/ethanol bath to −78 °C, and *n*-butyllithium (4.0 mL of 2.5 M solution in hexanes, 10.0 mmol) was introduced dropwise to the reaction mixture. After stirring at −78 °C for 1 h, a solution of zinc(II) bromide (2.25 g, 10.0 mmol) in anhydrous THF (20 mL) was added in small portions, and the resulting mixture was allowed to warm to 0 °C and stirred for an additional two hours. The reaction mixture was then transferred *via* a cannula to an oven-dried Schlenk flask that was flushed with nitrogen and charged with solid copper(II) chloride (44 mg, 0.32 mmol) and *O*-benzoyl-*N*-hydroxymorpholine (5.0 mmol). The obtained mixture was heated at 50 °C overnight and then quenched by adding diethyl ether (10 mL) and distilled water (5 mL). The heterogeneous mixture was filtered into a separatory funnel and extracted with 3 M HCl (20 mL). The aqueous layer was separated and neutralized with 10% aqueous NaOH (to pH ≈ 7). The precipitated

product was extracted into diethyl ether (3× 10 mL) and the organic layer was dried over anhydrous magnesium sulfate and evaporated under reduced pressure. The crude product was crystallized from boiling hexane to produce **10** as an orange crystalline solid. Yield: 0.49 g (34%), orange solid.

^{1}H NMR ($CDCl_3$, 399.95 MHz): δ 2.82–2.85 (m, 4 H, CH_2N), 3.81–3.83 (m, 6 H, CH_2O and CH of C_5H_4), 3.96 (vt, *J*′ = 2.0 Hz, 2 H, CH of C_5H_4), 4.26 (s, 5 H, CH of C_5H_5). ^{13}C{^{1}H} NMR ($CDCl_3$, 100.58 MHz): δ 50.24 (CH_2N), 54.59 (CH of C_5H_4), 63.60 (CH of C_5H_4), 66.55 (CH_2O), 67.12 (CH of C_5H_5), 113.67 (C^{ipso}–N). HR MS ESI+, *m/z* calc. for $C_{14}H_{18}FeNO$ ([M + H]$^+$): 272.0732, found 272.0736. Anal. Calc. for $C_{14}H_{17}FeNO$ (271.1): C 62.01, H 6.32, N 5.17%. Found: C 62.22, H 6.23, N 4.97%.

Synthesis of (10Me)[BF_4]. A flask equipped with a magnetic stirring bar was charged with **10** (27.1 mg, 0.10 mmol) and MeCN (5 mL). Meerwein salt (19.0 mg, 0.10 mmol) was added and the reaction mixture was stirred for 2 h. The resulting solution was evaporated under vacuum and the crude product was purified by crystallization from acetone and diethyl ether. Yield: 20.9 mg (73%), orange brown crystals.

^{1}H NMR ($CDCl_3$, 399.95 MHz): δ 3.43 (s, 3 H, CH_3), 3.56-3.64 (m, 2 H, CH_2N), 3.82-3.92 (m, 2 H, CH_2N), 3.95-4.10 (4 H, CH_2O), 4.45 (vt, *J*′ = 2.2 Hz, 2 H, CH of fc), 4.47 (s, 5 H, CH of C_5H_5), 4.58 (vt, *J*′ = 2.2 Hz, CH of fc). ^{13}C{^{1}H} NMR ($CDCl_3$, 100.58 MHz): δ 51.38 (CH_3), 61.14 (CH of fc), 61.73 (CH_2O), 64.41 (CH_2N), 69,04 (CH of fc), 71.65 (CH of C_5H_5). HR ESI+ MS, *m/z* calc. for $C_{15}H_{20}FeNO$ ([M – BF_4]$^+$): 286.0894, found 286.0890. Anal. Calc. for $C_{15}H_{20}FeNOBF_4$ (373.0): C 48.30, H 5.40, N 3.76%. Found: C 48.49, H 5.15, N 3.96%.

General procedure for the preparation of amines 12. An oven-dried, three-necked flask was charged with 1,1′-dibromoferrocene (0.69 g, 2.0 mmol), flushed with nitrogen, and sealed with a rubber septum. The educt was dissolved in anhydrous tetrahydrofuran (30 mL), and the solution was cooled with a dry ice/ethanol bath to –78 °C. *n*-Butyllithium (0.8 mL of 2.5 M solution in hexanes, 2.0 mmol) was added dropwise, and the reaction mixture was stirred under continuous cooling for 1 h. Next, a solution of zinc(II) bromide (0.45 mg, 2.0 mmol) in THF (10 mL) was added in small portions, and the resulting mixture was allowed to warm to 0 °C and stirred for another 2 h. The reaction mixture was then transferred *via* a cannula to an oven-dried Schlenk flask that was flushed with nitrogen and charged with solid copper(II) chloride (6.7 mg, 0.050 mmol) and the respective *O*-benzoyl-*N*-hydroxylamine (1.0 mmol). The reaction mixture was heated overnight to 50 °C and quenched by the addition of diethyl ether (10 mL) and distilled water (5 mL). The heterogeneous mixture was filtered into a separatory funnel and washed with brine (3× 10 mL). The organic layer was dried over anhydrous magnesium sulfate and evaporated under reduced pressure. The oily residue was purified by column chromatography as specified below.

Preparation of 12a. The amine **12a** was obtained by a slightly modified General procedure. Specifically, 1,1′-dibromoferrocene (3.44 g, 10.0 mmol) was dissolved in 50 mL of anhydrous THF, lithiated with *n*-butyllithium (6.3 mL of 1.6 M solution in hexanes, 10.0 mmol), and then reacted with a solution of $ZnBr_2$ (2.60 g, 10.0 mmol) in THF (20 mL). The reaction mixture was then transferred to a Schlenk flask charged with $CuCl_2$ (34 mg, 0.25 mmol) and *O*-benzoyl-*N*-hydroxymorpholine (1.04 g, 5.0 mmol) and heated to 50 °C overnight (18 h). The reaction was terminated as described in the General procedure, and the heterogeneous mixture was extracted with 3 M hydrochloric acid (20 mL). The aqueous layer was separated and neutralized by 10% aqueous NaOH to neutral pH. The precipitated product was extracted with diethyl ether (3× 10 mL). The organic extracts were combined, washed with brine (20 mL), dried over anhydrous magnesium sulfate, and evaporated, leaving **12a** as a brown oil. Yield: 1.01 g (61%).

^{1}H NMR ($CDCl_3$, 399.95 MHz): δ 2.84–2.88 (m, 4 H, CH_2N), 3.79 (vt, *J*′ = 2.0 Hz, 2 H, CH of fc), 3.81–3.86 (m, 4 H, CH_2O), 4.04 (vt, *J*′ = 1.9 Hz, 2 H, CH of fc), 4.20 (vt, *J*′ = 1.9 Hz, 2 H, CH of fc), 4.55 (vt, *J*′ = 1.9 Hz, 2 H, CH of fc). ^{13}C{^{1}H} NMR ($CDCl_3$, 100.58 MHz): δ 50.12 (CH_2N), 57.13 (CH of fc), 66.18 (CH of fc), 66.34 (CH of fc), 66.48 (CH_2O), 69.03 (CH of fc), 77.71 (C^{ipso}–Br of fc), 115.10 (C^{ipso}–N of fc). Anal. Calc. for $C_{14}H_{16}BrFeNO$ (350.0): C 48.04, H 4.61, N 4.00%. Found: C 48.28, H 4.39, N 3.77%.

Preparation of 12b. Compound **12b** was obtained following the General procedure, starting from 1,1′-dibromoferrocene (677 mg, 1.97 mmol), *n*-butyllithium (0.79 mL of 2.5 M solution in hexanes, 1.97 mmol), $ZnBr_2$ (444 mg, 1.97 mmol), $CuCl_2$ (6.7 mg, 0.050 mmol), and *O*-benzoyl-*N*-hydroxythiomorpholine (220 mg, 0.99 mmol). The crude product obtained after the aqueous workup was purified by column chromatography over silica gel using dichloromethane as an eluent. Evaporation of the second band afforded **12b** as a brown oil. Yield: 210 mg (58%).

^{1}H NMR ($CDCl_3$, 399.95 MHz): δ 2.74–2.81 (m, 4 H, CH_2N), 3.10–3.17 (m, 4 H, CH_2S), 3.81 (vt, *J*′ = 1.9 Hz, 2 H, CH of fc), 4.03 (vt, *J*′ = 1.9 Hz, 2 H, CH of fc), 4.18 (vt, *J*′ = 1.9 Hz, 2 H, CH of fc), 4.53 (vt, *J*′ = 1.9 Hz, 2 H, CH of fc). ^{13}C{^{1}H} NMR ($CDCl_3$, 100.58 MHz): δ 27.57 (CH_2S), 52.01 (CH_2N), 57.55 (CH of fc), 66.35 (2× CH of fc), 69.22 (CH of fc), 77.80 (C^{ipso}–Br of fc), 114.99 (C^{ipso}–N of fc). HR MS ESI+, *m/z* calc. for $C_{14}H_{17}BrFeNS$ ($[M + H]^+$): 365.9616, found 365.9606.

Preparation of 12c. Amine **12c** was prepared according to the General procedure using 1,1′-dibromoferrocene (688 mg, 2.0 mmol), *n*-butyllithium (0.8 mL of 2.5 M solution in hexanes, 2.0 mmol), $ZnBr_2$ (450 mg, 2.0 mmol), $CuCl_2$ (6.7 mg, 0.050 mmol), and *O*-benzoyl-*N*-hydroxyl-dimethylamine (165 mg, 0.99 mmol). The crude product obtained after the aqueous workup was purified by column chromatography over silica gel using dichloromethane-methanol as the eluent (50:1). The second band was collected and evaporated under vacuum, producing **12c** as a brown oil. Yield: 107 mg (35%).

^{1}H NMR ($CDCl_3$, 399.95 MHz): δ 2.62 (s, 6 H, CH_3), 3.74 (vt, *J*′ = 2.0 Hz, 2 H, CH of fc), 3.99 (vt, *J*′ = 2.0 Hz, 2 H, CH of fc), 4.16 (vt, *J*′ = 1.9 Hz, 2 H, CH of fc), 4.51 (vt, *J*′ = 1.9 Hz, 2 H, CH of fc). ^{13}C{^{1}H} NMR ($CDCl_3$, 100.58 MHz): δ 42.25 (CH_3), 57.48 (CH of fc), 65.88 (CH of fc), 66.17 (CH of fc), 68.73 (CH of fc), 77.88 (C^{ipso}–Br of fc), 116.89 (C^{ipso}–N of fc). HR MS ESI+, *m/z* calc. for $C_{12}H_{15}BrFeN$ ([M + H]$^{+}$): 307.9653, found 307.9655.

Preparation of phosphinoamines 1a–c, 2a, and 3a. General procedure. An oven-dried Schlenk flask equipped with a stirring bar was charged with the respective amine **12** (1 equiv.) and flushed with nitrogen. The starting material was dissolved in anhydrous THF (20 mL), and the solution was cooled to –78 °C using a dry ice/ethanol bath. Then, *n*-butyllithium (2.5 M solution in hexanes, 1.1 equiv.) was added dropwise, and the reaction mixture was stirred at –78 °C for 1 h. The corresponding chlorophosphine (1.2 equiv.) was added, and the reaction mixture was stirred at room temperature for 1 h. The reaction was terminated by adding distilled water (10 mL), and the resulting mixture was transferred to a separatory funnel and diluted with diethyl ether (10 mL). The organic layer was separated, washed with brine (2× 10 mL), dried over anhydrous magnesium sulfate, and evaporated under reduced pressure. The crude product was purified by column chromatography over silica gel as described below.

Preparation of 1a. Compound **1a** was obtained by the General procedure starting from **12a** (1.75 g, 5.0 mmol), *n*-BuLi (2.2 mL of 2.5 M in hexanes, 5.5 mmol), and chlorodiphenylphosphine (1.1 mL, 6.0 mmol). The crude product obtained after aqueous workup was purified by column chromatography over silica gel using hexane-diethyl ether (1:1) as the eluent. The first band was collected and evaporated, leaving **1a** as a brown oil. Subsequent crystallization from hot hexane produced orange crystalline solid. Yield: 1.55 g (68%). Analytical data were identical to those reported above.

Preparation of 1b. Lithiation of **12b** (0.22 g, 0.60 mmol) with *n*-BuLi in hexane (0.3 mL of 2.5 M solution in hexanes, 0.7 mmol) and reaction with chlorodiphenylphosphine (0.13 mL, 0.70 mmol) according to the General procedure produced crude **1b**, which purified by column chromatography over silica gel using hexane-ethyl acetate (10:1). The compound was isolated as a slowly crystallizing brown oil. Yield: 0.18 g (65%).

^{1}H NMR ($CDCl_3$, 399.95 MHz): δ 2.67–2.70 (m, 4 H, CH_2S), 2.92–2.94 (m, 4 H, CH_2N), 3.74 (vt, *J*′ = 2.0 Hz, 2 H, CH of fc), 3.83 (vt, *J*′ = 2.0 Hz, 2 H, CH of fc), 4.24 (vq, *J*′ = 1.9 Hz, 2 H, CH of fc), 4.51 (vt, *J*′ = 1.8 Hz, 2 H, CH of fc), 7.28–7.33 (m, 6 H, PPh_2), 7.34–7.40 (m, 4 H, PPh_2). ^{13}C{^{1}H} NMR ($CDCl_3$, 100.58 MHz): δ 27.55 (CH_2S), 51.88 (CH_2N), 55.93 (CH of fc), 64.92 (CH of fc), 69.97 (d, J_{PC} = 4 Hz, CH of fc), 72.27 (d, J_{PC} = 15 Hz, CH of fc), 74.91 (d, $^{1}J_{PC}$ = 5 Hz, C^{ipso}–P of fc), 114.15 (C^{ipso}–N of fc), 128.08 (d, J_{PC} = 7 Hz, CH of PPh_2), 128.37 (CH^{para} of PPh_2), 133.50 (d, J_{PC} = 19 Hz, CH of PPh_2), 139.41 (d, $^{1}J_{PC}$ = 9 Hz, C^{ipso} of PPh_2). ^{31}P{^{1}H} NMR ($CDCl_3$, 161.90 MHz): δ –15.8 (s). ESI+ MS: *m/z*

472.1 ([M + H]$^+$). Anal. Calc. for $C_{26}H_{26}FeNPS$ (471.4): C 66.25, H 5.56, N 2.97%. Found: C 66.00, H 5.50, N 2.82%.

Preparation of 1c. The reaction of **12c** (0.31 g, 1.0 mmol) with *n*-BuLi (0.44 mL of 2.5 M in hexanes, 1.1 mmol) and chlorodiphenylphosphine (0.20 mL, 1.1 mmol) according to the General procedure produced crude **1c**. The compound was purified by column chromatography over silica gel, eluting with hexane-ethyl acetate (5:1) with added triethylamine (0.1% v/v). Evaporation of the first band gave **1c** as a slowly crystallizing brown oil. Yield: 0.24 g (58%).

^{1}H NMR ($CDCl_3$, 399.95 MHz): δ 2.47 (s, 6 H, CH_3), 3.68 (vt, *J′* = 2.0 Hz, 2 H, CH of fc), 3.78 (vt, *J′* = 1.9 Hz, 2 H, CH of fc), 4.21 (vq, *J′* = 1.9 Hz, 2 H, CH of fc), 4.50 (vt, *J′* = 1.9 Hz, 2 H, CH of fc), 7.28–7.33 (m, 6 H, PPh_2), 7.34–7.40 (m, 4 H, PPh_2). ^{13}C{^{1}H} NMR ($CDCl_3$, 100.58 MHz): δ 42.17 (CH_3), 55.88 (CH of fc), 64.84 (CH of fc), 69.47 (d, J_{PC} = 4 Hz, CH of fc), 71.93 (d, J_{PC} = 15 Hz, CH of fc), 74.51 (d, $^1J_{PC}$ = 5 Hz, C^{ipso}–P of fc), 115.99 (C^{ipso}–N of fc), 128.03 (d, J_{PC} = 7 Hz, CH of PPh_2), 128.30 (CH^{para} of PPh_2), 133.46 (d, J_{PC} = 19 Hz, CH of PPh_2), 139.54 (d, $^1J_{PC}$ = 9 Hz, C^{ipso} of PPh_2). ^{31}P{^{1}H} NMR ($CDCl_3$, 161.90 MHz): δ –15.6 (s). ESI+ MS: *m/z* 414.1 ([M + H]$^+$). Anal. Calc. for $C_{24}H_{24}FeNP$ (413.3): C 69.75, H 5.85, N 3.39%. Found: C 69.08, H 5.70, N 3.19%.

Preparation of 2a. The reaction of **12a** (0.35 g, 1.0 mmol) with *n*-BuLi (0.4 mL of 2.5 M in hexanes, 1.1 mmol) and chlorodicyclohexylphosphine (0.24 mL, 1.1 mmol) according to the General procedure produced crude **2a**, which was purified by column chromatography over silica gel using hexane-diethyl ether (10:1) as the eluent. Following evaporation, the compound was obtained as an orange solid. Yield: 0.39 g (83%).

^{1}H NMR ($CDCl_3$, 400.13 MHz): δ 0.96–1.39 (m, 10 H, Cy), 1.60–2.00 (m, 12 H, Cy), 2.80–2.90 (m, 4 H, CH_2N), 3.79 (br s 2 H, CH of fc), 3.81–3.84 (m, 4 H, CH_2N), 3.92 (br s 2 H, CH of fc), 4.26 (br s 2 H, CH of fc), 4.46 (br s 2 H, CH of fc). ^{13}C{^{1}H} NMR ($CDCl_3$, 100.61 MHz): δ 26.46 (CH_2 of Cy), 27.40 (m, CH_2 of Cy), 30.23 (d, J_{CP} = 3 Hz, CH_2 of Cy), 30.35 (CH_2 of Cy), 33.53 (d, $^1J_{CP}$ = 3 Hz, CH of Cy), 50.12 (CH_2N), 55.36 (CH of fc), 65.42 (CH of fc), 66.54 (CH_2O), 68.15 (d, J_{CP} = 3 Hz, CH of fc), 70.79 (d, J_{CP} = 11 Hz, CH of fc), 75.80 (d, $^1J_{CP}$ = 16 Hz, C^{ipso}–P of fc), 113.95 (C^{ipso}–N of fc). ^{31}P{^{1}H} NMR ($CDCl_3$, 161.90 MHz): δ –7.2 (s). ESI+ MS: *m/z* 468.2 ([M + H]$^+$). Anal. Calc. for $C_{26}H_{38}FeNOP$ (467.4): C 66.81, H 8.19, N 3.00%. Found: C 66.59, H 7.98, N 3.09%.

Preparation of 3a. Compound **3a** was obtained following the General procedure, using **12a** (0.53 g, 1.5 mmol), *n*-BuLi (0.66 mL of 2.5 M in hexanes, 1.7 mmol) and chlorodi(2-furyl)phosphine (0.27 mL, 1.73 mmol). The crude product obtained after aqueous work-up was purified by column chromatography over silica gel using hexane-ethyl acetate (13:1) as the eluent. The second band was collected and evaporated, leaving **3a** as a brown oil that was further crystallized from pentane to give an orange crystalline material. Yield: 0.31 g (47%).

^{1}H NMR ($CDCl_3$, 600.17 MHz): δ 2.72–2.75 (m, 4 H, CH_2N), 3.67 (vt, *J′* = 2.0 Hz, 2 H, CH of fc), 3.77–3.81 (m, 6 H, CH of fc and CH_2O), 4.49 (vt, *J′* = 1.9 Hz, 2 H, CH of fc), 4.57 (vq, *J′* = 2.0 Hz 2 H,

CH of fc), 6.38 (dt, J = 3.3, 1.7 Hz, 2 H, CH of furyl), 6.66-6.68 (m, 2 H, CH of furyl), 7.62 (d, J = 1.9 Hz, 2 H, CH of furyl). $^{13}C\{^1H\}$ NMR ($CDCl_3$, 150.91 MHz): δ 50.05 (CH_2N), 53.38 (CH of fc), 64.80 (CH of fc), 66.49 (CH_2O), 69.87 (d, J_{CP} = 6 Hz, CH of fc), 71.63 (d, $^1J_{CP}$ = 6 Hz, C^{ipso}–P of fc), 72.77 (d, J_{CP} = 18 Hz, CH of fc), 110.55 (d, J_{CP} = 6 Hz, CH of furyl), 114.43 (C^{ipso}–N of fc), 119.64 (d, J_{CP} = 24 Hz, CH of furyl), 146.53 (d, J_{CP} = 2 Hz, CH of furyl), 152.64 (d, $^1J_{CP}$ = 7 Hz, C^{ipso} of furyl). $^{31}P\{^1H\}$ NMR ($CDCl_3$, 242.95 MHz): δ –64.7 (s). ESI+ MS: m/z 435.2 (M^+). Anal. Calc. for $C_{22}H_{22}FeNO_3P$ (435.2): C 60.71, H 5.09, N 3.22%. Found: C 66.58, H 4.44, N 2.97%.

Preparation of lithium 2,2,6,6-tetramethylpiperidide (LiTMP). Under nitrogen, 2,2,6,6-tetramethylpiperidine (2.26 g, 16.0 mmol) was dissolved in anhydrous THF (10 mL), and the solution was cooled to 0 °C. *n*-BuLi in hexanes (6.0 mL of 2.5 M solution, 15 mmol) was introduced dropwise, and the mixture was stirred at 0 °C for 30 min at 0 °C to complete the reaction. The resulting yellow solution of LiTMP was used directly in the following step as described below.

Preparation of amines 13a–c. General procedure. Bromoferrocene (2.65 g, 10.0 mmol) was dissolved in anhydrous tetrahydrofuran (20 mL) in a flame-dried Schlenk flask flushed with nitrogen. The reaction mixture was cooled with a dry ice-ethanol bath to −78 °C. Next, a freshly prepared solution of lithium tetramethylpiperidide (10.3 mmol) was introduced, and the reaction mixture was stirred at −78 °C for 1 h. A solution of zinc(II) bromide (2.25 g, 10.0 mmol) in anhydrous THF (20 mL) was added in small portions, and the resulting solution was allowed to warm to 0 °C and stirred for an additional 2 h. The reaction mixture was transferred *via* a cannula to an oven-dried Schlenk flask that was flushed with nitrogen and charged with solid copper(II) chloride (44 mg, 0.32 mmol) and the respective *O*-benzoyl-*N*-hydroxylamine (5.0 mmol). The resulting mixture was heated at 50 °C overnight, cooled to room temperature and quenched by adding diethyl ether (10 mL) and distilled water (5 mL). The heterogeneous mixture was filtered into a separatory funnel and washed with brine (3× 10 mL). The organic layer was dried over anhydrous magnesium sulfate and evaporated under reduced pressure. The oily residue was purified by column chromatography as described below.

Preparation of 13a. Amine **13a** was obtained following the General procedure. The crude product obtained after the aqueous workup was purified by column chromatography over silica gel, eluting with dichlorometane-methanol (20:1). Evaporation of the second band afforded **13a** as a brown oil. Yield: 0.72 g (41%), brown oil.

^1H NMR ($CDCl_3$, 399.95 MHz): δ 2.82–2.90 (m, 2 H, CH_2N), 3.04–3.13 (m, 2 H, CH_2N), 3.81–3.86 (m, 4 H, CH_2O), 3.92–3.97 (m, 2 H, CH of C_5H_3), 4.26 (s, 5 H, C_5H_5), 4.27–4.29 (m, 1 H, CH of C_5H_3). $^{13}C\{^1H\}$ NMR ($CDCl_3$, 100.58 MHz): δ 52.62 (CH_2N), 56.59 (CH of C_5H_3), 62.05 (CH of C_5H_3), 66.95 (CH_2O), 67.59 (CH of C_5H_3), 70.51 (C_5H_5), 72.77 (C^{ipso}–Br), 109.41 (C^{ipso}–N). HR MS ESI+, m/z calc. for $C_{14}H_{17}BrFeNO$ ($[M + H]^+$): 349.9845, found 349.9831.

Preparation of 13b. Compound **13b** was obtained following the General procedure. The crude product was purified by column chromatography over silica gel using cyclohexane-ethylacetate (30:1) as the eluent. Evaporation of the second band afforded **13b** as a brown oil. Yield: 1.28 g (35%).

^{1}H NMR ($CDCl_3$, 399.95 MHz): δ 2.73–2.86 (m, 4 H, CH_2S), 3.07–3.14 (m, 2 H, CH_2N), 3.26–3.35 (m, 2 H, CH_2N), 3.94 (m, 2 H, CH of C_5H_3), 4.22 (s, 5 H, C_5H_5), 4.27 (t, *J* = 2.1 Hz, 1 H, CH of C_5H_3). $^{13}C\{^1H\}$ NMR ($CDCl_3$, 100.58 MHz): δ 28.09 (CH_2S), 54.89 (CH_2N), 56.61 (CH of C_5H_3), 62.20 (CH of C_5H_3), 67.19 (CH of C_5H_3), 70.82 (C_5H_5), 74.37 (C^{ipso}–Br), 110.60 (C^{ipso}–N). HR MS ESI+, *m/z* calc. for $C_{14}H_{17}BrFeNS$ ($[M + H]^+$): 365.9609, found 365.9598.

Preparation of 13c. Amine **13c** was synthesized according to the General procedure. The crude product was purified by column chromatography over silica gel using cyclohexane-ethylacetate (30:1). The second band was collected and evaporated to dryness. The residue was subsequently purified by column chromatography over alumina using cyclohexane with a slow gradient to cyclohexane-ethylacetate (30:1). The first band was collected, yielding **13c** as a yellow oil. Yield: 1.32 g (43%).

^{1}H NMR ($CDCl_3$, 400.13 MHz): δ 2.70 (s, 6 H, NMe_2), 3.91–3.97 (m, 2 H, CH of C_5H_3), 4.24-4.27 (m, 6 H, CH of C_5H_3 and C_5H_5). $^{13}C\{^1H\}$ NMR ($CDCl_3$, 100.61 MHz): δ 44.70 (NMe_2), 56.17 (CH of C_5H_3), 61.86 (CH of C_5H_3), 67.50 (CH of C_5H_3), 70.43 (C_5H_5), 72.92 (C^{ipso}–Br), 111.08 (C^{ipso}–N). HR MS ESI+, *m/z* calc. for $C_{12}H_{15}BrFeN$ ($[M + H]^+$): 307.9732, found 307.9730.

Preparation of phosphinoamines 4a–c. General procedure. An oven-dried Schlenk flask equipped with a stirring bar was charged with the respective amine **13** (1.0 equiv.), flushed with nitrogen, and sealed with a rubber septum. The starting material was dissolved in anhydrous THF (20 mL), and the solution was cooled to –78 °C in a dry ice/ethanol bath. *n*-Butyllithium (2.5 M solution in hexanes, 1.1 equiv.) was added dropwise, and the reaction mixture was stirred at –78 °C for 1 h. After this time, the respective chlorophosphine (1.2 equiv.) was introduced and the resulting mixture was stirred at room temperature for 1 h and then quenched with distilled water (10 mL). The resulting mixture was transferred to a separatory funnel and diluted with diethyl ether (10 mL). The organic layer was separated, washed with brine (2× 10 mL), dried over anhydrous magnesium sulfate, and evaporated under vacuum. The product was purified by column chromatography over silica gel as specified below.

Preparation of 4a. Compound **4a** was synthesized following the General procedure, starting from compound **13a** (0.72 g, 2.1 mmol), *n*-BuLi in hexanes (1.0 mL of 2.5 M solution, 2.5 mmol), and chlorodiphenylphosphine (0.45 mL, 2.5 mmol). The crude product was purified by column chromatography on silica gel using a dichloromethane-methanol (75:1) as the eluent. The first band was collected and evaporated, leaving a brown oil, which was further crystallized from hot heptane to produce pure **4a** as an orange crystalline solid. Yield: 0.45 g (48%), orange crystals.

^{1}H NMR ($CDCl_3$, 399.95 MHz): 2.73 (dddd, J = 11.8, 6.4, 3.1, 1.0 Hz, 2 H, CH_2N), 3.22 (ddt, J = 12.2, 6.2, 3.0 Hz, 2 H, CH_2N), 3.50 (ddd, J = 2.6, 1.5, 1.0 Hz, 1 H, CH of of C_5H_3), 3.58–3.72 (m, 4 H, CH_2O), 4.07 (td, J = 2.6, 0.7 Hz, 1 H, CH of C_5H_3), 4.26 (s, 5 H, C_5H_5), 4.21 (dt, J = 2.6, 1.6 Hz, 1 H, CH of C_5H_3), 7.21–7.27 (m, 5 H, PPh_2), 7.34–7.39 (m, 3 H, PPh_2), 7.48–7.54 (m, 2 H, PPh_2). ^{13}C{^{1}H} NMR ($CDCl_3$, 100.58 MHz): δ 53.13 (d, J_{PC} = 8 Hz, CH_2N), 60.90 (d, J_{PC} = 3 Hz, CH of C_3H_5), 65.11 (CH of C_3H_5), 66.17 (d, $^{1}J_{PC}$ = 10 Hz, C^{ipso}–P of C_5H_3), 66.84 (CH_2O), 68.55 (d, J_{PC} = 3 Hz, CH of C_3H_5), 68.79 (C_5H_5), 117.20 (d, $^{2}J_{PC}$ = 17 Hz, C^{ipso}–N of C_5H_3), 127.93 (d, J_{PC} = 11 Hz, CH of PPh_2), 128.05 (CH^{para} of PPh_2), 128.08 (d, J_{PC} = 8 Hz, CH of PPh_2), 129.06 (CH^{para} of PPh_2), 132.56 (d, J_{PC} = 18 Hz, CH of PPh_2), 135.12 (d, J_{PC} = 21 Hz, CH of PPh_2), 137.57 (d, $^{1}J_{PC}$ = 11 Hz, C^{ipso} of PPh_2), 139.08 (d, $^{1}J_{PC}$ = 11 Hz, C^{ipso} of PPh_2). ^{31}P{^{1}H} NMR ($CDCl_3$, 161.90 MHz): δ −19.7 (s). MALDI+ MS: m/z 456.3 ([M + H]$^{+}$). Anal. Calc. for $C_{26}H_{26}FeNOP$ (455.3): C 68.58, H 5.76, N 3.08%. Found: C 68.21, H 5.67, N 2.75%.

Preparation of 4b. Compound **4b** was obtained following the General procedure from **13b** (567 mg, 1.55 mmol), *n*-BuLi in hexanes (0.68 mL of 2.5 M solution, 1.7 mmol), and chlorodiphenylphosphine (0.33 mL, 1.86 mmol). The compound was purified by column chromatography over silica gel using dichloromethane as the eluent. Evaporation of the second band produced **4a** as a slowly crystallizing brown oil. Yield: 0.37 g (50%), an orange-brown solid. The compound retains residual dichloromethane.

^{1}H NMR ($CDCl_3$, 600.17 MHz): δ 2.47–2.64 (m, 4 H, CH_2S), 2.99 (ddd, J = 12.2, 7.1, 3.0 Hz, 1 H, CH_2N), 3.46 (ddt, J = 12.4, 7.0, 2.7 Hz, 2 H, CH_2N), 3.52 (ddd, J = 2.5, 1.5, 1.0 Hz, 1 H, C_5H_3), 4.07 (td, J' = 2.6, 0.7 Hz, 1 H, C_5H_3), 4.10 (s, 5 H, C_5H_5), 4.22 (dt, J' = 2.6, 1.5 Hz, 1 H, C_5H_3), 7.24–7.28 (m, 5 H, PPh_2), 7.34–7.39 (m, 3 H, PPh_2), 7.48–7.55 (m, 2 H, PPh_2). ^{13}C{^{1}H} NMR ($CDCl_3$, 150.91 MHz): δ 27.91 (CH_2S), 55.57 (d, J_{CP} = 7 Hz, CH_2N), 62.06 (d, J_{CP} = 3 Hz, CH of C_5H_3), 65.17 (CH of C_5H_3), 67.40 (d, $^{1}J_{CP}$ = 9 Hz, C^{ipso}–P of C_5H_3), 68.28 (d, J_{CP} = 3 Hz, CH of C_5H_3), 69.09 (C_5H_5), 118.11 (d, $^{2}J_{PC}$ = 17 Hz, C^{ipso}–N), 128.01 (d, J_{PC} = 1 Hz, CH of PPh_2), 128.04 (CH^{para} of PPh_2), 128.06 (d, J_{PC} = 2 Hz, CH of PPh_2), 128.97 (CH^{para} of PPh_2), 132.72 (d, J_{PC} = 19 Hz, CH of PPh_2), 134.93 (d, J_{PC} = 21 Hz, CH of PPh_2), 137.56 (d, $^{1}J_{PC}$ = 10 Hz, C^{ipso} of PPh_2), 138.90 (d, $^{1}J_{PC}$ = 11 Hz, C^{ipso} of PPh_2). ^{31}P{^{1}H} NMR ($CDCl_3$, 161.90 MHz): δ −21.0 (s). MALDI+ MS: m/z 472.1 ([M+H]$^{+}$). Anal. Calc. for $C_{26}H_{26}FeNPS\cdot 0.1CH_2Cl_2$ (479.6): C 65.42, H 5.36, N 2.92%. Found: C 65.46, H 5.26, N 2.71%.

Preparation of 4c. Compound **4c** was obtained according to the General procedure using **13c** (684 mg, 2.22 mmol), *n*-BuLi (0.98 mL of 2.5 M in hexanes, 2.46 mmol), and chlorodiphenylphosphine (0.48 mL, 2.66 mmol). The product was purified by column chromatography over a silica gel column, eluting with a dichloromethane-methanol (20:1). The product, a brown oil, was isolated from the first fraction. Further purification was achieved by crystallization from hot hexane. Impurities crystallized out from the solution, while pure phosphinoamine remained dissolved. Therefore, the mixture was filtered and evaporated, leaving **4c** as a brown powder.

Yield: 587 mg (64%). The obtained analytical data are consistent with the values published in literature.[5]

^{1}H NMR ($CDCl_3$, 600.17 MHz): δ 2.66 (s, 6 H, Me), 3.47 (m, 1 H, C_5H_3), 4.07 (m, 1 H, C_5H_3), 4.10 (s, 5 H, C_5H_5), 4.18 (m, 1 H, C_5H_3), 7.21–7.27 (m, 5 H, PPh_2), 7.34–7.39 (m, 3 H, PPh_2), 7.49–7.55 (m, 2 H, PPh_2). ^{31}P{^{1}H} NMR ($CDCl_3$, 161.90 MHz): δ −21.0 (s).

Preparation of 5a. The ligand **5a** was obtained as described above in the General procedure starting with **13a** (700 mg, 2.0 mmol), *n*-BuLi in hexanes (0.88 mL of 2.5 M solution, 2.2 mmol), and chlorodicyclohexylphosphine (0.56 mL, 2.4 mmol). The crude product was purified by column chromatography over silica gel using hexane-diethyl-ether (1:1) as the eluent. The first band was collected and evaporated to give a brown oil, which was further crystallized from hot heptane to produce **5a** as an orange crystalline solid. Yield: 0.45 g (48%), orange crystals.

^{1}H NMR ($CDCl_3$, 400.13 MHz): δ ^{1}H NMR ($CDCl_3$, 400.13 MHz): δ 0.78-1.99 (m, 21 H, PCy_2), 2.36 (m, 1 H, PCy_2), 2.73 (m, 2 H, CH_2N), 3.57 (m, 2 H, CH_2N), 3.75 (m, 4 H, CH_2O), 3.94 (m, 1 H, CH of C_5H_3), 4.06 (m, 1 H, CH of C_5H_3), 4.13 (m, 1 H, CH of C_5H_3), 4.25 (s, 5 H, C_5H_5). ^{13}C{^{1}H} NMR ($CDCl_3$, 100.61 MHz): δ 26.51 (d, J_{CP} = 11 Hz, CH_2 of Cy), 26.92 (CH_2 of Cy), 27.30 (m, 2× CH_2 of Cy), 27.73 (m, 2× CH_2 of Cy), 29.66 (d, J_{CP} = 7 Hz, CH_2 of Cy), 29.87 (d, J_{CP} = 11 Hz, CH_2 of Cy), 30.66 (d, J_{CP} = 14 Hz, CH_2 of Cy), 32.16 (d, $^{1}J_{CP}$ = 18 Hz, CH of Cy), 33.16 (d, J_{CP} = 11 Hz, CH_2 of Cy), 35.03 (d, $^{1}J_{CP}$ = 14 Hz CH of Cy), 52.61 (d, J_{CP} = 11 Hz, CH_2N), 61.28 (d, J_{CP} = 3 Hz, CH of C_5H_3), 63.50 (CH of C_5H_3), 64.26 (d, J_{CP} = 22 Hz, C^{ipso}–P of C_5H_3), 67.01 (CH_2O), 67.12 (d, J_{CP} = 3 Hz, CH of C_5H_3), 68.29 (C_5H_5), 116.36 (d, $^{2}J_{CP}$ =12 Hz, C^{ipso}–N of C_5H_3). ^{31}P{^{1}H} NMR ($CDCl_3$, 161.98 MHz): δ −11.3 (s). ESI+ MS: *m/z* 468.2 ($[M + H]^+$). HR MS ESI+, *m/z* calc. for $C_{26}H_{29}FeNOP$ ($[M + H]^+$): 468.2119, found 468.2120.

Preparation of 6a. Compound **6a** was synthesized according to the General procedure, from **13a** (528 mg, 1.5 mmol), *n*-BuLi in hexanes (0.66 mL of 2.5 M solution, 1.65 mmol), and chlorodi(2-furyl)phosphine (0.27 mL, 1.73 mmol). The crude product was purified by chromatography over silica gel, eluting with hexane-ethylacetate (5:1). The second band was collected and evaporated to produce a brown oil, which was further crystallized from pentane to give **6a** as an orange crystalline solid. Yield: 0.28 g (42%), orange crystals.

^{1}H NMR ($CDCl_3$, 600.17 MHz): δ 2.65 (dddd, *J* = 11.8, 6.4, 3.0, 1.0 Hz, 2 H, CH_2N), 2.96–3.02 (m, 2 H, CH_2N), 3.72–3.81 (m, 4 H, CH_2O), 4.06 (s, 5 H, C_5H_5), 4.13 (td, *J* = 2.5, 1.4, Hz, 1 H, CH of C_5H_3), 4.15 (td, *J* = 2.6, 0.6, Hz, 1 H, CH of C_5H_3), 4.26 (ddd, *J* = 2.5, 1.5, 1.0 Hz, 1 H, CH of C_5H_3), 6.31 (dt, *J* = 3.2, 1.6 Hz, 1 H, CH of furyl), 6.47 (dt, *J* = 3.4, 1.8 Hz, 1 H, CH of furyl), 6.54 (ddd, *J* = 3.3, 1.2, 0.8 Hz, 1 H, CH of furyl), 6.86 (ddd, *J* = 3.2, 2.4, 0.8 Hz, 1 H, CH of furyl), 7.54 (dd, *J* = 1.9, 0.7 Hz, 1 H, CH of furyl), 7.73 (dt, *J* = 1.7, 0.6 Hz, 1 H, CH of furyl). ^{13}C{^{1}H} NMR ($CDCl_3$, 150.91 MHz): δ 54.22 (d, J_{CP} = 5 Hz, CH_2N), 59.02 (d, J_{CP} = 5 Hz, CH of C_5H_3), 66.17 (CH of C_5H_3), 66.29 (d, $^{1}J_{CP}$ = 4 Hz, C^{ipso}–P of C_5H_3), 66.92 (CH_2O), 69.29 (C_5H_5), 69.73 (d, J_{CP} = 5 Hz, CH of C_5H_3), 110.44 (d, J_{CP} = 5 Hz, CH of furyl), 110.71 (d, J_{CP} = 7 Hz, CH of furyl), 117.71 (d, $^{1}J_{CP}$ = 23 Hz, C^{ipso}–N of C_5H_3), 119.04 (d, J_{CP} = 21

Hz, CH of furyl), 121.07 (d, J_{CP} = 27 Hz, CH of furyl), 146.58 (d, J_{CP} = 2 Hz, CH of furyl), 146.74 (d, J_{CP} = 2 Hz, CH of furyl), 151.74 (d, $^{1}J_{CP}$ = 10 Hz, C^{ipso}–P of furyl), 152.63 (d, $^{1}J_{CP}$ = 9 Hz, C^{ipso}–P of furyl). $^{31}P\{^{1}H\}$ NMR ($CDCl_3$, 242.95 MHz): δ −69.6 (s). ESI+ MS: *m/z* 435.2 (M^+). HR MS ESI+, *m/z* calc. for $C_{22}H_{23}FeNO_3P$ ($[M + H]^+$): 436.0765, found 436.0752.

General procedure for preparation of the gold(I) complexes. A flask equipped with a magnetic stirring bar was charged with the respective phosphinoamine **1**–**6.** The ligand (0.10 mmol) was dissolved in anhydrous CH_2Cl_2 (5 mL). A solution of chloro(dimethylsulfide)gold (0.10 mmol) in the same solvent (5 mL) was added, and the reaction mixture was stirred for 30 min and then evaporated under reduced pressure. The solid residue was dissolved in CH_2Cl_2 (1 mL) and the solution was slowly mixed with pentane (10 mL). The obtained precipitate was isolated by decantation and dried in a stream of nitrogen. Crystals for X-ray diffraction analysis were obtained by a slow diffusion of pentane into a CH_2Cl_2 solution of the complex.

Preparation of [AuCl(1a-κ*P*)] (1aAu). The compound was prepared according to the General method. Yield: 69 mg (quantitative), yellow powder.

^{1}H NMR ($CDCl_3$, 399.95 MHz): δ 2.67–2.70 (m, 4 H, CH_2N), 3.74–3.77 (m, 4 H, CH_2O), 3.88–3.92 (m, 4 H, 2 CH of fc), 4.54 (d of vt, *J′* = 3.0, 1.7 Hz, 2 H, CH of fc), 4.70 (vt of d, *J′* = 1.8, 1.1 Hz, 2 H, CH of fc), 7.40–7.52 (m, 6 H, PPh_2), 7.55–7.62 (m, 4 H, PPh_2). $^{13}C\{^{1}H\}$ NMR ($CDCl_3$, 100.58 MHz): δ 49.99 (CH_2N), 55.96 (CH of fc), 65.80 (CH of fc), 66.22 (CH_2O), 67.69 (d, $^{1}J_{PC}$ = 75 Hz, C^{ipso}–P of fc), 71.60 (d, J_{PC} = 9 Hz, CH of fc), 72.54 (d, J_{PC} = 14 Hz, CH of fc), 115.69 (C^{ipso}–N of fc), 128.86 (d, J_{PC} = 12 Hz, CH of PPh_2), 131.17 (d, $^{1}J_{PC}$ = 64 Hz, C^{ipso} of PPh_2), 131.54 (d, $^{4}J_{PC}$ = 3 Hz, CH^{para} of PPh_2), 133.59 (d, J_{PC} = 14 Hz, CH of PPh_2). $^{31}P\{^{1}H\}$ NMR ($CDCl_3$, 161.90 MHz): δ 29.3 (s). ESI+ MS: *m/z* 688.3 ($[M + H]^+$). Anal. Calc. for $C_{26}H_{26}AuClFeNOP$ (687.7): C 45.41, H 3.81, N 2.04%. Found: C 45.13, H 3.58, N 1.85%.

Preparation of [AuCl(1b-κ*P*)] (1bAu). The compound was prepared following the General procedure. Yield: 70 mg (quantitative), yellow powder.

^{1}H NMR ($CDCl_3$, 399.95 MHz): δ 2.70–2.76 (m, 4 H, CH_2S), 2.95–3.00 (m, 4 H, CH_2N), 3.88 (vt, *J′* = 2.0 Hz, 2 H, CH of fc), 3.92 (vt, *J′* = 2.0 Hz, 2 H, CH of fc), 4.53 (d of vt, *J′* = 3.0, 1.9 Hz, 2 H, CH of fc), 4.68 (vt of d, *J′* = 1.8, 1.1 Hz, 2 H, CH of fc), 7.41–7.52 (m, 6 H, PPh_2), 7.54–7.62 (m, 4 H, PPh_2). $^{13}C\{^{1}H\}$ NMR ($CDCl_3$, 100.58 MHz): δ 27.57 (CH_2S), 51.89 (CH_2N), 56.31 (CH of fc), 65.78 (CH of fc), 67.74 (d, $^{1}J_{PC}$ = 75 Hz, C^{ipso}–P of fc), 71.77 (d, J_{PC} = 9 Hz, CH of fc), 72.66 (d, J_{PC} = 14 Hz, CH of fc), 115.48 (C^{ipso}–N of fc), 128.84 (d, J_{PC} = 12 Hz, CH of PPh_2), 131.12 (d, $^{1}J_{PC}$ = 64 Hz, C^{ipso} of PPh_2), 131.51 (d, $^{4}J_{PC}$ = 2 Hz, CH^{para} of PPh_2), 133.56 (d, J_{PC} = 14 Hz, CH of PPh_2). $^{31}P\{^{1}H\}$ NMR ($CDCl_3$, 161.90 MHz): δ 29.3 (s). MALDI+ MS: *m/z* 704.2 ($[M + H]^+$). Anal. Calc. for $C_{26}H_{26}AuClFeNPS$ (703.8): C 44.37, H 3.72, N 1.99%. Found: C 44.58, H 3.44, N 1.82%.

Preparation of [AuCl(1c-κ*P*)] (1cAu). The compound was prepared following the General procedure. Yield: 65 mg (quantitative), yellow powder.

^{1}H NMR ($CDCl_3$, 399.95 MHz): δ 2.48 (s, 6 H, CH_3), 3.80 (vt, *J′* = 2.0 Hz, 2 H, CH of fc), 3.87 (vt, *J′* = 2.0 Hz, 2 H, CH of fc), 4.48 (d of vt, *J* = 3.0, 1.9 Hz, 2 H, CH of fc), 4.69 (vt of d, *J* = 1.9, 1.1 Hz, 2 H, CH of fc), 7.40–7.51 (m, 6 H, PPh_2), 7.54–7.62 (m, 4 H, PPh_2). ^{13}C{^{1}H} NMR ($CDCl_3$, 100.58 MHz): δ 42.03 (CH_3), 56.09 (CH of fc), 65.88 (CH of fc), 67.28 (d, $^{1}J_{PC}$ = 75 Hz, C^{ipso}–P of fc), 71.27 (d, J_{PC} = 10 Hz, CH of fc), 72.44 (d, J_{PC} = 15 Hz, CH of fc), 117.41 (C^{ipso}–N of fc), 128.80 (d, J_{PC} = 12 Hz, CH of PPh_2), 131.33 (d, $^{1}J_{PC}$ = 64 Hz, C^{ipso}–P of PPh_2), 131.47 (d, $^{4}J_{PC}$ = 3 Hz, CH^{para} of PPh_2), 133.56 (d, J_{PC} = 14 Hz, CH of PPh_2). ^{31}P{^{1}H} NMR ($CDCl_3$, 161.90 MHz): δ 29.3 (s). MALDI+ MS: *m/z* 646.0 ([M + H]$^{+}$). Anal. Calc. for $C_{24}H_{24}AuClFeNP$ (645.7): C 44.64, H 3.75, N 2.17%. Found: C 45.03, H 3.72, N 1.97%.

Preparation of [AuCl(2a-κ*P*)] (2aAu). The complex was prepared according to the General procedure and isolated as a yellow powder. Yield: 69 mg (98%).

^{1}H NMR ($CDCl_3$, 400.13 MHz): δ 1.06–2.22 (m, 22 H, PCy_2), 2.88 (br s, 4 H, CH_2N), 3.84 (br s, 4 H, CH_2O), 3.95 (br s, 2 H, CH of fc), 4.08 (br s, 2 H, CH of fc), 4.46 (br s, 2 H, CH of fc), 4.64 (br s, 2 H, CH of fc). ^{13}C{^{1}H} NMR ($CDCl_3$, 100.61 MHz): δ 25.71 (CH_2 of Cy), 26.59 (d, J_{CP} = 3 Hz, CH_2 of Cy), 26.72 (d, J_{CP} = 4 Hz, CH_2 of Cy), 29.79 (CH_2 of Cy), 34.63 (d, $^{1}J_{CP}$ = 36 Hz, CH of Cy), 50.18 (CH_2N), 55.61 (CH of fc), 66.29 (CH of fc), 66.49 (CH_2O), 67.00 (d, $^{1}J_{CP}$ = 61 Hz, C^{ipso}–P of fc), 69.95 (d, J_{CP} = 8 Hz, CH of fc), 71.43 (d, J_{CP} = 11 Hz, CH of fc), 115.48 (C^{ipso}–N of fc). ^{31}P{^{1}H} NMR ($CDCl_3$, 161.98 MHz): δ 41.8. HR MS ESI+, *m/z* calc. for $C_{26}H_{28}AuFeNOP$ ([M – Cl]$^{+}$): 664.1706, found 664.1682. Anal. Calc. for $C_{26}H_{28}AuClFeNOP$ (699.8): C 44.62, H 5.47, H 2.00%. Found: C 44.50, H 5.25, N 2.07%.

Preparation of [AuCl(3a-κ*P*)] (3aAu). The complex was prepared following the General procedure and isolated as a yellow solid. Yield: 65 mg (97%), yellow powder.

^{1}H NMR ($CDCl_3$, 600.17 MHz): δ 2.77 (m, 4 H, CH_2N), 3.81 (m, 4 H, CH_2N), 3.85 (s, 4 H, CH of fc), 4.68 (s, 2 H, CH of fc), 4.81 (s, 2 H, CH of fc), 6.51 (s, 2 H, CH of furyl), 7.05 (m, 2 H, CH of furyl), 7.45 (m, 2 H, CH of furyl). ^{13}C{^{1}H} NMR ($CDCl_3$, 150.91 MHz): δ 50.11 (CH_2N), 55.85 (CH of fc), 65.66 (CH of fc), 66.22 (CH_2O), 71.58 (d, J_{CP} = 11 Hz, CH of fc), 72.88 (d, J_{CP} = 17 Hz, CH of fc), 111.27 (d, J_{CP} = 9 Hz, CH of furyl), 115.87 (C^{ipso}–N of fc), 123.36 (d, J_{CP} = 25 Hz, CH of furyl), 148.84 (d, J_{CP} = 6 Hz, CH of furyl). Note: The signal due to the C^{ipso}–P of fc and furyl were not detected. ^{31}P{^{1}H} NMR ($CDCl_3$, 242.95 MHz): δ −14.0 (s). ESI+ MS: *m/z* 667.0 (*M*$^{+}$). Anal. Calc. for $C_{22}H_{22}AuClFeNO_3P$ (677.7): C 39.58, H 3.32, N 2.10%. Found: C 39.38, H 3.30, N 2.00%.

Preparation of [AuCl(4a-κ*P*)] (4aAu). The compound was prepared following the General procedure. Yield: 69 mg (quantitative), yellow powder.

^{1}H NMR ($CDCl_3$, 399.95 MHz, 50 °C): δ 2.51 (ddd, *J* = 11.4, 6.2, 3.1, 2 H, CH_2N), 2.90 (ddd, *J* = 11.0, 6.7, 2.9 Hz, 2 H, CH_2N), 3.69–3.82 (m, 4 H, CH_2O), 3.94 (dt, *J* = 2.9, 1.5 Hz, 1 H, CH of C_5H_3), 4.19 (s, 5 H, C_5H_5), 4.33 (td, *J* = 2.7, 1.1 Hz, 1 H, CH of C_5H_3), 4.41 (ddd, *J* = 2.8, 2.0, 1.3 Hz, 1 H, CH of C_5H_3), 7.34–7.44 (m, 3 H, PPh_2), 7.45–7.61 (m, 5 H, PPh_2), 7.82–7.90 (m, 2 H, PPh_2). ^{13}C{^{1}H} NMR

($CDCl_3$, 150.93 MHz, 25 °C): δ 55.23 (CH_2N), 61.37 (d, J_{PC} = 6 Hz, CH of C_3H_5), 65.71 (d, $^1J_{PC}$ = 74 Hz, C^{ipso}–P of C_5H_3), 66.57 (CH_2O), 67.98 (d, J_{PC} = 8 Hz, CH of C_3H_5), 69.12 (d, J_{PC} = 5 Hz, CH of C_3H_5), 70.78 (C_5H_5), 117.06 (d, $^2J_{PC}$ = 17 Hz, C^{ipso}–N of C_5H_3), 128.81 (d, J_{PC} = 12 Hz, CH of PPh_2), 128.94 (d, J_{PC} = 12 Hz, CH of PPh_2), 129.80 (d, $^1J_{PC}$ = 66 Hz, C^{ipso} of PPh_2), 131.36 (d, $^4J_{PC}$ = 3 Hz, CH^{para} of PPh_2), 131.89 (d, $^4J_{PC}$ = 3 Hz, CH^{para} of PPh_2), 132.50 (d, $^1J_{PC}$ = 59 Hz, C^{ipso} of PPh_2), 132.89 (d, J_{PC} = 14 Hz, CH of PPh_2), 134.84 (d, J_{PC} = 15 Hz, CH of PPh_2). $^{31}P\{^1H\}$ NMR ($CDCl_3$, 161.90 MHz, 50 °C): δ 22.9 (s). ESI+ MS: *m/z* 684.1 ($[M - Cl + MeOH]^+$). Anal. Calc. for $C_{26}H_{26}AuClFeNOP$ (687.7): C 45.41, H 3.81, N 2.04%. Found: C 45.14, H 3.55, N 1.90%.

Preparation of [AuCl(4b-κ*P*)] (4bAu). The compound was prepared following the General procedure. Yield: 70 mg (quantitative), yellow powder.

^1H NMR ($CDCl_3$, 399.95 MHz): δ 2.65–2.83 (m, 6 H, CH_2N and CH_2S), 3.19–3.28 (m, 2 H, CH_2N), 3.97 (dt, *J* = 2.7, 1.6 Hz, 1 H, CH of C_5H_3), 4.19 (s, 5 H, C_5H_5), 4.33–4.37 (m, 2 H, CH of C_5H_3), 7.36–7.45 (m, 3 H, PPh_2), 7.46–7.56 (m, 3 H, PPh_2), 7.58–7.66 (m, 2 H, PPh_2), 7.85–7.92 (m, 2 H, PPh_2). $^{13}C\{^1H\}$ NMR ($CDCl_3$, 100.58 MHz): δ 27.92 (CH_2S), 57.24 (CH_2N), 61.96 (d, J_{PC} = 6 Hz, CH of C_3H_5), 65.99 (d, $^1J_{PC}$ = 75 Hz, C^{ipso}–P of C_5H_3), 67.94 (d, J_{PC} = 8 Hz, CH of C_3H_5), 68.95 (d, J_{PC} = 4 Hz, CH of C_3H_5), 70.89 (C_5H_5), 118.32 (d, $^2J_{PC}$ = 14 Hz, C^{ipso}–N of C_5H_3), 128.80 (d, J_{PC} = 12 Hz, CH of PPh_2), 128.97 (d, J_{PC} = 12 Hz, CH of PPh_2), 129.62 (d, $^1J_{PC}$ = 66 Hz, C^{ipso}–P of PPh_2), 131.43 (d, $^4J_{PC}$ = 3 Hz, CH^{para} of PPh_2), 131.84 (d, $^4J_{PC}$ = 3 Hz, CH^{para} of PPh_2), 132.30 (d, $^1J_{PC}$ = 59 Hz, C^{ipso}–P of PPh_2), 133.00 (d, J_{PC} = 14 Hz, CH of PPh_2), 134.75 (d, J_{PC} = 15 Hz, CH of PPh_2). $^{31}P\{^1H\}$ NMR ($CDCl_3$, 161.90 MHz, 50 °C): δ 23.4 (s). MALDI+ MS: *m/z* 668.3 ($[M - Cl]^+$). Anal. Calc. for $C_{26}H_{26}AuClFeNOP$ (687.7): C 44.37, H 3.72, N 1.99%. Found: C 44.53, H 3.58, N 1.74%.

Preparation of [AuCl(4c-κ*P*)] (4cAu). The complex was prepared by following the General procedure, resulting as a yellow powdery solid. Yield: 63 mg (95%).

^1H NMR ($CDCl_3$, 399.95 MHz): δ 2.50 (s, 6 H, CH_3), 3.84 (ddd, *J* = 2.7, 2.0, 1.5 Hz, 1 H, CH of C_5H_3), 4.19 (s, 5 H, C_5H_5), 4.30 (td, *J* = 2.7, 1.0 Hz, 1 H, CH of C_5H_3), 4.38 (ddd, *J* = 2.6, 2.0, 1.4 Hz, 1 H, CH of C_5H_3), 7.35–7.62 (m, 8 H, PPh_2), 7.78–7.87 (m, 2 H, PPh_2). $^{13}C\{^1H\}$ NMR ($CDCl_3$, 100.58 MHz): δ 46.71 (CH_3), 60.62 (d, J_{PC} = 7 Hz, CH of C_3H_5), 64.01 (d, $^1J_{PC}$ = 73 Hz, C^{ipso}–P of C_5H_3), 67.30 (d, J_{PC} = 9 Hz, CH of C_3H_5), 69.29 (d, J_{PC} = 6 Hz, CH of C_3H_5), 70.58 (C_5H_5), 118.77 (d, $^2J_{PC}$ = 13 Hz, C^{ipso}–N of C_5H_3), 128.68 (d, J_{PC} = 12 Hz, CH of PPh_2), 128.79 (d, J_{PC} = 11 Hz, CH of PPh_2), 130.33 (d, $^1J_{PC}$ = 65 Hz, C^{ipso}–P of PPh_2), 130.92 (d, $^4J_{PC}$ = 3 Hz, CH^{para} of PPh_2), 131.68 (d, $^4J_{PC}$ = 2 Hz, CH^{para} of PPh_2), 132.29 (d, $^1J_{PC}$ = 60 Hz, C^{ipso}–P of PPh_2), 133.02 (d, J_{PC} = 14 Hz, CH of PPh_2), 134.79 (d, J_{PC} = 15 Hz, CH of PPh_2). $^{31}P\{^1H\}$ NMR ($CDCl_3$, 161.90 MHz): δ 24.6 (s). ESI+ MS: *m/z* 646.0 ($[M + H]^+$). Anal. Calc. for $C_{24}H_{24}AuClFeNP$ (645.7): C 44.64, H 3.75, N 2.17%. Found: C 44.47, H 3.60, N 2.05%.

Preparation of [AuCl(5a-κ*P*)] (5aAu). The compound was prepared according to the General procedure. Yield: 68 mg (97%), yellow powder.

^{1}H NMR ($CDCl_3$, 600.17 MHz): δ 1.15–1.58 (m, 10 H, Cy), 1.66–2.03 (m, 9 H, Cy), 2.01–2.12 (m, 1 H, Cy), 2.34–2.41 (m, 1 H, Cy), 2.47–2.55 (m, 1 H, Cy), 2.74 (ddd, *J* = 11.3, 6.3, 3.1 Hz, 2 H, CH_2N), 3.15 (br s, 2 H, CH_2N), 3.76–3.84 (m, 4 H, CH_2O), 4.29 (td, *J* = 2.8, 1.4 Hz, 1 H, CH of C_5H_3), 4.35 (s, 5 H, C_5H_5), 4.37 (td, *J* = 2.7, 1.1 Hz, 1 H, CH of C_5H_3), 4.45 (dt, *J* = 2.5, 1.2 Hz, 1 H, CH of C_5H_3). ^{13}C{^{1}H} NMR ($CDCl_3$, 150.91 MHz): δ 25.70 (d, J_{CP} = 2 Hz, CH_2 of Cy), 25.80 (d, J_{CP} = 2 Hz, CH_2 of Cy), 26.72 (d, J_{CP} = 14 Hz, CH_2 of Cy), 26.83 (d, J_{CP} = 12 Hz, CH_2 of Cy), 27.01 (d, J_{CP} = 1 Hz, CH_2 of Cy), 27.11 (CH_2 of Cy), 29.17 (CH_2 of Cy), 30.52 (CH_2 of Cy), 31.24 (d, J_{CP} = 3 Hz, CH_2 of Cy), 31.94 (d, J_{CP} = 2 Hz, CH_2 of Cy), 35.03 (d, $^{1}J_{CP}$ = 36 Hz, CH of Cy), 36.06 (d, $^{1}J_{CP}$ = 35 Hz, CH of Cy), 53.42 (CH_2N), 63.73 (d, J_{CP} = 5 Hz, CH of C_5H_3), 63.75 (d, $^{1}J_{CP}$ = 57 Hz, C^{ipso}–P of C_5H_3), 67.14 (CH_2O), 67.53 (d, J_{CP} = 9 Hz, CH of C_5H_3), 70.60 (d, J_{CP} = 13 Hz, CH of C_5H_3), 70.85 (C_5H_5), 115.65 (d, $^{1}J_{CP}$ = 5 Hz, C^{ipso}–N of C_5H_3). ^{31}P{^{1}H} NMR ($CDCl_3$, 242.95 MHz): δ 43.3 (s). ESI+ MS: *m*/*z* 699.4 (M^+). Anal. Calc. for $C_{26}H_{38}AuClFeNOP \cdot 0.5CH_2Cl_2$ (742.3): C 42.88, H 5.30, N 1.89%. Found: C 42.96, H 5.23, N 1.81%.

Preparation of [AuCl(6a-κ*P*)] (6aAu). The compound was prepared following the General procedure. Yield: 63 mg (95%), yellow powder.

^{1}H NMR ($CDCl_3$, 600.17 MHz): δ 2.52-2.65 (m, 2 H, CH_2N), 2.81-2.95 (m, 2H, CH_2N), 3.84-3.93 (m, 2 H, CH_2O), 3.94-4.02 (m, 2 H, CH_2O), 4.16 (s, 5 H, C_5H_5), 4.34 (s, 1 H, CH of C_5H_3), 4.36 (s, 1 H, CH of C_5H_3), 4.52 (s, 1 H, CH of C_5H_3), 6.41 (m, 1 H, CH of furyl), 6.61 (m, 1 H, CH of furyl), 6.92 (m, 1 H, CH of furyl), 7.33 (m, 1 H, CH of furyl), 7.64 (m, 1 H, CH of furyl), 7.85 (m, 1 H, CH of furyl). ^{13}C{^{1}H} NMR ($CDCl_3$, 150.91 MHz): δ 55.41 (d, J_{CP} = 11Hz, CH_2N), 60.15 (d, $^{2}J_{CP}$ = 7 Hz, CH of C_5H_3), 66.57 (CH of C_5H_3), 68.38 (d, $^{3}J_{CP}$ = 9 Hz, CH of C_5H_3), 69.64 (d, J_{CP} = 4 Hz, CH_2O), 70.85 (C_5H_5), 111.14 (d, $^{3}J_{CP}$ = 9 Hz, CH^4 of furyl), 111.37 (d, $^{3}J_{CP}$ = 10 Hz, CH^4 of furyl), 122.52 (d, $^{2}J_{CP}$ = 24 Hz, CH^3 of furyl), 124.59 (d, $^{2}J_{CP}$ = 28 Hz, CH^3 of furyl), 148.78-149.01 (m, CH^5 of furyl). The signals due to C^{ipso} at C_5H_3 and the furyl groups were not observed. ^{31}P{^{1}H} NMR ($CDCl_3$, 242.95 MHz): δ –25.5 (s). ESI+ MS: *m*/*z* 667.0 (M^+). Anal. Calc. for $C_{22}H_{22}AuClFeNO_3P \cdot ½CH_2Cl_2$ (710.1): C 38.06, H 3.26, N 1.97%. Found: C 37.99, H 2.83, N 2.13%.

Gold-catalyzed cyclization of *N*-propargylbenzamide. In a glass vial, *N*-propargylbenzamide (31.8 mg, 0.20 mmol) and a gold(I) complex (2.0 μmol) were dissolved in CD_2Cl_2 (0.50 mL). The obtained solution was transferred into the NMR tube and mixed with a stock solution of silver(I) bis(triflimide) (0.34 mL of 5.98 mM $AgNTf_2$, 2.0 μmol). The contents of the NMR tube were mixed, and the tube was inserted into the NMR spectrometer, where the solution was monitored continuously for 6 h (the ^{1}H NMR spectra were recorded every 10 minutes) at 25 °C. Yields were determined from the ratio of the NMR signal due to the CH_2 groups of the product (δ_H 4.65) and the starting material (δ_H 4.25).

Analytical data for **14**. ^{1}H NMR ($CDCl_3$, 300 MHz): δ 2.28 (t, *J* = 2.5 Hz, 1 H), 4.25 (dd, *J* = 2.5 Hz, 5.1 Hz, 2 H), 6.35-6.50 (bs, 1 H), 7.40-7.46 (m, 2 H), 7.48-7.53 (m, 1 H), 7.79 (d, J = 7.0 Hz, 2 H). Analytical data for **15**. ^{1}H NMR ($CDCl_3$, 300 MHz): δ 4.36 (q, *J* = 2.7 Hz, 1 H), 4.65 (t, *J* = 2.9 Hz, 2 H),

4.81 (q, *J* = 3.0 Hz, 1 H) 7.40-7.47 (m, 2 H) 7.47-7.54 (m, 1 H), 7.94-8.01 (m, 2 H). The data match those in the literature.[4]

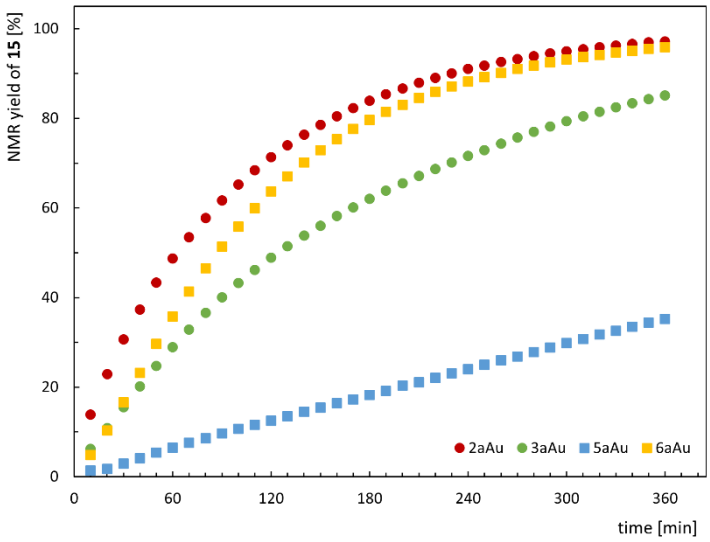

Figure S1. Kinetic profiles for the Au-catalyzed cyclisation of *N*-propargylbenzamide (**14**). The reaction was performed at 25 °C in CD_2Cl_2 in the presence of 1 mol% of Au catalyst. The data are the average of two independent runs. Note: 1.5 equiv. of $AgNTf_2$ were used for activation of complexes **3aAu**, **5aAu** and **6aAu**, that were otherwise inactive.

Gold-catalyzed oxidative cyclization of phenylacetylene with acetonitrile using pyridine *N*-oxide as an oxidant. A Schlenk flask equipped with a magnetic stirring bar was charged with pyridine *N*-oxide (30.9 mg, 0.33 mmol), the respective gold(I) complex (13.0 µmol), and $AgNTf_2$ (4.9 mg, 13.0 µmol), and the solid educts were dissolved in anhydrous MeCN (2.5 mL). Phenylacetylene (27 µL, 0.25 mmol) was introduced, and the resulting mixture was stirred at 60 °C for 24 h. Next, the mixture was allowed to cool to room temperature, and anisole (27 µL, 0.25 mmol) was added as an internal standard. An aliquot (0.1 mL) was withdrawn, filtered through a PTFE syringe filter into an NMR tube, and diluted with $CDCl_3$ (0.5 mL). The solution was analyzed by ^{1}H NMR. The NMR yield was determined by comparing the intensity of the signals due to the methyl groups of anisole (δ_H 3.75) and the product (δ_H 2.35). Once the reaction had finished, the mixture was concentrated under vacuum, and the cyclization product was isolated by column chromatography on silica gel using a cyclohexane/ethyl acetate mixture (83:17) as the eluent.

Analytical data for 5-methyl-2-phenyl-oxazole (**17**). ^{1}H NMR ($CDCl_3$, 300 MHz): δ 2.39 (s, 3 H, CH_3), 6.87 (s, 1 H, CH), 7.41–7.46 (m, 3 H, CH of Ph), 8.02–8.04 (m, 2H, CH of Ph). The analytical data correspond with those reported in the literature.[6]

X-ray crystallography

Full-set diffraction data were collected with a Bruker D8 VENTURE Kappa Duo instrument equipped with a PHOTON 100 detector and a Cryostream Cooler. The data for **1b** and **8** were recorded using CuKα radiation (λ = 1.54178 Å). In all other cases, Mo Kα radiation (λ = 0.71073 Å) was utilized. The structures were solved by direct methods using SHELXT-2014/2018[7] and subsequently refined with SHELXL-2014/2017.[8] The non-hydrogen atoms were refined with anisotropic displacement parameters. All hydrogen atoms were included in their calculated positions and refined as riding atoms with U_{iso}(H) set to 1.2U_{eq}(C), using the standard parameters implemented in SHELXL. Structure-specific details are as follows.

One of the P-bound phenyl groups in the structure of **4a** exhibited a disorder. This group was refined as a regular hexagon over two positions in a 53:47 ratio. The phenyl groups in the structure of **1aAu** were also disordered and were modelled over two positions for most atoms. The refined occupancies were 63:37 and 57:43 for the rings C(12-16) and C(17-22), respectively. In addition, the disordered atoms had to be refined with displacement parameters approximating isotropic behavior (ISOR command in SHELXL). A disorder also affected the tetrafluoroborate anion in the struture of **10Me[BF_4]**. The anion was refined with two positions for three of its fluorine atoms (i.e., it appeared disordered by rottation along the B1−F4 bond) in approximately 60:40 ratio. ISOR command was applied to some of the disordered fluorine atoms.

Compound **4b** crystallized as an inversion twin (space group *Pca*2_1). The refined contributions from the two enantiomeric domains were ≈93:9. The related Au(I) complex **4bAu** crystallized as a two-component non-merohedral twin space (group *P*−1) with approximately equally populated domains (≈50:50).

Furthermore, the solvent molecule in the structure of **2aAu**·CH_2Cl_2 was partly disordered and had to be refined with the chlorine atoms distributed over two positions in a 53:47 ratio. Complex **5aAu** also crystallized as a dichloromethane solvate **5aAu**·½$CHCl_2$ with the solvent molecules extensively disordered within the structure voids. The contribution of the disordered solvent to the overall scattering was numerically eliminated using PLATON/SQUEEZE.[9] In total, 35 electrons were removed per the unit cell (triclinic, *P*−1), which approximately matches the expected value (48 electrons).

Selected crystallographic data and structure refinement parameters are presented in Table S1. All geometric data and structural diagrams were obtained using a recent version of the PLATON program.[10] The numerical values were rounded to one decimal place with respect to their standard deviations. Complete crystallographic data were deposited with the Cambridge Crystallographic Data Centre (CCDC) and can be accessed *via* www.ccdc.cam.ac.uk/structures. The deposition numbers are quoted in Table S1.

Table S1. Selected crystallographic data and structure refinement parameters.[a]

Compound	**1a**	**1b**	**1c**
Formula	$C_{26}H_{26}FeNOP$	$C_{26}H_{26}FeNPS$	$C_{24}H_{24}FeNP$
M	455.30	471.36	413.26
Crystal system	orthorombic	monoclinic	monoclinic
Space group	*Pbca* (no. 61)	$P2_1/c$ (no. 14)	$P2_1/c$ (no. 14)
T [K]	120(2)	150(2)	150(2)
a [Å]	17.2028(9)	9.9729(4)	15.0255(4)
b [Å]	9.3853(5)	15.2520(7)	11.5476(3)
c [Å]	26.593(1)	14.9371(6)	12.0575(4)
α [°]	90	90	90
β [°]	90	107.388(3)	109.175(1)
γ [°]	90	90	90
V [Å]^3	4293.6(4)	2168.2(2)	1976.0(1)
Z	8	4	4
F(000)	1904	984	864
μ(Mo Kα) [mm^{-1}]	0.795	7.265	0.852
Diffrns collected	38420	23509	30743
Independent diffrns	4924	4279	4529
Observed diffrns[a]	3926	3344	4377
R_{int}[b] [%]	5.30	8.91	1.82
No. of parameters	271	271	246
R[b] obsd diffrns [%]	4.14	4.17	2.21
wR[b] all data [%]	9.75	9.01	6.04
S[c]	1.053	1.015	1.054
Δρ [e Å^{-3}]	0.74, –0.36	0.34, –0.42,	0.31, –0.25,
CCDC deposition no.	2517192	2517197	2517196

[a] Diffractions with $I > 2\sigma(I)$. [b] Definitions: $R_{int} = \Sigma \left| F_o^2 - F_o^2(\text{mean}) \right| / \Sigma F_o^2$, where F_o^2(mean) is the average intensity of symmetry-equivalent diffractions. $R = \Sigma \left| \left| F_o \right| - \left| F_c \right| \right| / \Sigma \left| F_o \right|$, $wR = [\Sigma\{w(F_o^2 - F_c^2)^2\}/\Sigma w(F_o^2)^2]^{1/2}$. [c] Goodness of fit, $S = \{\Sigma[w(F_o^2 - F_c^2)^2]/(n - p)\}^{½}$, where n is the number of diffractions used for the refinement and p is the total number of refined parameters.

Table S1 continued

Compound	**1aS**	**2a**	**3a**
Formula	$C_{26}H_{26}FeNOPS$	$C_{26}H_{38}FeNOP$	$C_{22}H_{22}FeNO_3P$
M	487.36	467.39	435.22
Crystal system	orthorhombic	monoclinic	monoclinic
Space group	*Pbca* (no. 61)	$P2_1/n$ (no. 14)	$P2_1/c$ (no. 14)
T [K]	120(2)	150(2)	120(2)
a [Å]	18.0566(8)	6.0188(5)	10.3068(4)
b [Å]	9.2923(5)	10.3743(8)	8.2551(3)
c [Å]	26.486(1)	37.385(3)	22.7564(9)
α [°]	90	90	90
β [°]	90	90.447(3)	90.595(1)
γ [°]	90	90	90
V [Å]^3	4443.9(4)	2334.3(3)	1936.1(1)
Z	8	4	4
F(000)	2032	1000	904
μ(Mo Kα) [mm^{-1}]	0.864	0.733	0.885
Diffrns collected	45693	26872	43568
Independent diffrns	5109	5346	4418
Observed diffrns[a]	4433	5026	4218
R_{int}[b] [%]	4.06	2.54	2.72
No. of parameters	280	271	253
R[b] obsd diffrns [%]	3.86	3.64	2.45
wR[b] all data [%]	8.18	8.38	6.64d
S[c]	1.118	1.210	1.034
Δρ [e Å^{-3}]	0.72, –0.56	0.36, –0.27	0.33, –0.33
CCDC deposition no.	2517193	2517194	2517195

Table S1 continued

Compound	**4a**	**4b**	**5a**
Formula	$C_{26}H_{26}FeNOP$	$C_{26}H_{26}FeNPS$	$C_{26}H_{38}FeNOP$
M	455.30	471.36	467.39
Crystal system	orthorhombic	orthorhombic	monoclinic
Space group	*Pbca* (no. 61)	*P*ca2$_1$ (no. 29)	*P*2$_1$/c (no. 14)
T [K]	120(2)	120(2)	120(2)
a [Å]	15.201(2)	15.766(1)	19.3758(7)
b [Å]	14.255(1)	19.195(2)	10.1323(4)
c [Å]	19.957(2)	14.390(1)	12.2398(5)
α [°]	90	90	90
β [°]	90	90	102.565(1)
γ [°]	90	90	90
V [Å]^3	4324.4(8)	4354.7(6)	2345.4(2)
Z	8	8	4
F(000)	1904	1968	1000
μ(Mo Kα) [mm^{-1}]	0.789	0.876	0.729
Diffrns collected	243017	93850	64755
Independent diffrns	6300	9993	5822
Observed diffrns[a]	5895	9740	5553
R_{int}[b] [%]	3.32	3.00	3.02
No. of parameters	302	542	271
R[b] obsd diffrns [%]	2.46	2.29	2.28
wR[b] all data [%]	6.76	5.98	6.07
S[c]	1.058	1.047	1.022
Δρ [e Å^{-3}]	–0.26, 0.44	0.63, –0.19	0.35, –0.25
CCDC deposition no.	2517203	2517206	2517204

Table S1 continued

Compound	**6a**	**1aAu**	**1bAu**
Formula	$C_{22}H_{22}FeNO_3P$	$C_{26}H_{26}AuClFeNOP$	$C_{26}H_{26}AuClFeNPS$
M	435.22	687.71	703.77
Crystal system	triclinic	monoclinic	monoclinic
Space group	P–1 (no. 2)	$P2_1/c$ (no. 14)	$P2_1/n$ (no. 14)
T [K]	120(2)	130(2)	120(2)
a [Å]	9.3802(3)	15.1704(9)	9.6322(2)
b [Å]	10.1241(4)	13.789(8)	19.2608(4)
c [Å]	10.3269(4)	11.3953(6)	13.0816(2)
α [°]	100.938(1)	90	90
β [°]	93.135(1)	91.084(2)	99.414(1)
γ [°]	97.712(1)	90	90
V [Å]^3	950.9(6)	2381.5(2)	2394.3(8)
Z	2	4	4
F(000)	452	1336	1368
μ(Mo Kα) [mm^{-1}]	0.901	6.961	7.008
Diffrns collected	43924	23927	34644
Independent diffrns	5553	5473	5468
Observed diffrns[a]	5454	5109	5400
R_{int}[b] [%]	2.36	2.19	2.45
No. of parameters	253	355	289
R[b] obsd diffrns [%]	2.15	1.58	1.45
wR[b] all data [%]	5.93	3.41	3.39
S[c]	1.048	1.098	1.105
Δρ [e Å^{-3}]	0.42, –0.31	0.56–0.70	0.77, –0.70
CCDC deposition no.	2517205	2517198	2517202

Table S1 continued

Compound	**1cAu**	**2aAu·CHCl$_3$**	**3aAu**
Formula	$C_{24}H_{24}AuClFeNP$	$C_{27}H_{39}AuCl_4FeNOP$	$C_{22}H_{22}AuClFeNO_3P$
M	645.68	819.18	667.64
Crystal system	triclinic	monoclinic	monoclinic
Space group	*P*–1 (no. 2)	$P2_1/n$ (no. 14)	$P2_1/n$ (no. 14)
T [K]	150(2)	120(2)	120(2)
a [Å]	10.2998(4)	10.1180(3)	8.8936(3)
b [Å]	11.2164(4)	23.6712(9)	11.0024(3)
c [Å]	22.2753(7)	12.7592(4)	22.6977(7)
α [°]	78.599(1)	90	90
β [°]	77.682(1)	100.560(1)	99.410(1)
γ [°]	62.824(1)	90	90
V [Å]^3	2221.7(1)	3004.1(2)	2191.1(1)
Z	4	4	4
F(000)	1248	1616	1288
μ(Mo Kα) [mm^{-1}]	7.452	5.792	7.569
Diffrns collected	51605	47570	31993
Independent diffrns	10171	6865	5023
Observed diffrns[a]	9934	6773	4880
R_{int}[b] [%]	3.06	1.82	2.37
No. of parameters	527	344	271
R[b] obsd diffrns [%]	1.51	1.70	1.44
wR[b] all data [%]	3.75	4.03	3.23
S[c]	1.128	1.081	1.089
Δρ [e Å^{-3}]	0.73, –0.72	1.19, –1.28	–0.62, 0.56
CCDC deposition no.	2517201	2517199	2517200

Table S1 continued

Compound	**4aAu**	**4bAu**·$2CH_2Cl_2$	**4cAu**
Formula	$C_{26}H_{26}AuClFeNOP$	$C_{28}H_{30}AuCl_5FeNPS$	$C_{24}H_{24}AuClFeNP$
M	687.71	873.62	645.68
Crystal system	monoclinic	triclinic	triclinic
Space group	$P2_1/c$ (no. 14)	$P\bar{1}$ (no. 2)	$P\bar{1}$ (no. 2)
T [K]	120(2)	120(2)	120(2)
a [Å]	9.7338(5)	9.511(1)	9.7832(5)
b [Å]	13.0064(7)	17.971(2)	10.5794(5)
c [Å]	19.357(1)	19.045(3)	11.4784(6)
α [°]	90	108.334(4)	72.733(2)
β [°]	100.267(2)	92.424(5)	80.170(2)
γ [°]	90	92.944(5)	72.030(2)
V [Å]^3	2411.4(2)	3079.9(7)	1075.0(1)
Z	4	4	2
F(000)	1336	1704	624
μ(Mo Kα) [mm^{-1}]	6.875	5.803	7.700
Diffrns collected	103640	27727	55525
Independent diffrns	7038	27727	6248
Observed diffrns[a]	6822	25127	6198
R_{int}[b] [%]	2.66	5.34	5.77
No. of parameters	289	686	264
R[b] obsd diffrns [%]	1.41	3.80	1.55
wR[b] all data [%]	3.30	10.7	4.09
S[c]	1.121	1.028	1.159
Δρ [e Å^{-3}]	0.91, –0.52	2.33, –1.09	0.99, –1.00
CCDC deposition no.	2517207	2517210	2517209

Table S1 continued

Compound	**5aAu·½CH$_2$Cl$_2$**	**8**
Formula	$C_{26.5}H_{39}AuCl_2FeNOP$	$C_{22}H_{20}FeNPS$
M	742.27	417.27
Crystal system	triclinic	triclinic
Space group	*P*–1 (no. 2)	*P*–1 (no. 2)
T [K]	120(2)	120(2)
a [Å]	10.5333(3)	9.3036(4)
b [Å]	11.7347(4)	9.4666(4)
c [Å]	13.1950(4)	11.2315(5)
α [°]	99.359(1)	73.973(1)
β [°]	104.167(1)	88.758(1)
γ [°]	114.437(1)	78.416(1)
V [Å]^3	1373.9(7)	930.78(7)
Z	2	2
F(000)	734	432
μ(Mo Kα) [mm^{-1}]	6.134	8.383
Diffrns collected	30432	13587
Independent diffrns	6283	3522
Observed diffrns[a]	6155	3501
R_{int}[b] [%]	2.10	2.60
No. of parameters	289	235
R[b] obsd diffrns [%]	1.27	2.65
wR[b] all data [%]	3.04	6.79
S[c]	1.047	1.060
Δρ [e Å^{-3}]	0.55, –0.41	–0.33, 0.36
CCDC deposition no.	2517208	2517404

Table S1 continued

Compound	**10**	**(10Me)[BF_4]**	**12a**
Formula	$C_{14}H_{17}FeNO$	$C_{15}H_{20}BF_4FeNO$	$C_{14}H_{16}BrFeNO$
M	271.13	372.98	350.04
Crystal system	monoclinic	monoclinic	monoclinic
Space group	$P2_1/c$ (no. 14)	$P2_1/c$ (no. 14)	$P2_1/c$ (no. 14)
T [K]	120(2)	100(2)	120(2)
a [Å]	15.4561(7)	8.3381(5)	10.3806(5)
b [Å]	10.0553(4)	9.6955(5)	9.2842(4)
c [Å]	7.8796(3)	18.900(1)	27.334(1)
α [°]	90	90	90
β [°]	104.080(2)	90.750(2)	91.979(2)
γ [°]	90	90	90
V [Å]^3	1187.82(9)	1527.8(2)	2632.7(2)
Z	4	4	8
F(000)	568	768	1408
μ(Mo Kα) [mm^{-1}]	1.251	1.032	4.167
Diffrns collected	20474	34808	54119
Independent diffrns	2718	3780	6026
Observed diffrns[a]	2552	3730	5896
R_{int}[b] [%]	2.21	2.50	2.31
No. of parameters	154	237	325
R[b] obsd diffrns [%]	2.22	4.55	1.65
wR[b] all data [%]	5.66	9.82	4.27
S[c]	1.067	1.208	1.056
Δρ [e Å^{-3}]	0.44, −0.33	1.06, −0.81	0.37, −0.42
CCDC deposition no.	2517190	2522540	2517191

Compound **8** crystallizes with the symmetry of the common[11] triclinic space group *P*–1 (Figure S2). The 1,1′-disubstituted ferrocene unit in its structure assumes an approximately 1,3′ conformation[12] as indicated by the torsion angle τ of −139.7(1)° (τ is the torsion angle C1-Cg1-Cg2-C6, where Cg1 and Cg2 are the centroids of the cyclopentadienyl rings C(1-5) and C(6-10), respectively). The Fe1-C(1-10) distances range 2.038(2)-2.084(2) Å, and the dihedral angle between the least-squares cyclopentadienyl planes is 3.14(9)°. However, while the C(6-10) ring is practically ideally planar (within 0.001 Å), the N-substituted cyclopentadienyl ring is distorted toward an envelope with the C1 atom displaced by 0.028(2) Å from the plane of the remaining atoms C(2-5). This feature is common to the structures of 1′-phosphinoferrocene-1-amines and their complexes reported in this study (*vide infra*). It can also be detected in the structure of aminoferrocene as the simplest representative of this class of compounds, although it wasn't noticed there (*cf*. Fe-C(N) 2.097(3) Å *vs*. 2.028(4)-2.061(4) Å for the remaining ring carbon atoms).[13]

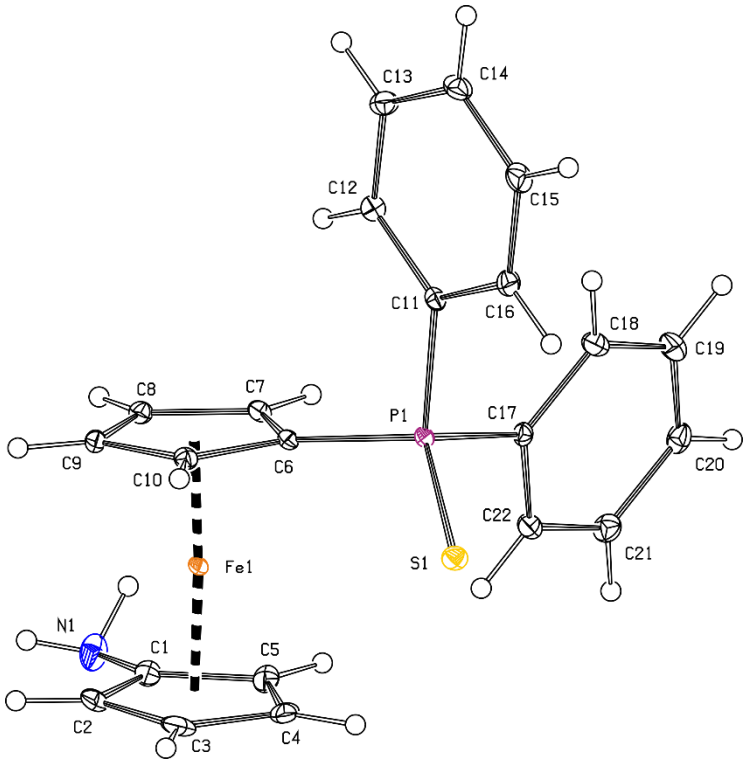

Figure S2. PLATON plot of the molecular structure of **8**. Displacement ellipsoids enclose the 30% probability level. Selected distances and angles (in Å and deg): C1-N1 1.400(2), P1-S1 1.9657(5), P1-C6 1.784(2), P1-C11 1.821(2), P1-C17 1.817(2), C6-P1-C11 104.56(7), C6-P1-C17 106.15(8), C11-P1-C17 104.66(7), S1-P1-C6 115.05(5), S1-P1-C11 112.45(5), S1-P1-C17 113.05(5).

The diphenylthiophosphoryl group in the structure of **8** has the usual tetrahedral arrangement. One phenyl ring is directed above the ferrocene unit and the other to its side, pointing toward the NH_2 substituent. This situation can be illustrated by the angles subtended by

the Cg1-Cg2 vector and the P1-C11 and P1-C17 bonds of −173.33(5)° and 76.93(6)°, respectively. The P-C and P-S distances fall within the usual ranges.[14]

4-Ferrocenylmorpholine (**10**) crystallizes in the monoclinic space group $P2_1/c$ with one molecule in the asymmetric unit (Figure S3). The dihedral angle subtended by the mean cyclopentadienyl planes is only 1.31(8)°. However, such a small tilt angle does not fully correspond to the variation in the individual Fe1-C(1-10) distances, which range from 2.036(1) Å (C3) to 2.088(1) Å (C1). While the carbon atoms in the non-substituted cyclopentadienyl ring are coplanar within 0.004 Å, only the carbon atoms C(2-4) form a plane with similar parameters (within 0.001 Å), from which the pivotal atom C1 is displaced by 0.032(1) Å. In other words, compound **10** exhibits the same structural distortion as observed in the structure of aminoferrocene and compound **8**. The morpholine moiety adopts a chair conformation with the ring puckering parameter[15] θ = 4.3(1)° near the ideal value (θ = 0/180°) and the pivotal C1-N1 bond in an equatorial position. The C1-N1 distance of 1.409(2) Å is similar to that in 4-phenylmorpholine[16] (1.411 Å, value from the Cambridge Structure Database,[17] CCDC entry: 2214385).

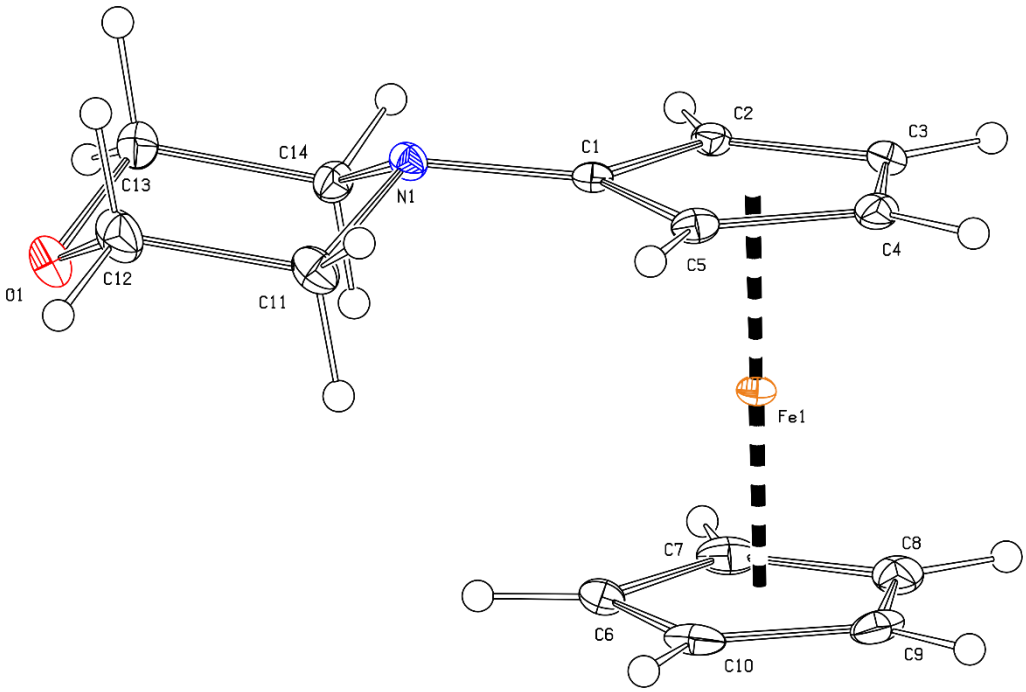

Figure S3. PLATON plot of the molecular structure of **10** showing displacement ellipsoids at the 30% probability level.

Compound **(10Me)[BF$_4$]** also crystallizes with the symmetry of the space group $P2_1/c$ and with a partially disordered tetrafluoroborate anion (Figure S4). Importantly, the ferrocene unit in this structure does not exhibit the characteristic deformation observed for the parent amine **10**.

The Fe1-C(1-10) distances range from 2.005(2) Å to 2.056(3) Å, and the dihedral angle between the least-squares cyclopentadienyl planes is 2.6(2)°; the shortest Fe-C distances is determined for the C1 atom bearing the ammonium group. The angles around N1 are approximately tetrahedral (107.3(2)-110.7(2)°) and the morpholinyl group retains a chair conformation (θ = 4.4(2)°). Compared to **10**, however, the morpholinyl group in the salt is rotated from the plane of the bonding cyclopentadienyl ring. This rotation can be illustrated by the angles between the vectors defined by atoms C11/C14 and C2/5, which are 117.9(1)° for **(10Me)[BF_4]** and 179.59(8)° for **10**. The changed conformation in the ammonium salt can be explained by the lack of conjugation between the lone pair at N1 and the cyclopentadienyl ring, albeit steric factors and solid-state effects can also play a role (the ferrocene and morpholinyl CH groups are involved in weak hydrogen bonding interactions with the anion). Correspondingly, the C1-N1 bond in **(10Me)[BF_4]** (1.477(3) Å) is longer than in the parent amine **10** (C1-N1 1.409(2) Å).

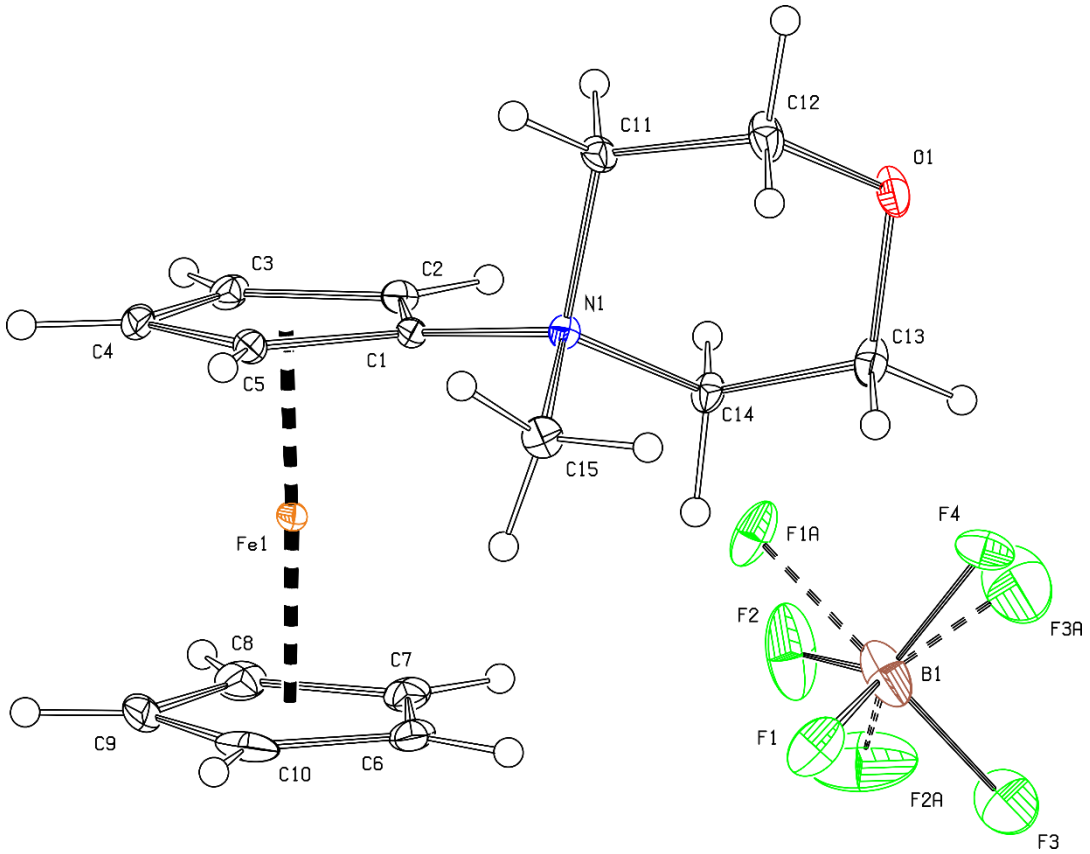

Figure S4. PLATON plot of the molecular structure of **(10Me)[BF_4]** showing displacement ellipsoids at the 30% probability level.

The crystal structure of 1-bromo-1′-(4-morpholinyl)ferrocene (**12a**) contains two crystallographically independent molecules that slightly differ in the tilting of the ferrocene cyclopentadienyl rings and mutual orientation of the attached substituents (Figure S5, parameters in Table S2). Even in the structure of **12a**, the C1 (C21 in molecule 2) atoms are displaced by

approximately 0.05 Å from the plane defined by the four remaining ring atoms [C(2-5) and C(22-25)]. The morpholinyl groups retain their usual geometry and chair conformation (θ = 178.0(1)° and 178.5(1)° for molecules 1 and 2, respectively).

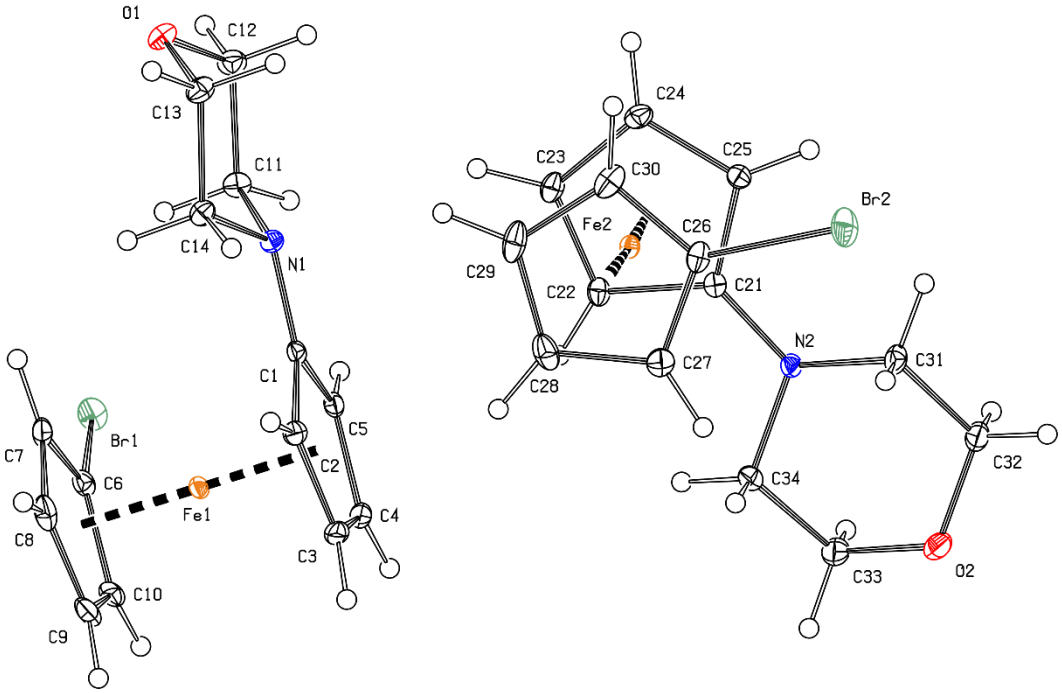

Figure S5. PLATON plot of the molecular structure of **12a** showing displacement ellipsoids at the 30% probability level.

Table S2. Selected distances and angles for **12a** (in Å and deg).[a]

Parameter	Molecule 1	Parameter	Molecule 2
Fe1-C(1-10)	2.020(1)-2.102(1)	Fe2-C(21-30)	2.015(1)-2.105(1)
tilt	1.32(8)	tilt	4.79(8)
τ	71.5(1)	τ	64.4(1)
C1-N1	1.397(2)	C21-N2	1.397(2)
C6-Br1	1.887(1)	C26-Br2	1.888(1)

[a] Tilt is the dihedral angle of the least-squares cyclopentadienyl planes, and τ is the torsion angle C1-Cg1-Cg2-C6, where Cg1 and Cg2 are the centroids of the cyclopentadienyl rings C(1-5) and C(6-10) in molecule 1 and similarly in molecule 2.

The molecular structures of phosphinoamines **1a-c**, **2a**, and **3a** are generally similar (Figures S6 and S7; geometric data in Table S3). All compounds exhibit the characteristic distortion of the ferrocene unit, involving a bending of the nitrogen-substituted carbon atom C1 out of the plane of the substituted cyclopentadienyl ring, away from the iron center. However, this

distortion varies in extent, as exemplified by the perpendicular distance (Δ) of atom C1 from the plane defined by the remaining ring carbon atoms C(2-5), which are otherwise coplanar within 0.001 Å in all structures. The largest displacement (0.045(2) Å) is observed for the morpholine derivative **1a**, while the other compounds show a smaller distance of approximately 0.03 Å. The cyclopentadienyl-bound nitrogen atoms are pyramidal, and the (thio)morpholinyl groups adopt chair conformations and bind in equatorial positions. The parameters describing the (thio)morpholine moieties are unexceptional in view of those determined for compound **10**.

In all the structures, one P-C(Ph/Cy/Fur) bond is directed above the ferrocene unit, and the other to the side (*cf*. the structure of **8**). This leads to two possible arrangements that differ in the positioning of the phosphorus lone pair, which is either directed toward the nitrogen substituent (**1c** and **2a**) or away from it (all other compounds); the C-P-C angles vary only marginally in the entire series. The planes of the flat phenyl and 2-furyl groups subtend dihedral angles of 75.2(1)° in **1a**, 86.3(1)° in **1b**, 75.01(7)° in **1c**, and 63.42(7)° in **3a**. The cyclohexyl groups in **2a** have chair conformations [θ = 177.5(2)° for C(11-16), and 0.0(2)° for C(17-22)] with the P-C bonds in the equatorial positions. The arrangement of the respective phosphine substituents is similar to that in (diphenylphosphino)ferrocene[18] or functional di(2-furyl)-[19] and (dicyclohexyl)-phosphinoferrocenes.[20] The compounds differ mainly by the orientation of the substituents: the conformation of the 1,1′-disubstituted ferrocene unit can be described as approximately 1,2′ for **1a** and **1c**, 1,3′ for **2a** and **1b**, and an intermediate conformation for **3a**.

Table S3. Selected distances and angles for phosphines **1a-c**, **2a**, and **3a** (in Å and deg).[a]

Parameter	**1a**	**2a**	**3a**	**1b**	**1c**
Fe1-C(1-10)	2.024(2)-2.106(2)	2.035(2)-2.094(2)	2.036(1)-2.102(1)	2.037(3)-2.095(3)	2,036(1)-2.098(1)
tilt	5.4(1)	3.1(1)	1.40(7)	1.3(2)	0.96(7)
Δ	0.045(2)	0.029(2)	0.031(1)	0.030(3)	0.037(1)
τ	−85.6(2)	148.0(1)	−111.35(8)	−147.9(2)	−78.34(9)
C1-N1	1.404(3)	1.412(2)	1.395(2)	1.414(4)	1.394(2)
θ	176.9(2)	180.0(2)	178.3(1)	4.2(2)	n.a.
C6-P1	1.814(2)	1.825(2)	1.813(1)	1.817(3)	1.812(1)
P1-C11	1.839(2)	1.868(2)	1.810(1)	1.845(3)	1.835(1)
P1-C17	1.831(2)	1.862(2)	1.808(1)	1.838(3)	1.838(1)
C6-P1-C11	100.79(9)	101.13(9)	100.36(5)	100.6(1)	103.71(5)
C6-P1-C17	101.81(9)	101.28(8)	102.38(5)	102.7(1)	102.14(5)
C11-P1-C17	100.36(9)	103.10(9)	100.66(5)	99.6(1)	99.88(5)

[a] Tilt is the dihedral angle of the least-squares cyclopentadienyl planes, and τ is the torsion angle C1-Cg1-Cg2-C6, where Cg1 and Cg2 are the centroids of the cyclopentadienyl rings C(1-5) and C(6-10) in molecule 1. Δ is the distance of C1 from the least-squares plane defined by the remaining ring carbon atoms C(2-5), and θ is the ring puckering parameter describing the conformation of the (thio)morpholinyl group (values in degrees). n.a. = not applicable.

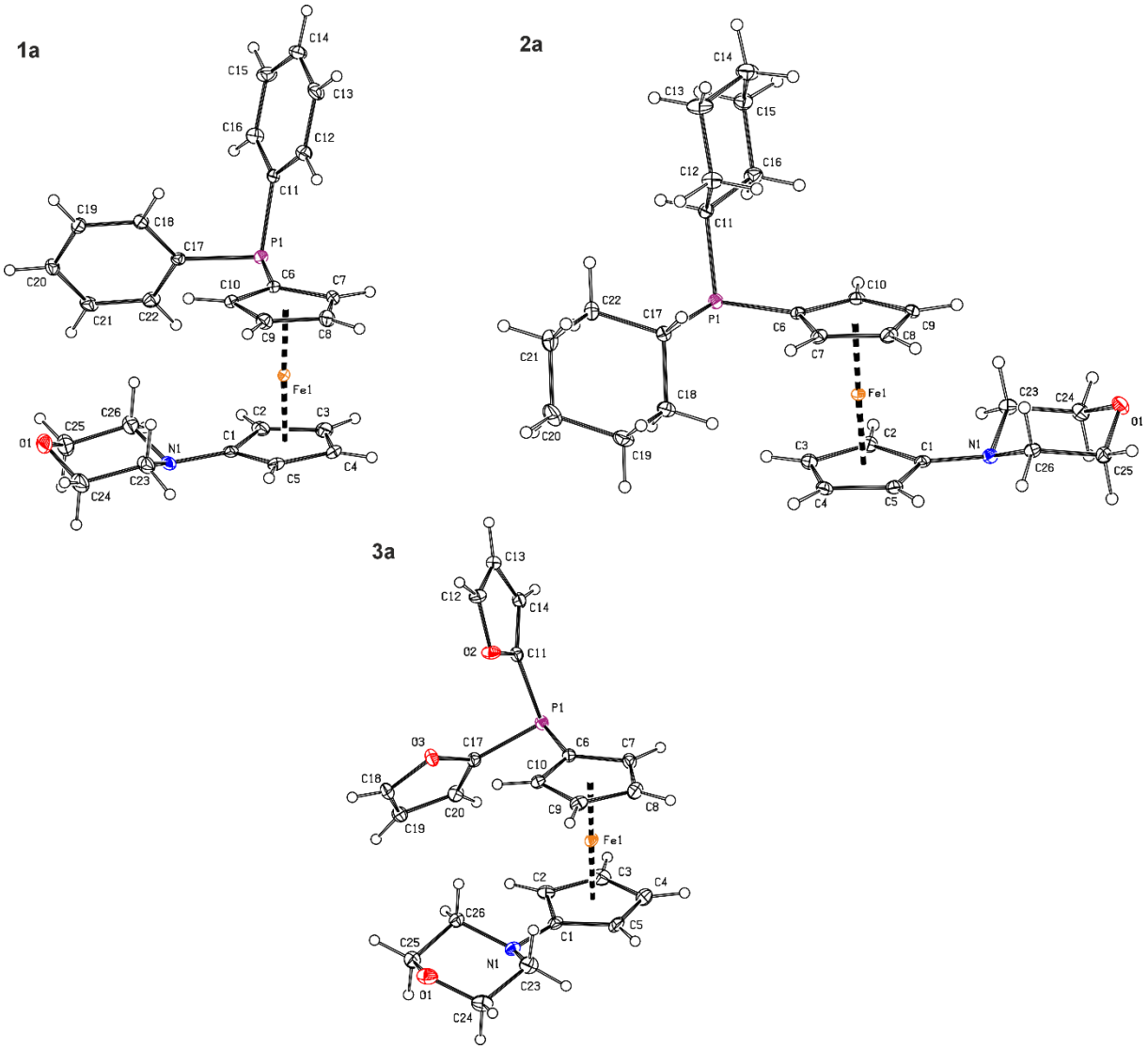

Figure S6. PLATON plot of the molecular structures of **1a**, **2a**, and **3a** showing displacement ellipsoids at the 30% probability level.

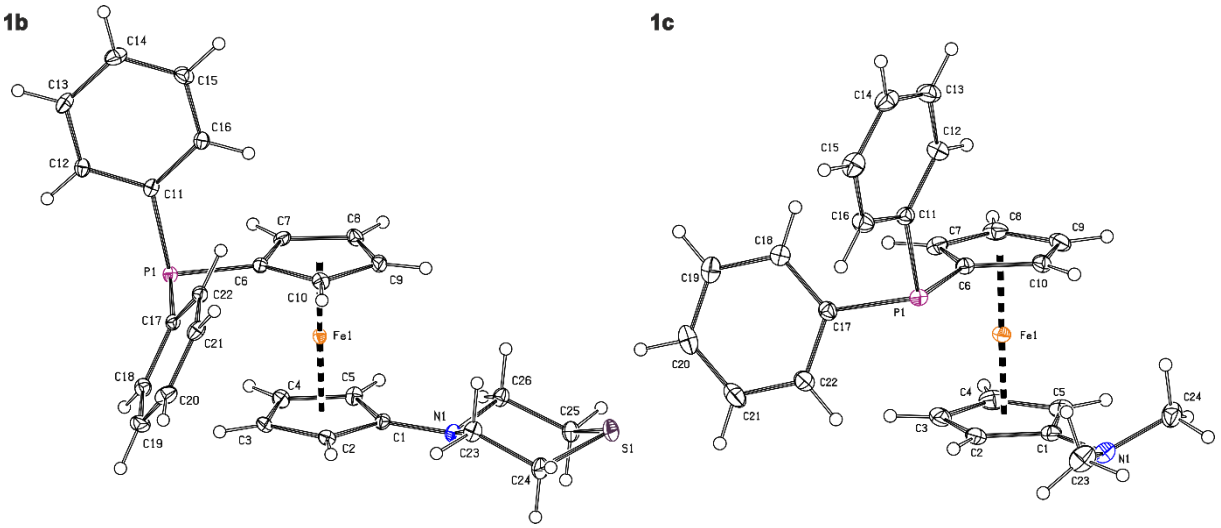

Figure S7. PLATON plot of the molecular structures of **1b** and **1c** showing displacement ellipsoids at the 30% probability level.

Compared to the parent phosphine, phosphine sulfide **1aS** (Figure S8, Table S4) exhibits wider C-P-C angles and shorter P-C distances, as observed for (diphenylphophino)ferrocene[18] and the corresponding phosphine sulfide.[14] The P1-S1 distance is 1.9491(8) Å and the S1-P1-C(6,11,17) angles are 111.79(7)-115.83(7)°. Otherwise, the geometry of **1aS** is similar to that of **1a**, including the distortion of the ferrocene unit and the arrangement of the morpholinyl group.

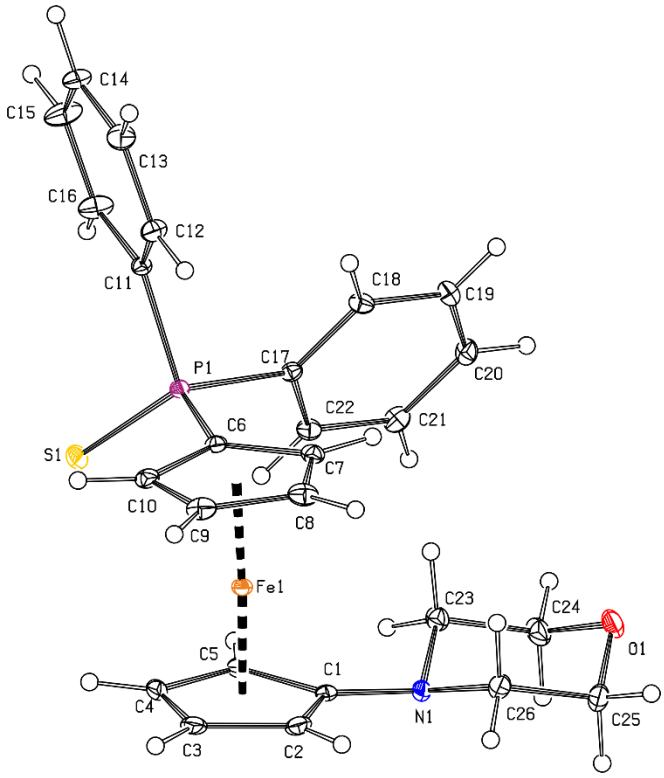

Figure S8. PLATON plot of the molecular structures of **1aS**. Displacement ellipsoids enclose the 30% probability level.

Table S4. Selected distances and angles for **1aS** (in Å and deg).[a]

Fe1-C(1-10)	2.020(2)-2.110(2)	τ	82.1(1)
tilt	5.7(1)	Δ	0.046(2)
C1-N1	1.398(3)	θ	177.4(2)
C6-P1	1.787(2)	C6-P1-C11	103.44(9)
P1-C11	1.820(2)	C6-P1-C17	105.93(9)
P1-C17	1.813(2)	C11-P1-C17	105.36(9)

[a] Tilt is the dihedral angle of the least-squares cyclopentadienyl planes, and τ is the torsion angle C1-Cg1-Cg2-C6, where Cg1 and Cg2 are the centroids of the cyclopentadienyl rings C(1-5) and C(6-10) in molecule 1 and similarly in molecule 2. Δ is the distance of C1 from the least-squares plane defined by the remaining ring carbon atoms C(2-5), and θ is the ring puckering parameter describing the conformation of the morpholinyl group (in degrees).

The structures of the 1,2-isomeric phosphinoamines **4a**, **4b**, **5a**, and **6a** are shown in Figures S9 and S10. Pertinent geometric parameters are collected in Table S5. The compounds are planar-chiral but racemic. Whereas compounds **4a**, **5a,** and **6a** crystallized in centric space groups (*Pbca*, $P2_1/c$, and $P\bar{1}$, respectively), the thiomorpholine derivative **4b** crystallized as a racemic twin in the acentric space group $Pca2_1$ with two virtually identical molecules in the asymmetric unit.

The molecular structures are similar. The functional substituents at the ferrocene unit are bonded quite symmetrically; the differences between the C2-C1-N1/C5-C1-N1 angles for the nitrogen group and the C1-C2-P1/C3-C2-P1 angles for the phosphine moiety are less than 6° in the pairs. Even so, the substituents do not induce any significant torsion at the C1-C2 edge of the cyclopentadienyl ring (see Table S5). Consequently, the ferrocene unit retains its regular geometry; the distortion of the substituted cyclopentadienyl ring discussed above is not detected for **4a**, **4b**, **5a**, and **6a**, at least not in a similar extent. Nevertheless, a minor deformation can be detected at the C1-N1 bond, which is deflected from the plane of the cyclopentadienyl ring C(1-5) (by 5.83(7)° in **4a**, 6.2(2)/6.6(2)° in **4b**, and 5.64(7)° in **5a**), while the C2-P1 bonds lie in the ring plane (angles < 1°). Only compound **6a** shows similar distortion for both substituents (4.54(5)° for the C2-P1 bond and 2.64(6)° for the C1-N1 bond). In all structures, one P-C(Ph/Cy/Fur) bond is directed above the ferrocene unit and the other to the side, away from the nitrogen groups, and the (thio)morpholinyl substituents adopt their usual chair conformation.

Table S5. Selected distances and angles for phosphines **4a**, **4b**, **5a**, and **6a** (in Å and deg).[a]

Parameter	**4a**	**4b** (molecule 1)	**4b** (molecule 2)[c]	**5a**	**6a**
Fe1-C(1-10)	2.031(1)-2.078(1)	2.043(2)-2.064(3)	2.044(2)-2.063(2)	2.035(1)-2.069(1)	2.041(1)-2.059(1)
tilt	2.29(6)	2.7(1)	2.2(1)	2.00(7)	2.57(6)
N1-C1-C2-P1	6.0(1)	−8.0(3)	6.3(3)	−7.2(2)	−2.3(1)
C1-N1	1.405(1)	1.410(3)	1.415(3)	1.409(1)	1.417(1)
θ	178.7(1)	178.3(2)	0.0(2)	1.7(1)	179.1(1)
C2-P1	1.821(1)	1.815(2)	1.814(2)	1.824(1)	1.8101(9)
P1-C11	1.834(1)	1.837(2)	1.836(2)	1.865(1)	1.806(1)
P1-C17	–[b]	1.837(2)	1.830(2)	1.870(1)	1.816(1)
C2-P1-C11	100.89(4)	101.3(1)	100.7(1)	100.88(4)	98.68(4)
C2-P1-C17	–[b]	100.3(1)	100.3(1)	100.51(5)	102.74(4)
C11-P1-C17	–[b]	103.1(1)	102.1(1)	104.47(4)	99.09(4)

[a] The parameters are defined as for **12a** (see footnote to Table S#). θ is the ring puckering parameter describing the conformation of the (thio)morpholinyl group (values in degrees). [b] Value affected by disorder. [c] Atomic labelling of molecule 2 is analogous to that of molecule 1.

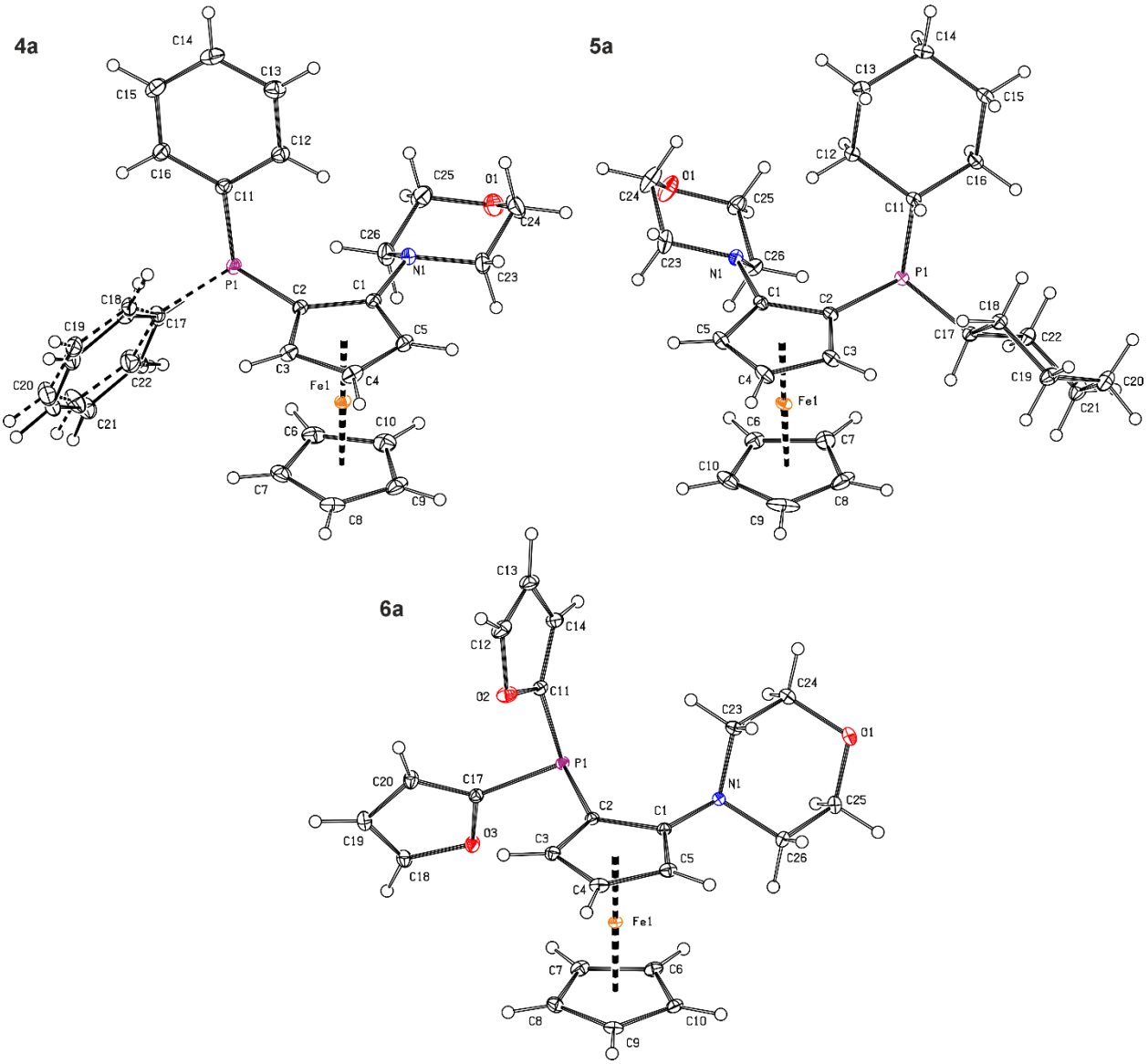

Figure S9. PLATON plot of the molecular structures of **4a**, **5a** and **6a**. Displacement ellipsoids enclose the 30% probability level. Both orientations of the disordered phenyl ring C(17-22) in the structure of **4a** are shown.

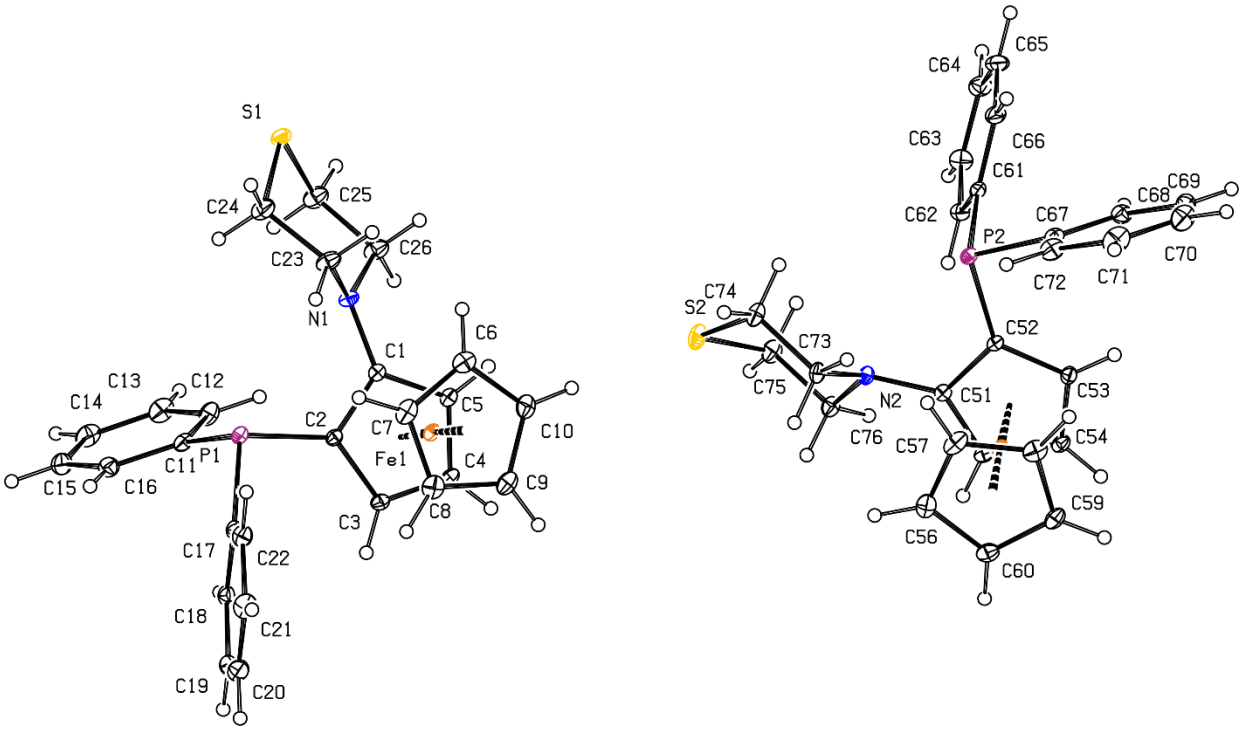

Figure S10. PLATON plot of the molecular structure of **4b** (two crystallographically independent molecules). Displacement ellipsoids are depicted at the 30% probability level.

The structures of gold(I) complexes **1a-cAu**, **2aAu**·$CHCl_3$, and **3aAu** are presented in Figure S11, and the relevant geometric parameters are outlined in Table S6. Compound **1cAu** (Figure S12) crystallizes with two structurally independent but very similar molecules (space group *P*–1; the two molecules differ slightly in conformation), and complex **1aAu** exhibits a rotational disorder at the P-bound phenyl rings. The solvent molecule in the structure of **2aAu**·$CHCl_3$ is also partly disordered.

The structures comprise linear P-Au-Cl units (176-178°) with interatomic distances within the normal ranges.[19b,21] The coordination results in shortening of the P-C bonds and opening of the C-P-C angles relative to the free phosphinoamines, similar to those observed upon thionation of the phosphine groups. The orientation of the substituents at the phosphorus atom with respect to the central ferrocene unit remains similar, with the Au-Cl fragment taking the position at the side of the ferrocene unit. The ferrocene units exhibit distortion resulting from displacement of the nitrogen-bound atom C1 from the plane of the remaining cyclopentadienyl ring carbon atoms C(2-5) (by ≈0.030 Å in **1bAu** and ≈0.045 Å in all other complexes), similar to the free ligands. Their conformations are near 1,3′ (for **1bAu** and **2aAu**·$CHCl_3$; ideal value: $\tau = \pm 144°$) or intermediate with $\tau \approx 90°$ (in all other compounds), corresponding to a more open 1,2′ arrangement.

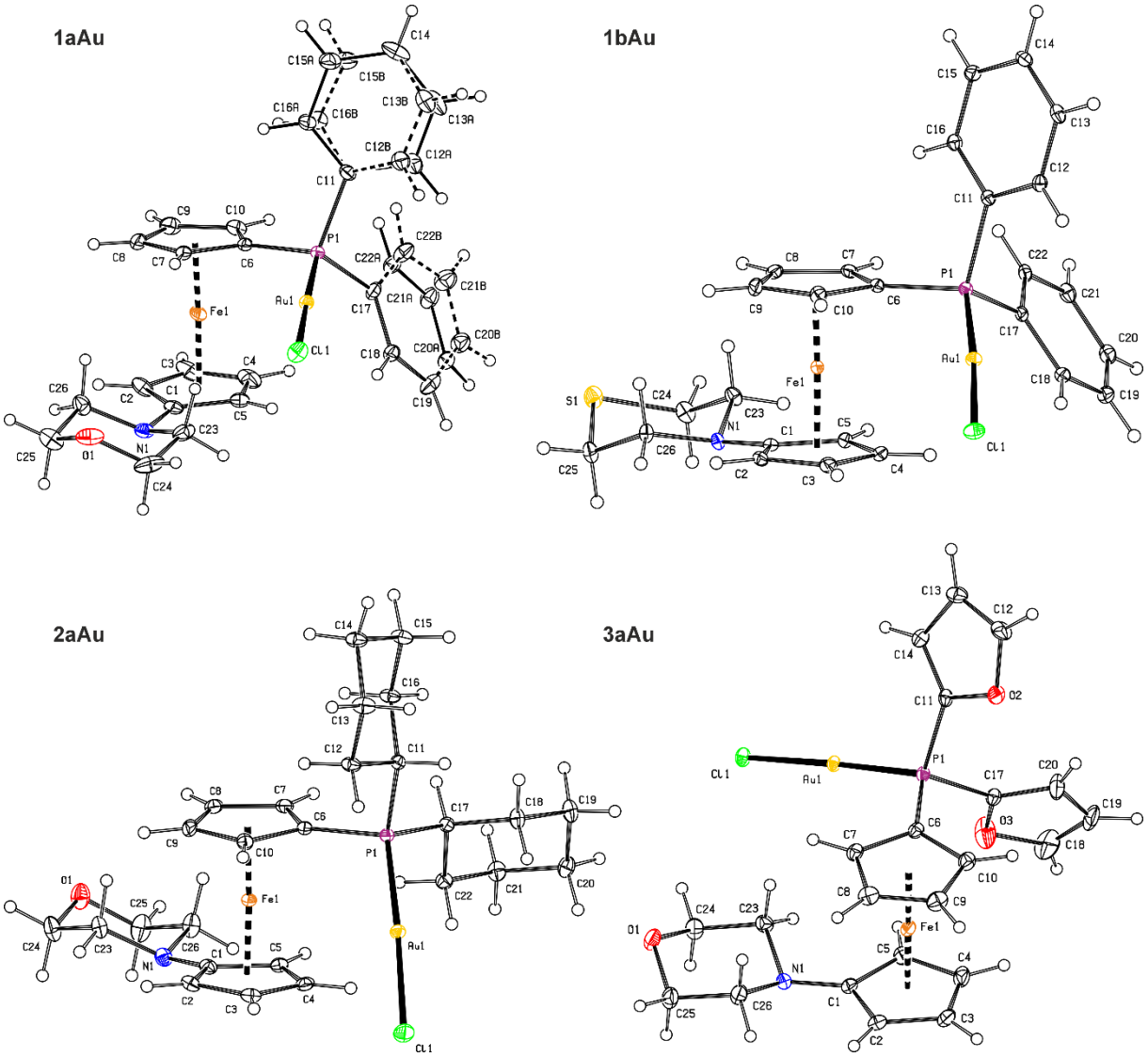

Figure S11. PLATON plot of the molecular structures of **1aAu**, **1bAu**, **2aAu** and **3aAu**. Displacement ellipsoids enclose the 30% probability level. Both orientations of the disordered phenyl ring C(17-22) in the structure of **1aAu** are shown.

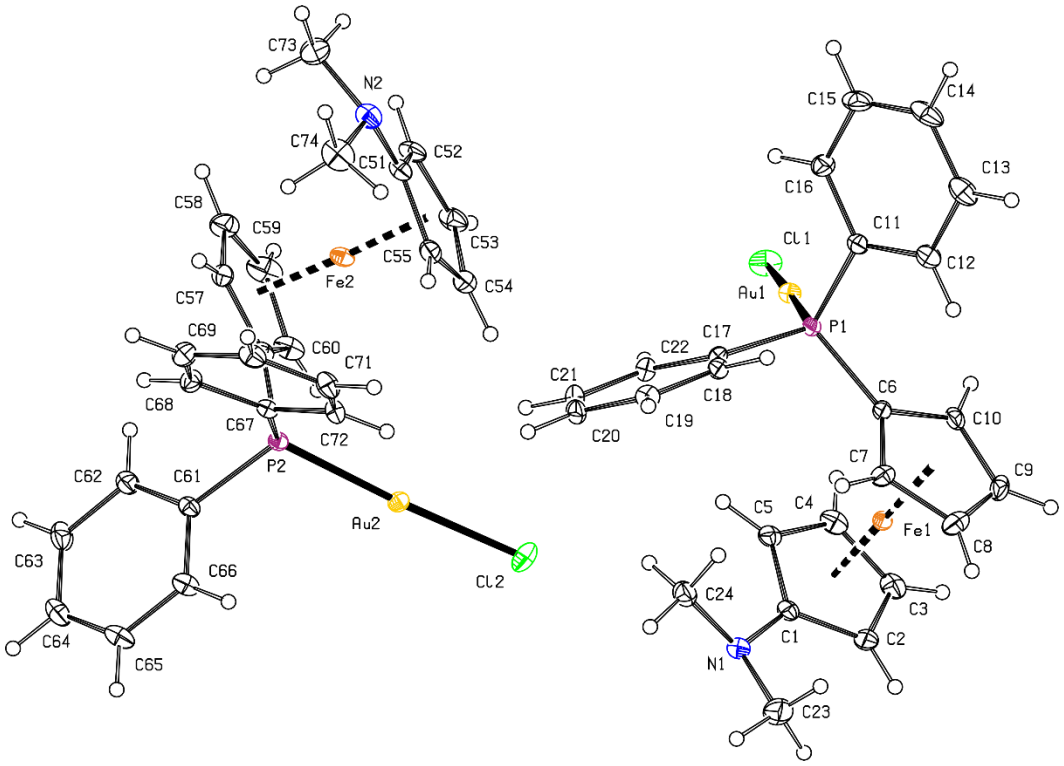

Figure S12. PLATON plot of the molecular structure of **1cAu**. Displacement ellipsoids correspond to the 30% probability level.

Table S6. Selected distances and angles for complexes **1a-cAu**, **2aAu**·$CHCl_3$ and **3aAu** (in Å and deg).[a]

Parameter	**1aAu**	**1bAu**	**1cAu** (mol 1/mol 2)[b]	**2aAu**·$CHCl_3$	**3aAu**
Au1-P1	2.2286(6)	2.2343(6)	2.2324(6)/2.2306(6)	2.2320(7)	2.2189(5)
Au1-Cl1	2.2762(7)	2.2844(5)	2.2877(7)/2.2864(7)	2.2913(7)	2.2902(5)
P1-Au1-Cl1	178.40(2)	176.35(2)	178.12(3)/176.83(3)	176.71(2)	177.49(3)
Fe1-C(1-10)	2.023(2)-2.128(2)	2.025(2)-2.100(2)	2.020(2)-2.121(2)/ 2.024(2)-2.110(2)	2.035(2)-2.105(2)	2.030(2)-2.118(2)
tilt	4.7(1)	0.9(1)	3.4(1)/3.3(1)	3.6(1)	3.2(1)
τ	87.6(2)	−150.6(1)	−88.2(2)/−95.4(2)	−149.4(2)	−84.5(2)
Δ	0.045(2)	0.031(2)	0.044(2)/0.047(2)	0.042(2)	0.045(2)
C1-N1	1.395(3)	1.400(2)	1.387(3)/1.393(3)	1.397(3)	1.393(3)
θ	175.5(2)	6.2(2)	n.a.	178.1(3)	3.4(2)
C6-P1	1.782(2)	1.785(2)	1.782(2)/1.782(2)	1.794(2)	1.778(2)
P1-C11	1.822(2)	1.820(2)	1.823(2)/1.821(2)	1.836(2)	1.783(2)
P1-C17	1.812(2)	1.816(2)	1.813(2)/1.813(2)	1.840(2)	1.795(2)
C6-P1-C11	105.22(9)	104.53(8)	103.98(9)/105.08(9)	105.7(1)	107.47(9)
C6-P1-C17	107.7(1)	107.83(9)	106.5(1)/107.1(1)	108.1(1)	106.75(9)
C11-P1-C17	104.6(1)	105.32(9)	106.00(9)/105.56(8)	105.15(9)	103.20(9)

[a] The parameters are defined as for the free phosphinoamines (see footnote to Table S3). n.a. = not applicable. [b] Atomic labelling of molecule 2 is analogous to that of molecule 1.

The structures of **4aAu**, **4bAu**·2CH_2Cl_2, **4cAu**, and **5aAu**·½CH_2Cl_2 (Figures S13 and S14; Table S7) also reveal linear P-Au-Cl units (174-179°) with the Au-P and Au-Cl distances similar to those determined for complexes obtained from the isomeric ligands comprising the 1,1′-disubstituted ferrocene unit. Complexes featuring the (diphenylphosphino)ferrocene ligands, **4aAu**, **4bAu,** and **4cAu**, have very similar arrangements. The P-Au-Cl arms in their molecules are directed toward the ferrocene iron atom, albeit under different angles as indicated by the angles at which the pivotal P1-Au1 bond intersects the parent cyclopentadienyl ring C(1-5): 36.89(7)° for **4aAu**, 26.8(3)/32.3(2)° (two independent molecules) for **4bAu**, and 11.85(8)° for **4cAu**. One phenyl ring is always directed above the ferrocene unit and the other to the side, away from the nitrogen substituent, which brings the gold center to the vicinity of the nitrogen atom. The Au1···N1 distances of 3.229(1) Å for **4aAu**, 3.175(6)/3.133(6) Å for **4bAu**, and 2.987(2) Å for **4cAu** are longer than the sum of the respective covalent radii (2.07 Å)[22] but below the sum of the van der Waals radii (3.98 Å).[23] In contrast, the P-Au-Cl moiety in the molecule of **5aAu** is directed away from the nitrogen substituent, although still "below" the ferrocene unit (the angle between the P1-Au1 bond and the ring C(1-5) is 47.40(7)°). The P1-C17 bond lies approximately in the plane of the substituted cyclopentadienyl ring and is thus directed toward the morpholinyl substituent, whereas the P1-C11 bond is directed above. The complexes exhibit shorter P-C distances and wider C-P-C angles than the corresponding free phosphinoamines. The ferrocene units are practically undistorted and exhibit no significant torsional deformation at the N1-C1-C2-P1 moiety (torsion angles below 6°). The amine substituents also retain their normal geometry.

Table S7. Selected distances and angles for **4aAu**, **4bAu**·2CH_2Cl_2, **4cAu**, and **5aAu**·½CH_2Cl_2 (in Å and deg).[a]

Parameter	**4aAu**	**4bAu**·2CH_2Cl_2 (mol 1/mol 2)	**4cAu**	**5aAu**· ½CH_2Cl_2
Au1-P1	2.2327(5)	2.229(2)/2.228(1)	2.2331(6)	2.2362(4)
Au1-Cl1	2.2922(5)	2.296(2)/2.288(2)	2.2999(6)	2.2898(6)
P1-Au1-Cl1	177.18(2)	179.04(6)/178.64(6)	176.38(2)	174.34(2)
Fe1-C(1-10)	2.026(2)-2.064(2)	2.024(8)-2.064(6)/2.036(6)-2.069(6)	2.032(2)-2.069(2)	2.023(2)-2.063(2)
tilt	4.0(1)	2.1(4)/1.6(4)	5.0(1)	5.9(1)
N1-C1-C2-P1	–6.6(2)	2.5(8)/–4.0(8)	–6.6(2)	–2.2(3)
C1-N1	1.415(2)	1.417(8)/1.420(8)	1.408(3)	1.421(2)
θ	175.2(2)	5.2(5)/177.6(5)	n.a.	178.0(2)
C2-P1	1.792(2)	1.791(6)/1.787(6)	1.789(2)	1.808(2)
P1-C11	1.819(2)	1.819(6)/1.823(6)	1.821(2)	1.838(2)
P1-C17	1.814(2)	1.824(6)/1.820(6)	1.817(2)	1.827(2)
C2-P1-C11	104.52(7)	105.7(3)/106.1(3)	106.46(8)	105.79(8)
C2-P1-C17	105.11(7)	107.8(3)/108.3(3)	107.35(9)	109.45(8)
C11-P1-C17	107.15(8)	102.2(3)/103.3(3)	104.37(9)	107.59(8)

[a] The parameters are defined as for the phosphinoamine ligands (see footnote to Table S5). n.a. = not applicable. [b] Atomic labelling of molecule 2 is analogous to that of molecule 1.

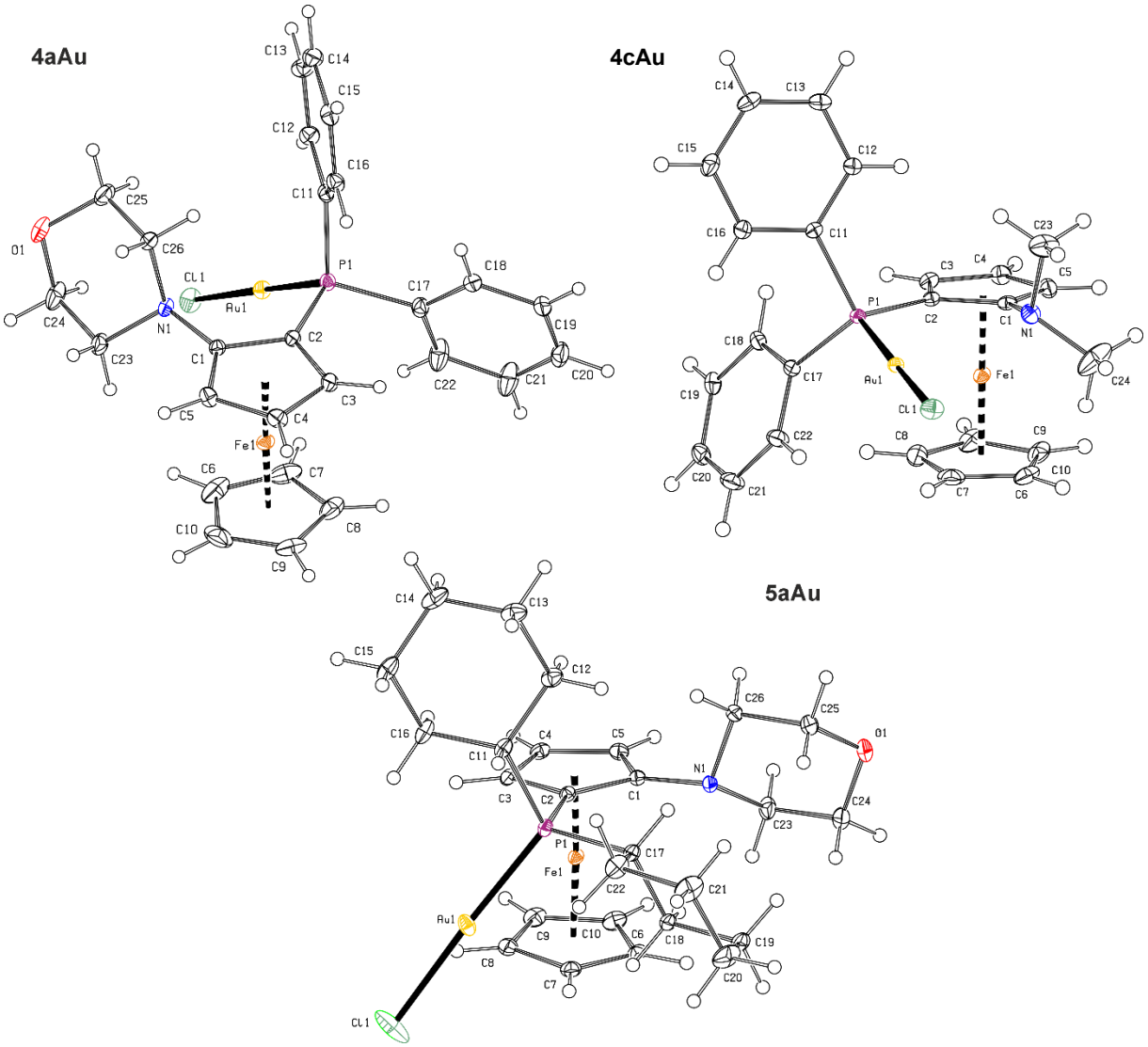

Figure S13. PLATON plot of the molecular structures of **4aAu**, **4cAu**, and **5aAu**. Displacement ellipsoids correspond to the 30% probability level.

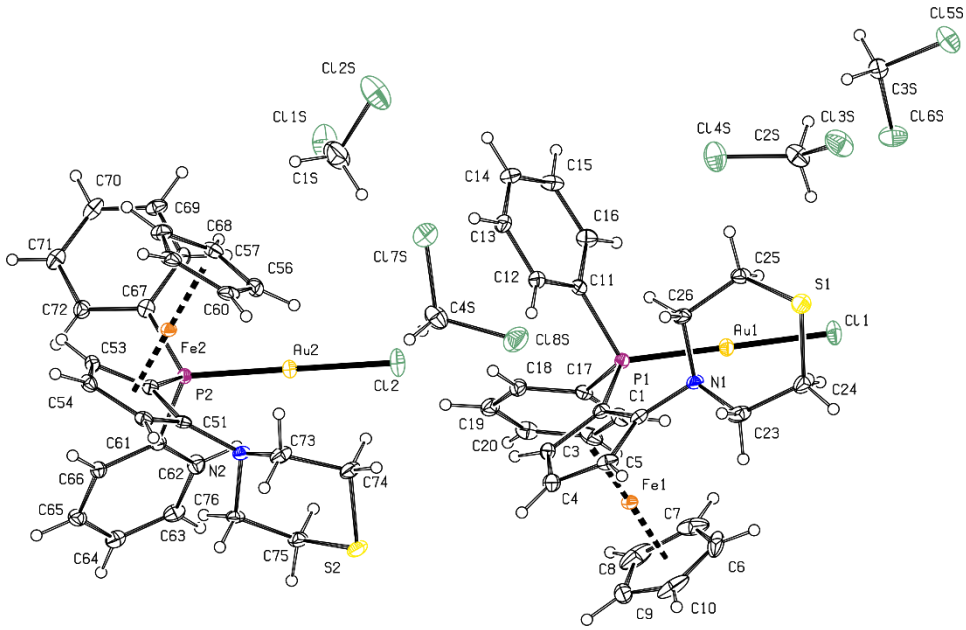

Figure S14. PLATON plot of the molecular structures of **4bAu**·2CH_2Cl_2 with the displacement at the 30% probability level.

DFT calculations

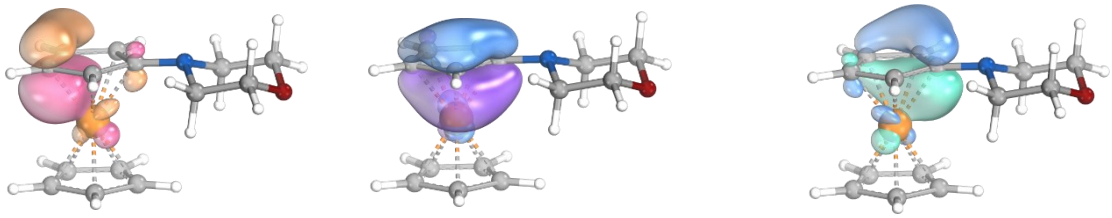

π(Cp(1-5)) → Fe [5.08(∑C1-C5)/0.83(Fe)]

π(Cp1-5) → Fe [(0.87(C1)/1.08(C2)/1.02(C3)/1.02(C4)/1.08(C5)/0.83(Fe)]

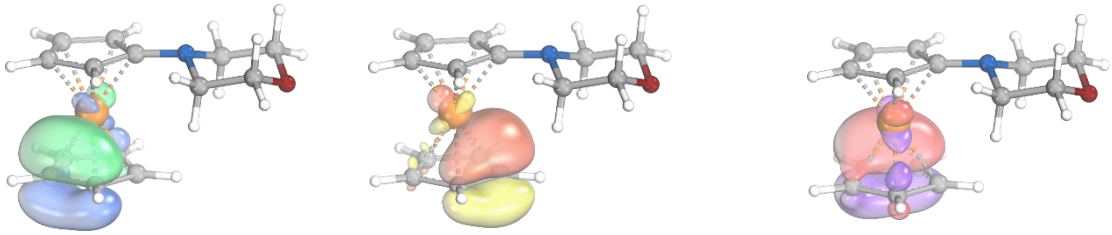

π(Cp(6-10)) → Fe [5.17(∑C6-C10)/0.78(Fe)]

π(C6-10) → Fe [(1.01(C6)/1.01(C7)/1.07(C8)/1.04(C9)/1.04(C10)/0.78(Fe)]

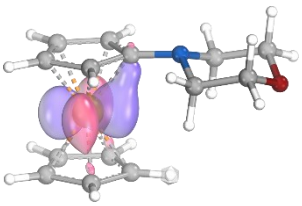

d(Fe) →ππ*(Cp)

[1.77(Fe)/0.07(C1)/0.03(C6)/0.04(C7)/0.04(C10)]

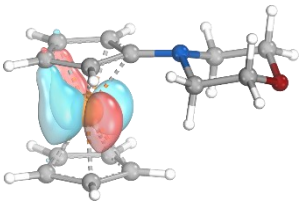

d(Fe) → π*(Cp)

[1.74(Fe)/0.06(C3)/0.06(C4)/0.03(C7)/0.03(C8)/

0.03(C9)/0.03(C10)]

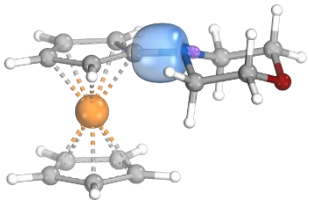

σ(C–N) [0.87(C1)/1.12(N)]

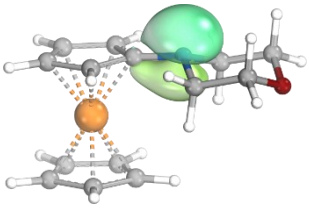

N(lp) [1.78(N)/0.10(C1)]

Figure S15. Selected Intrinsic bond orbitals (IBOs) representing Fe–Cp bonding in **10**. Values in parentheses indicate IBO electron populations assigned to the indicated atoms or fragments. The contributions of carbon atoms within each cyclopentadienyl ring are reported both as summed values (C1–C5 and C6–C10) as well as individual per-atom populations.

Table S8. QTAIM descriptors at the Fe–C bond critical points (bcp) for **10** (in atomic units): electron density (ρ_{bcp}), Laplacian of the electron density ($\nabla^2\rho_{bcp}$), total energy density (H_{bcp}), the ratio of potential and kinetic energy density ($|V|/G$), and the ratios of kinetic (G/ρ_{bcp}) and total energy density (H/ρ_{bcp}) to electron density, together with experimental and calculated Fe–C bond distances and Mayer bond orders (MBO) for the substituted cylopentadienyl ring.[a]

Atom	Fe-C bond length [Å]		ρ_{bcp}	$\nabla^2\rho_{bcp}$	H_{bcp}	$\lvert V\rvert/G$	G/ρ_{bcp}	H/ρ_{bcp}	MBO
	exp.	calc.[a]							
C1	2.088(1)	2.095	0.084	0.252	–0.027	1.3	1.07	–0.32	0.31
C2	2.048(1)	2.047	0.090	0.280	–0.030	1.3	1.11	–0.34	0.47
C3	2.036(3)	2.031	0.093	0.287	–0.032	1.31	1.12	–0.35	0.46
C4	2.036(1)	2.031	0.093	0.287	–0.032	1.31	1.12	–0.35	0.46
C5	2.054(1)	2.047	0.090	0.280	–0.030	1.3	1.11	–0.34	0.47

[a] Calculated at the PBE0-D3/def2-TZVP level of theory

Table S9. QTAIM descriptors at the Fe–C bond critical points (bcp) for **(10Me)[BF_4]** (in atomic units): electron density (ρ_{bcp}), Laplacian of the electron density ($\nabla^2\rho_{bcp}$), total energy density (H_{bcp}), the ratio of potential and kinetic energy density ($|V|/G$), and the ratios of kinetic (G/ρ_{bcp}) and total energy density (H/ρ_{bcp}) to electron density , together with experimental and calculated Fe–C bond distances and Mayer bond orders (MBO) for the substituted cyclopentadienyl ring.[a]

Atom	Fe-C bond length [Å]		ρ_{bcp}	$\nabla^2\rho_{bcp}$	H_{bcp}	$\lvert V\rvert/G$	G/ρ_{bcp}	H/ρ_{bcp}	MBO
	exp.	calc.[a]							
C1	2.005(2)	1.998	0.099	0.303	–0.037	1.33	1.15	–0.39	0.42
C2	2.043(1)	2.040	0.091	0.293	–0.031	1.30	1.14	–0.34	0.43
C3	2.048(1)	2.056	0.088	0.280	–0.029	1.29	1.12	–0.39	0.47
C4	2.056(1)	2.055	0.088	0.280	–0.029	1.29	1.12	–0.33	0.43
C5	2.050(2)	2.040	0.091	0.293	–0.031	1.29	1.14	–0.33	0.46

[a] Calculated at the PBE0-D3/def2-TZVP level of theory

Considerations regarding the observed distortion, inferred from the IBO analysis, can be extended to phosphinoamine **1a** (Figure S16). The two pnictogen substituents differ markedly in their overall electron-donor and acceptor character. While the amine substituent is strongly electron-donating, because its resonance donation (positive mesomeric effect) outweighs its modest inductive electron-withdrawing ability, diphenylphosphinyl group (PPh_2) behaves as a mildly electron-withdrawing group (as reflected, for example, by its positive Hammett σ_p value).[24] This difference is consistent with the distinct influence of each substituent on the donor/acceptor properties of the corresponding cyclopentadienyl ring in **1a**.[25] Based on the IBO descriptors, the amine-substituted ring is a slightly better donor (π(Cp1)→Fe: [5.06(ΣC1–C5)/0.86(Fe)]) and, conversely, a poorer acceptor in back-donation (e_2(Fe)→π*(Cp1): [3.50(Fe)/0.17(C1–C5)]), whereas the diphenylphosphino-substituted ring is a weaker donor (π(Cp2)→Fe: [5.14(ΣC6–C10)/0.76(Fe)]) but a better acceptor in back-donation (e_2(Fe)→π*(Cp2): [3.50(Fe)/0.22(C6–C10)]). Unlike the nitrogen lone pair, which can adopt substantial p-character and therefore conjugate effectively with an adjacent aromatic π-system, the lone pair on pyramidal P(III) centres is generally more s-rich and is consequently a weak π-donor, *i.e.*, it engages far less efficiently in π-conjugation with a ring π-system than the amine lone pair.[26]

While in **1a** the influences of the two pnictogen substituents are at least partially separated (each residing on a different cyclopentadienyl ring), in the isomeric, planar-chiral derivative **4a** the groups are attached to the same cyclopentadienyl ring in adjacent positions. In that situation, steric and electronic effects are difficult to disentangle and likely operate simultaneously. The opposing electronic tendencies of the amine (donating) and PPh_2 (mildly withdrawing) groups can be expected to partially compensate, consistent with the similar donor and acceptor properties obtained for the two cyclopentadienyl rings in **4a** (see Figure S17; π(Cp1)→Fe: [5.09(ΣC1–C5)/0.80(Fe)] *vs.* π(Cp2)→Fe: [5.13(ΣC6–C10)/0.80(Fe)]; and e_2(Fe)→π*(Cp1): [3.50(Fe)/0.21(C1–C5)] *vs.* e_2(Fe)→π*(Cp2): [3.50(Fe)/0.20(C6–C10)]). In addition, it is reasonable to expect that the envelope-like bending observed in the structures of the morpholine derivatives **1a** and **10** is, in the case **4a**, sterically hindered by the proximal bulky diphenylphosphanyl substituent.

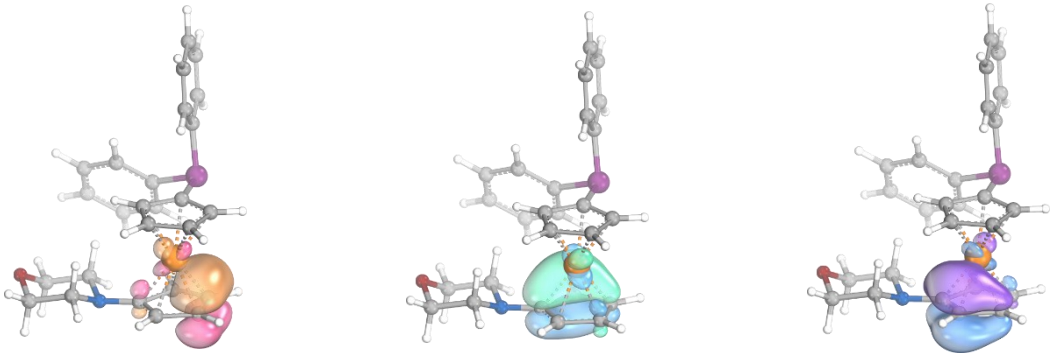

π(Cp1) → Fe [5.06(∑C1-C5)/0.86(Fe)]
π(Cp1) → Fe [(0.87(C1)/1.06(C2)/1.03(C3)/1.01(C4)/1.09(C5)/0.86(Fe)]

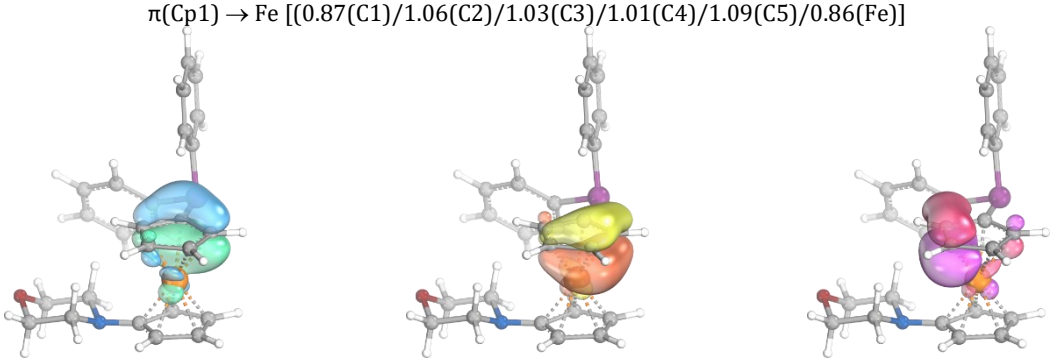

π(Cp2) → Fe [5.13(∑C6-C10)/0.75(Fe)]
π(Cp2) → Fe [(1.08(C6)/0.98(C7)/1.03(C8)/1.01(C9)/1.03(C10)/0.75(Fe)]

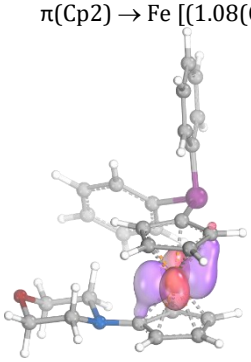

d(Fe) → π*(Cp)
[1.76(Fe)/0.05(C1)/0.02(C2)/ 0.08(C7)/0.03(C6)]

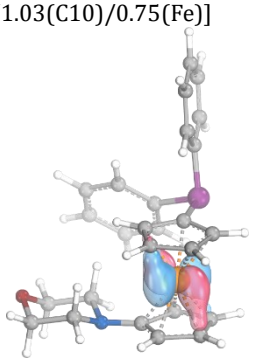

d(Fe) → π*(Cp)
[1.74(Fe)/0.04(C3)/0.06(C4)/ 0.06(C9)/0.04(10)]

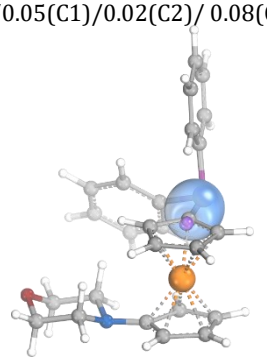

σ(C–P) [1.16(C1)/0.81(P)]

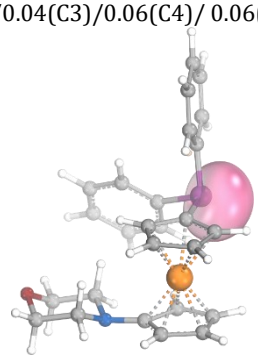

P(lp) [1.93(P)/0.07(other)]

Figure S16. Selected Intrinsic bond orbitals (IBOs) representing Fe–Cp bonding in **1a**. Values in parentheses indicate IBO electron populations assigned to the indicated atoms or fragments. The contributions of carbon atoms within each cyclopentadienyl ring are reported both as summed values (C1–C5 and C6–C10) as well as individual per-atom populations.

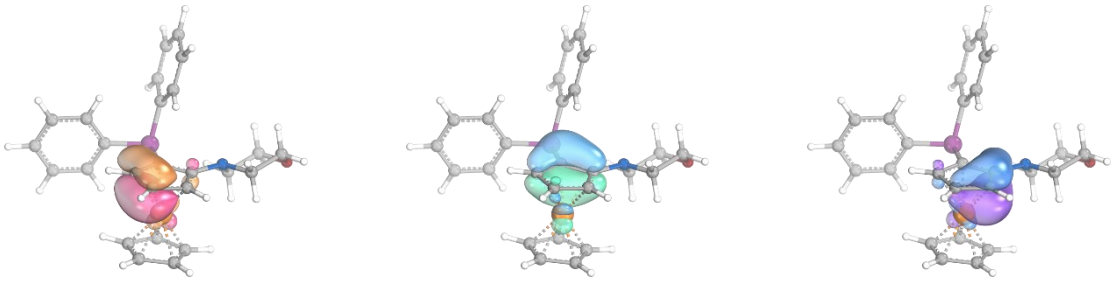

π(Cp1) → Fe [5.09(∑C1-C5)/0.80(Fe)]
π(Cp1) → Fe [(0.88(C1)/1.11(C2)/1.00(C3)/1.02(C4)/1.08(C5)/0.80(Fe)]

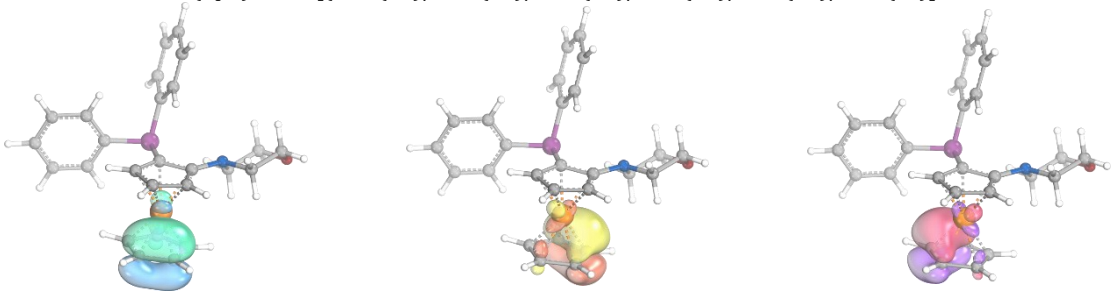

π(Cp2) → Fe [5.13(∑C6-C10)/0.80(Fe)]
π(Cp2) → Fe [(1.00(C6)/1.04(C7)/1.07(C8)/1.03(C9)/1.05(C10)/0.80(Fe)]

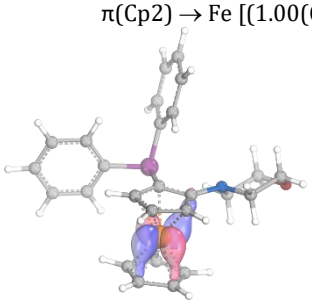

d(Fe) → π*(Cp)
[1.76(Fe)/0.07(C1)/0.02(C5)/0.05(C8)/0.05(C9)]

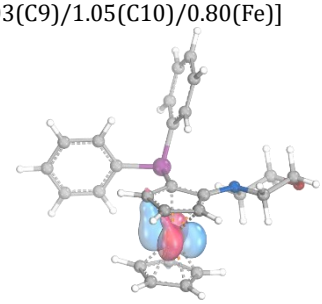

d(Fe) → π*(Cp)
[1.74(Fe)/0.07(C3)/0.05(C4)/0.07(C6)/0.03(C7)]

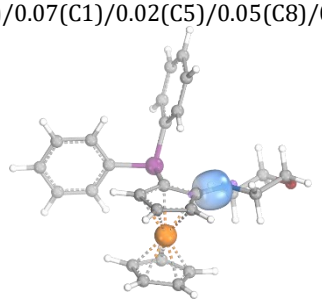

σ(C–N) [0.87(C1)/1.12(N)]

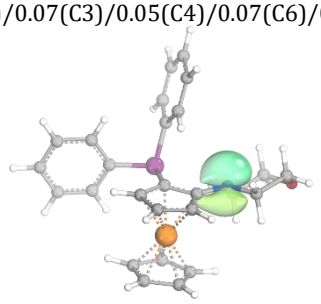

N(lp) [1.78(N)/0.09(C1)]

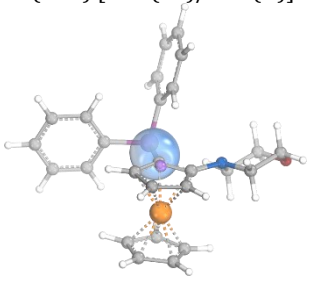

σ(C–P) [1.16(C1)/0.81(N)]

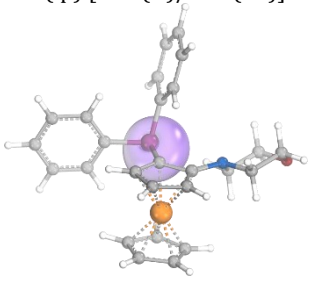

P(lp) [1.90(P)/0.1(other)]

Figure S17. Selected Intrinsic bond orbitals (IBOs) representing Fe–Cp bonding in **4a**. Values in parentheses indicate IBO electron populations assigned to the indicated atoms or fragments. The contributions of carbon atoms within each cyclopentadienyl ring are reported both as summed values (C1–C5 and C6–C10) as well as individual per-atom populations.

a)

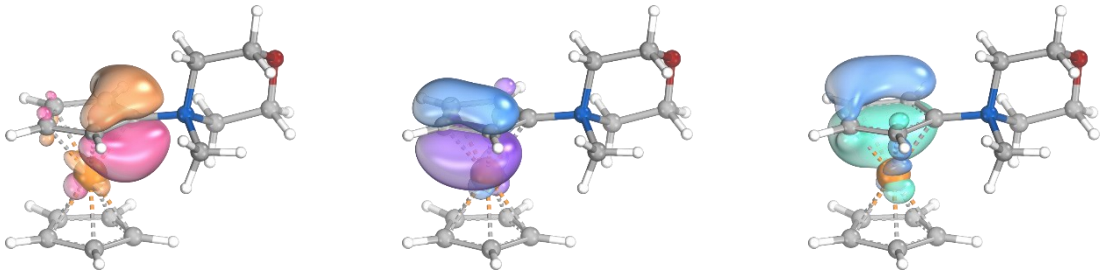

π(C(1-5)) → Fe [5.19(∑C1-C5)/0.73(Fe)]

π(Cp1-5) → Fe [(1.16(C1)/1.01(C2)/1.01(C3)/0.99(C4)/1.02(C5)/0.73(Fe)]

b)

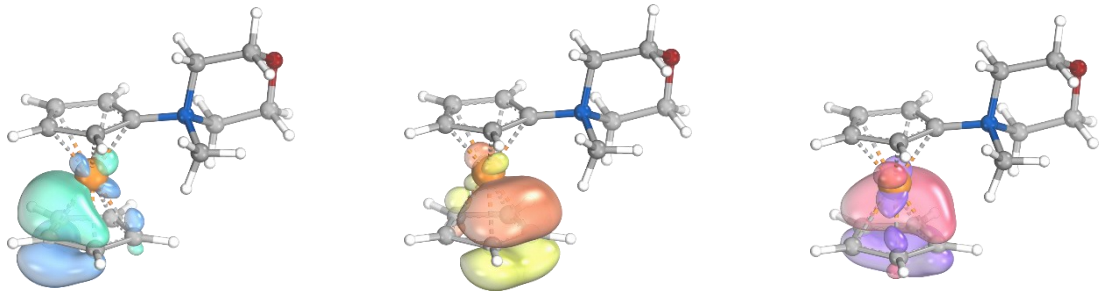

π(Cp(6-10)) → Fe [5.04(∑C6-C10)/0.91(Fe)]

π(Cp6-10) → Fe [(1.02(C6)/1.03(C7)/0.98(C8)/1.01(C9)/1.01(C10)/0.91(Fe)]

c)

d(Fe) → π*(Cp)

[1.74(Fe)/0.05(C4)/0.08(C5)/0.03(C6)/0.05(C10)]

d(Fe) → π*(Cp)

[1.75(Fe)/0.07(C2)/0.05(C3)/0.02(C7)/0.05(C8)]

d)

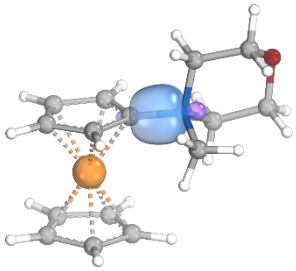

σ(C–N) [0.78(C1)/1.20(N)]

Figure S18. Selected Intrinsic bond orbitals (IBOs) representing Fe–Cp bonding in **10Me[BF$_4$]**. Values in parentheses indicate IBO electron populations assigned to the indicated atoms or fragments. The contributions of carbon atoms within each cyclopentadienyl ring are reported both as summed values (C1–C5 and C6–C10) as well as individual per-atom populations.

Analysis of the possible Au···N interactions in Au(I) complexes

DFT calculations were also performed to investigate the nature of the possible Au···N interactions in the Au(I) complexes of the homoannular phosphinoamine ligands. Complex **4cAu** was chosen as the model compound. Computational analyses of secondary interactions[27] consistently show a bond critical point between the "interacting" atoms and an NCI attractive region between the metal and the donor, indicating a stabilizing interaction, while orbital-based methods often find little to no true covalent character. We have performed the NCI analysis[28] (see the scatter plot of the reduced density gradient in Figure S18a, and the corresponding sign(λ_2)ρ isosurface map in Figure S18b), which indeed revealed the presence of an attractive noncovalent interaction between gold and the nitrogen atom. Topological analysis of the electron density at the Au···N bond critical point (bcp) is consistent with a weak, predominantly closed-shell interaction (Table S10). The electron density at the bcp (ρ_{bcp}) is low and its Laplacian ($\nabla^2\rho_{bcp}$) is small but positive,[29] suggesting a charge depletion in the internuclear region. The energy–density criterion places the interaction at the closed-shell/intermediate boundary ($|V|/G \approx 1.01$) with a very small negative total energy density, indicating that the Au···N contact is primarily noncovalent with prevailing electrostatic contribution.[30] In line with these results, IBO analysis has shown only partial delocalization of the nitrogen atom lone electron pair to the ferrocene backbone, but no interaction with the gold atom (Figure S19).

a) **b)**

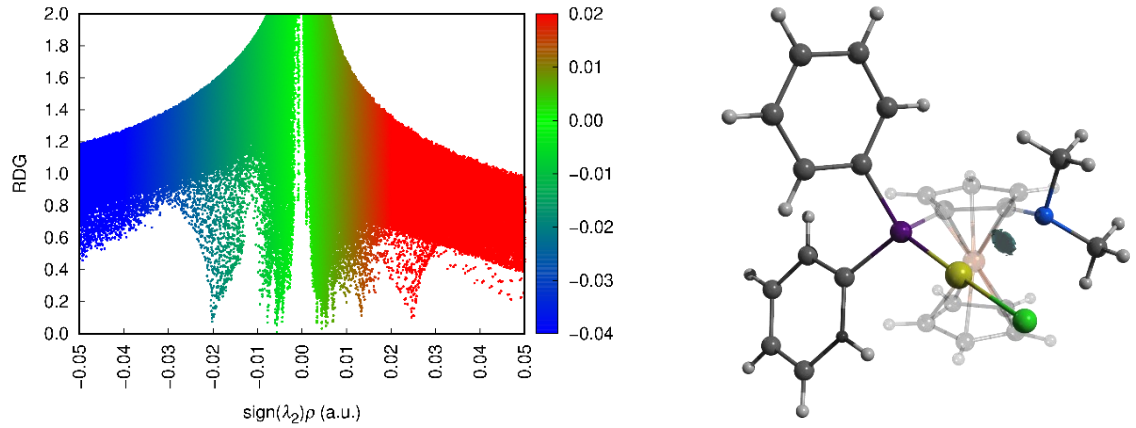

Figure S19. (a) Scatter plot of the reduced density gradient (RDG) versus the product of electron density and the sign of the second Hessian eigenvalue (sign(λ_2)ρ) for complex **4cAu**. (b) NCI plot for the same compound (RDG isosurfaces with $S(r)$ = 0.4). For clarity, the RDG isosurface has been set to show only the regions with negative sign(λ_2)ρ values in range from –0.05 to –0.01, corresponding to attractive noncovalent interactions.

Table S10. QTAIM descriptors at the Au–N bond critical point (bcp) in **4cAu** (in atomic units): electron density (ρ_{bcp}), Laplacian of the electron density ($\nabla^2\rho_{bcp}$), total energy density (H_{bcp}), the ratio of potential and kinetic energy density ($|V|/G$), and the ratios of kinetic (G/ρ_{bcp}) and total energy density (H/ρ_{bcp}) to electron density.[a]

ρ_{bcp}	$\nabla^2\rho_{bcp}$	H_{bcp}	$\lvert V\rvert/G$	G/ρ_{bcp}	H/ρ_{bcp}
0.020	0.058	$-7.08\cdot10^{-5}$	1.01	0.71	–0.003

[a] Calculated at the PBE0-D3/def2-TZVP:ECP(Au) level of theory.

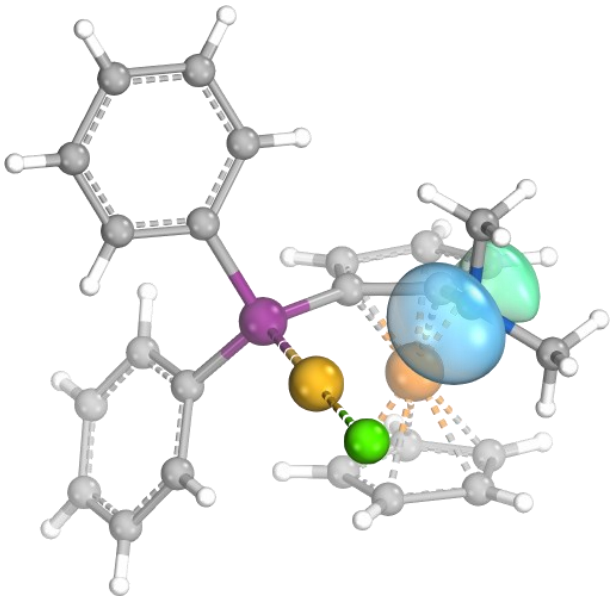

N(lp) [1.86(N)/0.04(C1)/0.10(other)]

Figure S20. Intrinsic bond orbital (IBO) representing the lone electron pair at the nitrogen atom in the gold complex **4cAu**. Values in parentheses indicate the fraction of bonding electrons assigned to the individual atoms.

Computationals details

Theoretical calculations were performed using the Gaussian 16 program package.[31] The geometry optimizations were started from atomic coordinates determined by single-crystal X-ray diffraction analysis, using PBE0[32] density functional in conjunction with def2-TZVP[33] basis set and associated effective core potential (ECP) for gold[34] with added Grimme's D3 dispersion correction.[35] Wavefunction for the NCI analysis have been obtained by single point calculation at the PBE0-D3/def2-TZVP:ECP(Au) level of theory using geometry determined by the X-ray crystallography. The analysis of calculated electron densities by the Atoms in Molecules approach (QTAIM) were performed using the Multiwfn software package (version 3.8).[36] Intrinsic bond orbital (IBO) analysis and visualization of the obtained orbitals were performed using the IboView software.[37]

Copies of the NMR spectra

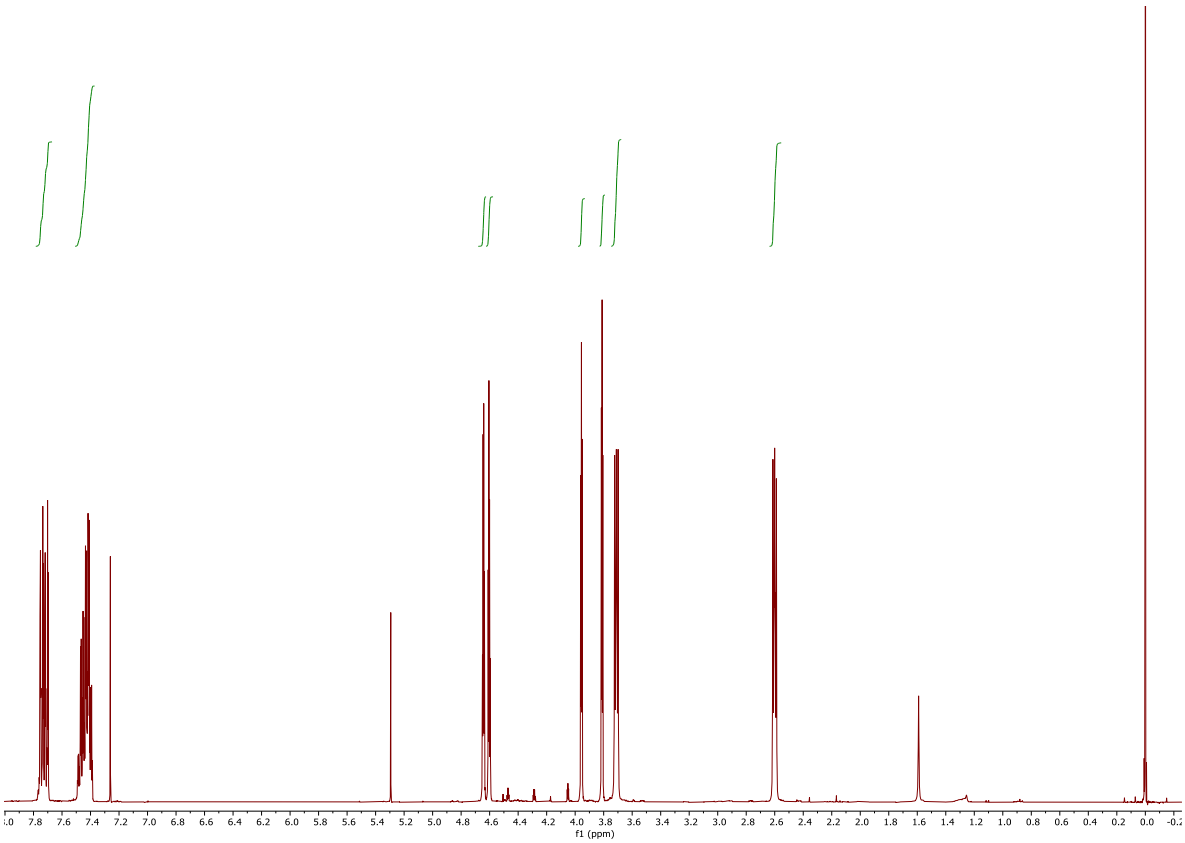

Figure S21. ^{1}H NMR spectrum (399.95 MHz, $CDCl_3$) of compound **1aS**.

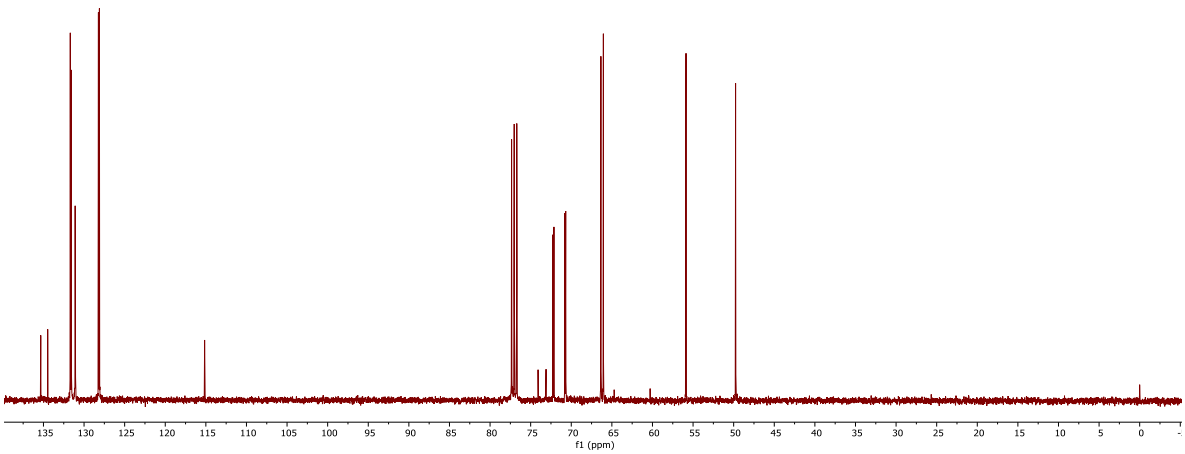

Figure S22. $^{13}C\{^{1}H\}$ NMR spectrum (100.58 MHz, $CDCl_3$) of compound **1aS**.

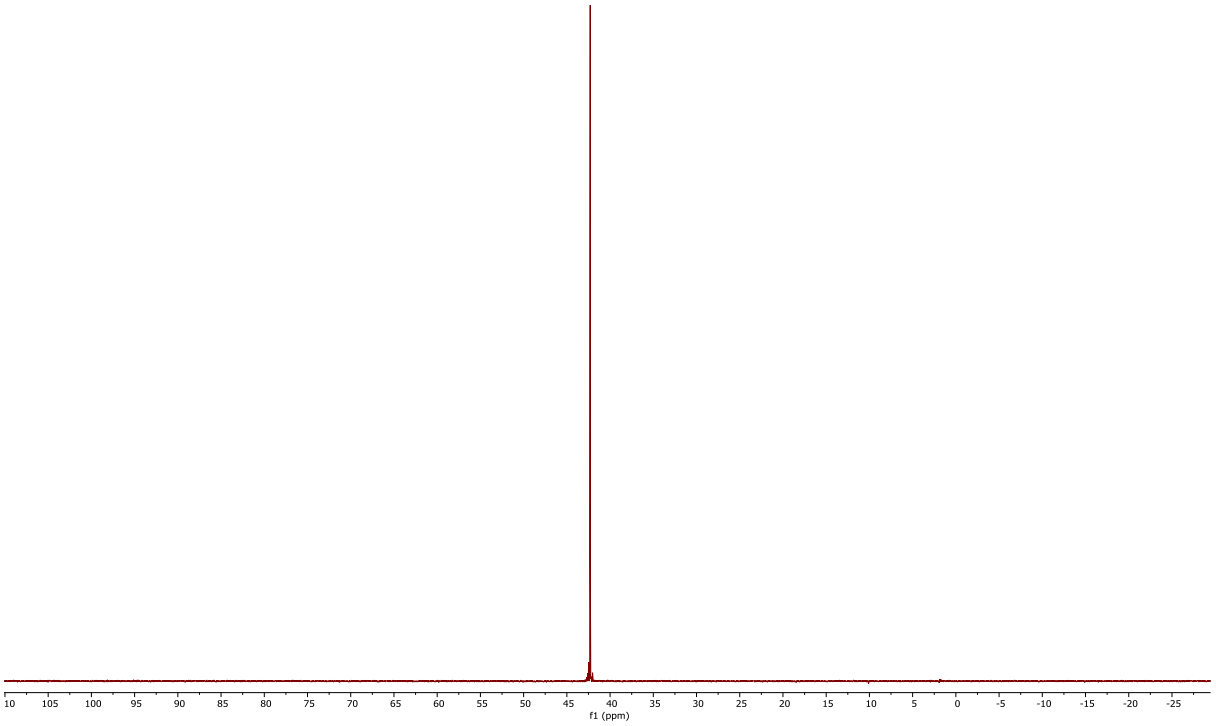

Figure S23. $^{31}P\{^{1}H\}$ NMR spectrum (161.90 MHz, $CDCl_3$) of compound **1aS**.

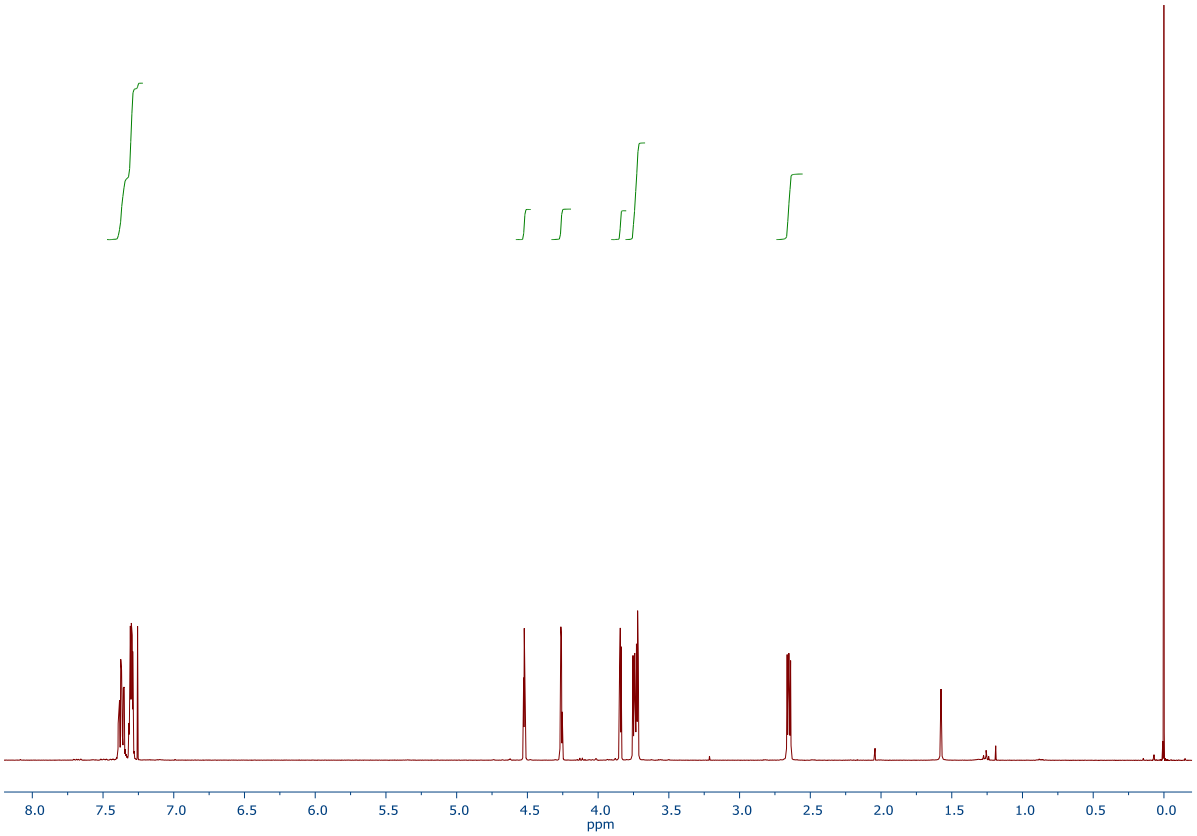

Figure S24. ^{1}H NMR spectrum (399.95 MHz, $CDCl_3$) of compound **1a**.

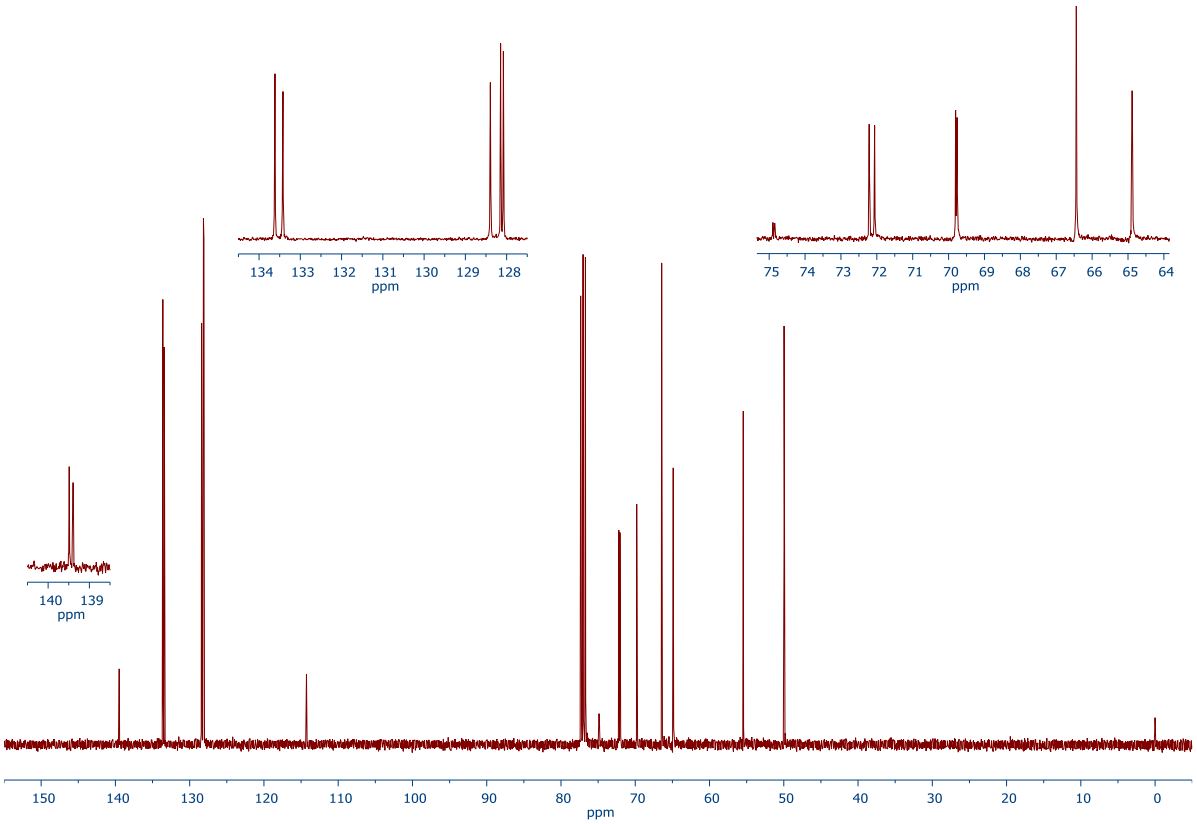

Figure S25. $^{13}C\{^{1}H\}$ NMR spectrum (100.58 MHz, $CDCl_3$) of compound **1a**.

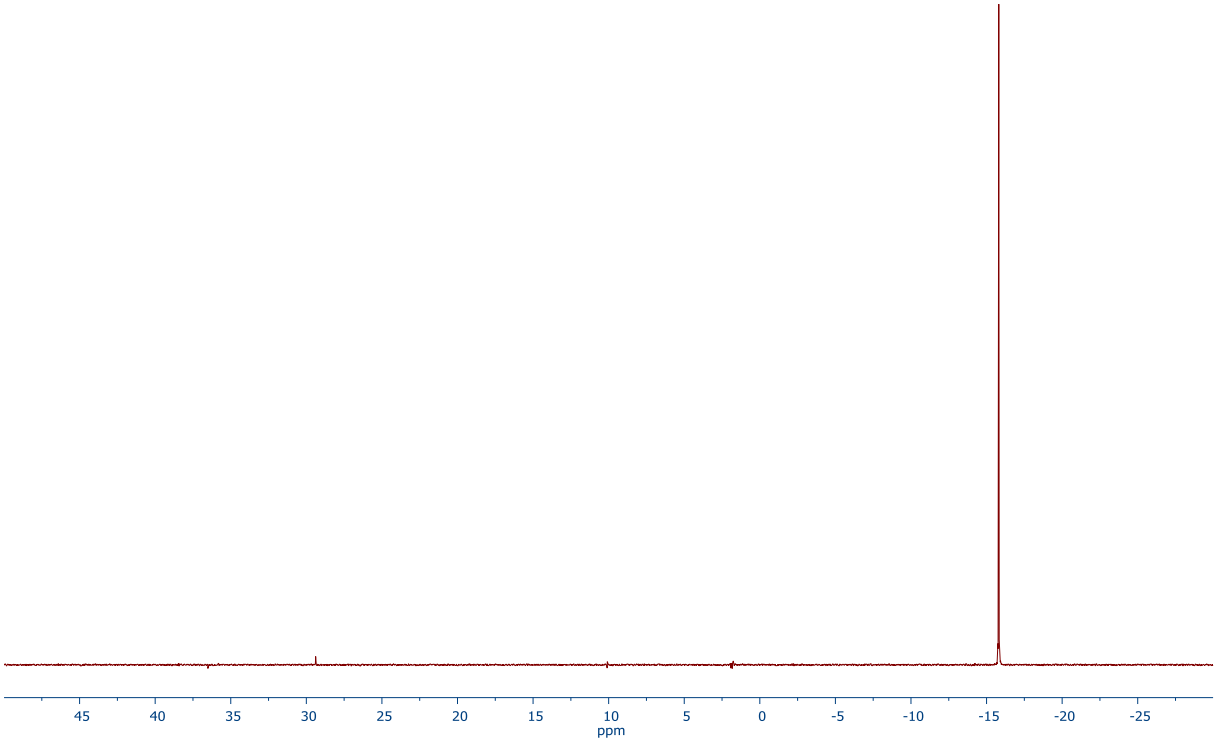

Figure S26. $^{31}P\{^{1}H\}$ NMR spectrum (161.90 MHz, $CDCl_3$) of compound **1a**.

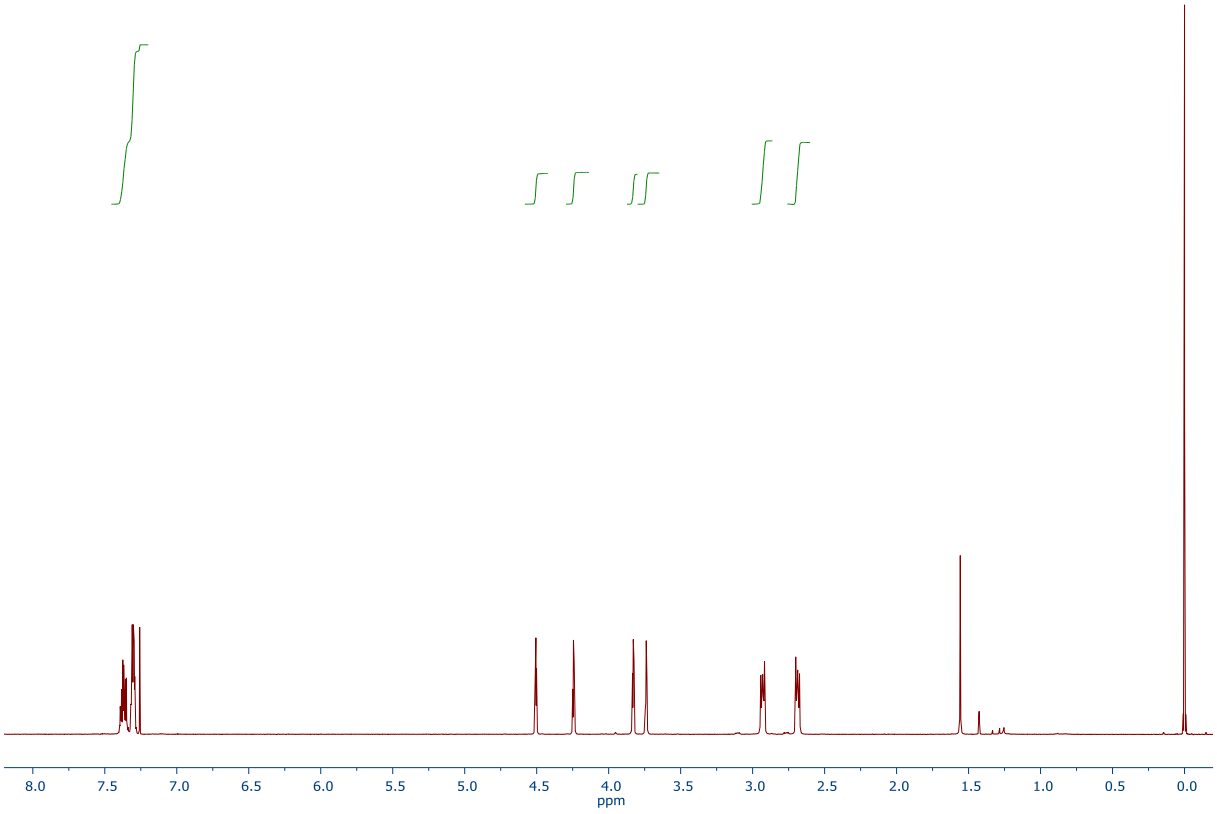

Figure S27. ^{1}H NMR spectrum (399.95 MHz, $CDCl_3$) of compound **1b**.

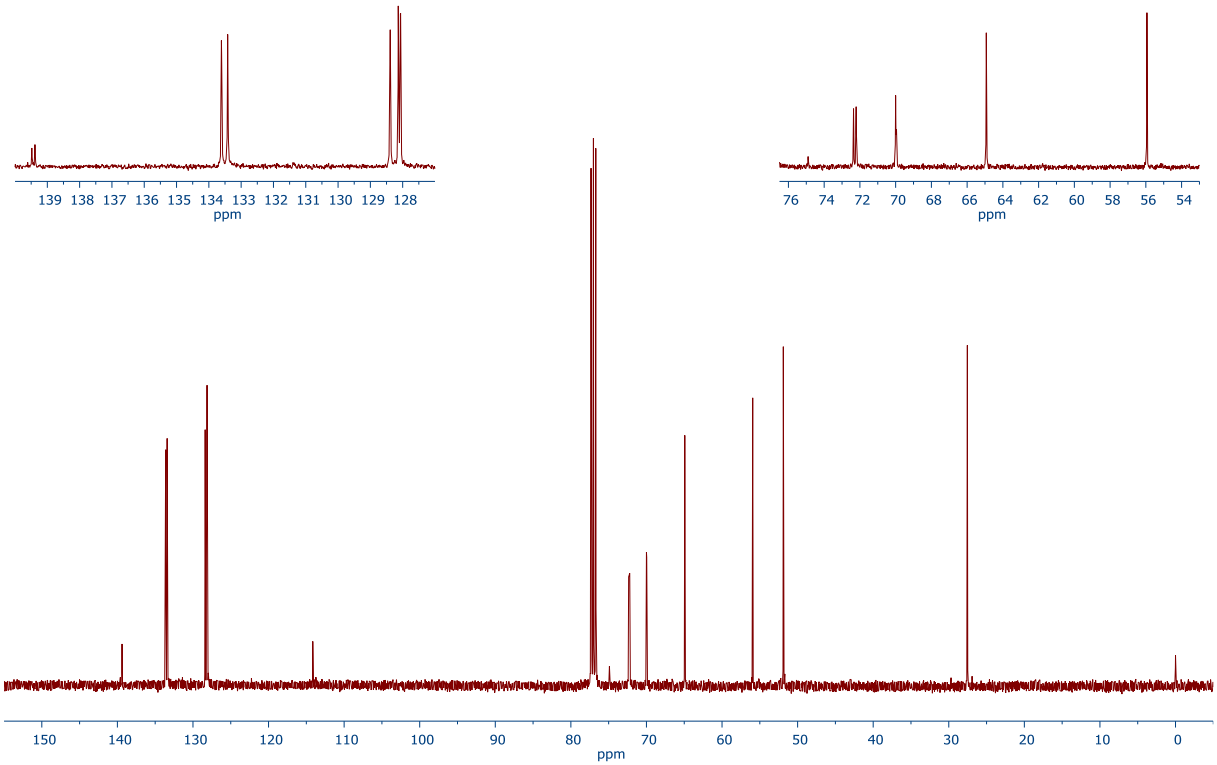

Figure S28. $^{13}C\{^{1}H\}$ NMR spectrum (100.58 MHz, $CDCl_3$) of compound **1b**.

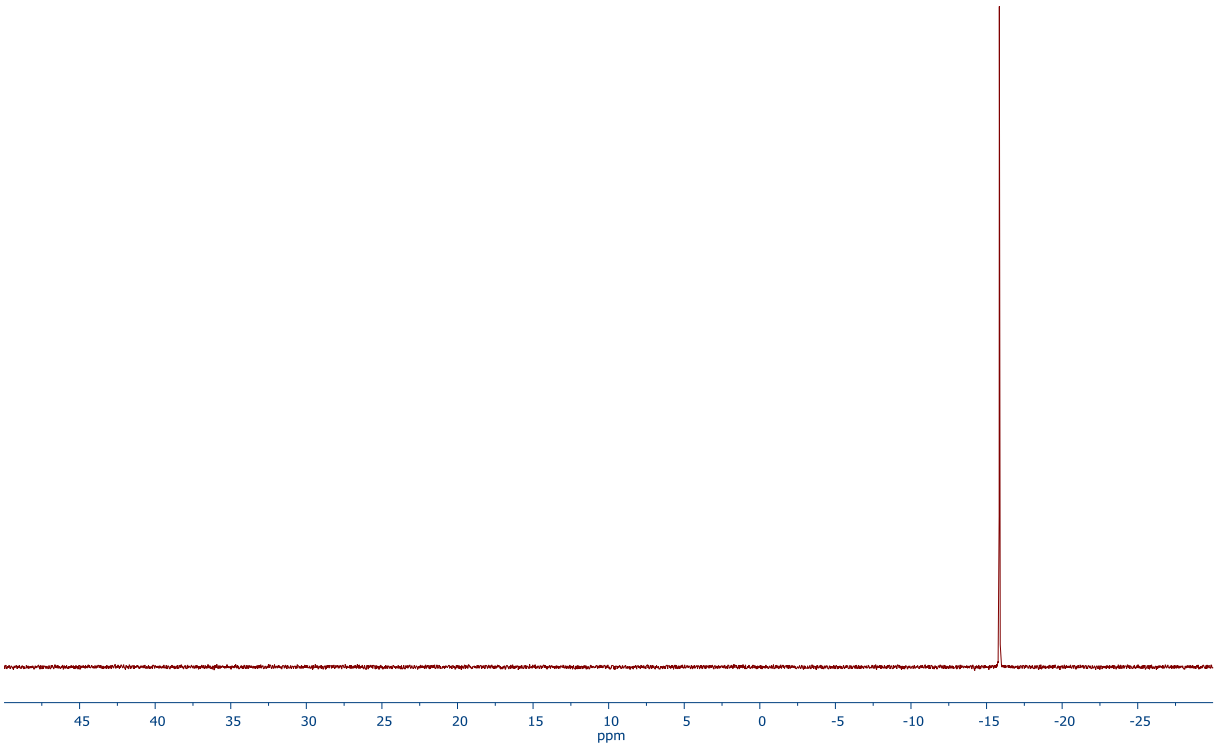

Figure S29. $^{31}P\{^{1}H\}$ NMR spectrum (161.90 MHz, $CDCl_3$) of compound **1b**.

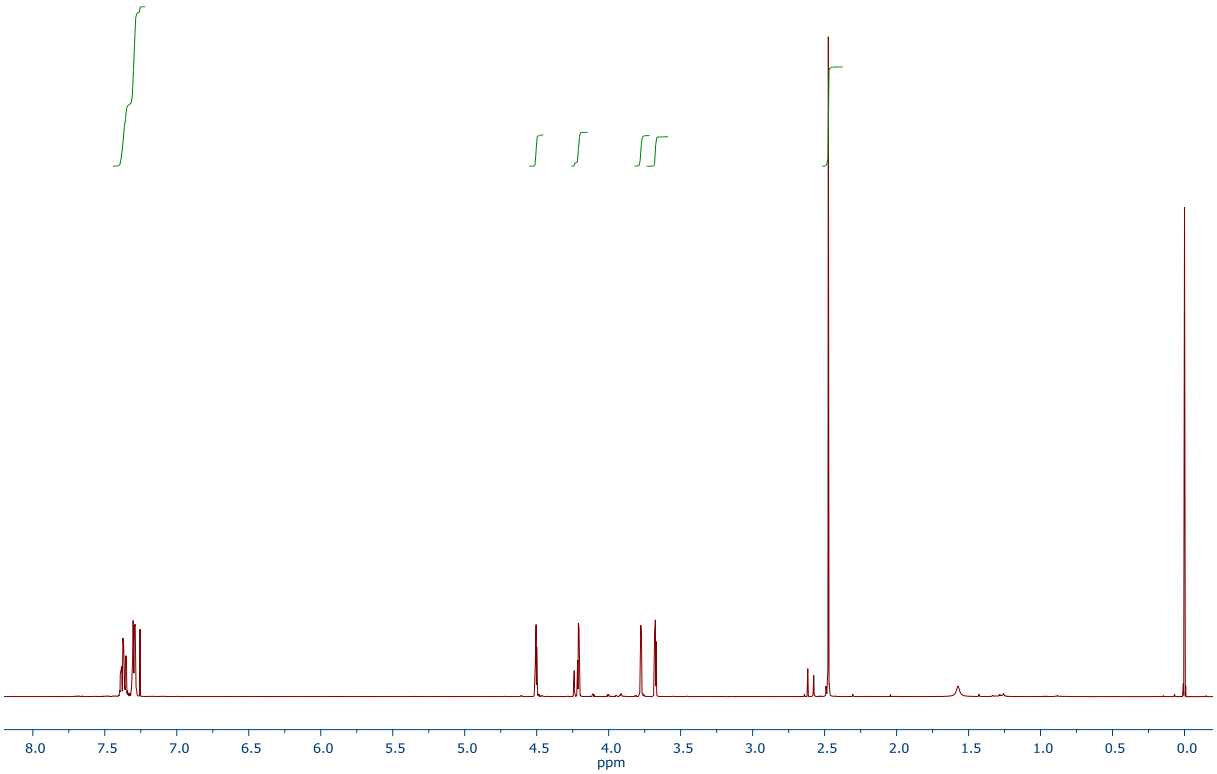

Figure S30. ^{1}H NMR spectrum (399.95 MHz, $CDCl_3$) of compound **1c**.

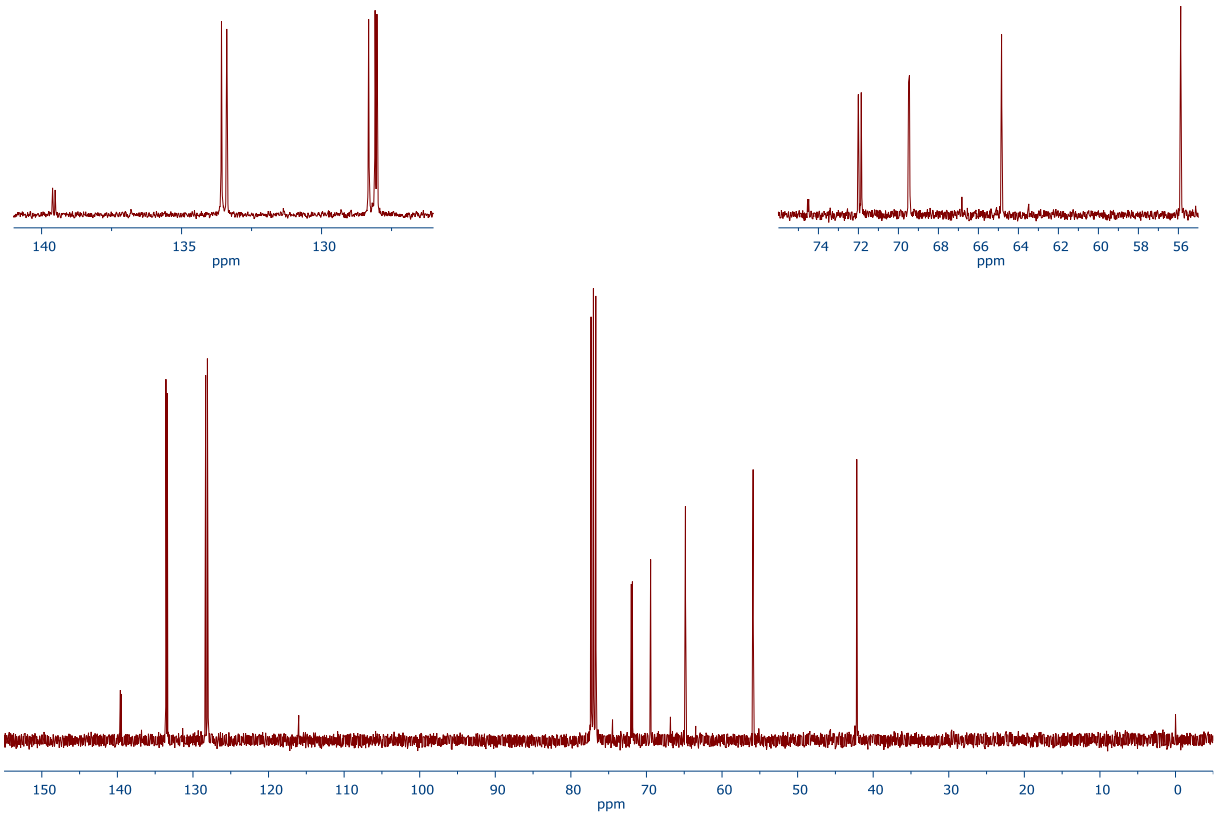

Figure S31. $^{13}C\{^{1}H\}$ NMR spectrum (100.58 MHz, $CDCl_3$) of compound **1c**.

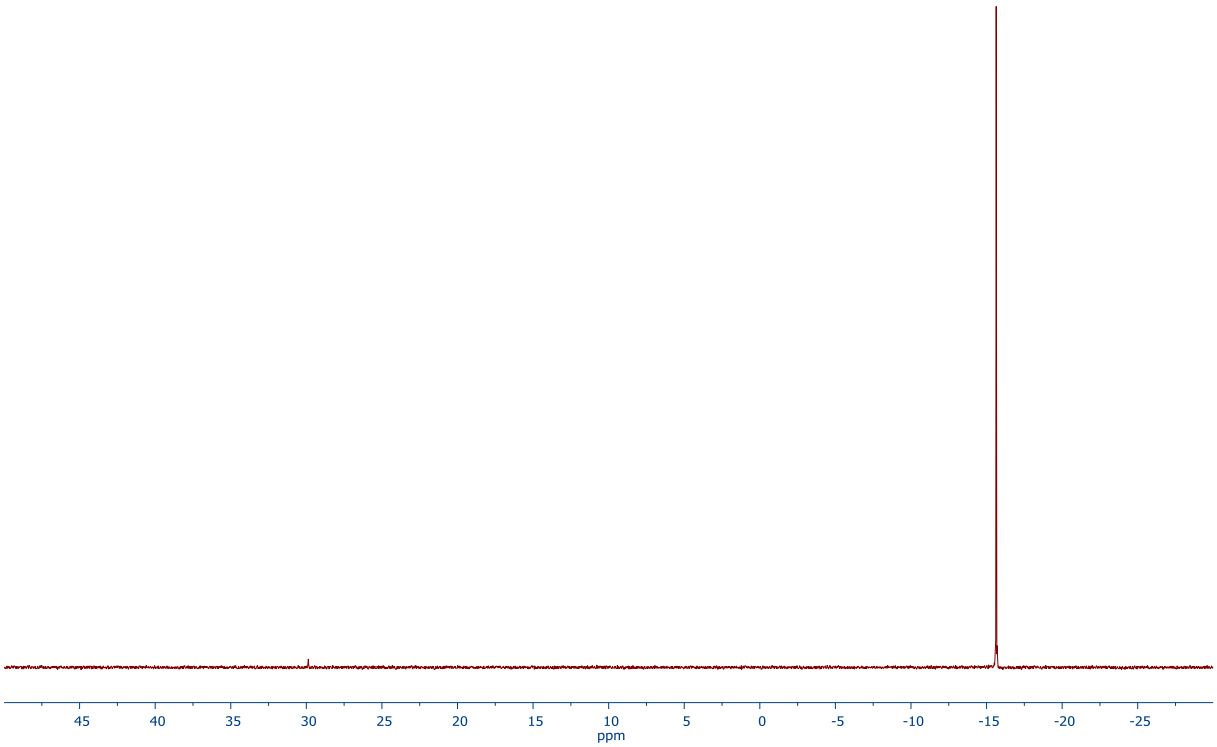

Figure S32. $^{31}P\{^{1}H\}$ NMR spectrum (161.90 MHz, $CDCl_3$) of compound **1c**.

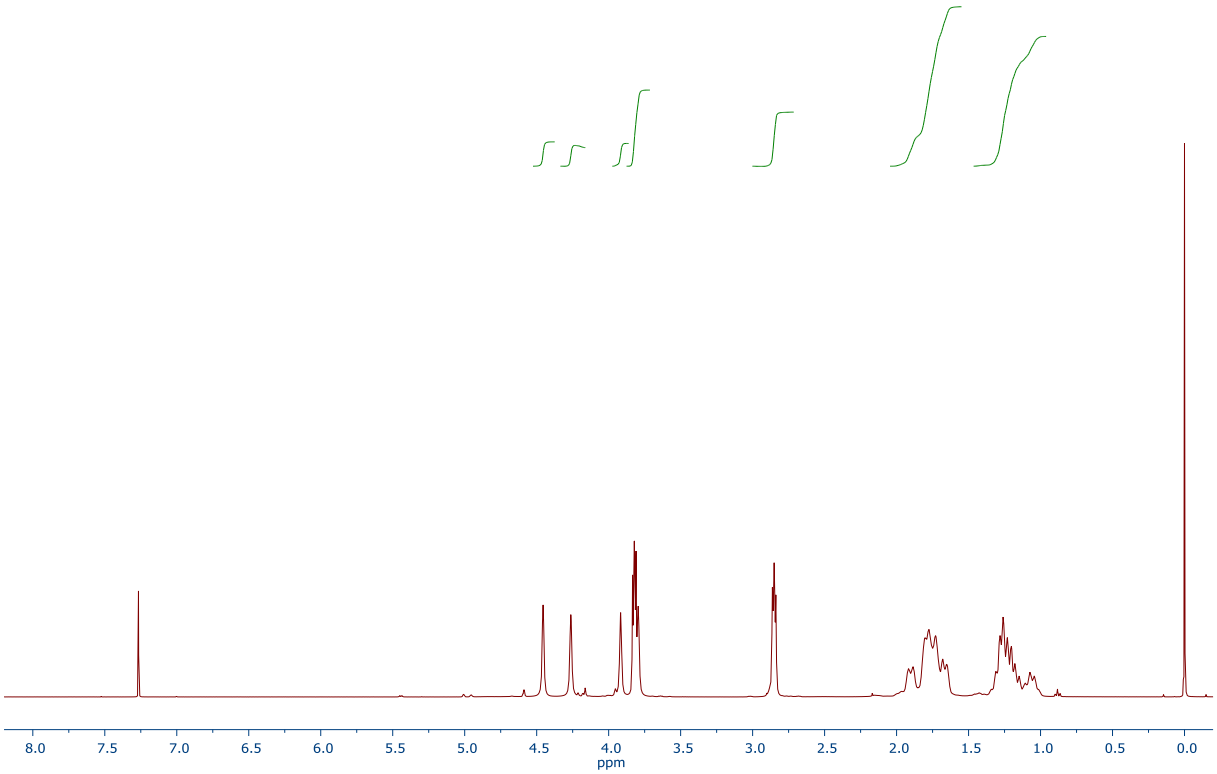

Figure S33. ^{1}H NMR spectrum (400.13 MHz, $CDCl_3$) of compound **2a**.

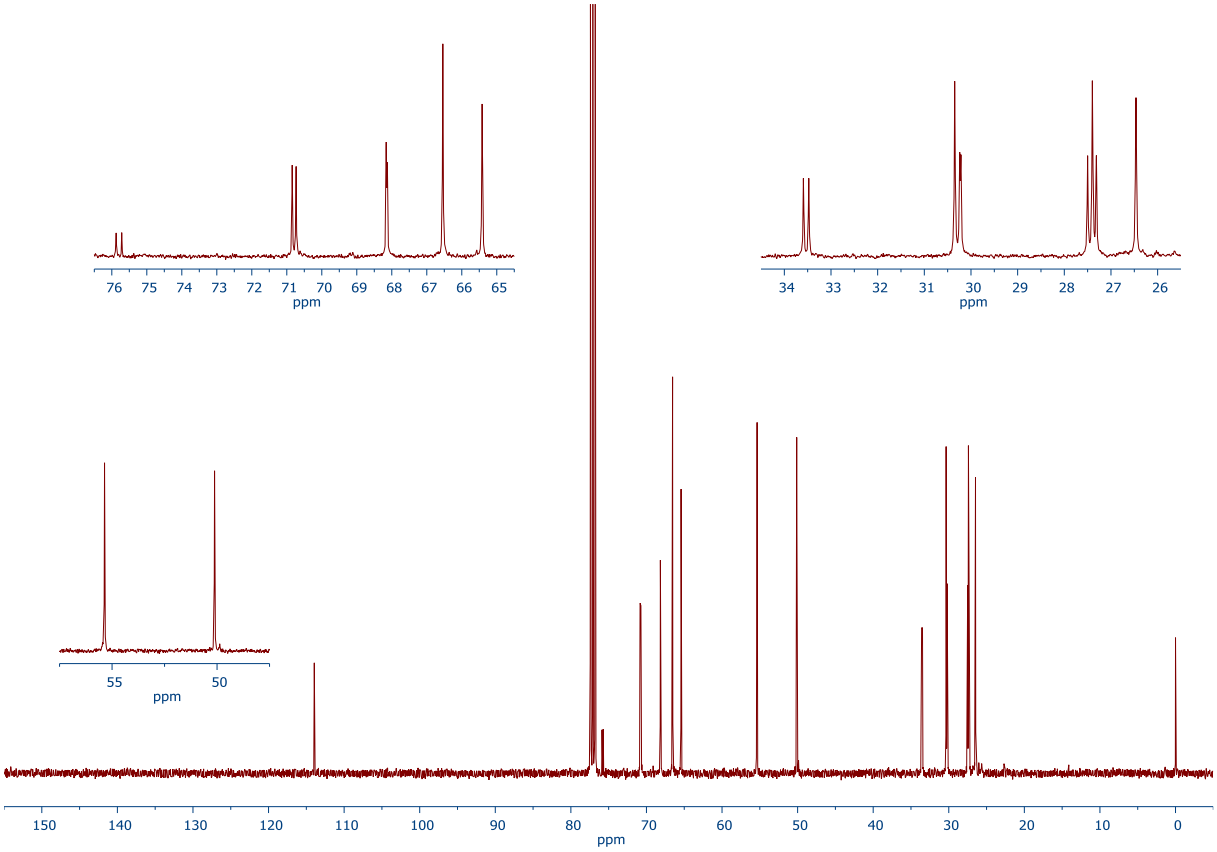

Figure S34. $^{13}C\{^{1}H\}$ NMR spectrum (100.62 MHz, $CDCl_3$) of compound **2a**.

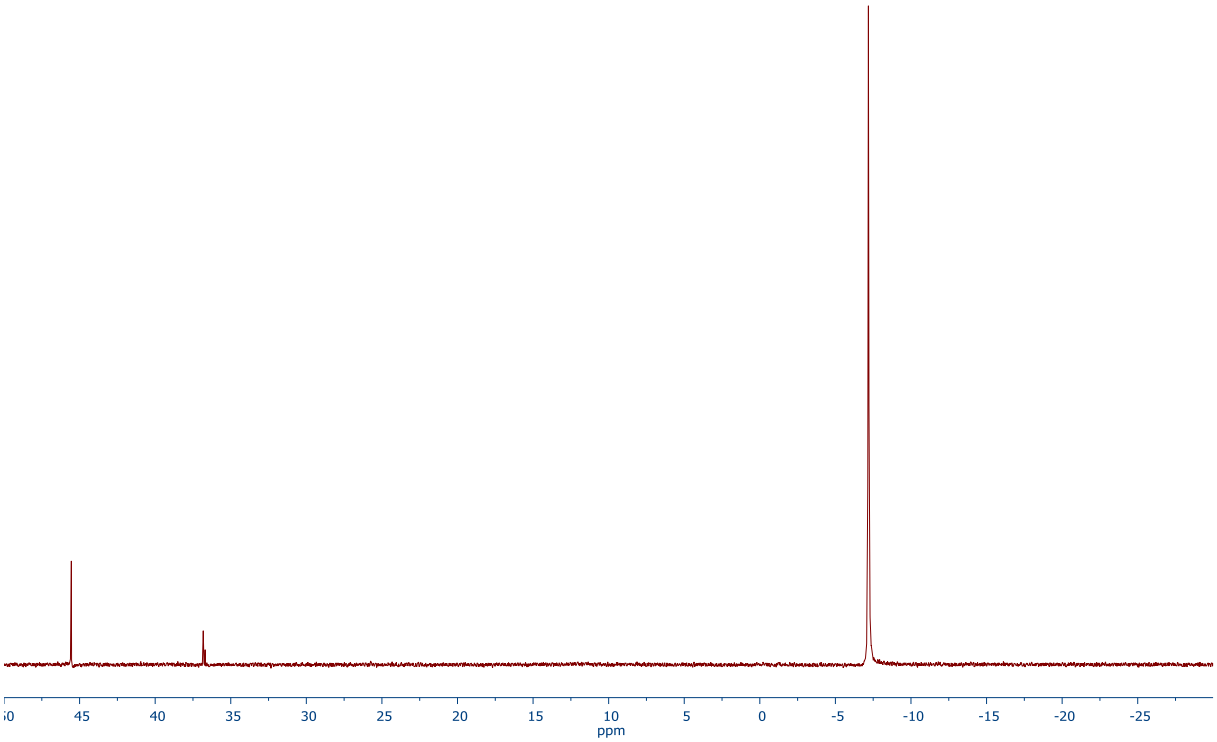

Figure S35. $^{31}P\{^{1}H\}$ NMR spectrum (161.97 MHz, $CDCl_3$) of compound **2a**.

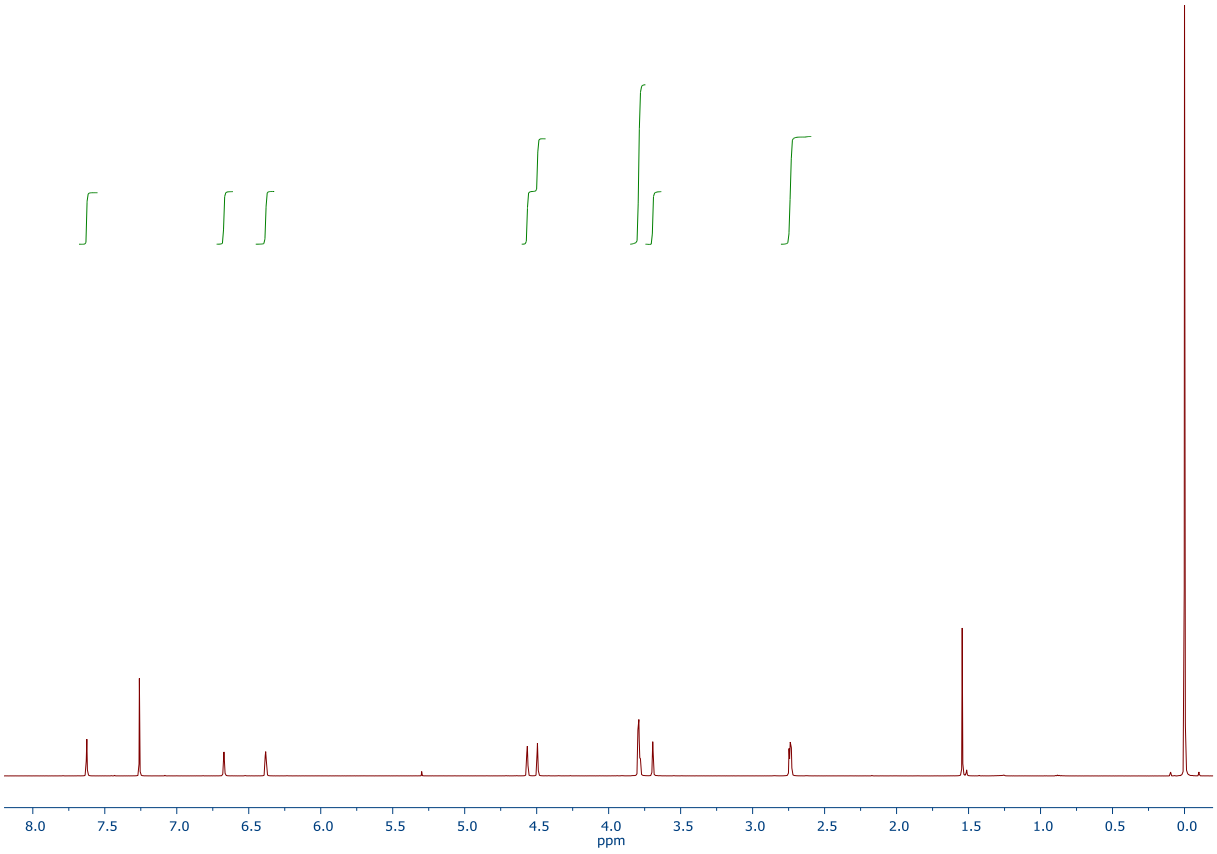

Figure S36. ^{1}H NMR spectrum (399.95 MHz, $CDCl_3$) of compound **3a**.

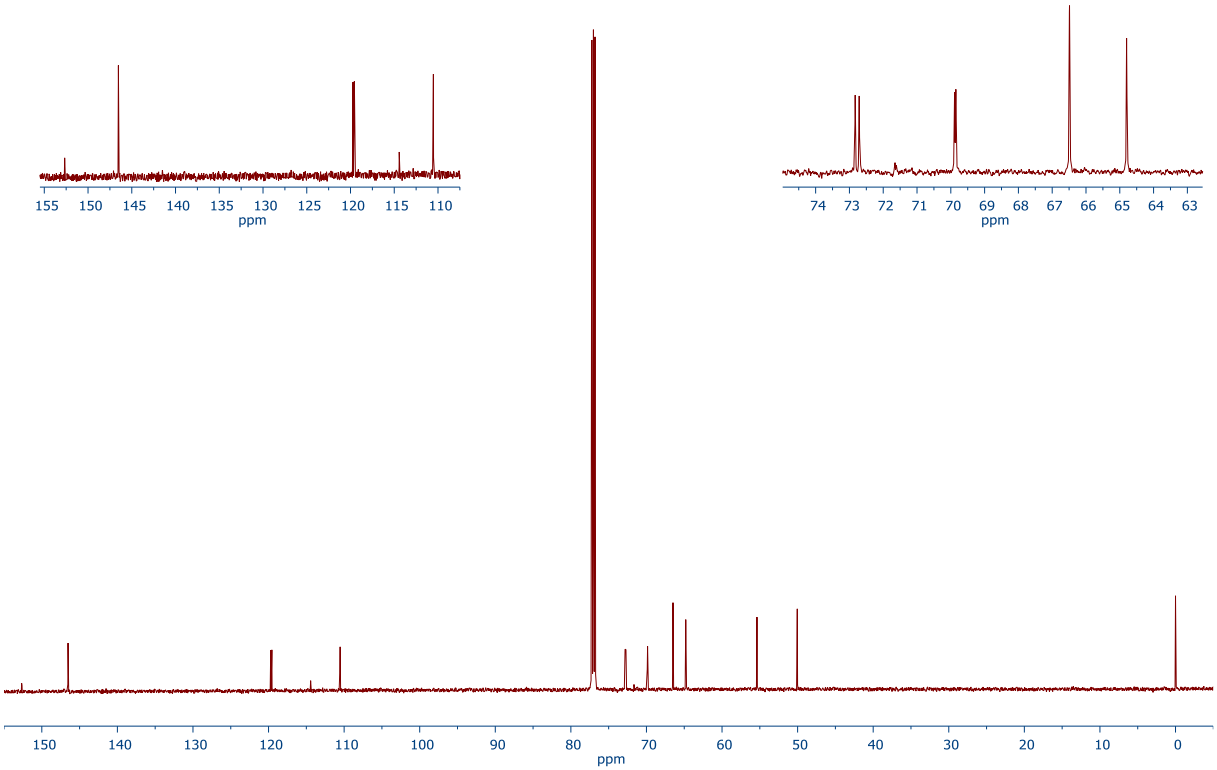

Figure S37. $^{13}C\{^{1}H\}$ NMR spectrum (100.58 MHz, $CDCl_3$) of compound **3a**.

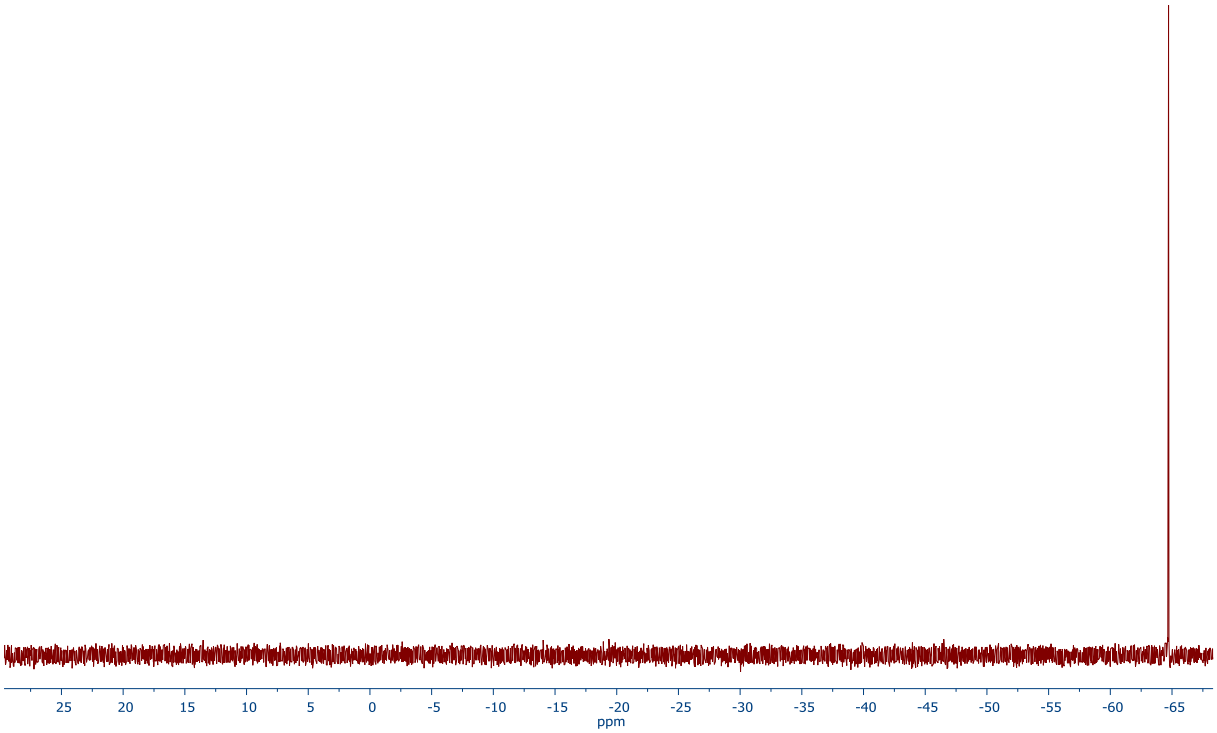

Figure S38. $^{31}P\{^{1}H\}$ NMR spectrum (161.90 MHz, $CDCl_3$) of compound **3a**.

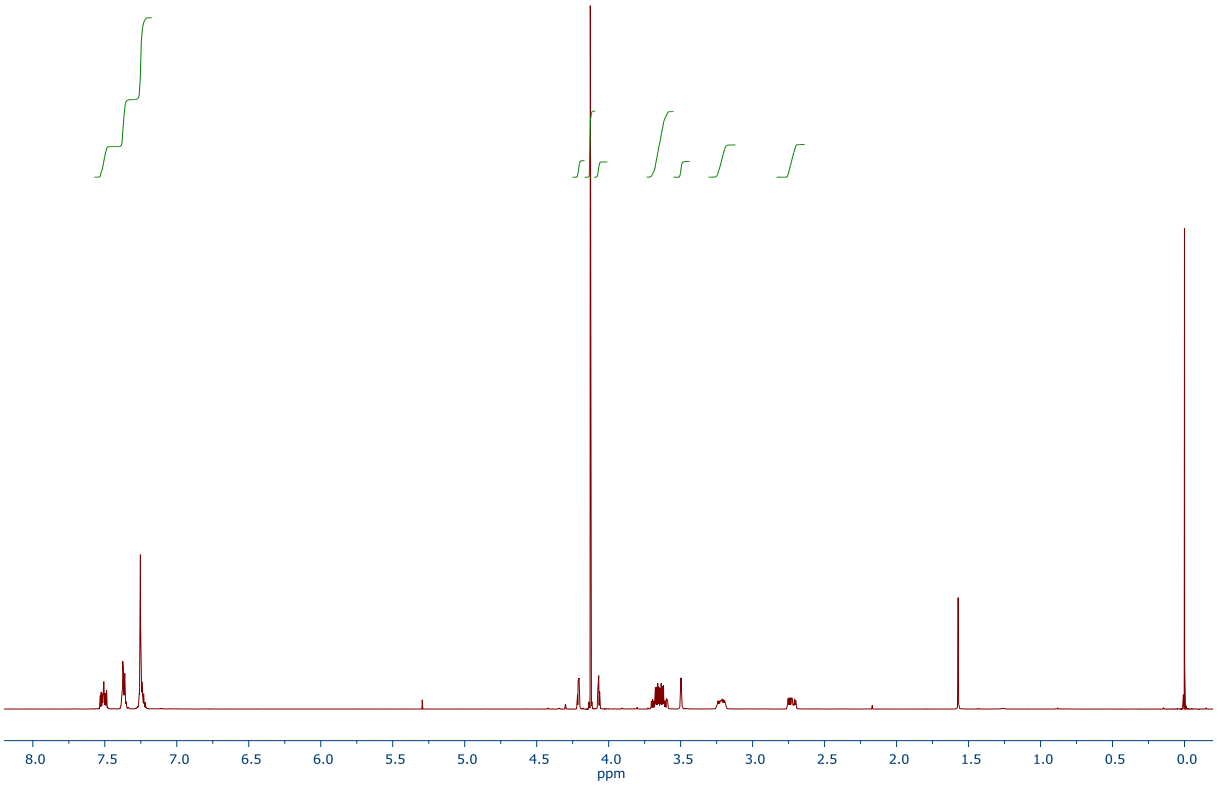

Figure S39. ^{1}H NMR spectrum (399.95 MHz, $CDCl_3$) of compound **4a**.

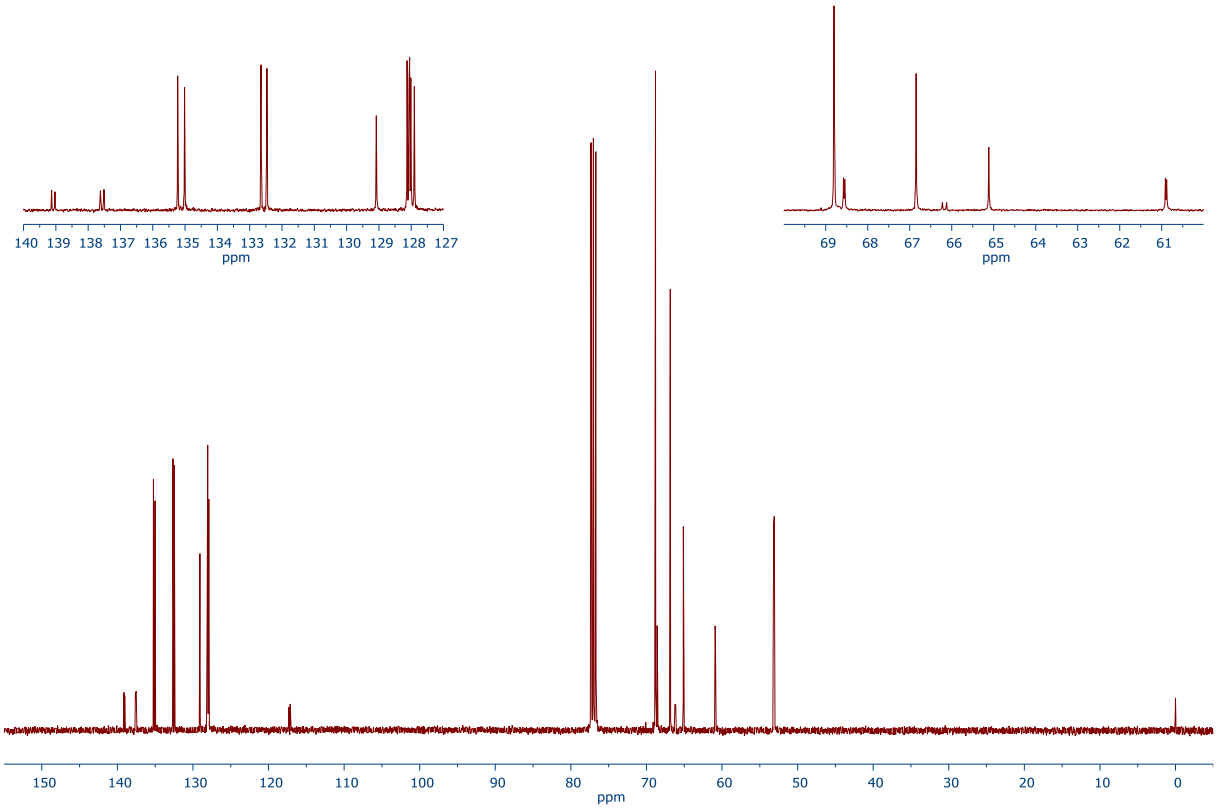

Figure S40. $^{13}C\{^{1}H\}$ NMR spectrum (100.58 MHz, $CDCl_3$) of compound **4a**.

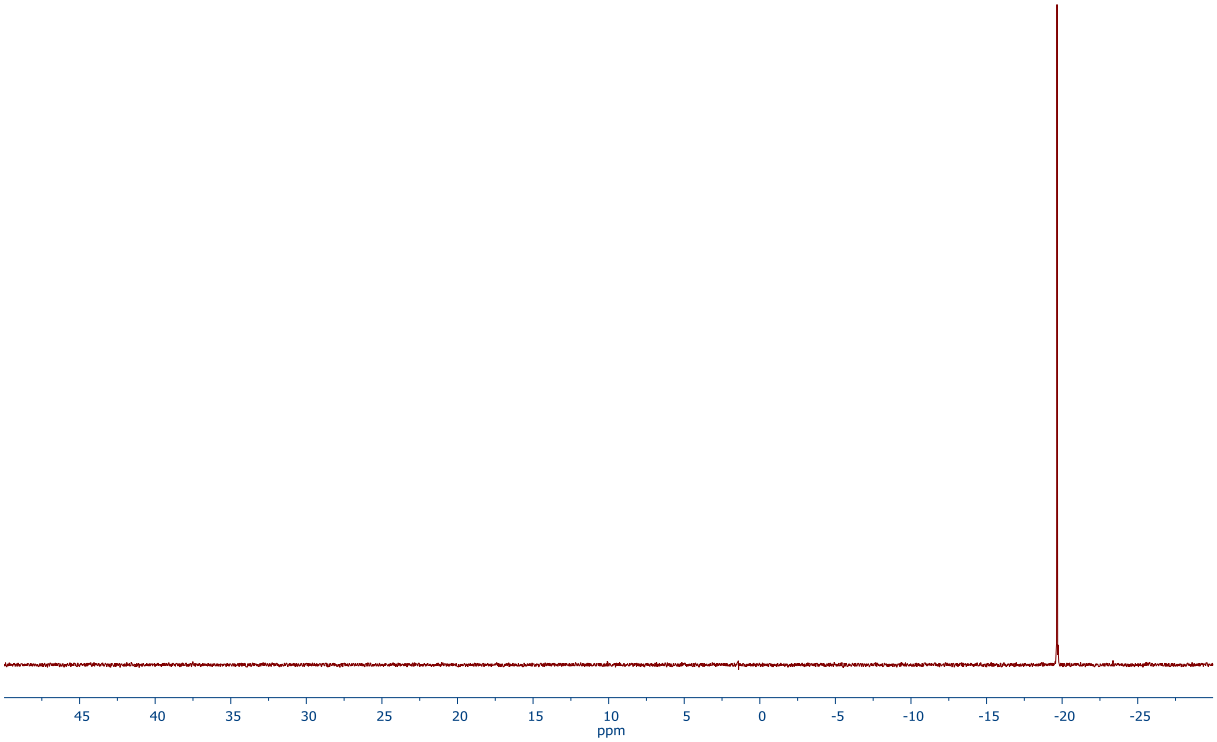

Figure S41. $^{31}P\{^{1}H\}$ NMR spectrum (161.90 MHz, $CDCl_3$) of compound **4a**.

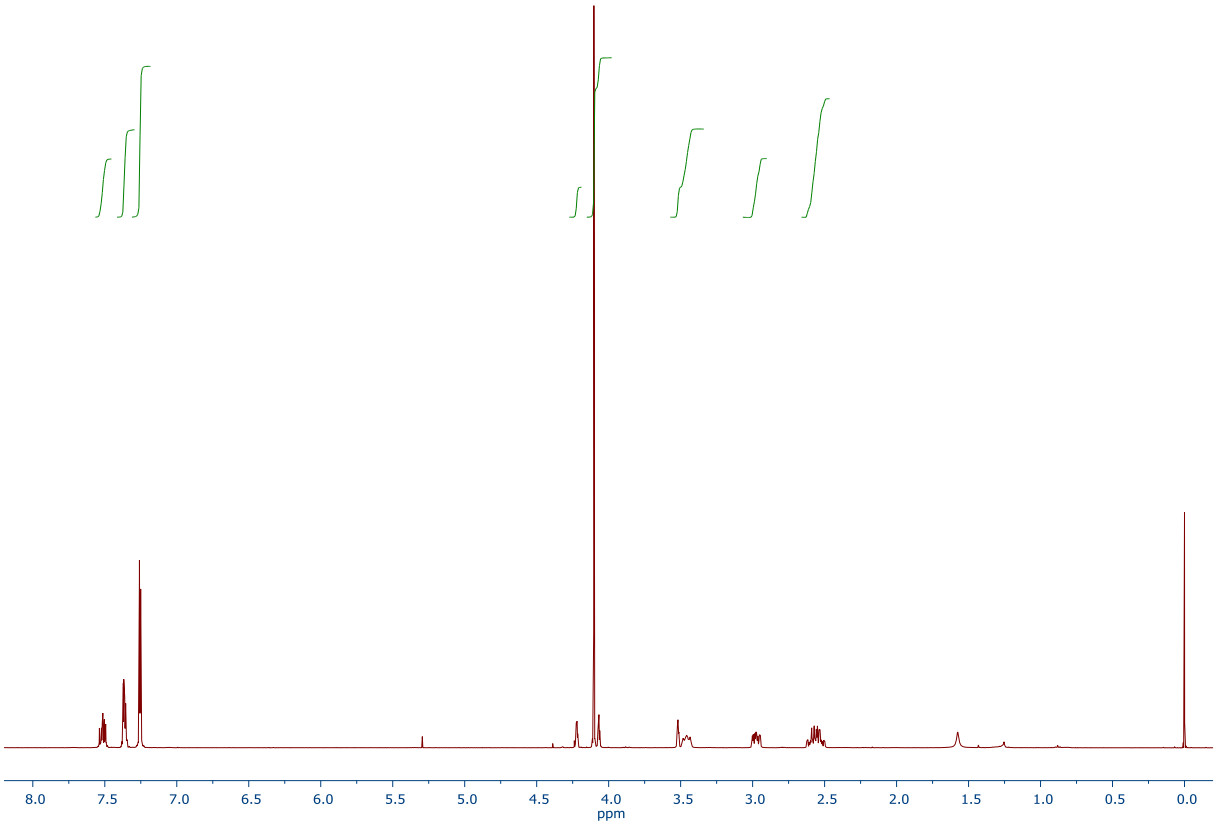

Figure S42. ^{1}H NMR spectrum (399.95 MHz, $CDCl_3$) of compound **4b**.

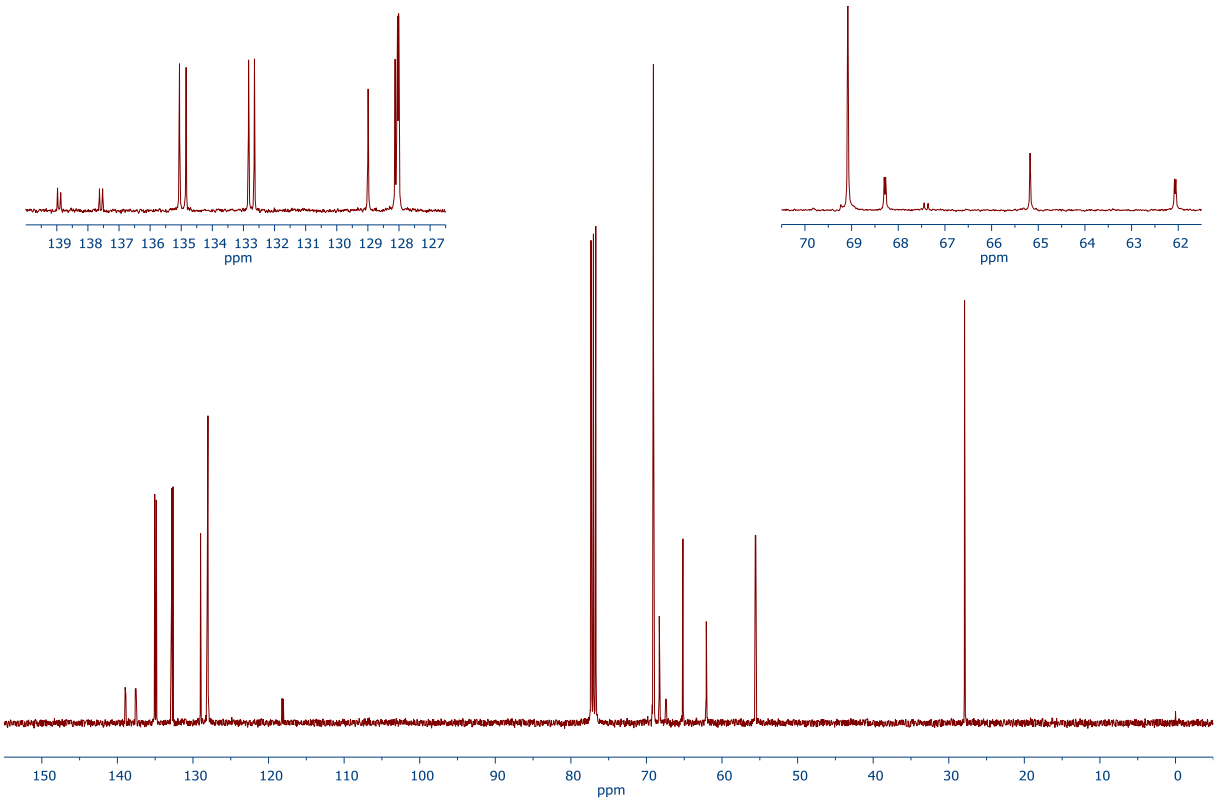

Figure S43. $^{13}C\{^{1}H\}$ NMR spectrum (100.58 MHz, $CDCl_3$) of compound **4b**.

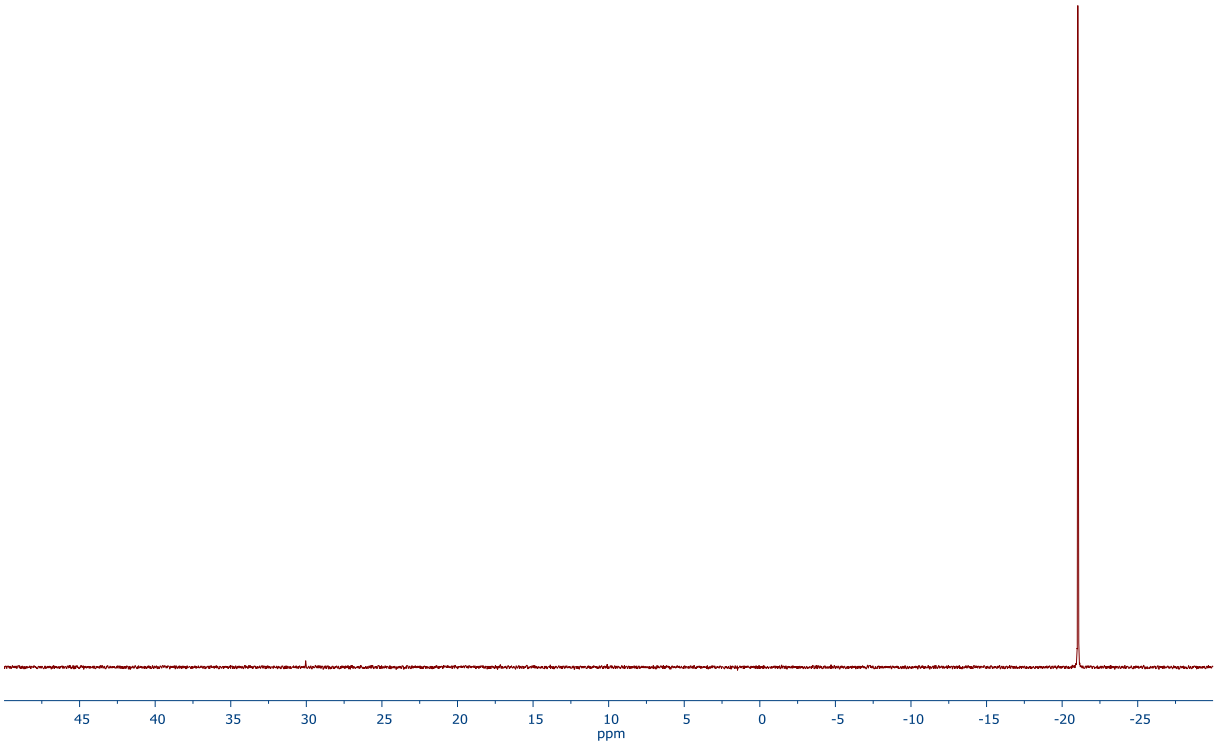

Figure S44. $^{31}P\{^{1}H\}$ NMR spectrum (161.90 MHz, $CDCl_3$) of compound **4b**.

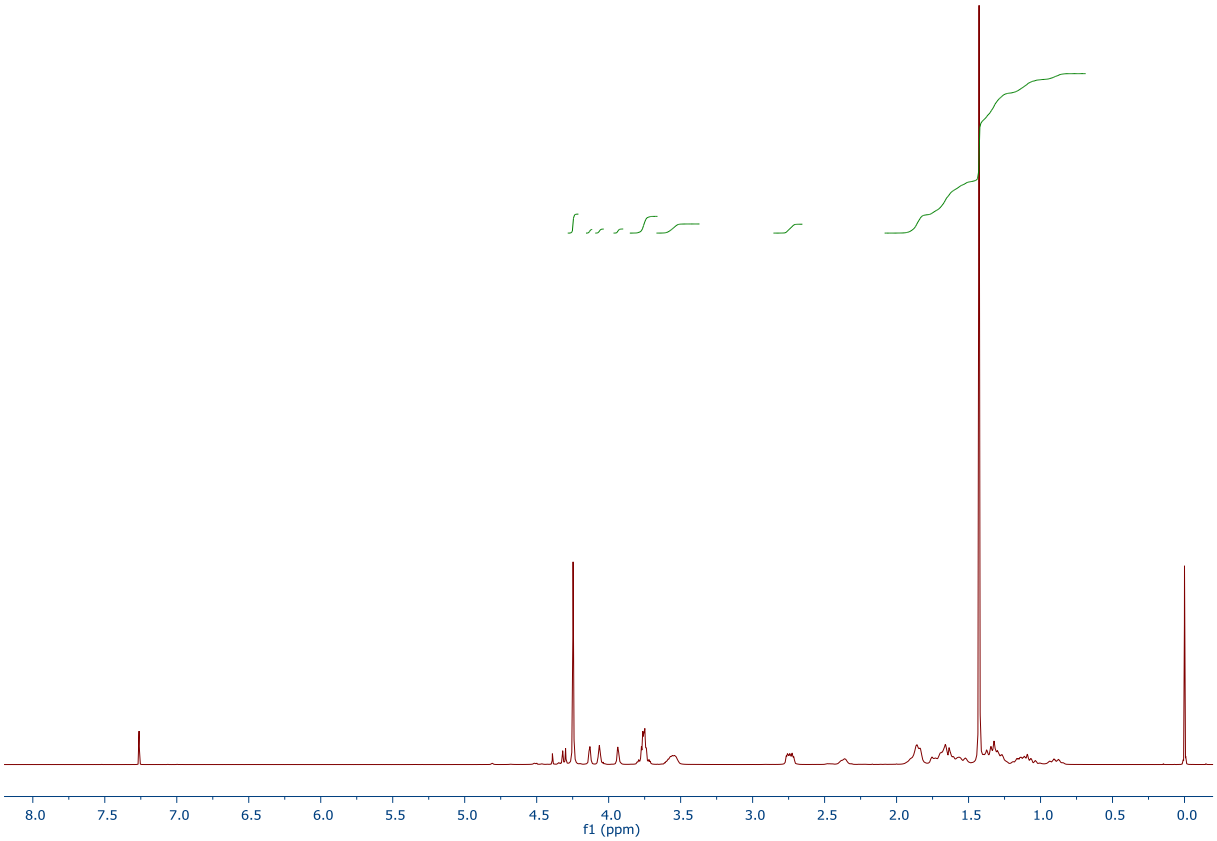

Figure S45. ^{1}H NMR spectrum (399.95 MHz, $CDCl_3$) of compound **5a**.

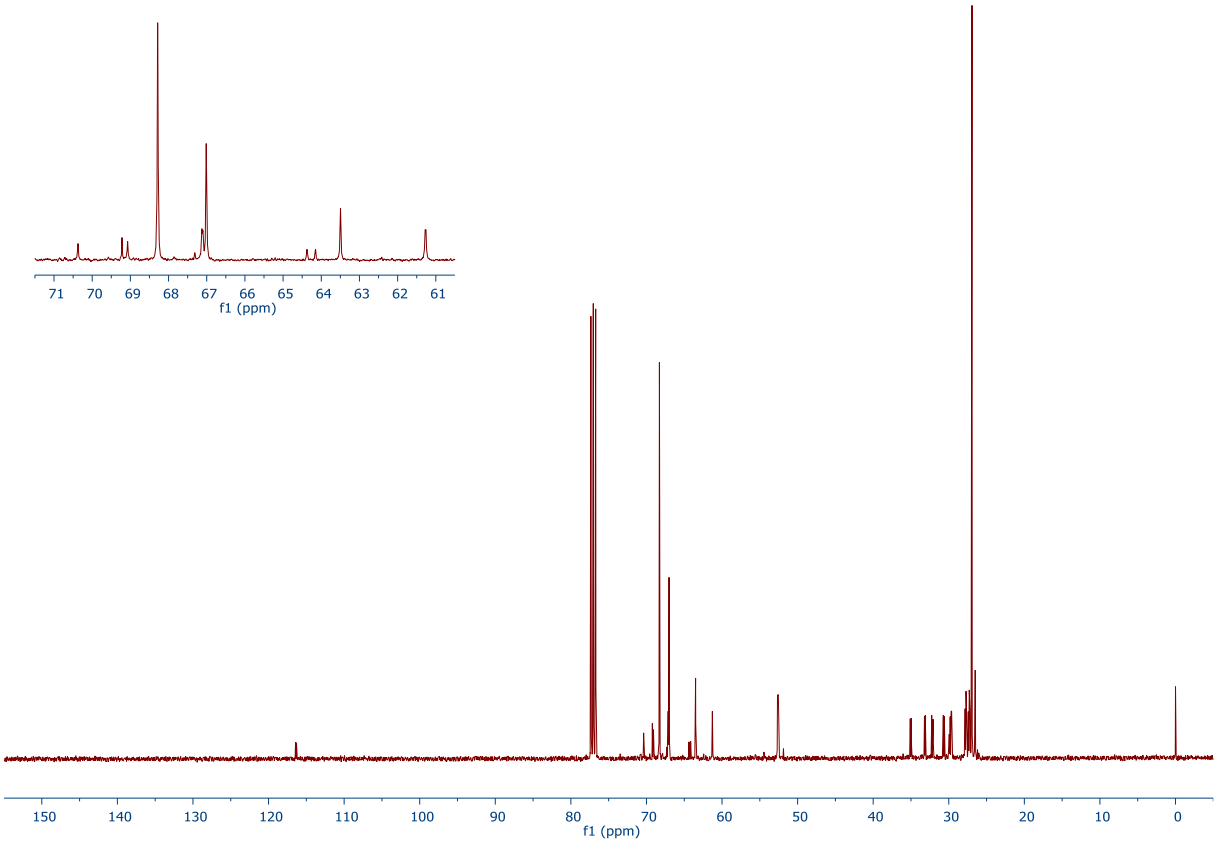

Figure S46. $^{13}C\{^{1}H\}$ NMR spectrum (100.58 MHz, $CDCl_3$) of compound **5a**.

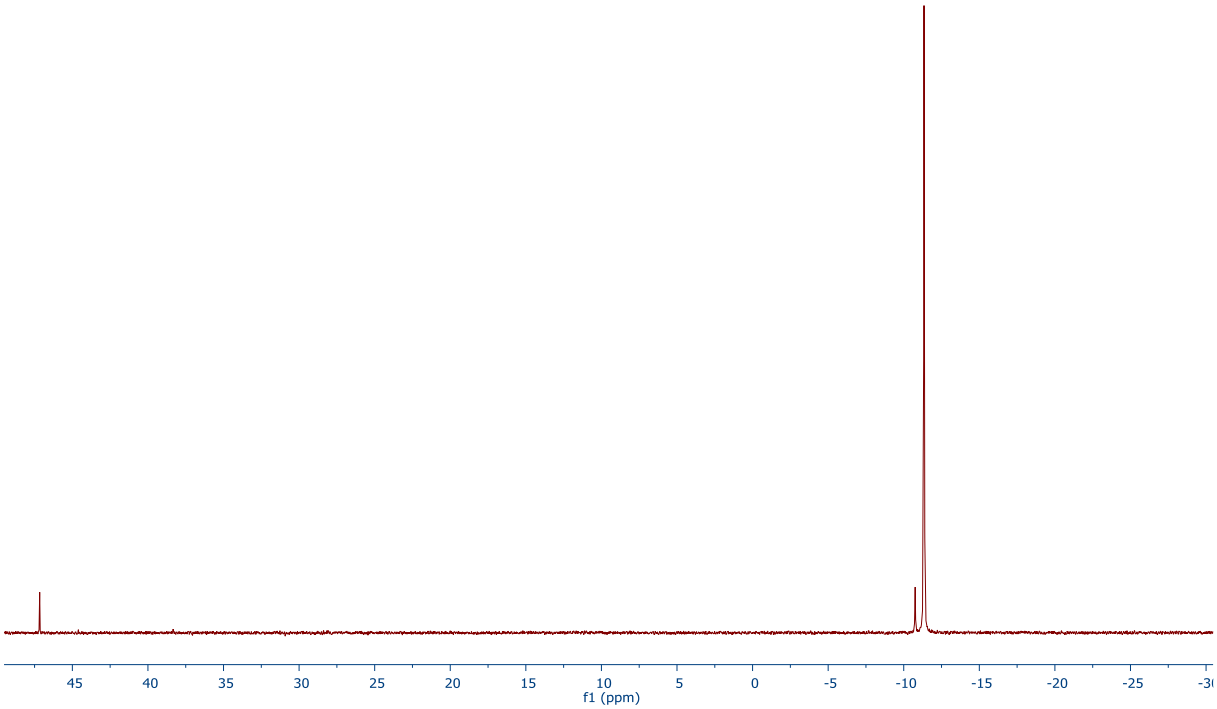

Figure S47. $^{31}P\{^{1}H\}$ NMR spectrum (161.90 MHz, $CDCl_3$) of compound **5a.**

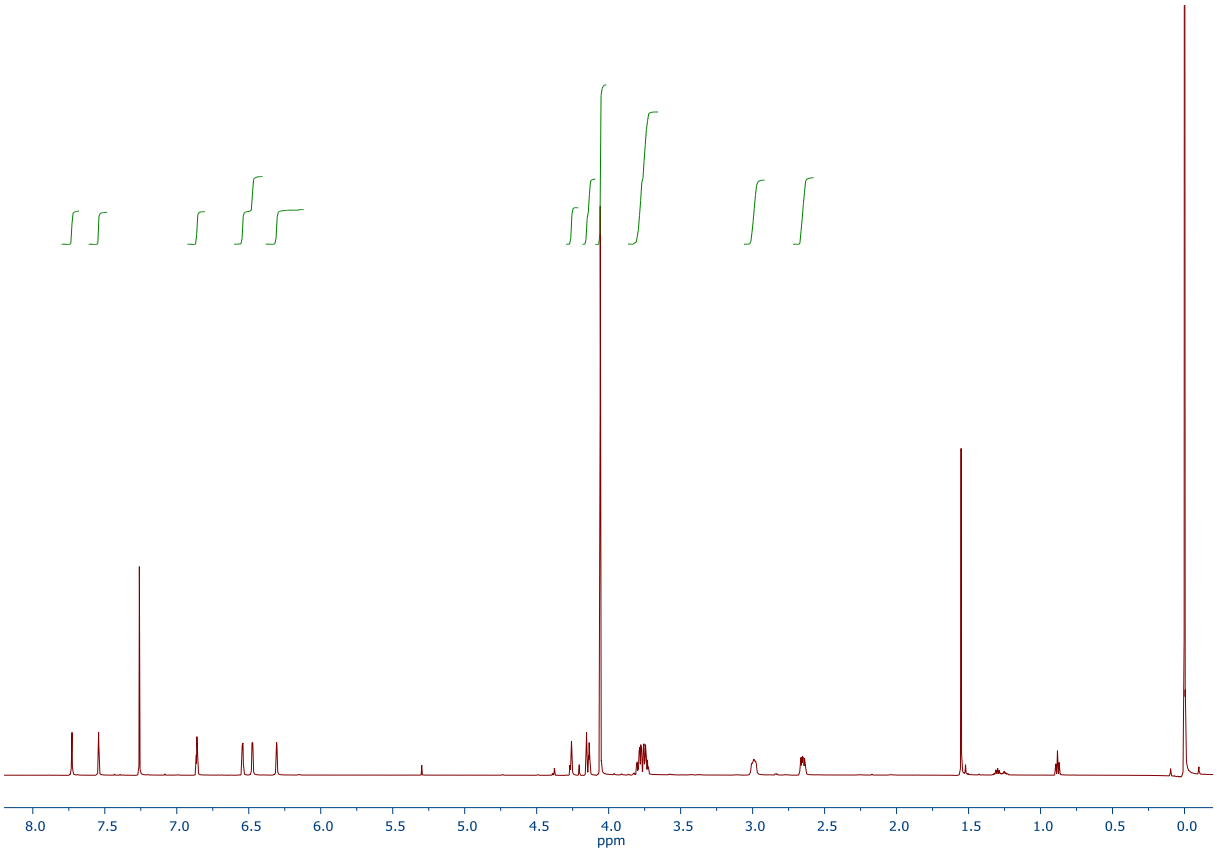

Figure S48. ^{1}H NMR spectrum (600.17 MHz, $CDCl_3$) of compound **6a**.

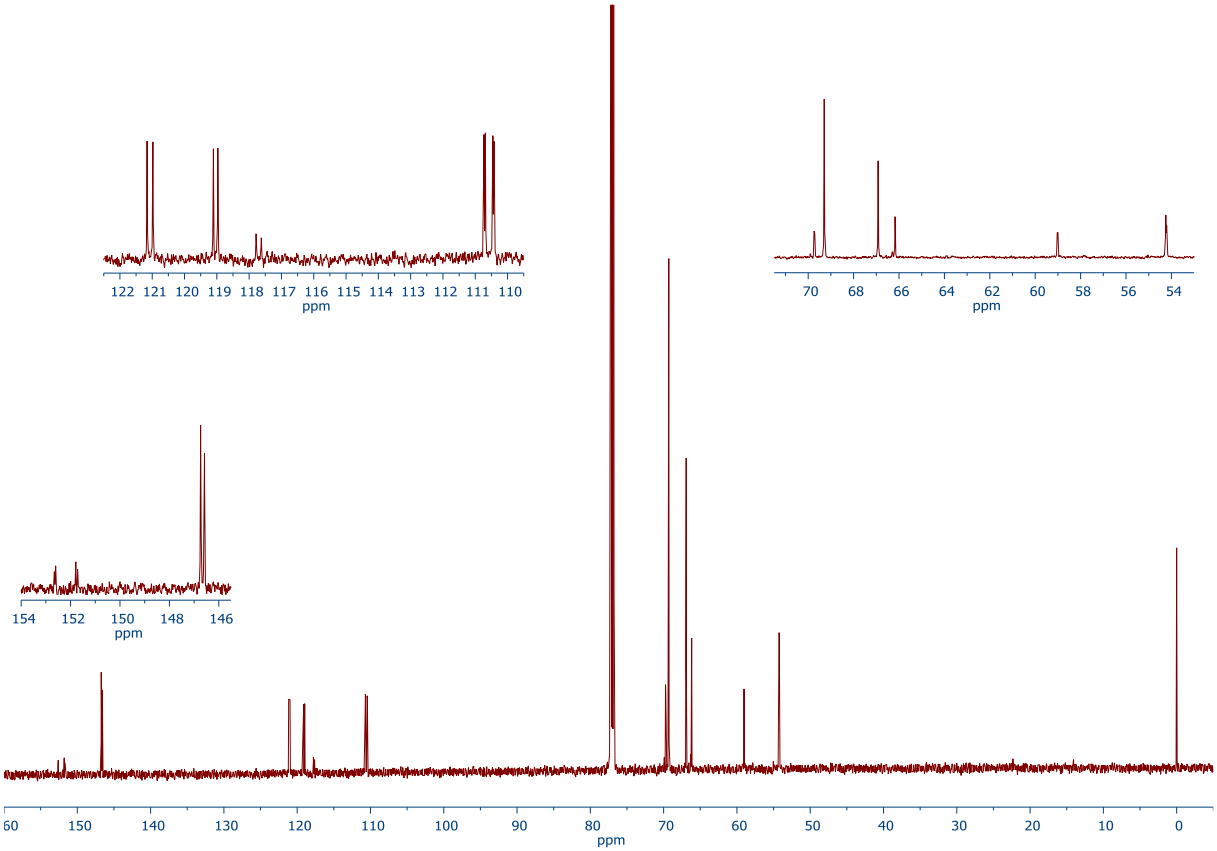

Figure S49. $^{13}C\{^{1}H\}$ NMR spectrum (150.93 MHz, $CDCl_3$) of compound **6a**.

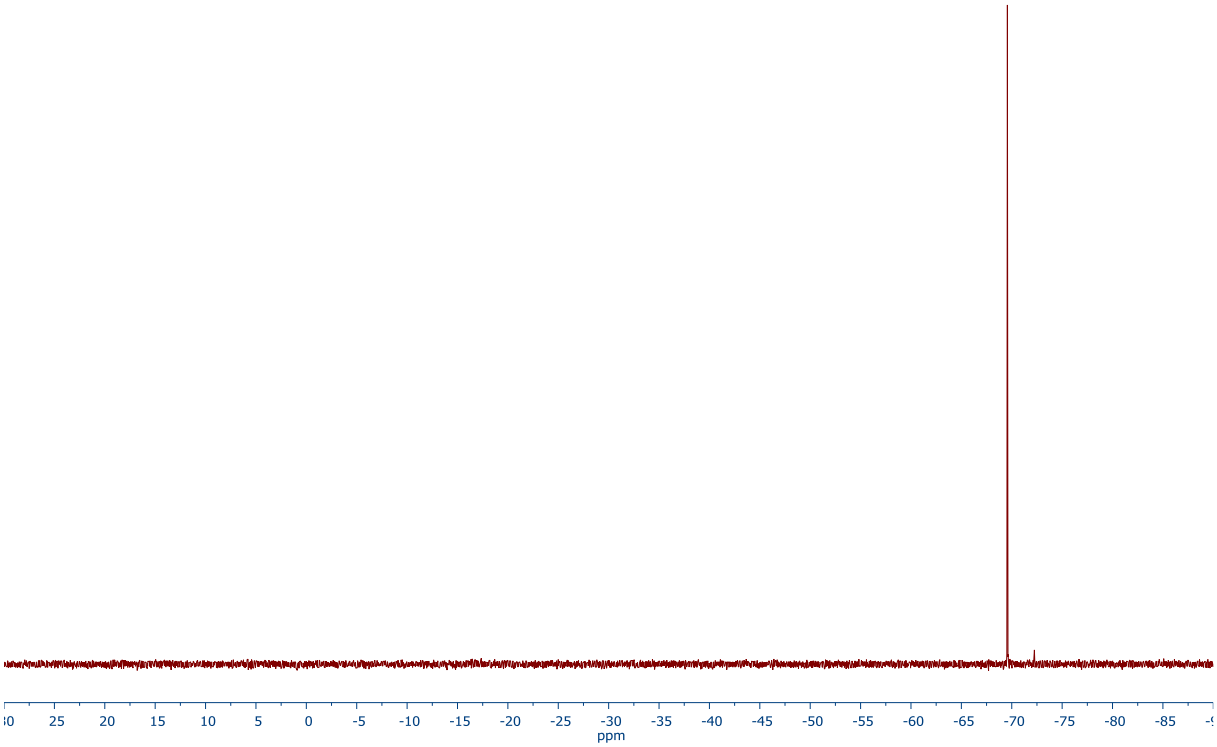

Figure S50. $^{31}P\{^{1}H\}$ NMR spectrum (161.90 MHz, $CDCl_3$) of compound **6a**.

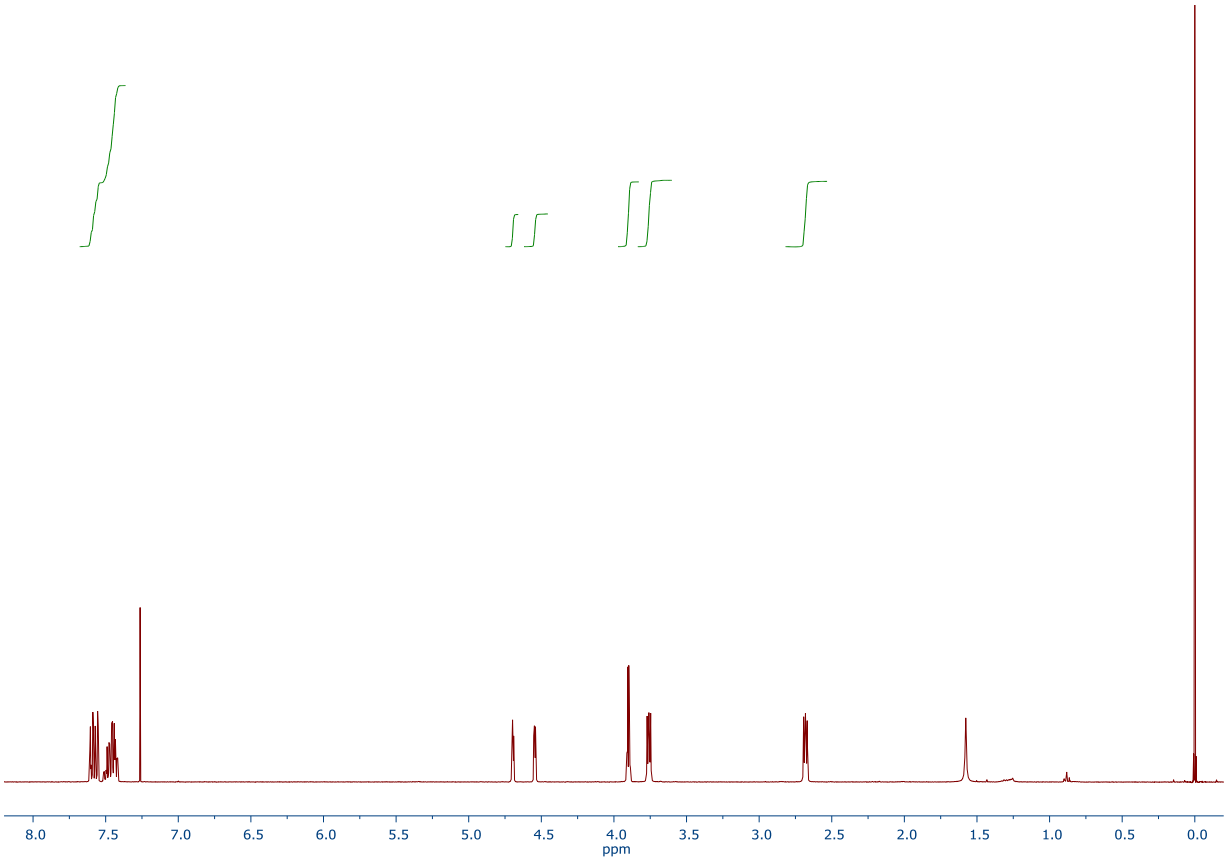

Figure S51. ^{1}H NMR spectrum (399.95 MHz, $CDCl_3$) of compound **1aAu**.

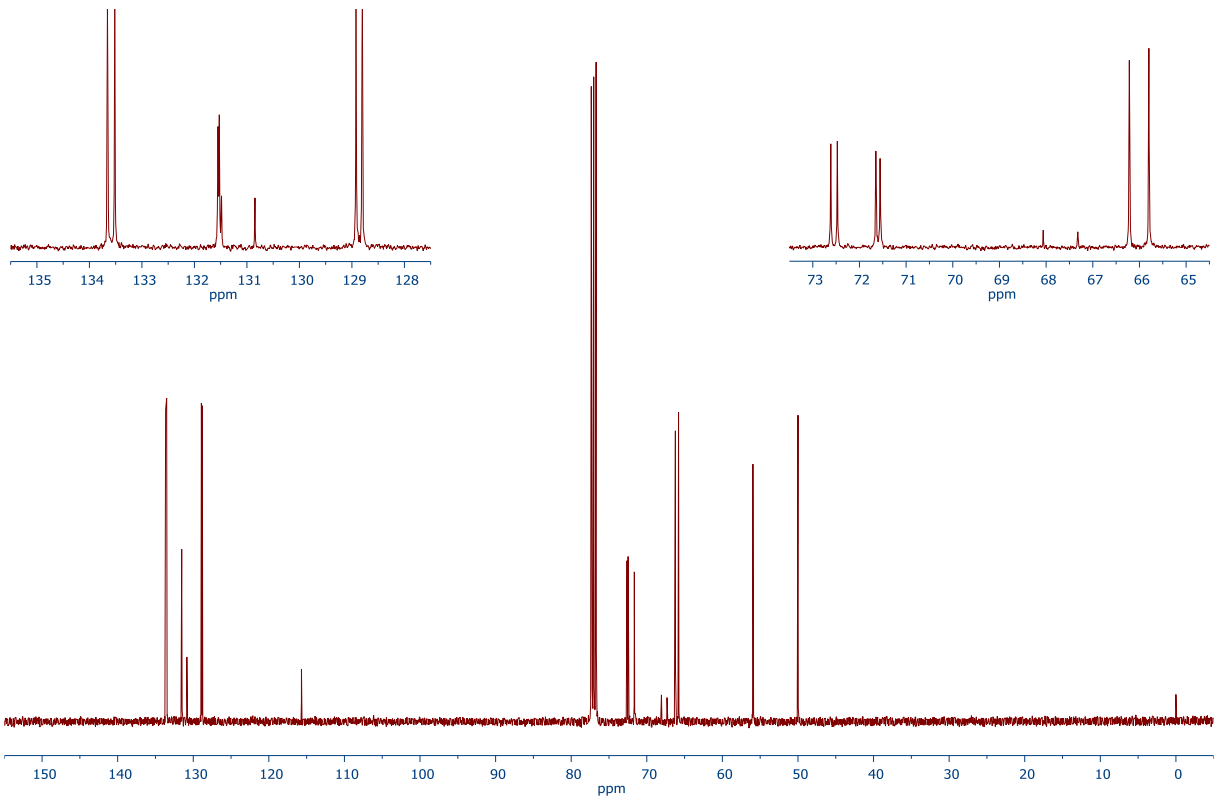

Figure S52. $^{13}C\{^{1}H\}$ NMR spectrum (100.58 MHz, $CDCl_3$) of compound **1aAu**.

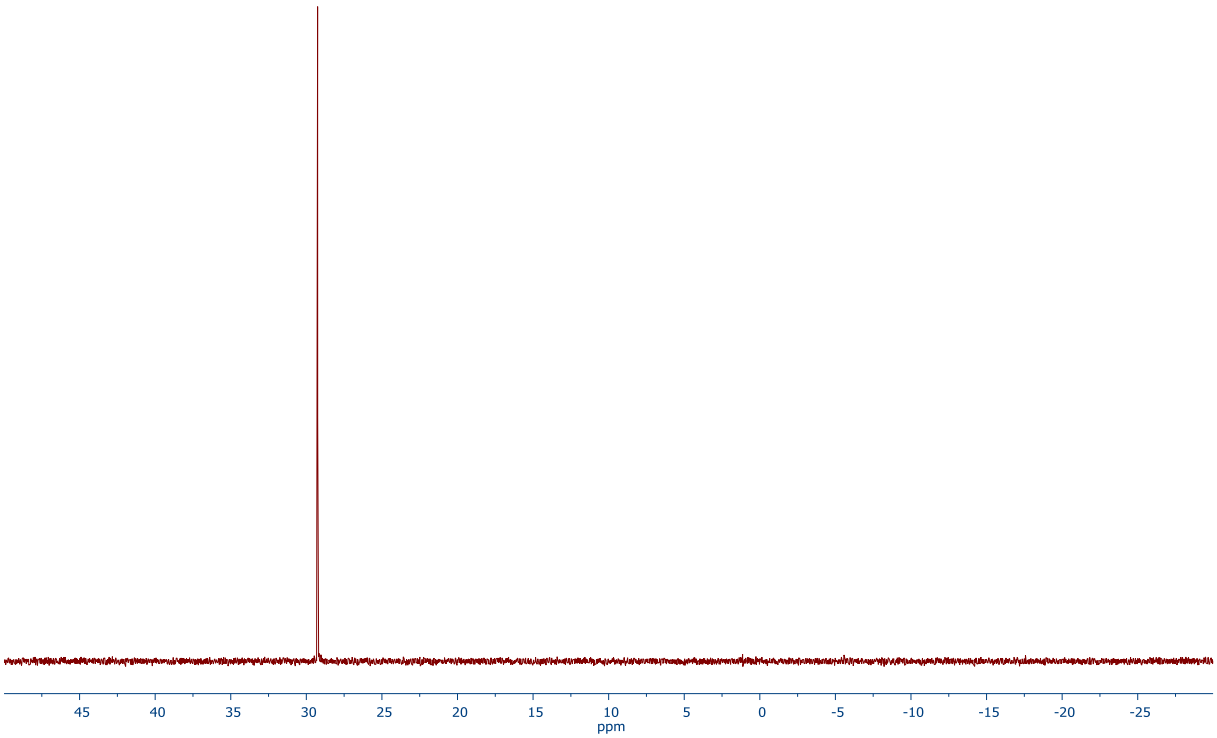

Figure S53. $^{31}P\{^{1}H\}$ NMR spectrum (161.90 MHz, $CDCl_3$) of compound **1aAu**.

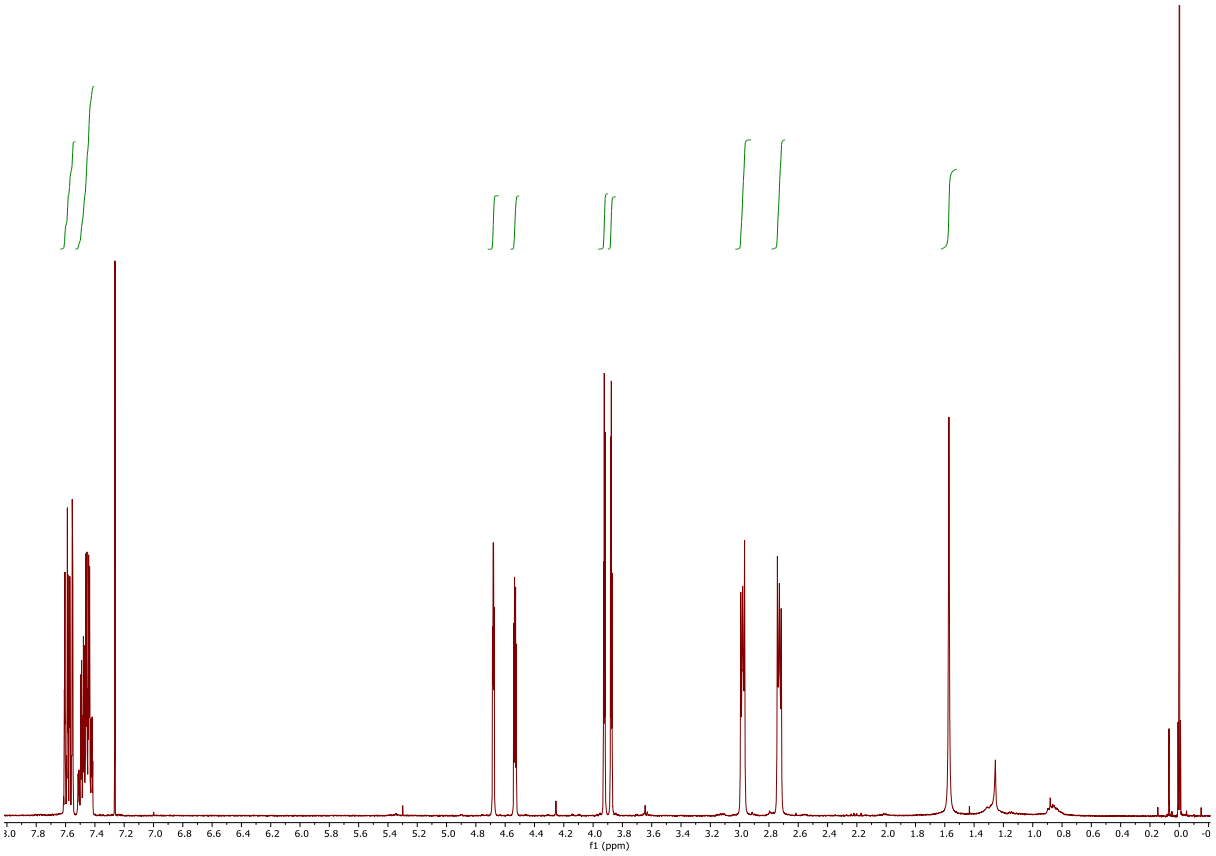

Figure S54. ^{1}H NMR spectrum (399.95 MHz, $CDCl_3$) of compound **1bAu**.

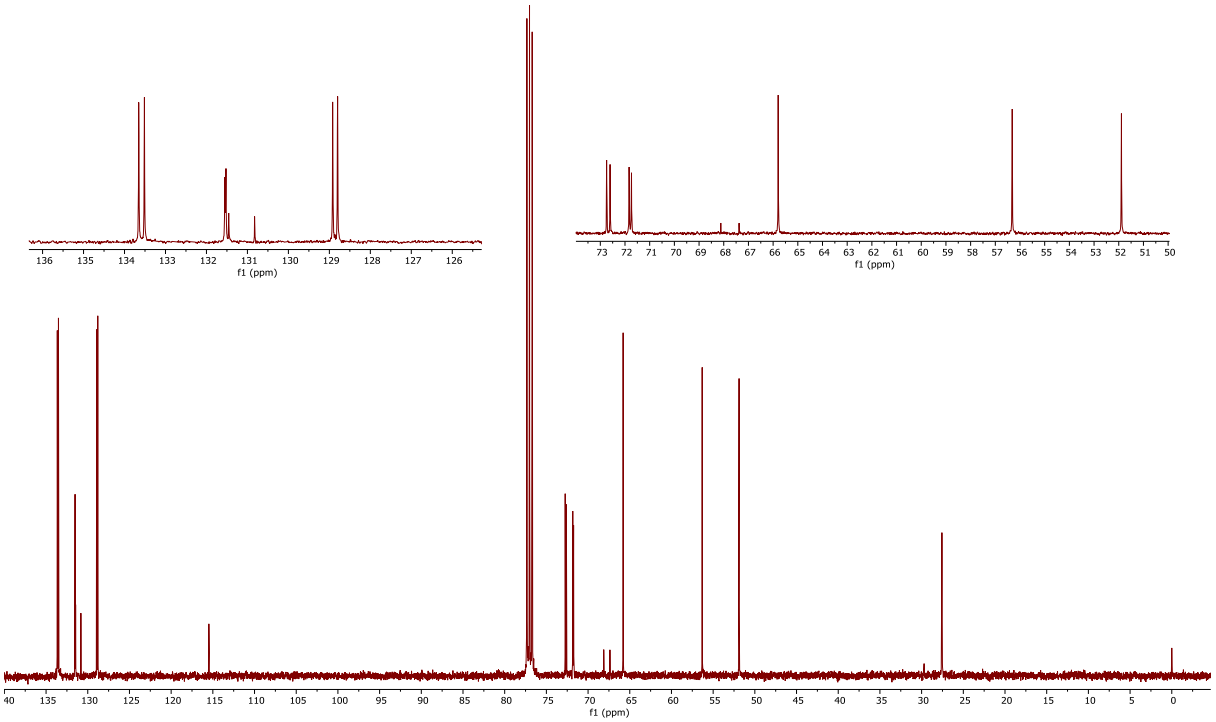

Figure S55. $^{13}C\{^{1}H\}$ NMR spectrum (100.58 MHz, $CDCl_3$) of compound **1bAu**.

Figure S56. $^{31}P\{^{1}H\}$ NMR spectrum (161.90 MHz, $CDCl_3$) of compound **1bAu**.

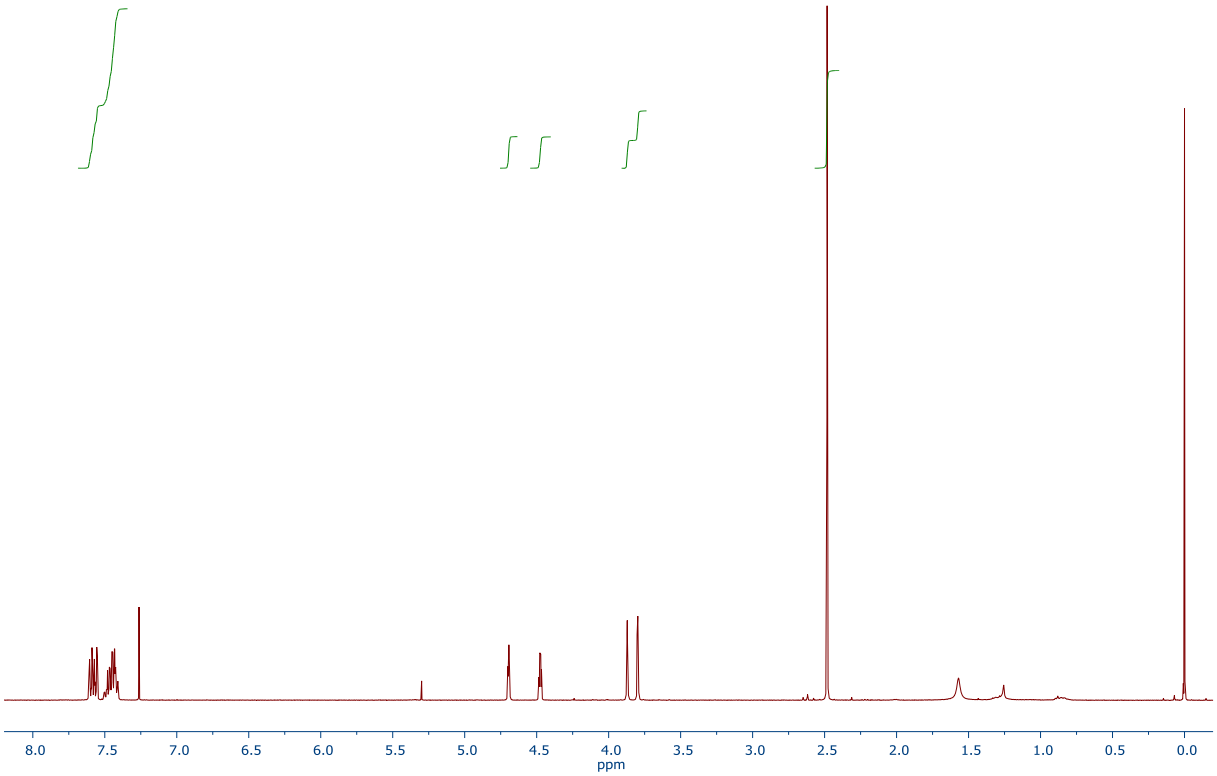

Figure S57. ^{1}H NMR spectrum (399.95 MHz, $CDCl_3$) of compound **1cAu**.

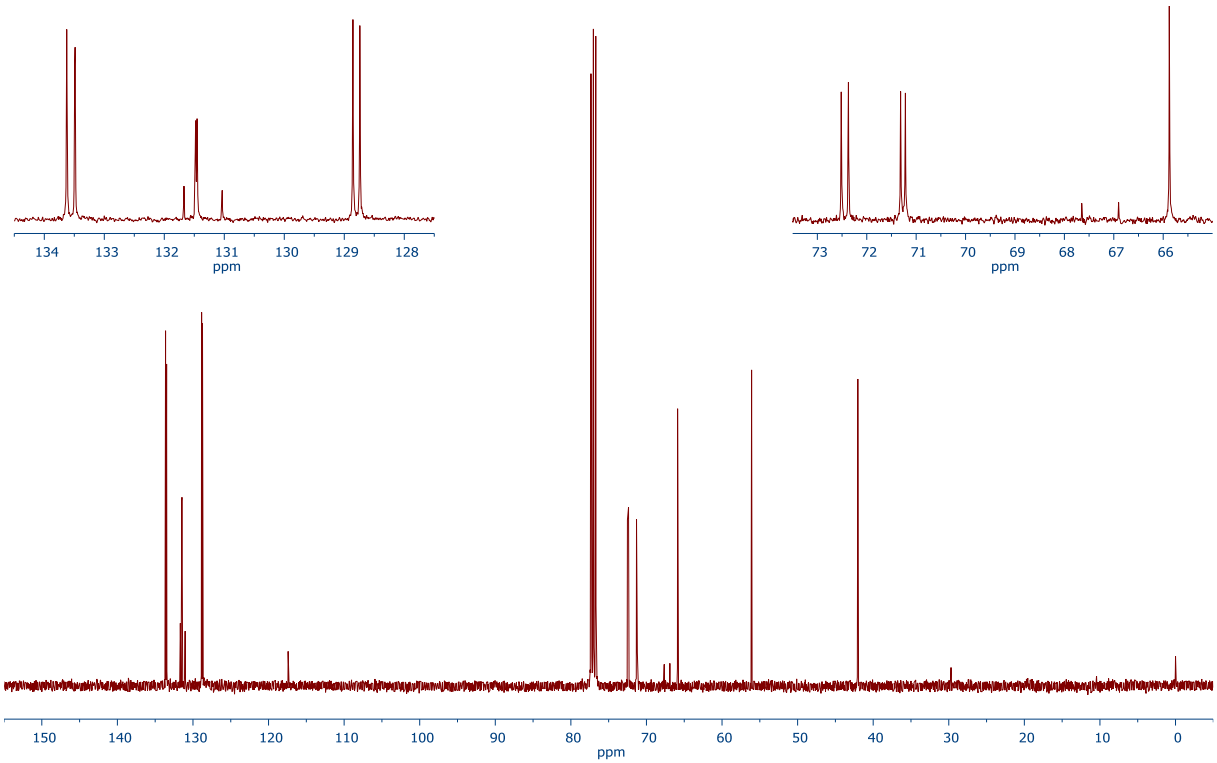

Figure S58. $^{13}C\{^{1}H\}$ NMR spectrum (100.58 MHz, $CDCl_3$) of compound **1cAu**.

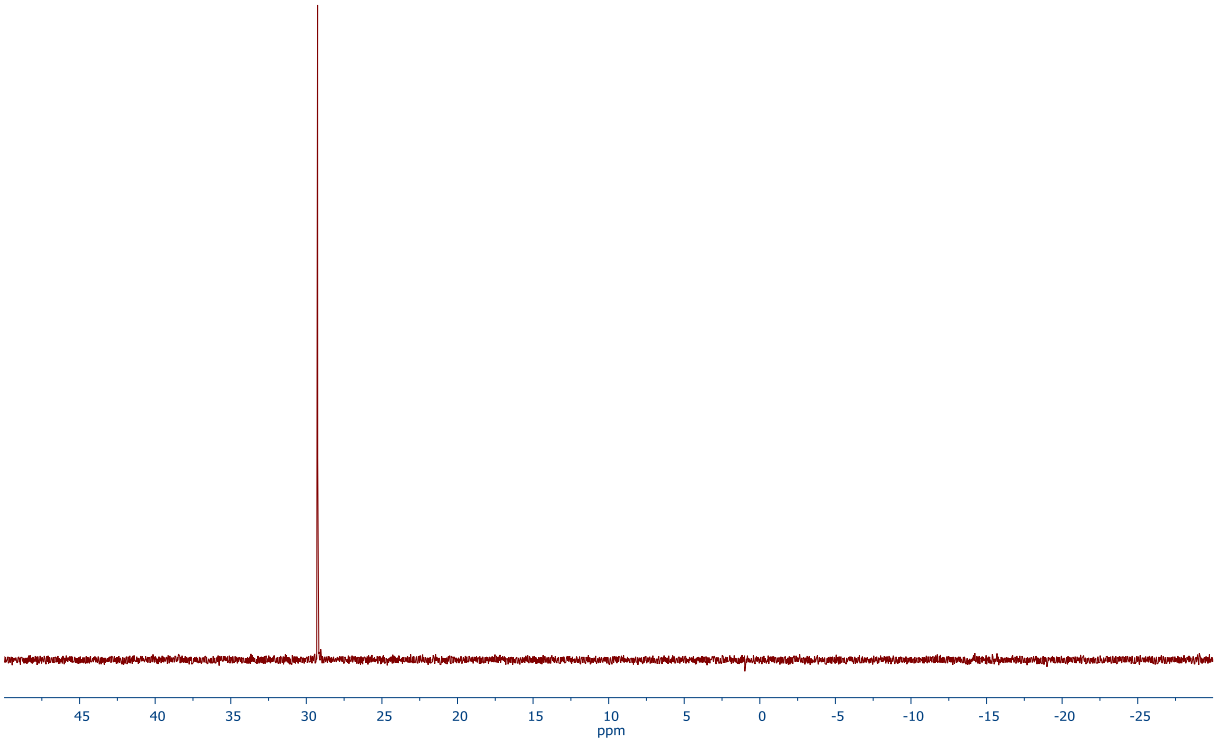

Figure S59. $^{31}P\{^{1}H\}$ NMR spectrum (161.90 MHz, $CDCl_3$) of compound **1cAu**.

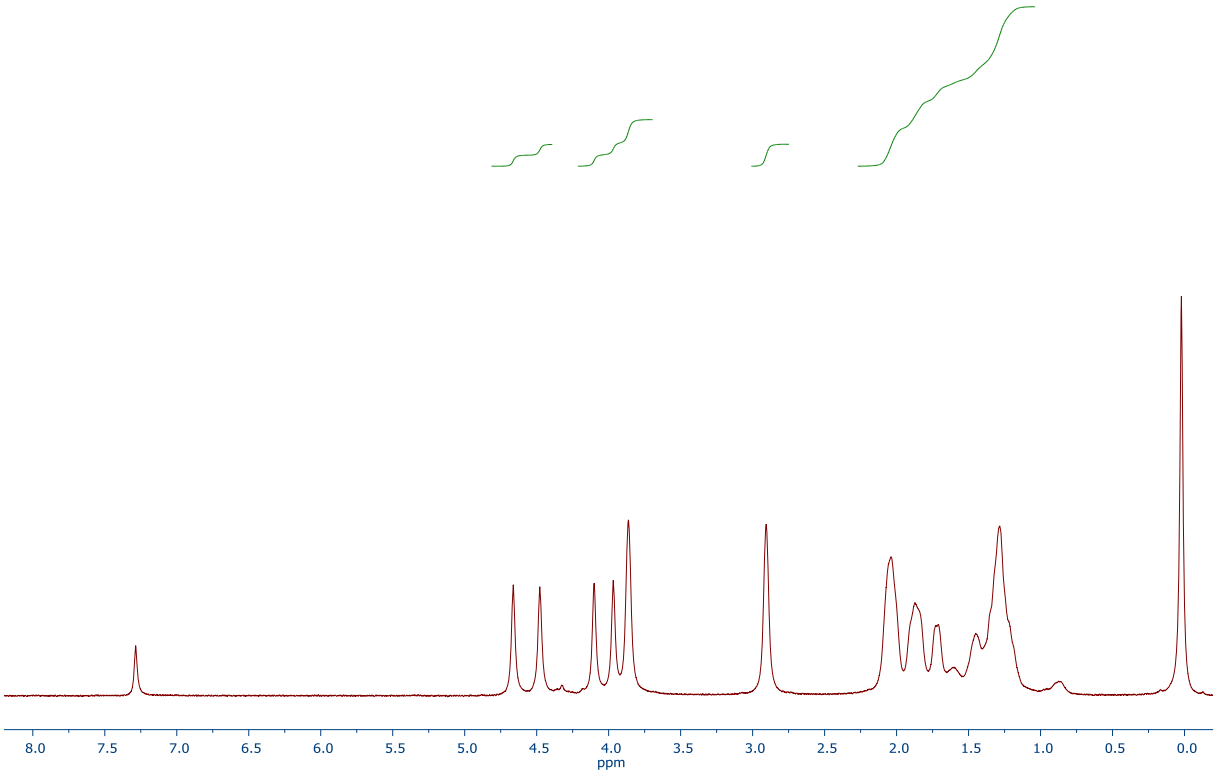

Figure S60. ^{1}H NMR spectrum (400.13 MHz, $CDCl_3$) of compound **2aAu**.

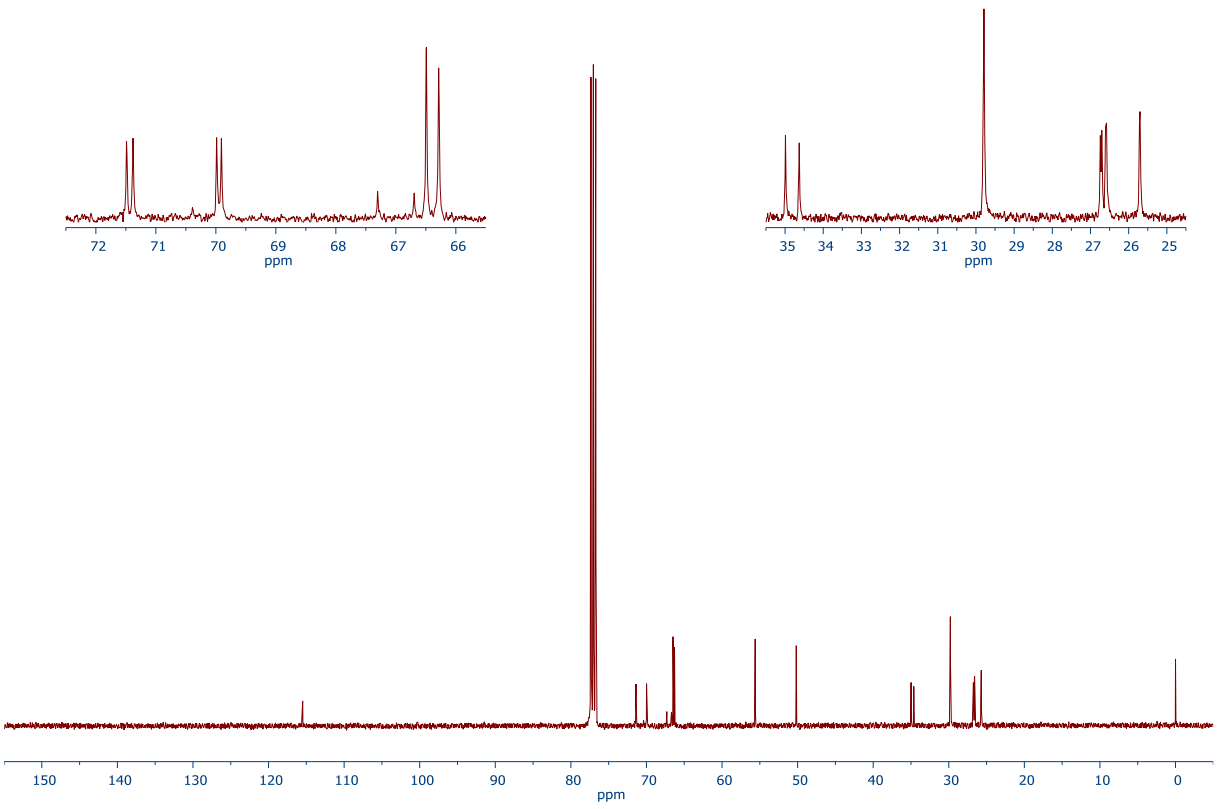

Figure S61. $^{13}C\{^{1}H\}$ NMR spectrum (100.62 MHz, $CDCl_3$) of compound **2aAu**.

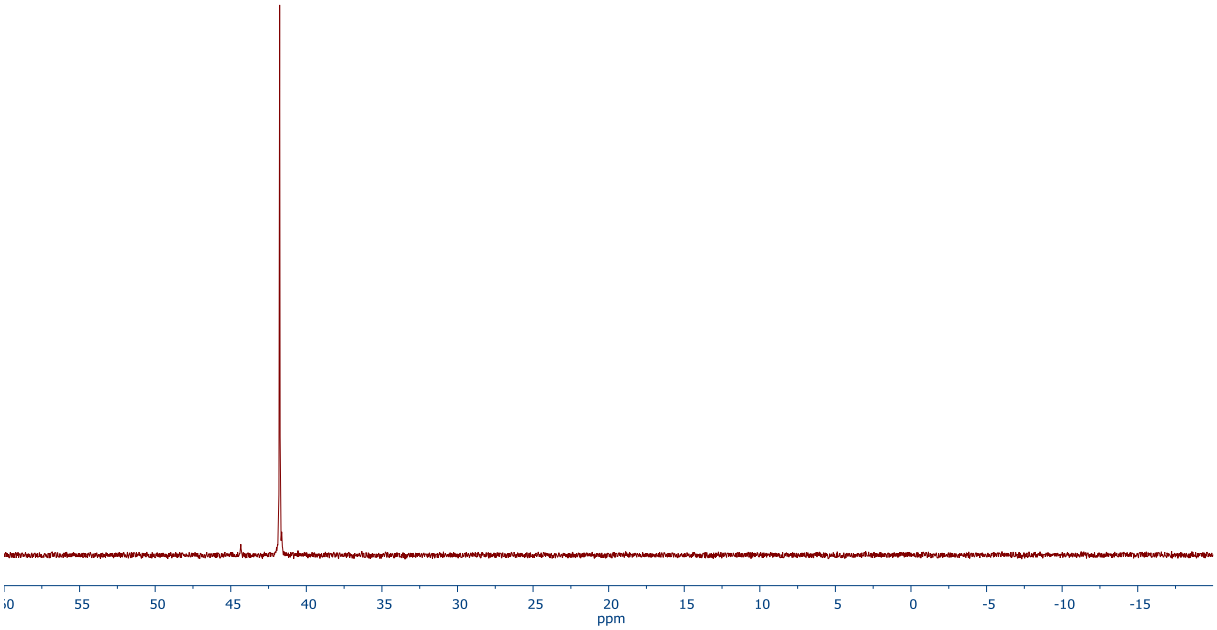

Figure S62. $^{31}P\{^{1}H\}$ NMR spectrum (161.97 MHz, $CDCl_3$) of compound **2aAu**.

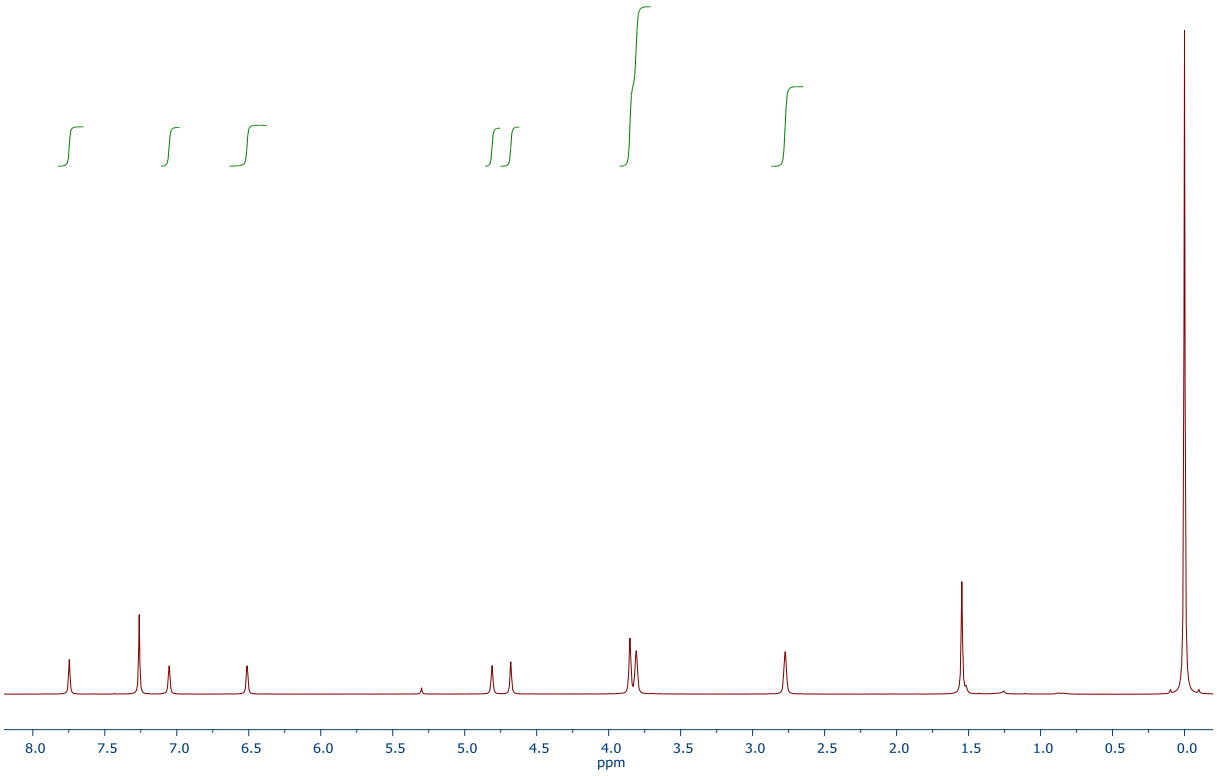

Figure S63. ^{1}H NMR spectrum (600.17 MHz, $CDCl_3$) of compound **3aAu**.

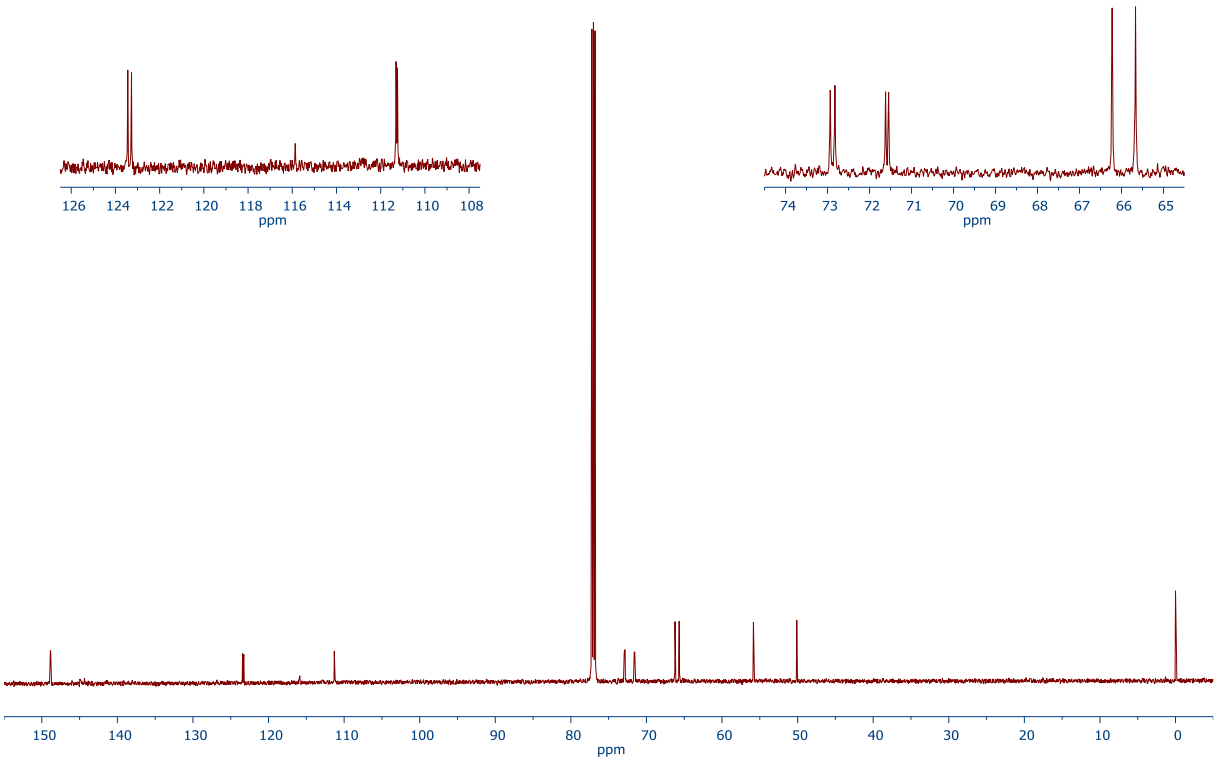

Figure S64. $^{13}C\{^{1}H\}$ NMR spectrum (150.93 MHz, $CDCl_3$) of compound **3aAu**.

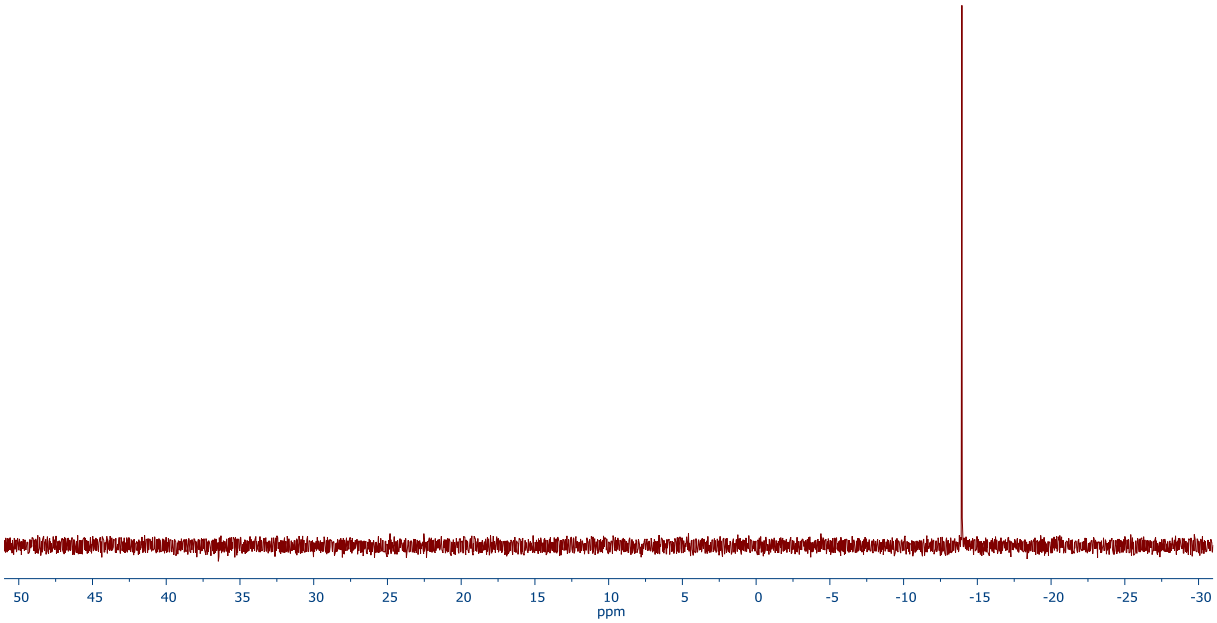

Figure S65. $^{31}P\{^{1}H\}$ NMR spectrum (242.96 MHz, $CDCl_3$) of compound **3aAu**.

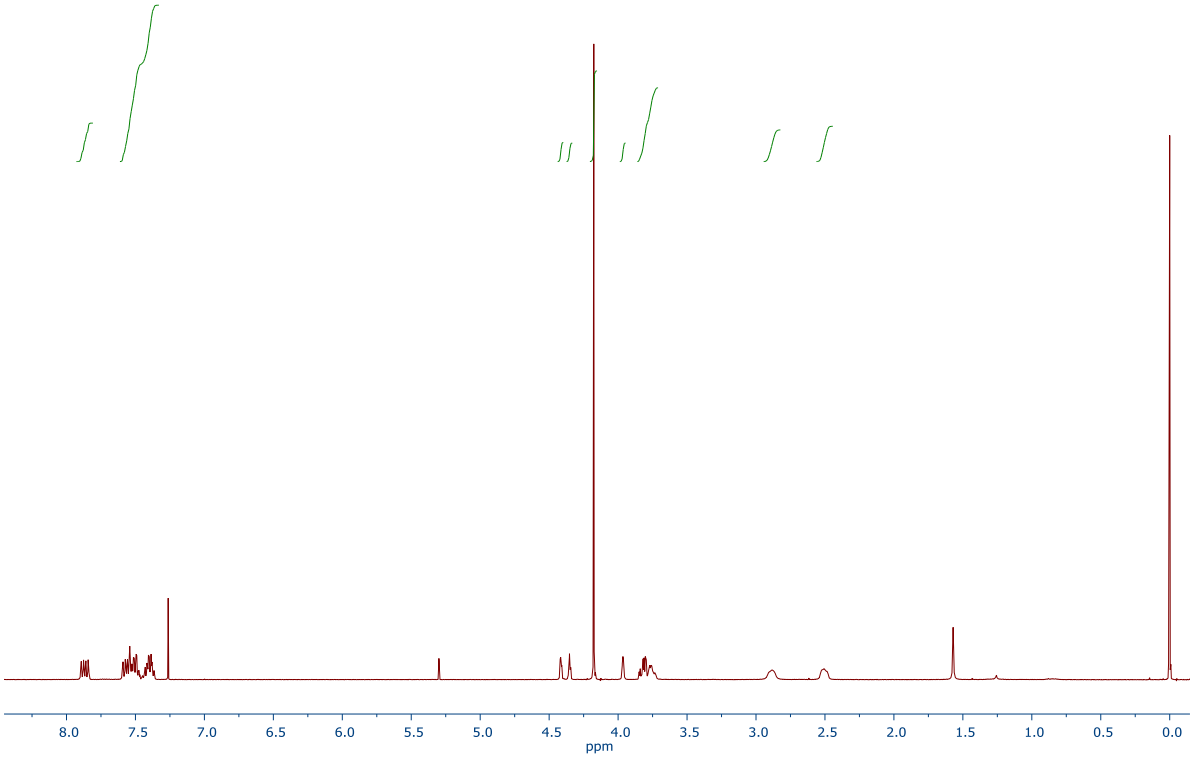

Figure S66. ^{1}H NMR spectrum (399.95 MHz, $CDCl_3$) of compound **4aAu**.

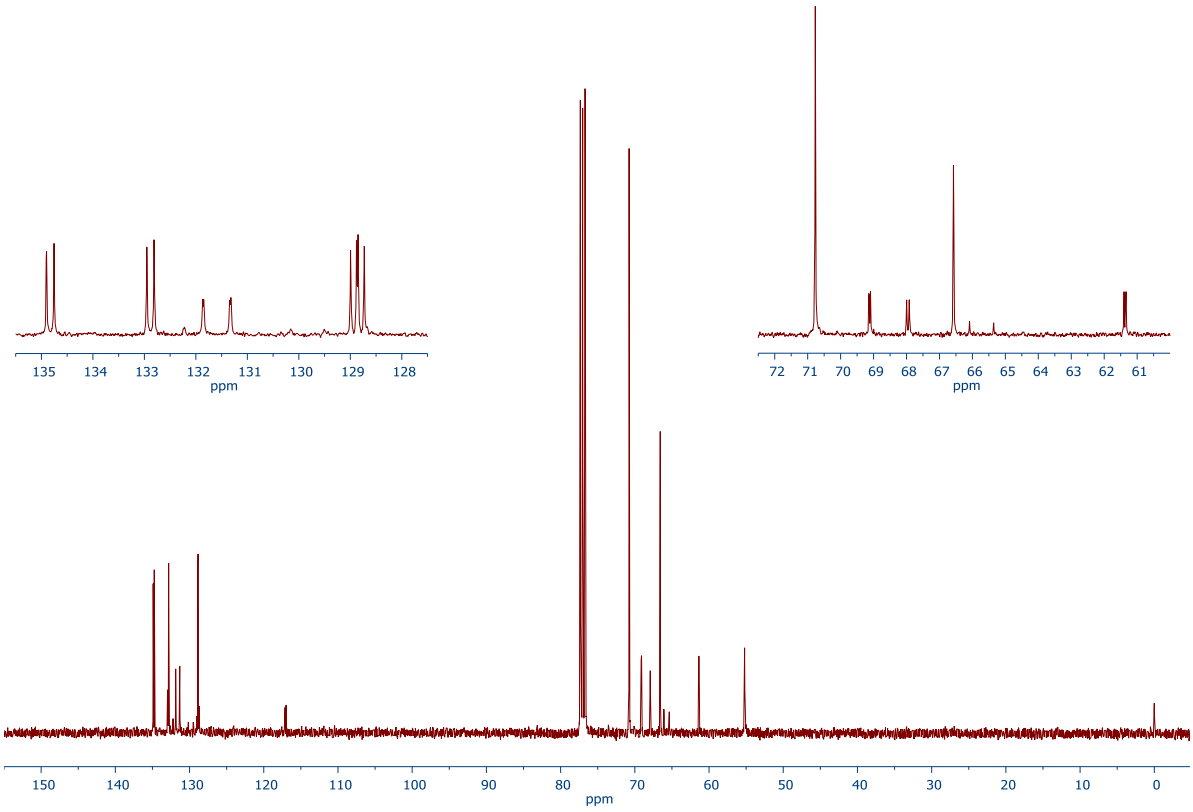

Figure S67. $^{13}C\{^{1}H\}$ NMR spectrum (100.58 MHz, $CDCl_3$) of compound **4aAu**.

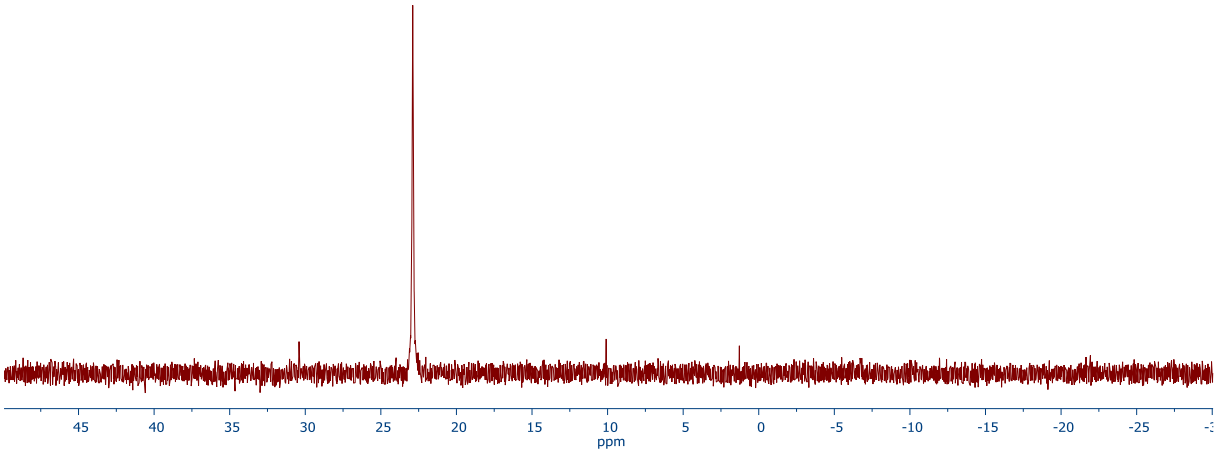

Figure S68. $^{31}P\{^{1}H\}$ NMR spectrum (161.90 MHz, $CDCl_3$) of compound **4aAu**.

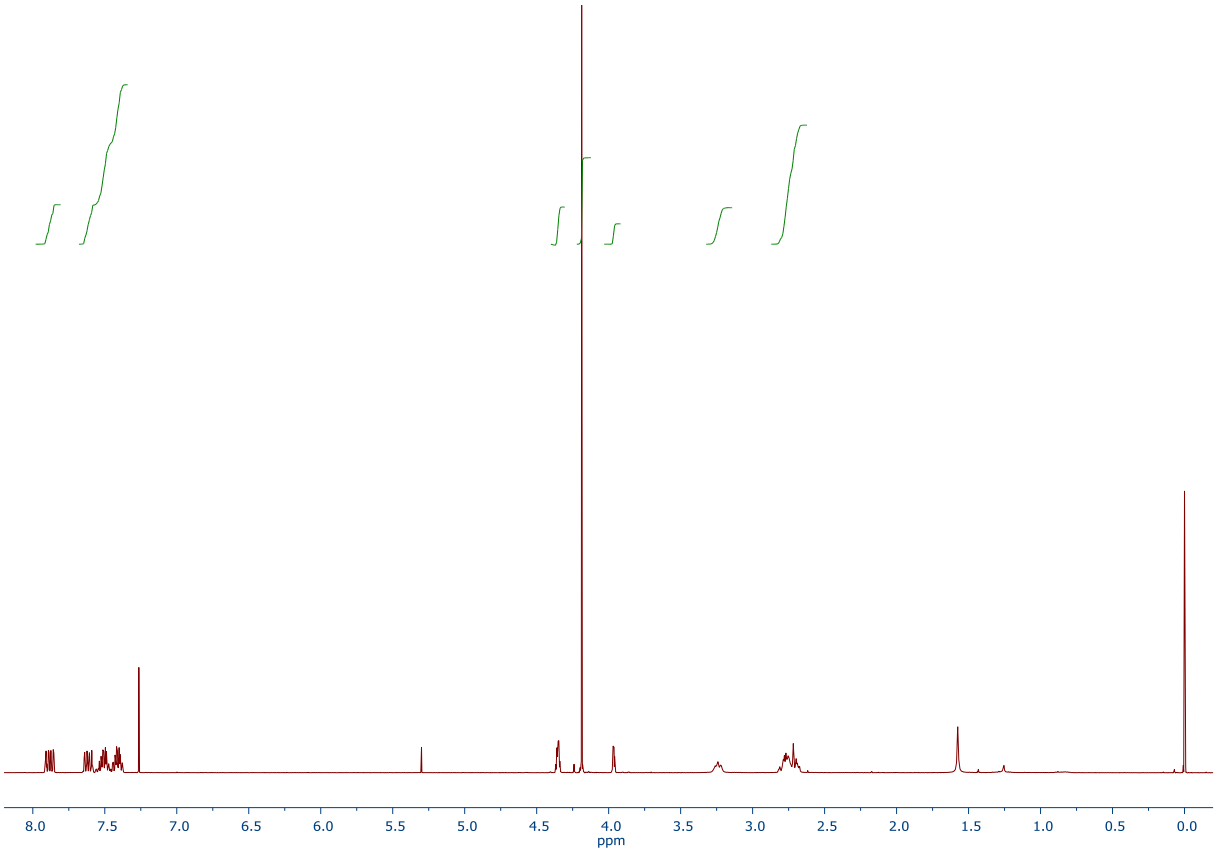

Figure S69. ^{1}H NMR spectrum (399.95 MHz, $CDCl_3$) of compound **4bAu**.

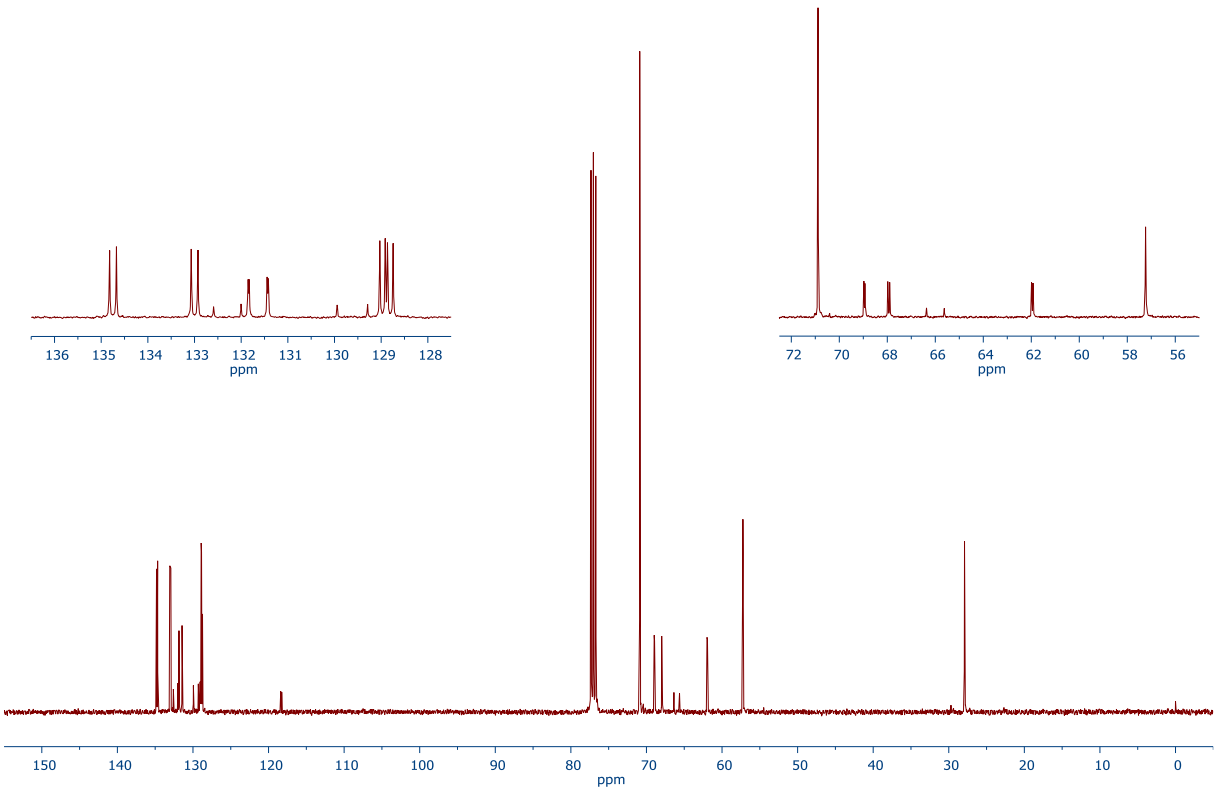

Figure S70. $^{13}C\{^{1}H\}$ NMR spectrum (100.58 MHz, $CDCl_3$) of compound **4bAu**.

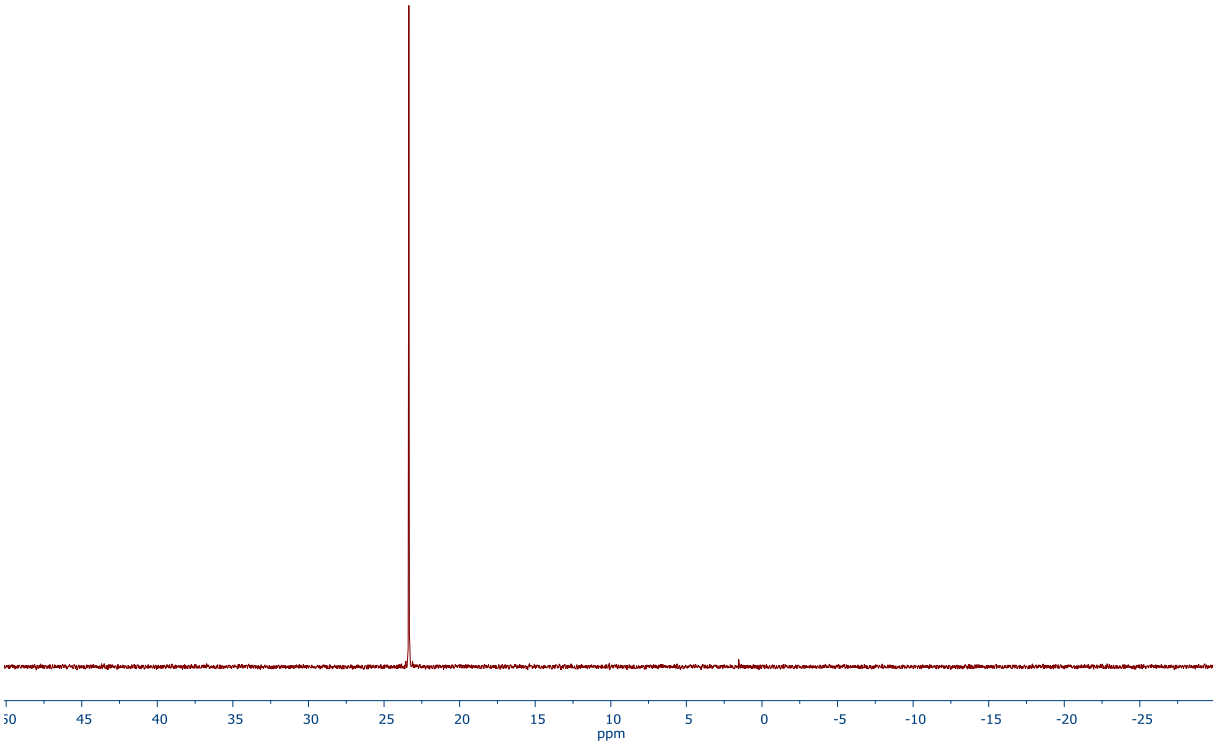

Figure S71. $^{31}P\{^{1}H\}$ NMR spectrum (161.90 MHz, $CDCl_3$) of compound **4bAu**.

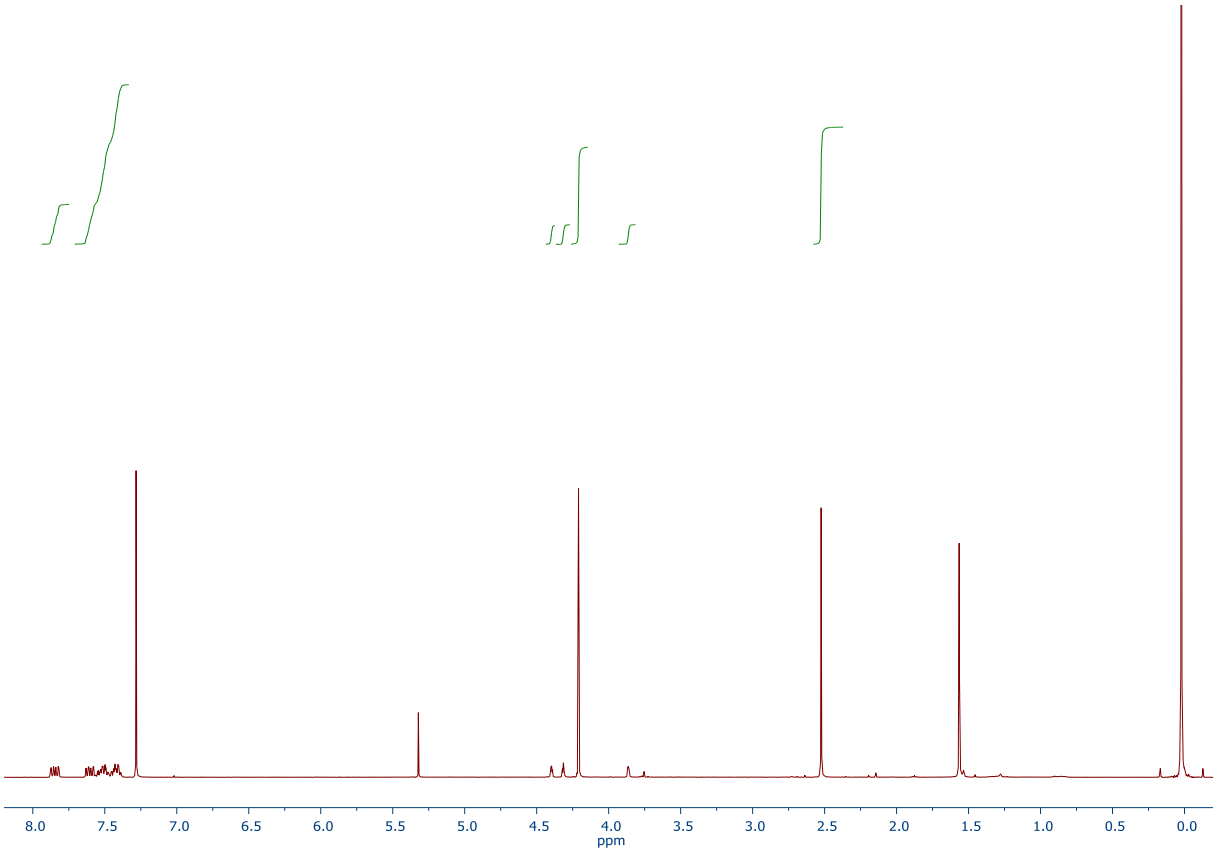

Figure S72. ^{1}H NMR spectrum (400.13 MHz, $CDCl_3$) of compound **4cAu**.

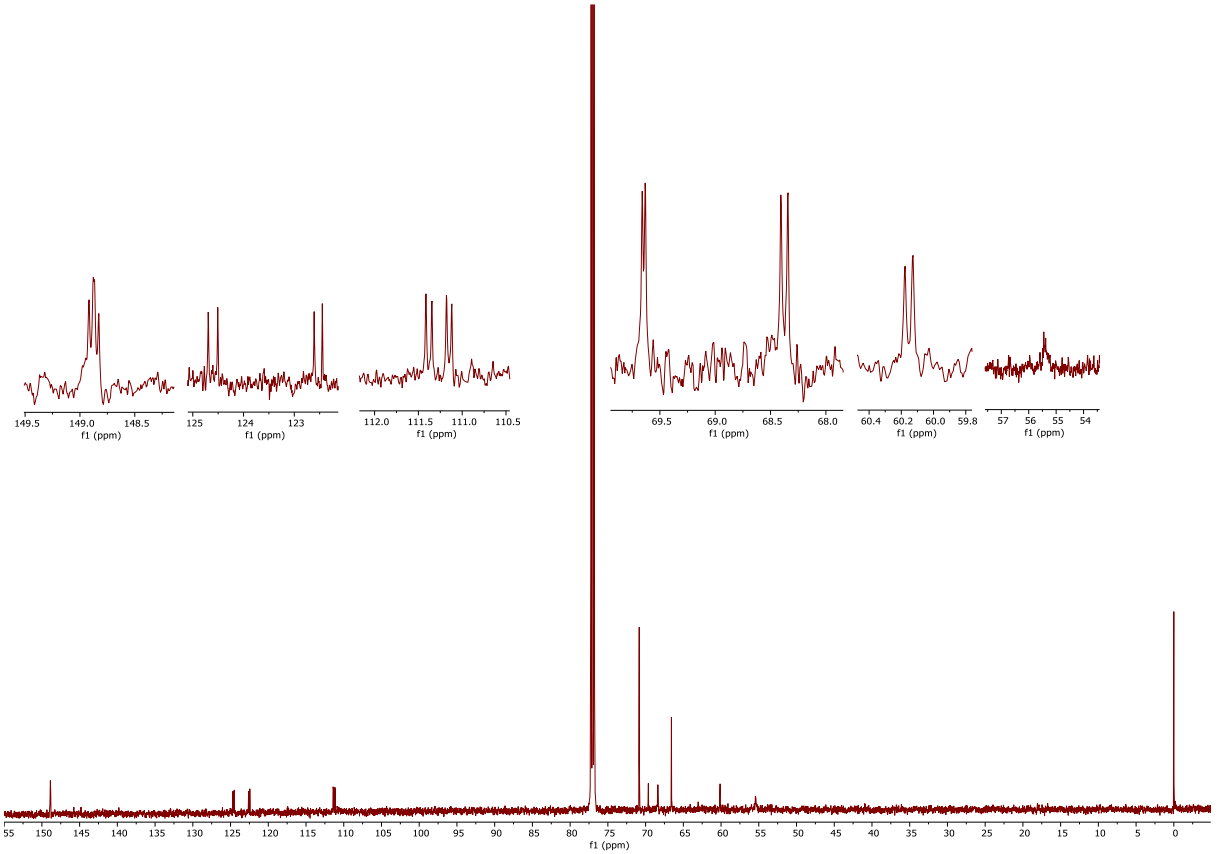

Figure S73. $^{13}C\{^{1}H\}$ NMR spectrum (100.58 MHz, $CDCl_3$) of compound **4cAu**.

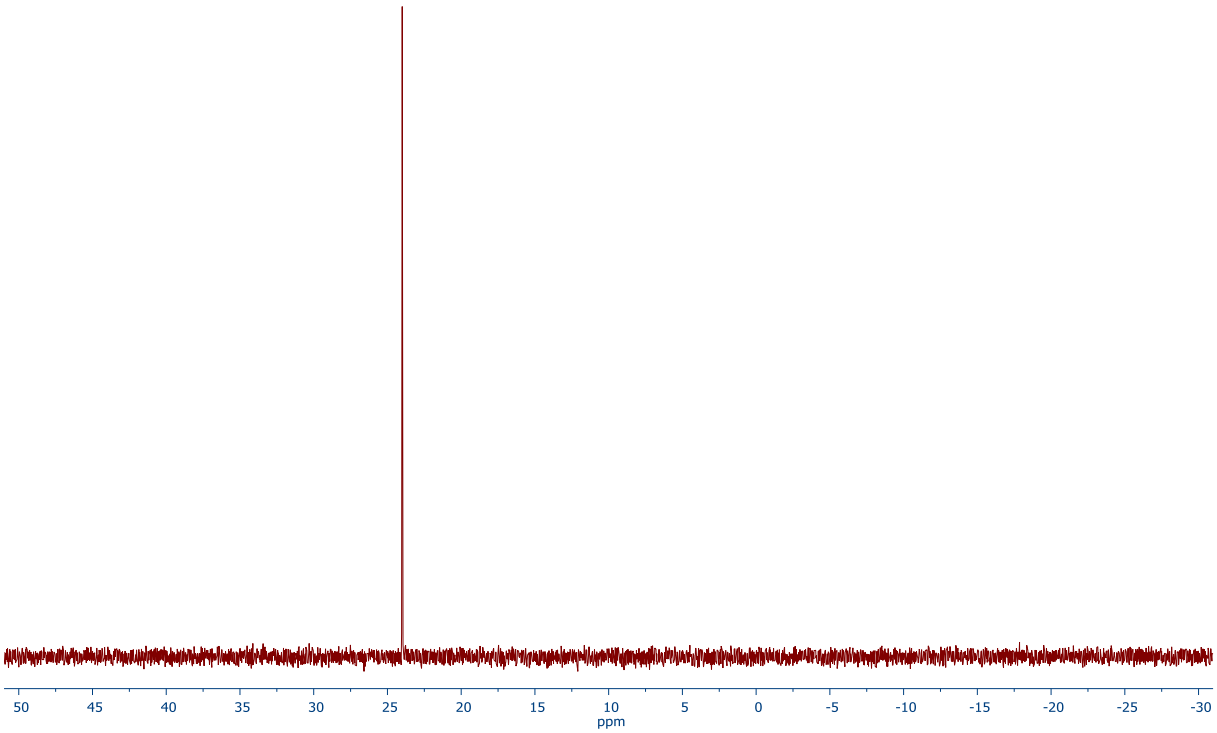

Figure S74. $^{31}P\{^{1}H\}$ NMR spectrum (161.97 MHz, $CDCl_3$) of compound **4cAu**.

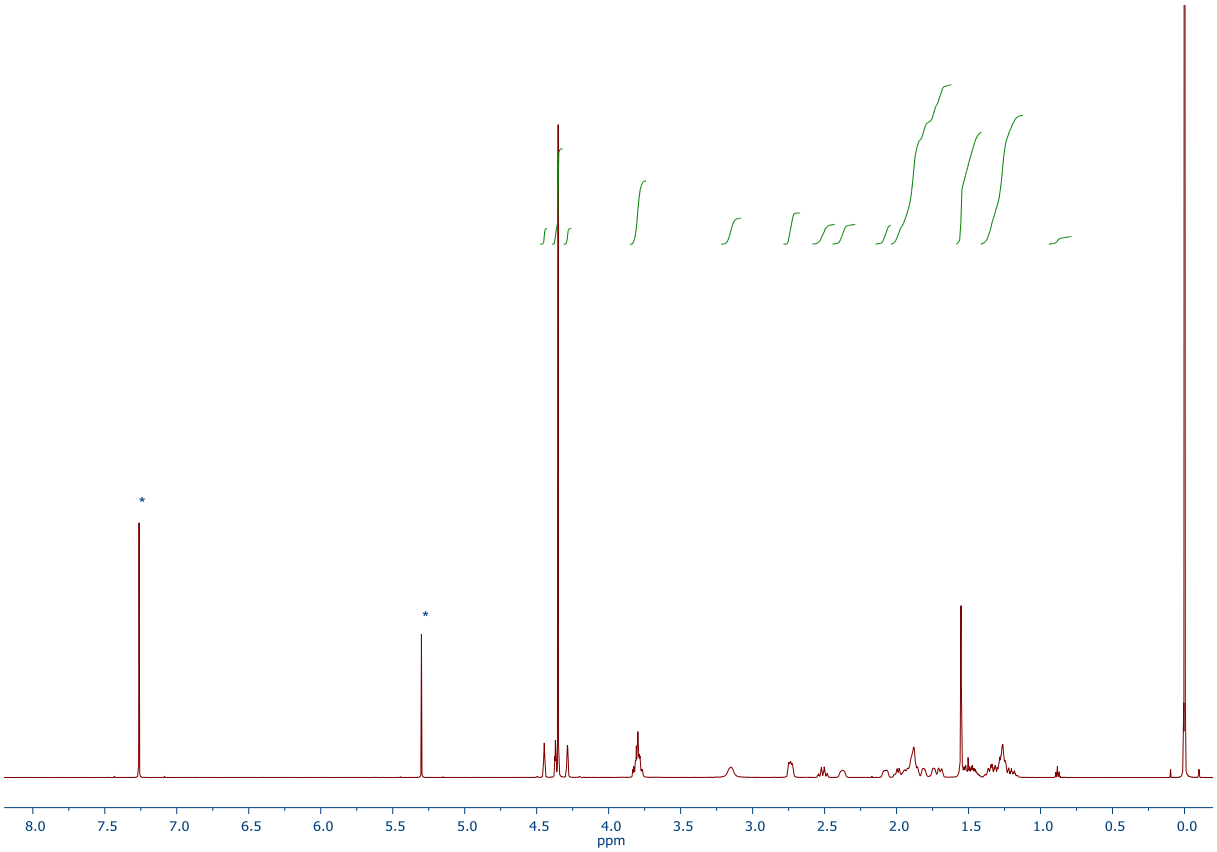

Figure S75. ^{1}H NMR spectrum (600.17 MHz, $CDCl_3$) of compound **5aAu**.

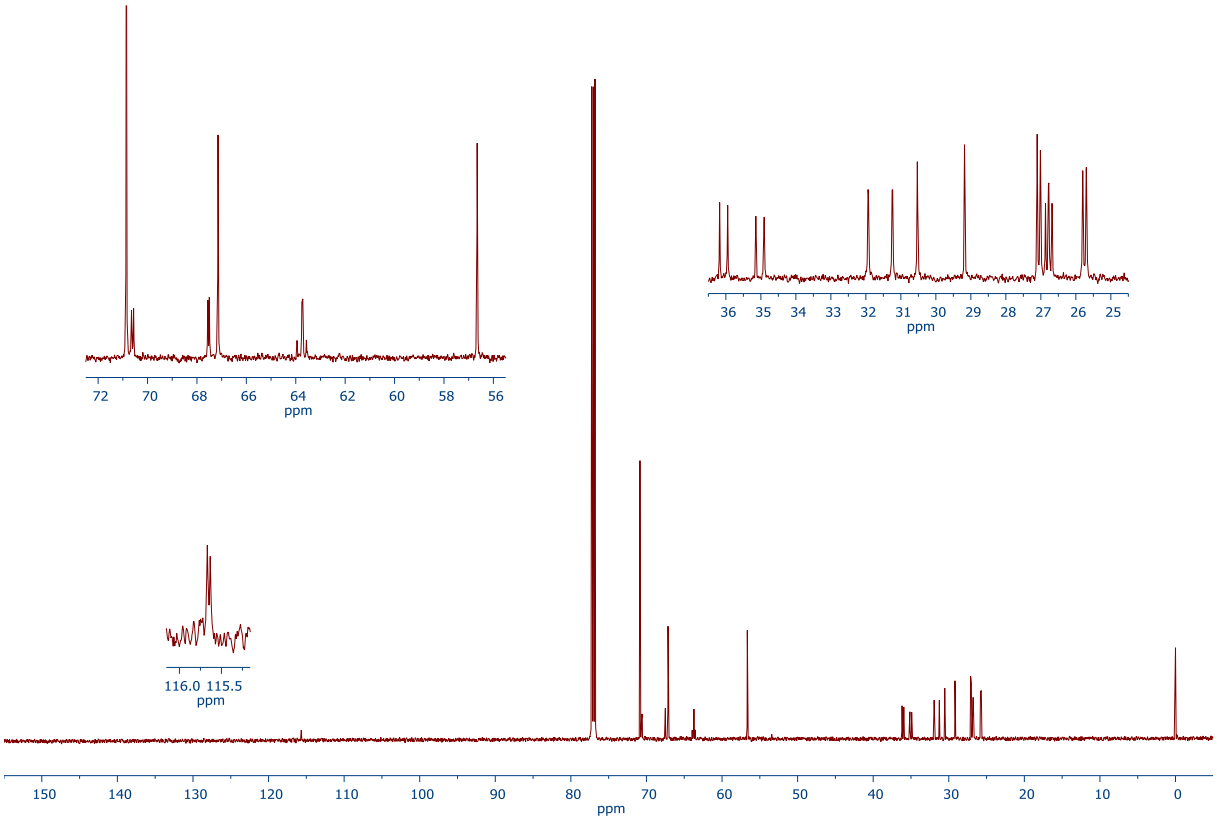

Figure S76. $^{13}C\{^{1}H\}$ NMR spectrum (150.93 MHz, $CDCl_3$) of compound **5aAu**.

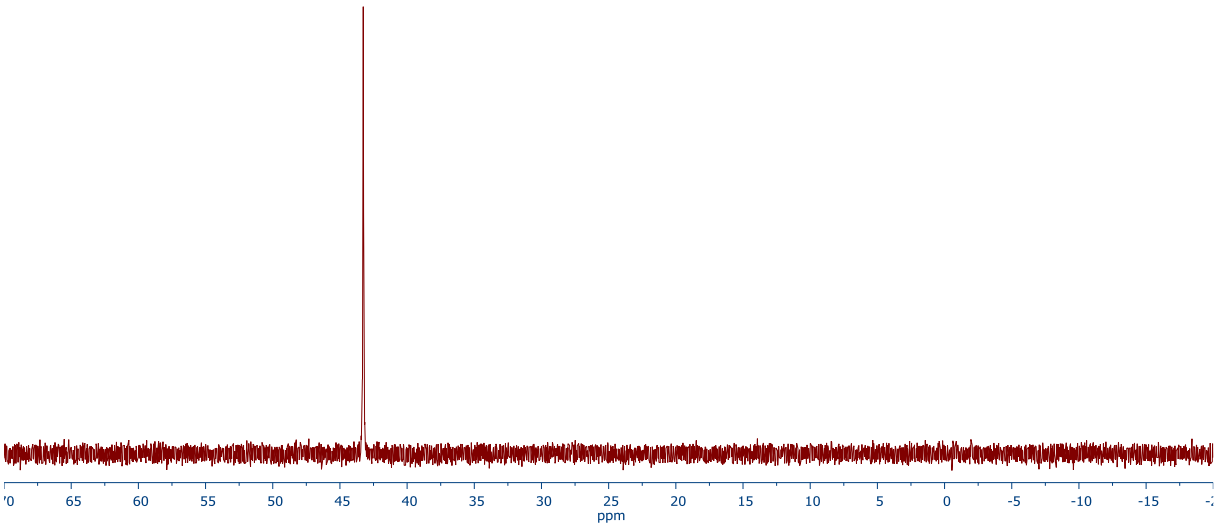

Figure S77. $^{31}P\{^{1}H\}$ NMR spectrum (242.96 MHz, $CDCl_3$) of compound **5aAu**.

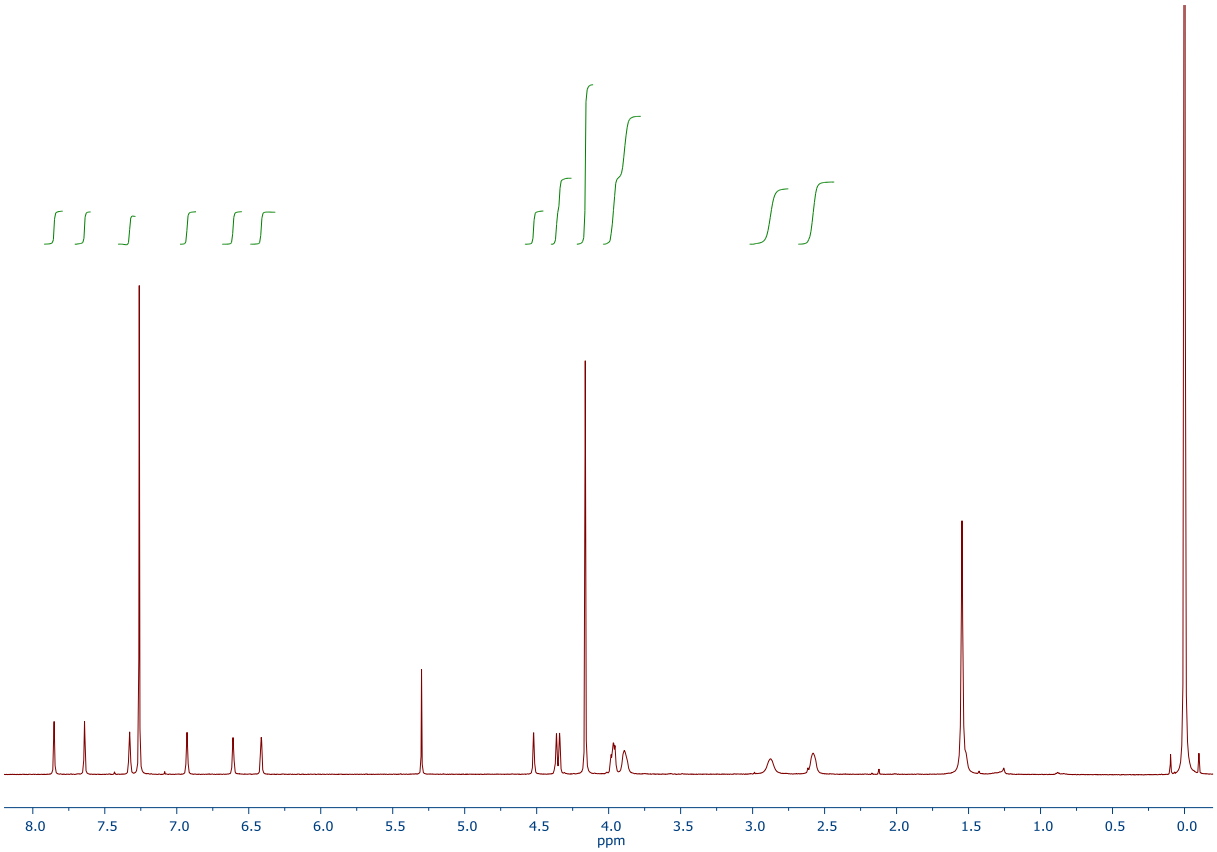

Figure S78. ^{1}H NMR spectrum (600.17 MHz, $CDCl_3$) of compound **6aAu**.

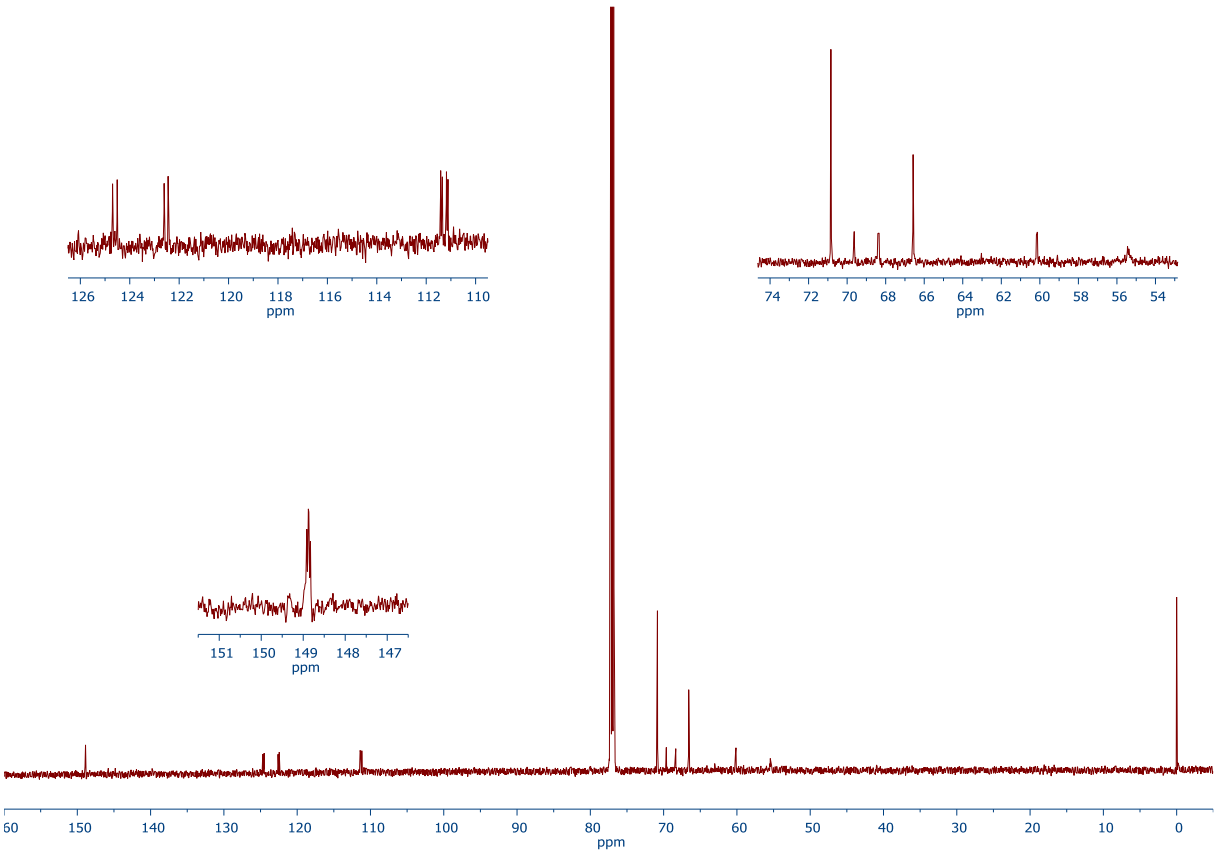

Figure S79. $^{13}C\{^{1}H\}$ NMR spectrum (150.93 MHz, $CDCl_3$) of compound **6aAu**.

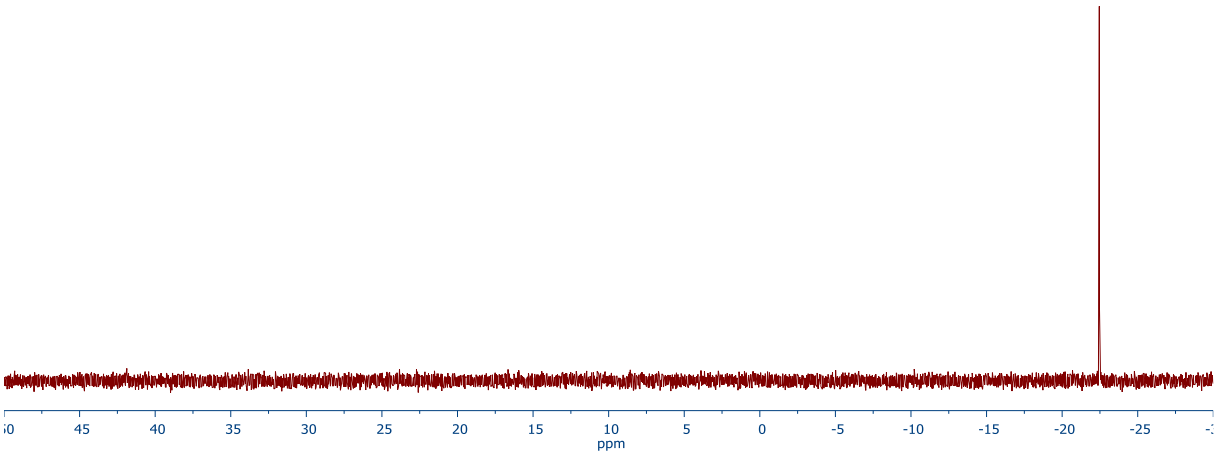

Figure S80. $^{31}P\{^{1}H\}$ NMR spectrum (242.96 MHz, $CDCl_3$) of compound **6aAu**.

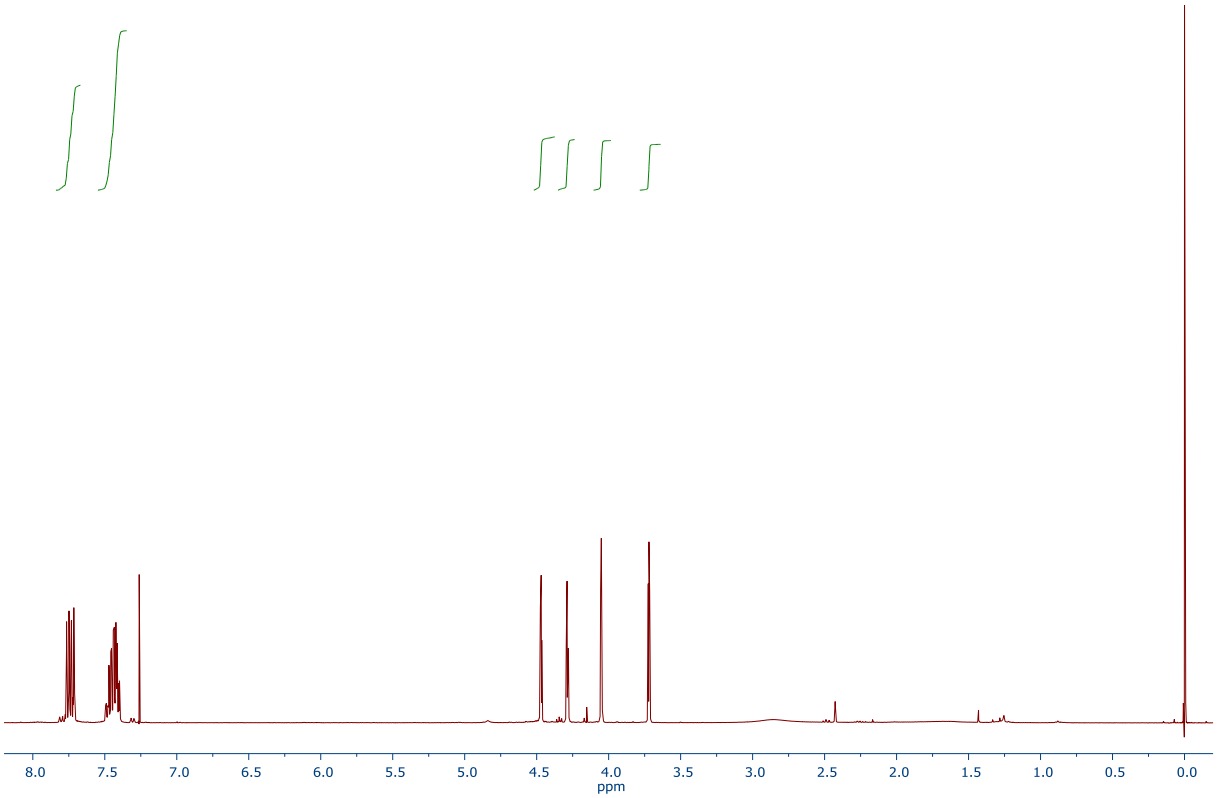

Figure S81. ^{1}H NMR spectrum (399.95 MHz, $CDCl_3$) of compound **8**.

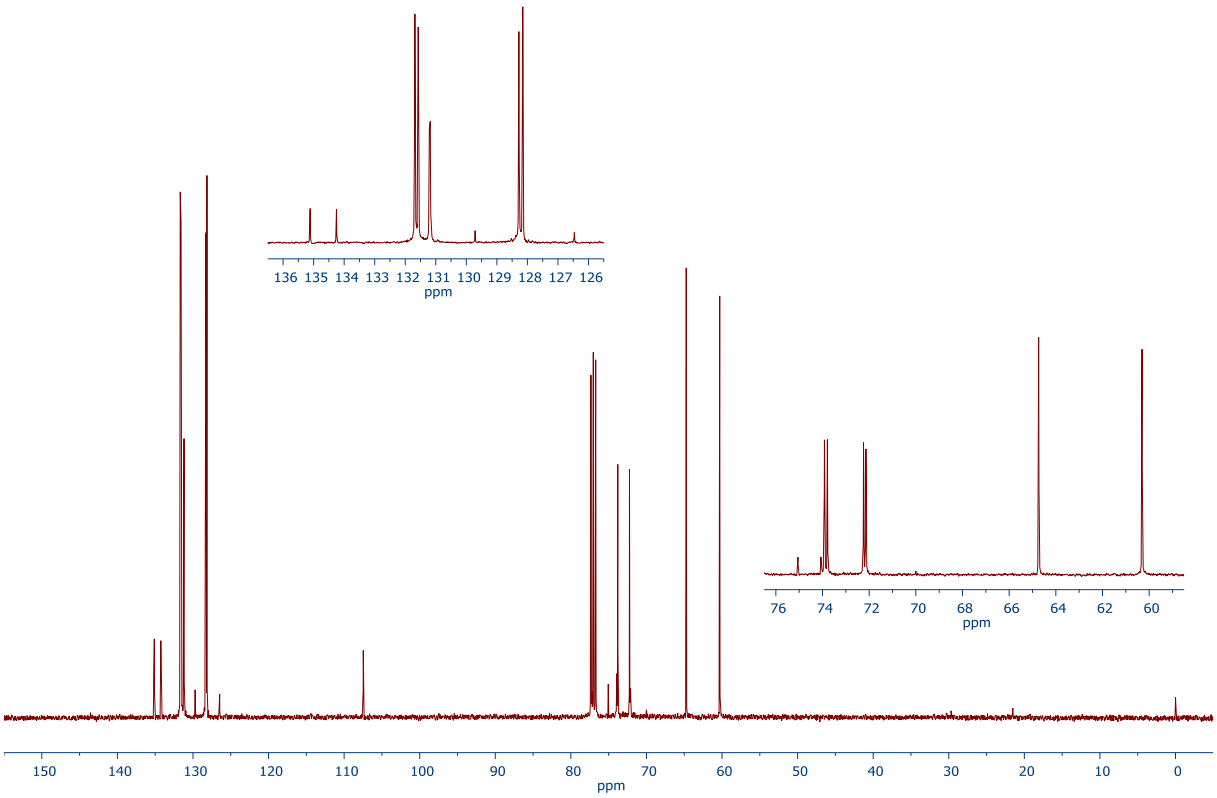

Figure S82. $^{13}C\{^{1}H\}$ NMR spectrum (100.58 MHz, $CDCl_3$) of compound **8**.

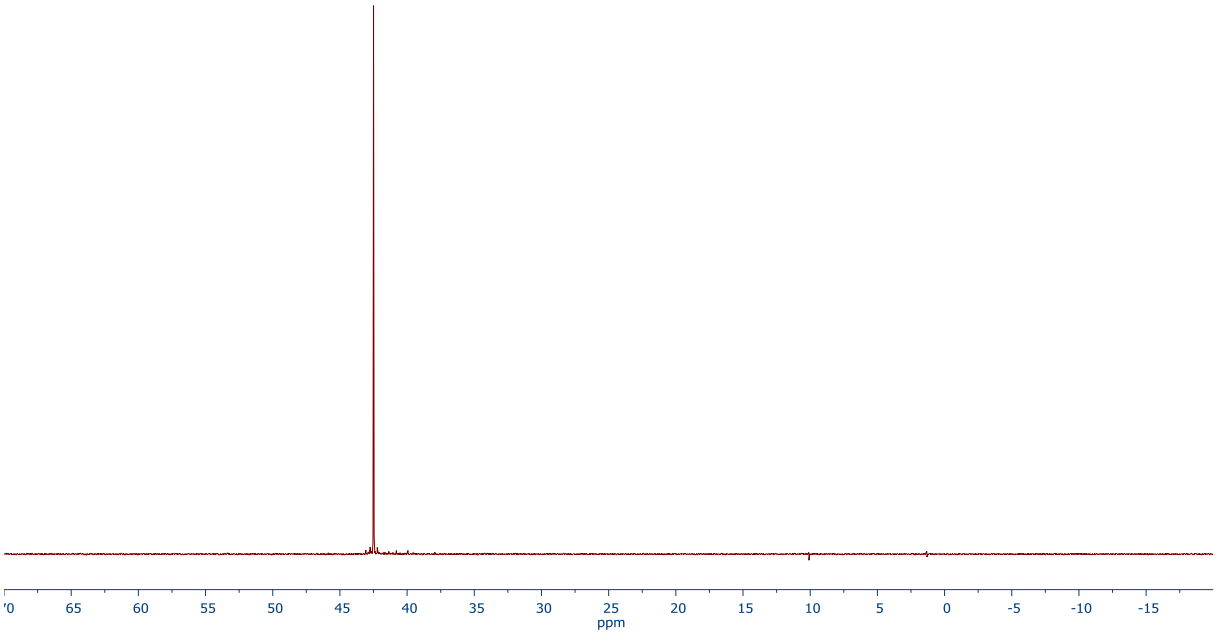

Figure S83. $^{31}P\{^{1}H\}$ NMR spectrum (161.90 MHz, $CDCl_3$) of compound **8**.

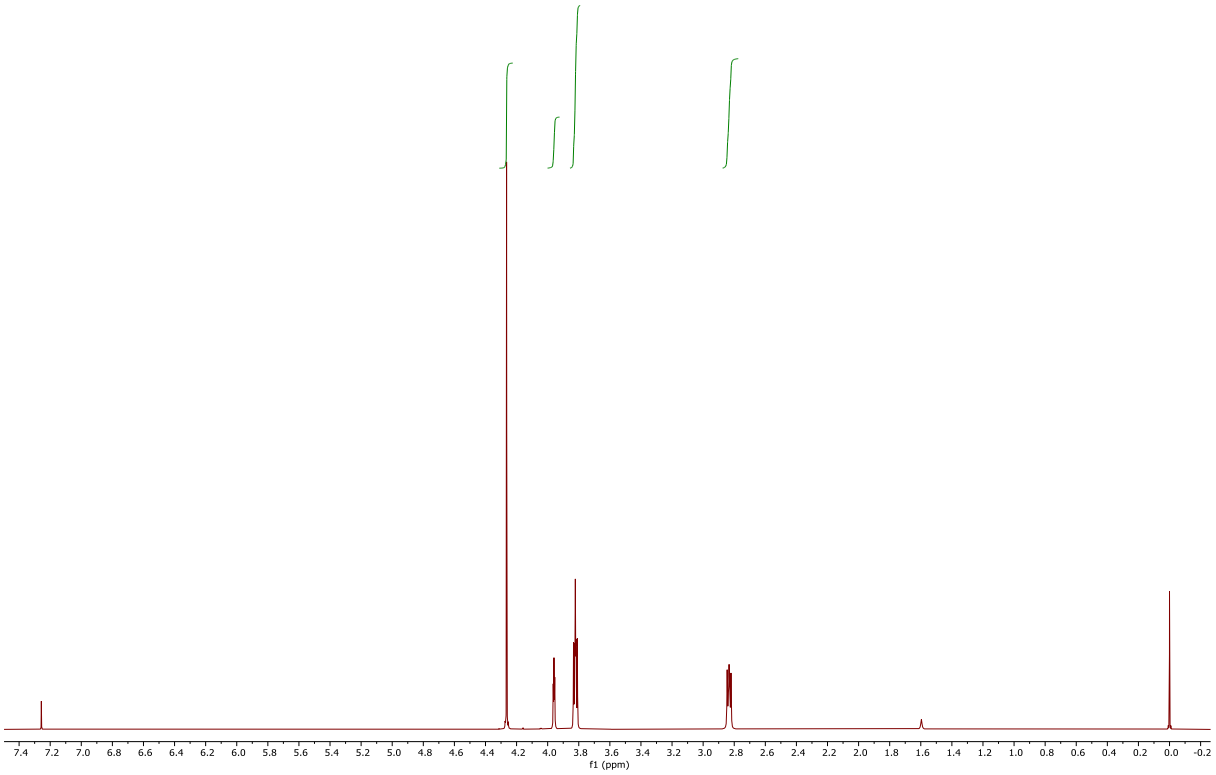

Figure S84. ^{1}H NMR spectrum (399.95 MHz, $CDCl_3$) of compound **10**.

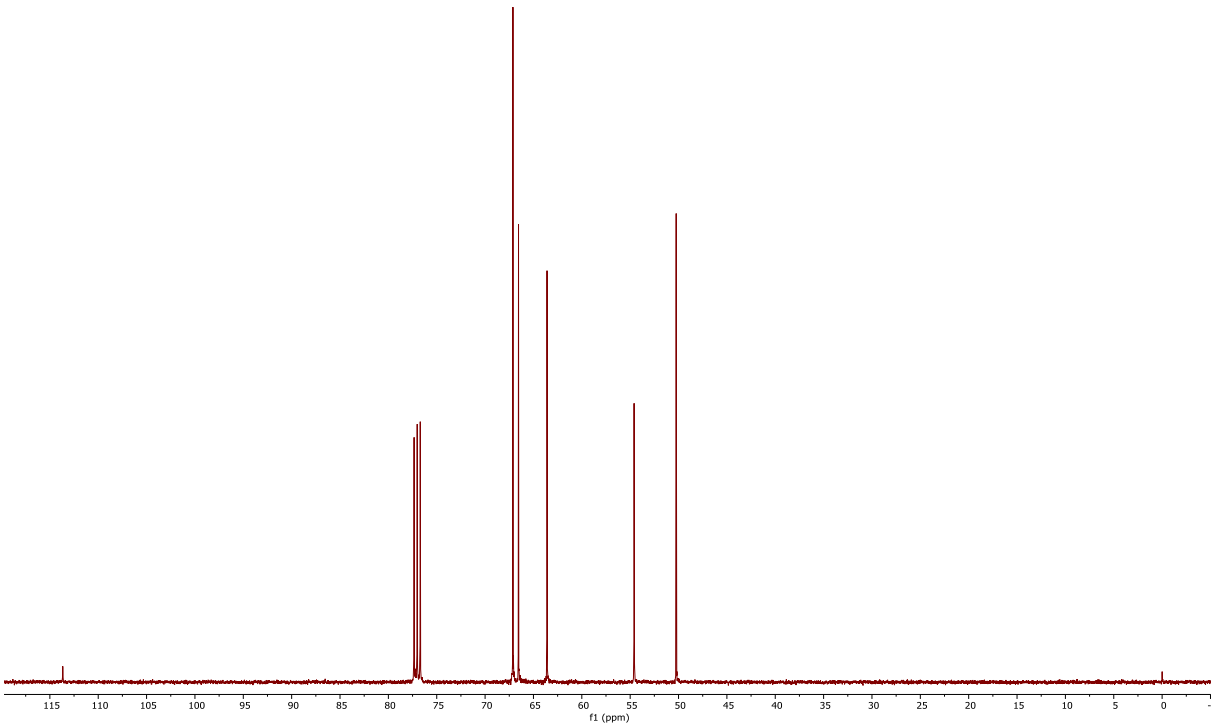

Figure S85. $^{13}C\{^{1}H\}$ NMR spectrum (100.58 MHz, $CDCl_3$) of compound **10**.

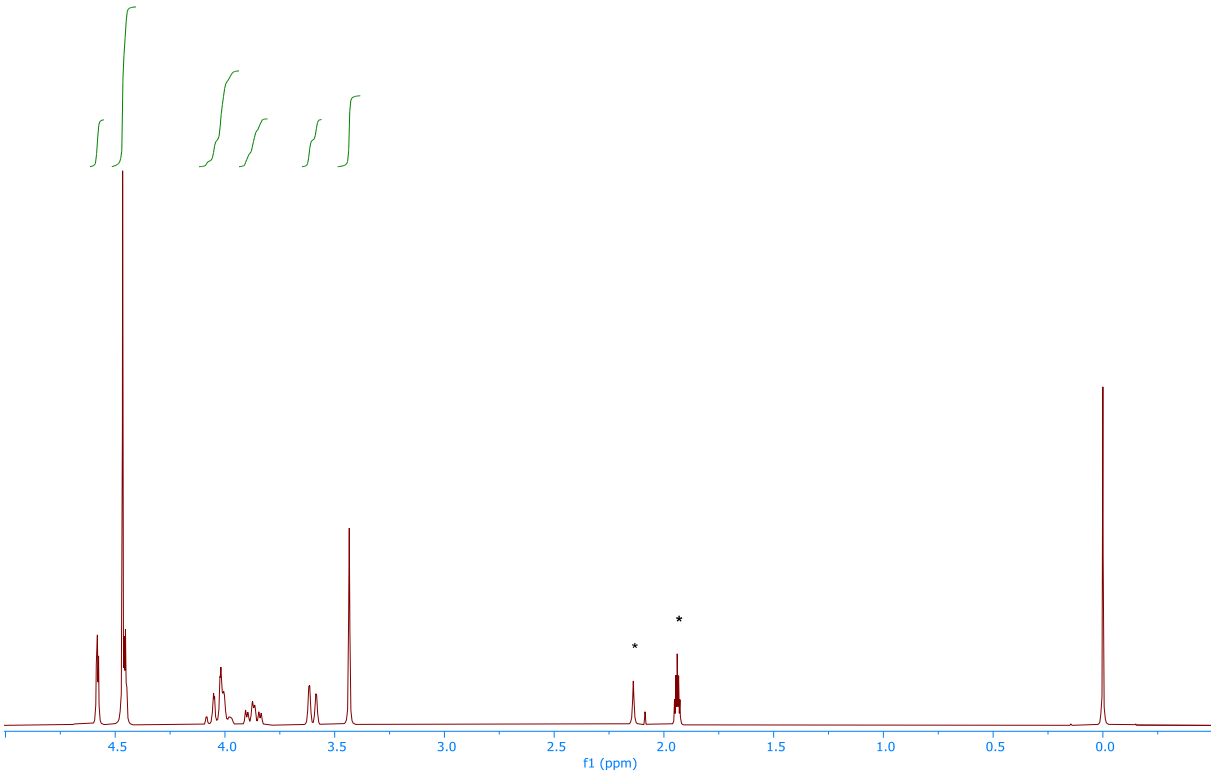

Figure S86. ^{1}H NMR spectrum (399.95 MHz, $CDCl_3$) of compound **(10Me)[BF_4]**.

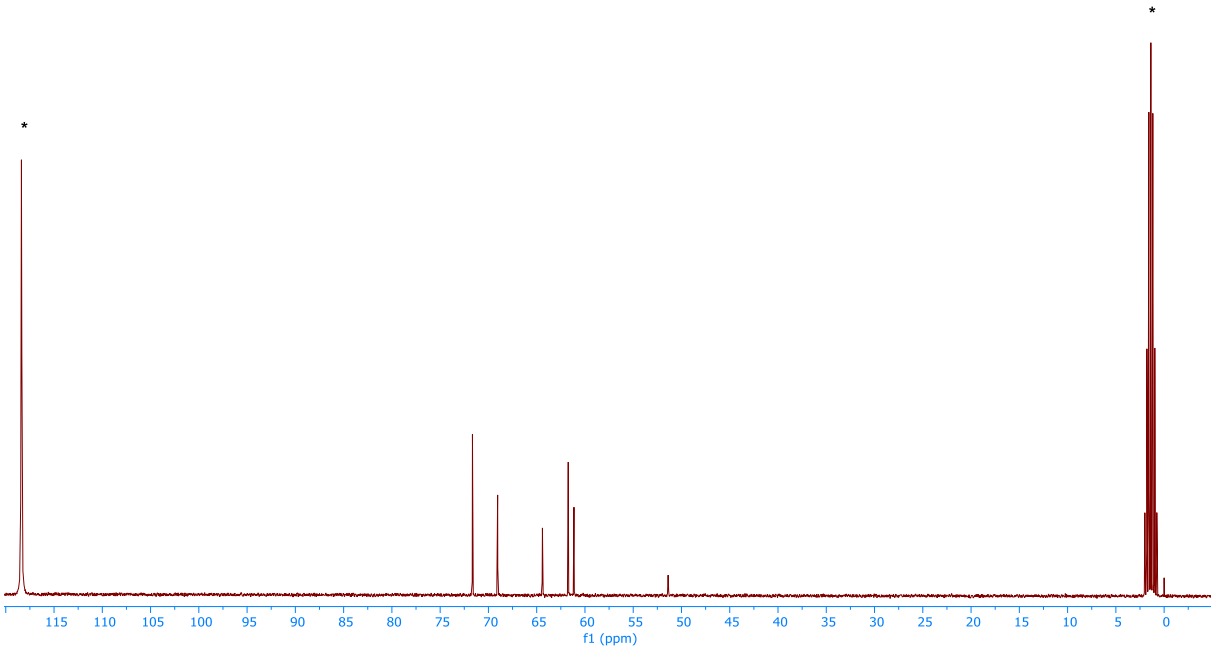

Figure S87. $^{13}C\{^{1}H\}$ NMR spectrum (100.58 MHz, $CDCl_3$) of compound **(10Me)[BF_4]**.

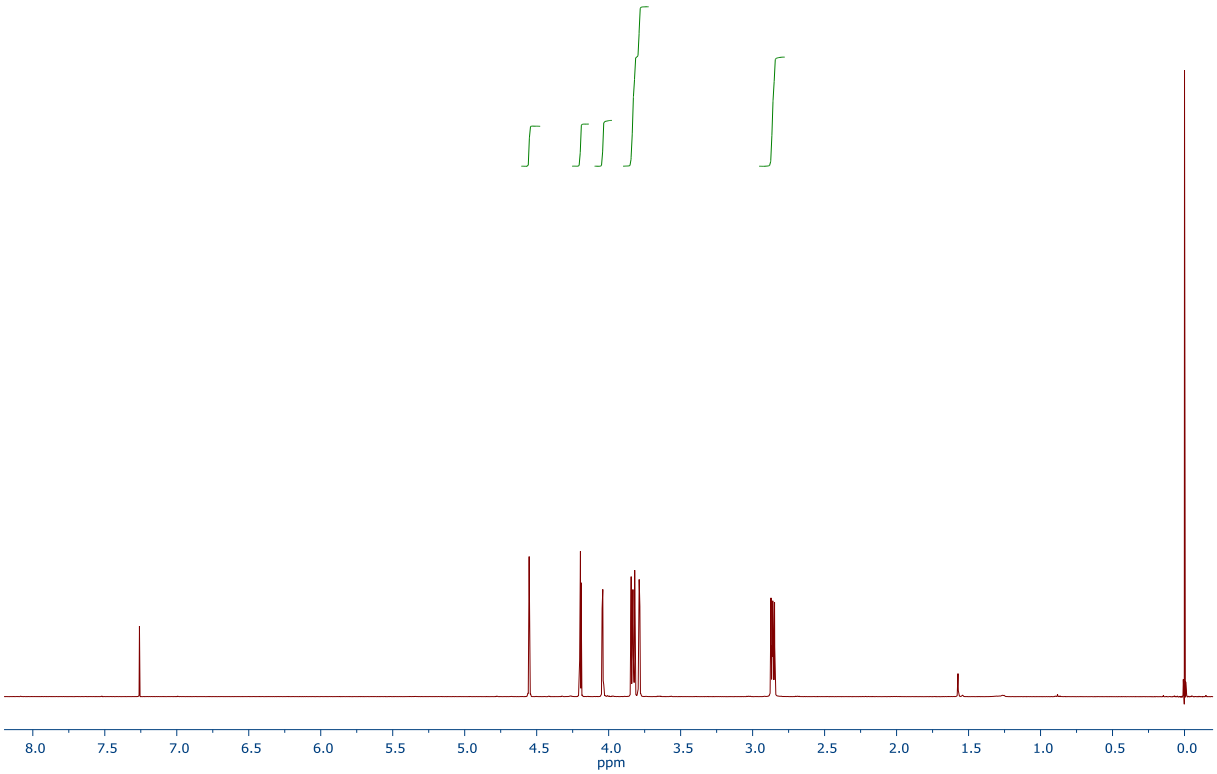

Figure S88. ^{1}H NMR spectrum (399.95 MHz, $CDCl_3$) of compound **12a**.

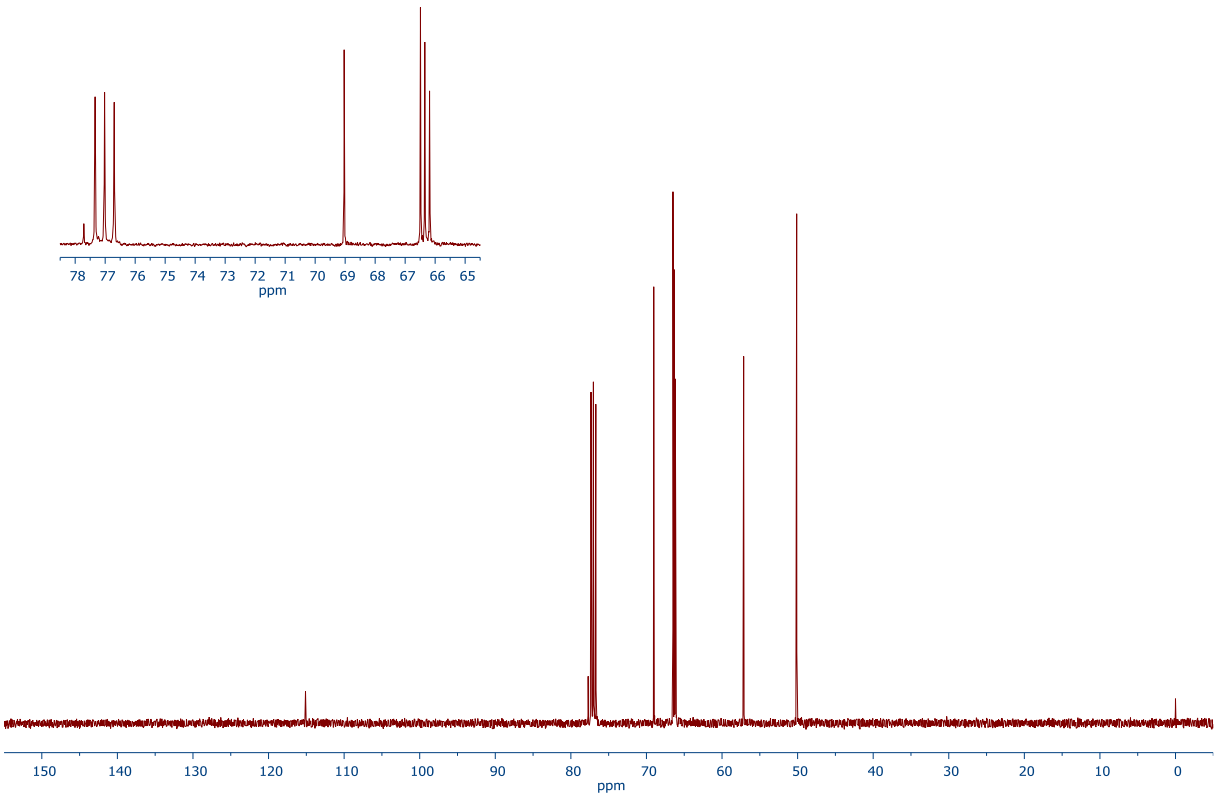

Figure S89. $^{13}C\{^{1}H\}$ NMR spectrum (100.58 MHz, $CDCl_3$) of compound **12a.**

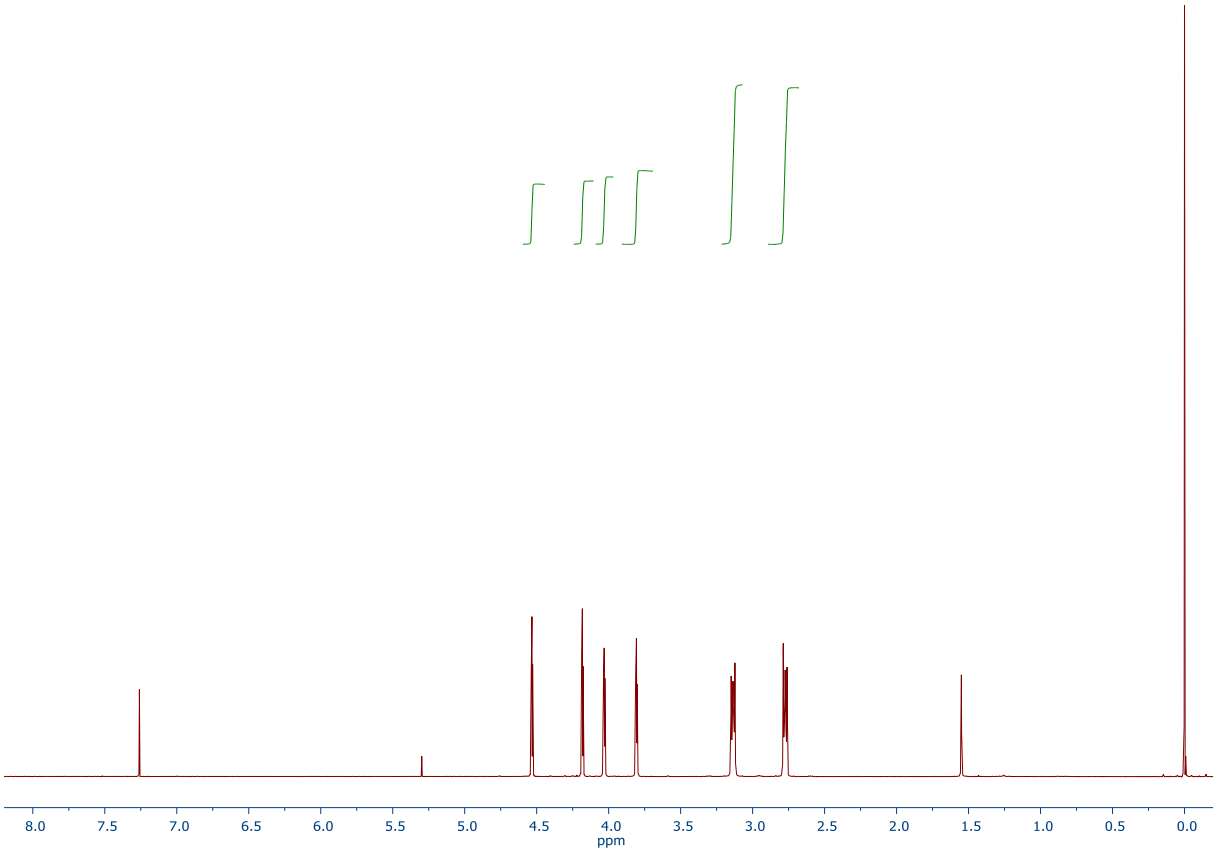

Figure S90. ^{1}H NMR spectrum (399.95 MHz, $CDCl_3$) of compound **12b**.

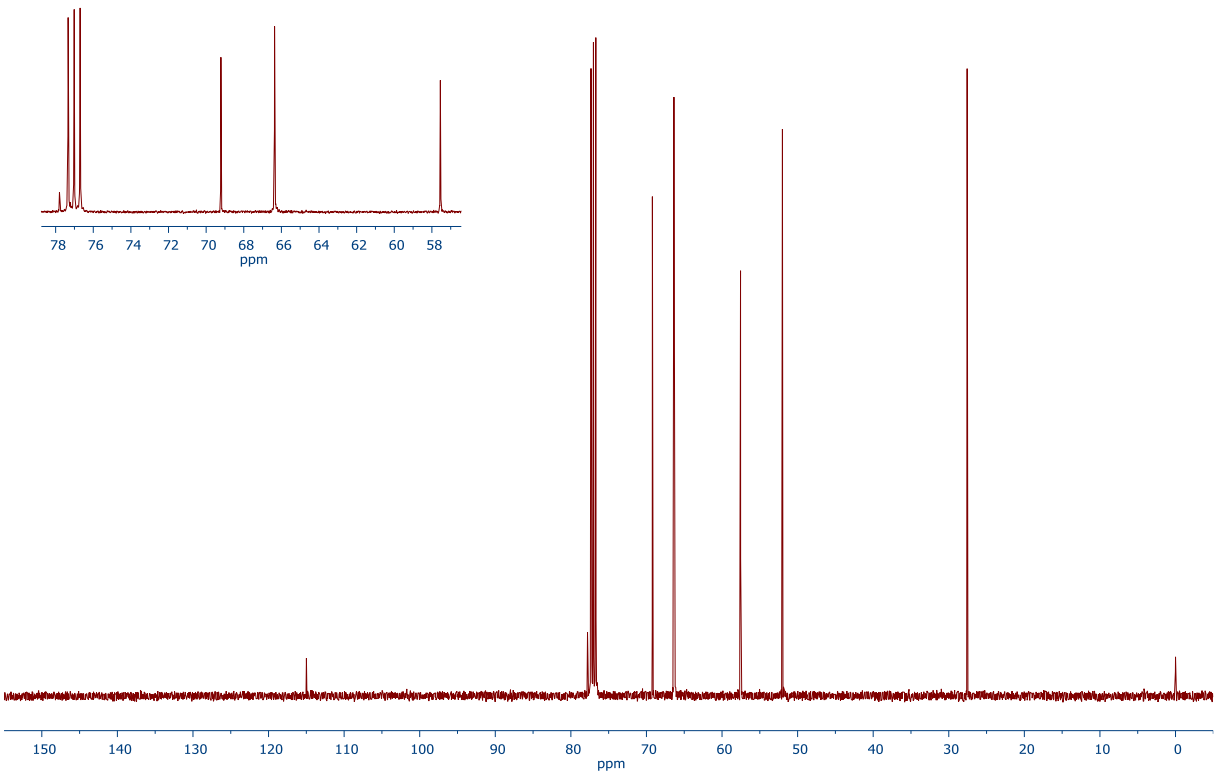

Figure S91. $^{13}C\{^{1}H\}$ NMR spectrum (100.58 MHz, $CDCl_3$) of compound **12b.**

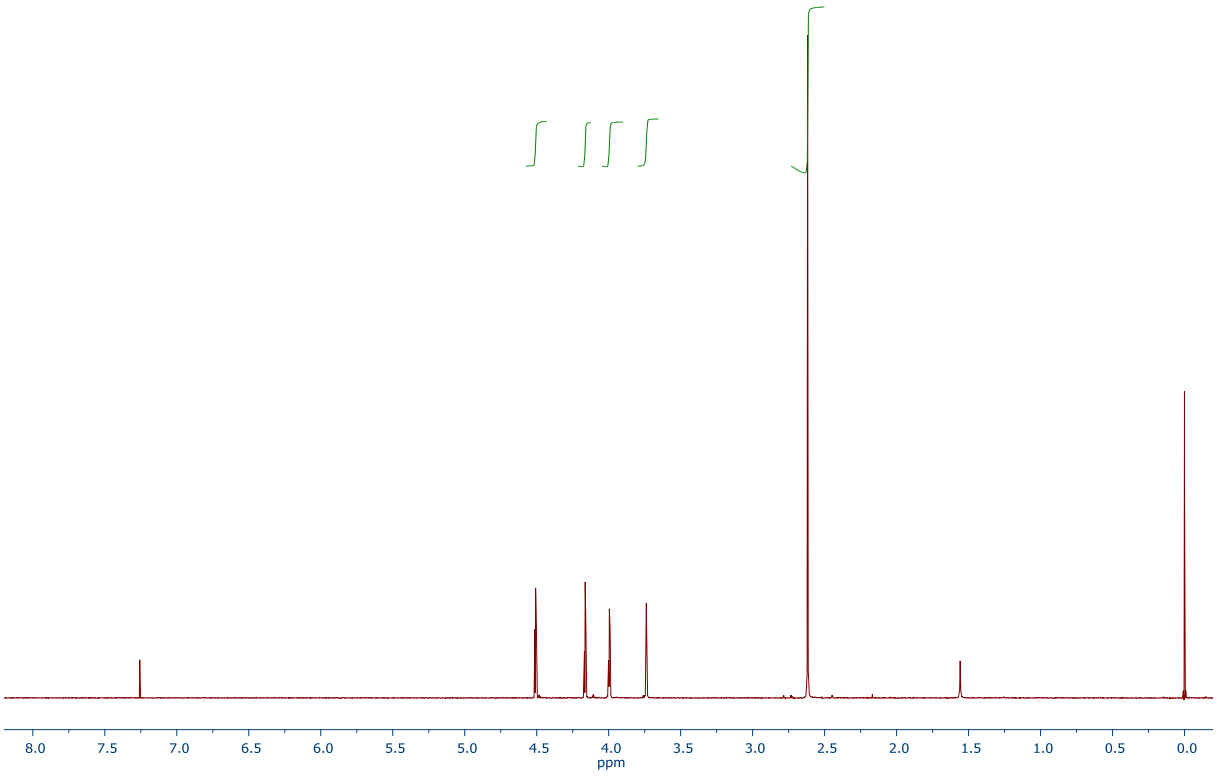

Figure S92. ^{1}H NMR spectrum (399.95 MHz, $CDCl_3$) of compound **12c**.

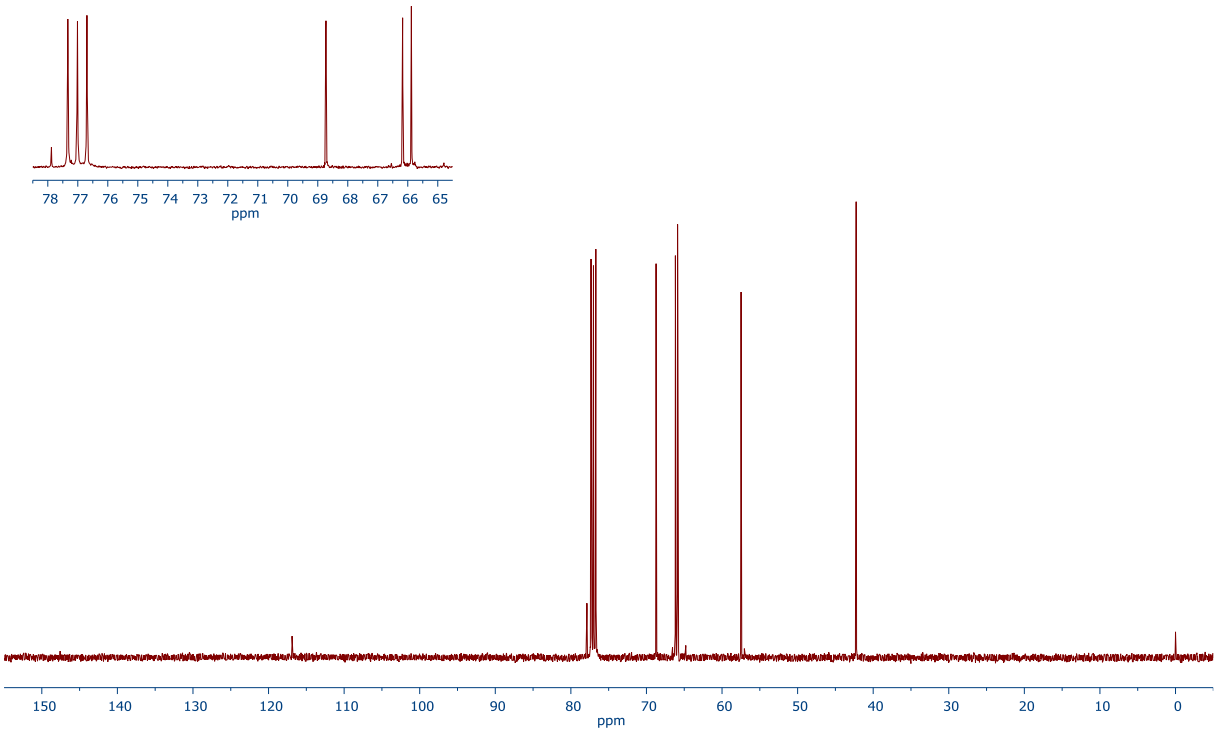

Figure S93. $^{13}C\{^{1}H\}$ NMR spectrum (100.58 MHz, $CDCl_3$) of compound **12c.**

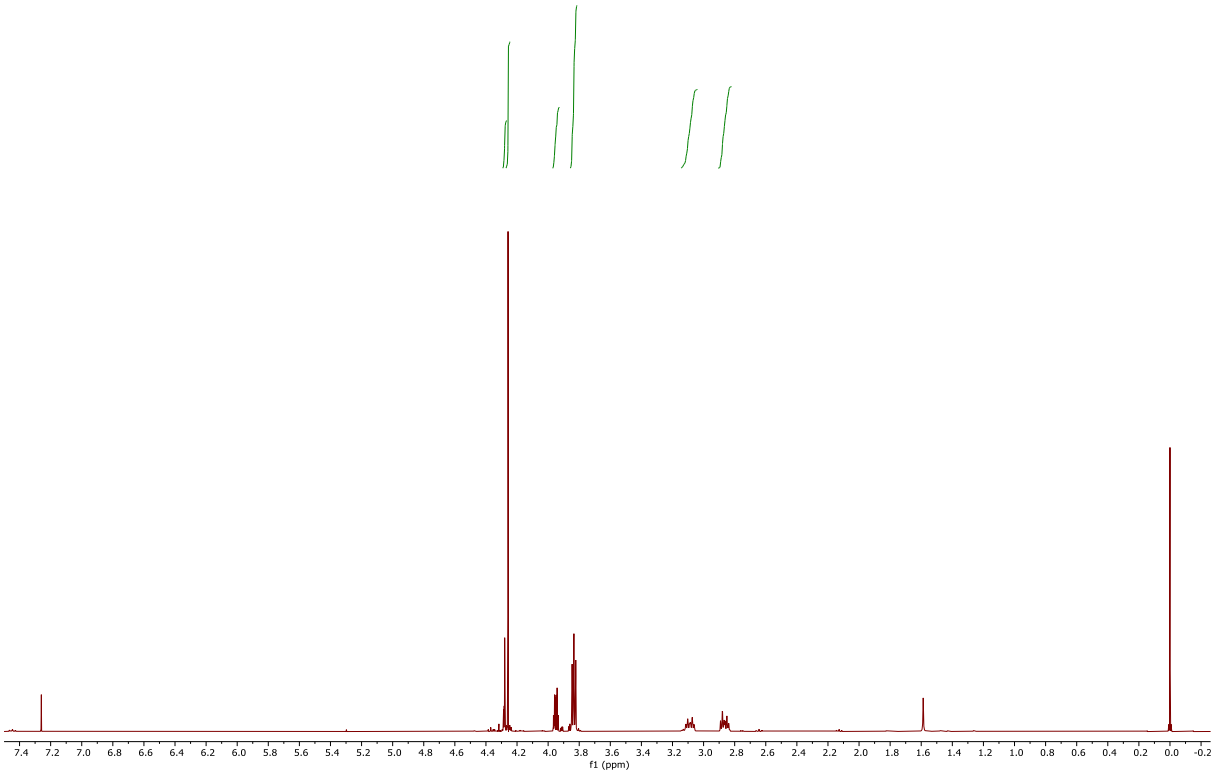

Figure S94. ^{1}H NMR spectrum (600.17 MHz, $CDCl_3$) of compound **13a**.

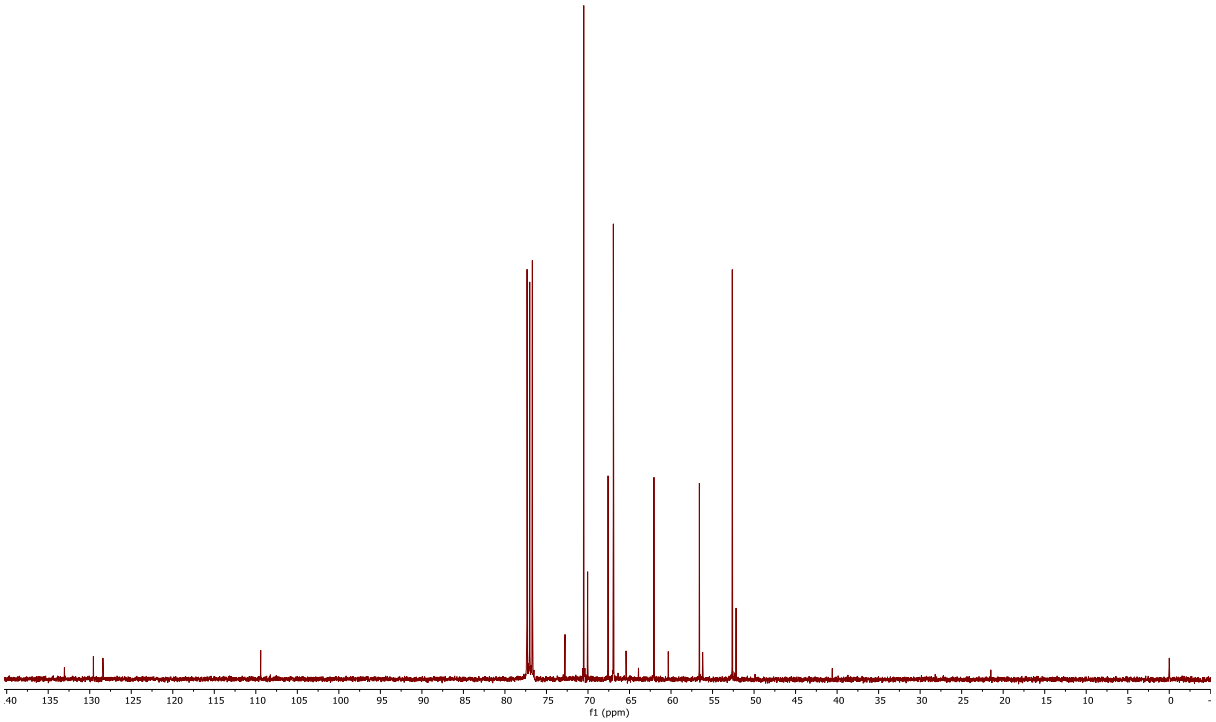

Figure S95. $^{13}C\{^{1}H\}$ NMR spectrum (150.93 MHz, $CDCl_3$) of compound **13a.**

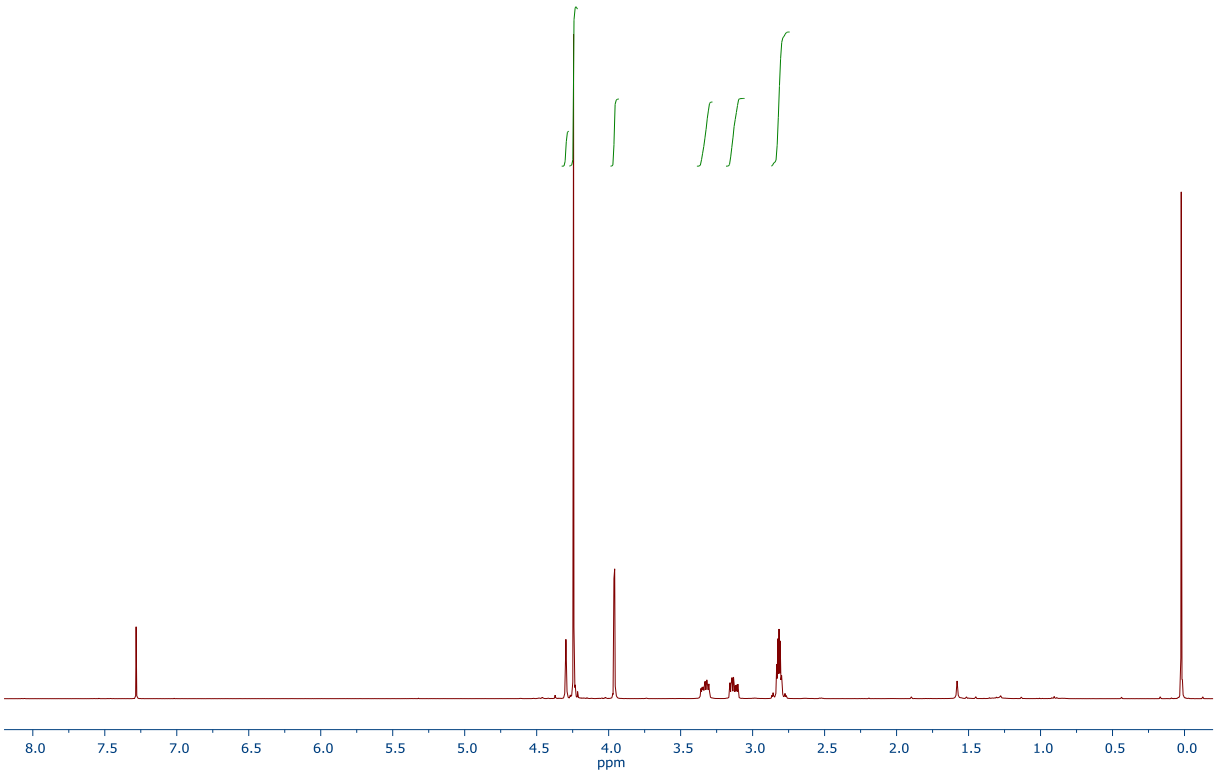

Figure S96. ^{1}H NMR spectrum (400.13 MHz, $CDCl_3$) of compound **13b**.

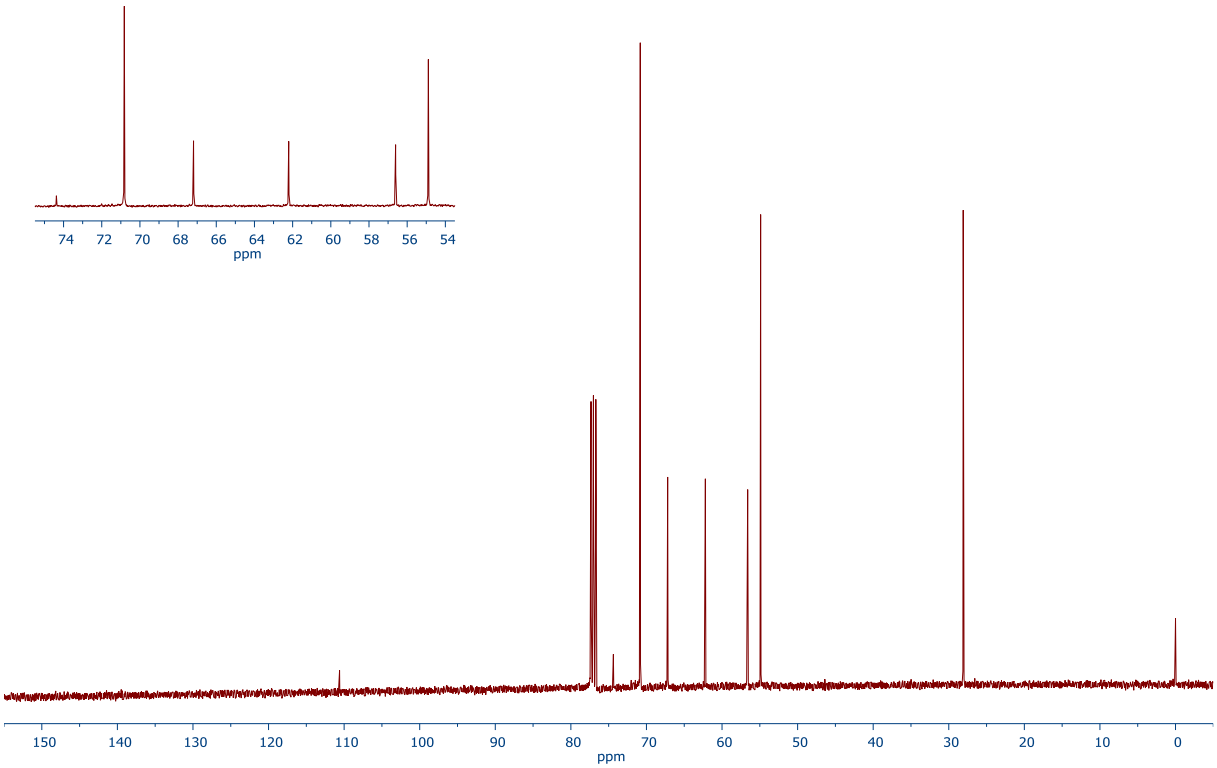

Figure S97. $^{13}C\{^{1}H\}$ NMR spectrum (100.62 MHz, $CDCl_3$) of compound **13b.**

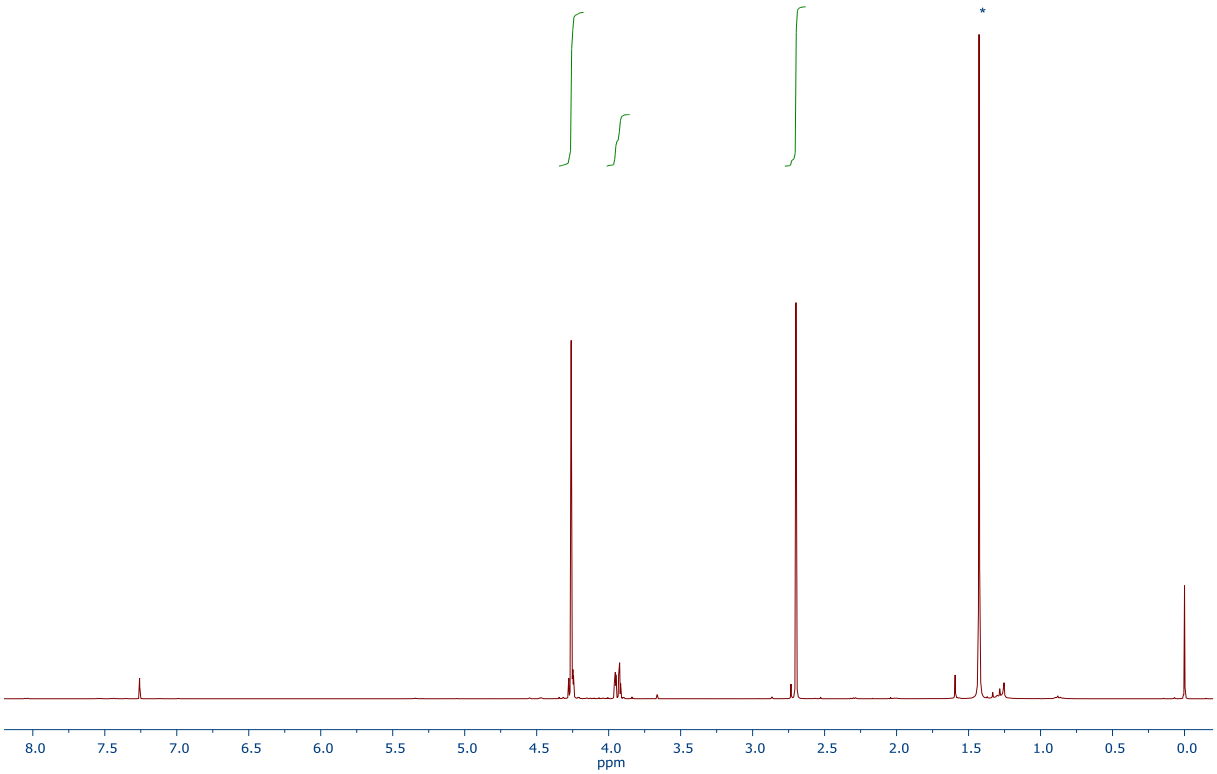

Figure S98. ^{1}H NMR spectrum (400.13 MHz, $CDCl_3$) of compound **13c**.

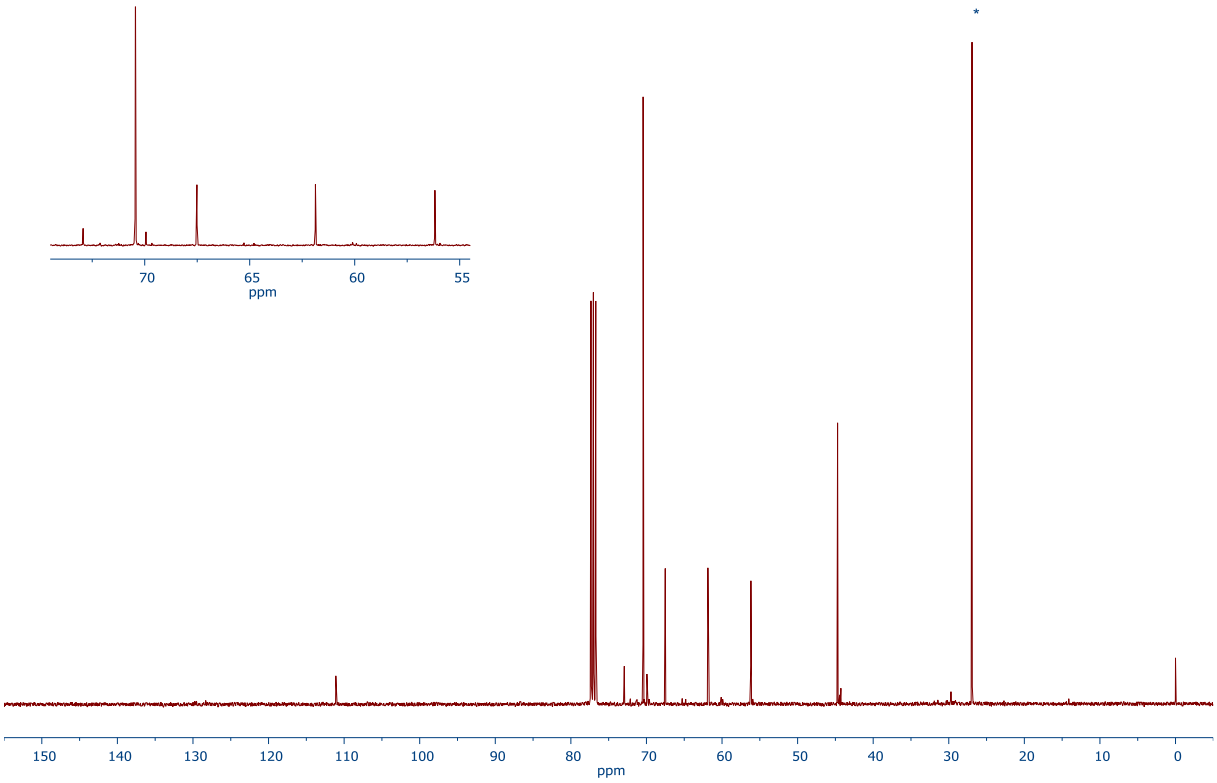

Figure S99. $^{13}C\{^{1}H\}$ NMR spectrum (100.62 MHz, $CDCl_3$) of compound **13c.**

References

1 K. Škoch, I. Císařová, J. Schulz, U. Siemeling and P. Štěpnička, *Dalton Trans.*, 2017, **46**, 10339–10354.

2 D. P. Day, T. Dann, R. J. Blagg and G. G. Wildgoose, *J. Organomet. Chem.*, 2014, **770**, 29–34.

3 H. Zhao, X. Chen, H. Jiang and M. Zhang, *Org. Chem. Front.*, 2018, **5**, 539–543.

4 X. Meng and S. Kim, *Org. Biomol. Chem.*, 2011, **9**, 4429–4431.

5 C. Metallinos, J. Zaifman, L. Belle, L. Dodge and M Pilkington, *Organometallics*, 2009, **28**, 4534–4543.

6 (a) A. Wang, X. Xie, C. Zhang, Y. Liu, *Chem. Commun.*, 2020, **56**, 15581–15584; (b) R. K. Kawade, R. Liu, *Org. Lett.* 2013, **15**, 4094–4097; (c) Y. Zheng, T. Zhang, W. Shen, *Org. Biomol. Chem.* 2021, **19**, 9688–9691.

7 G. M. Sheldrick, *Acta Crystallogr., Sect. A: Found. Adv.,* 2015, **71**, 3–8.

8 G. M. Sheldrick, *Acta Crystallogr., Sect. C: Struct. Chem.*, 2015, **71**, 3–8.

9 P. van der Sluis and A. L. Spek, *Acta Crystallogr., Sect. A: Found. Adv.*, 1990, **46**, 194–201.

10 (a) A. L. Spek, *J. Appl. Crystallogr*., 2003, **36**, 7–13; (b) A. L. Spek, *Acta Crystallogr. D, Biol. Crystallogr.*, 2009, **65**, 148–155.

11 https://www.ccdc.cam.ac.uk/media/CSD-Space-Group-Statistics-Space-Group-Frequency-Ordering-2023.pdf (retrieved on November 28, 2025).

12 S. I. Kirin, H.-B. Kraatz and N. Metzler-Nolte, *Chem. Soc. Rev.*, 2006, **35**, 348–354.

13 K. Heinze and M. Schlenker, *Eur. J. Inorg. Chem.*, 2004, 2974–2988.

14 M. J. Verschoor-Kirss, O. Hendricks, C. M. Verschoor, R. Conry and R. U. Kirss, *Inorg. Chim. Acta*, 2016, **450**, 30–38.

15 D. Cremer and J. A. Pople, *J. Am. Chem. Soc.*, 1975, **97**, 1354–1358.

16 D. Jiang, T. Lu, C. Du, F. Liu, Z. Yan, D. Hu, A. Shang, L. Gao, P. Lu and Y. Ma, *Sci. China Chem.*, 2023, **66**, 1132–1138.

17 Cambridge Structural Database, version 6.00 of April 2025.

18 J. A. Adeleke and L.-K. Liu, *Acta Crystallogr., Sect. C: Cryst. Struct. Commun*., 1993, **49**, 680–682.

19 (a) O. Bárta, I. Císařová, E. Mieczyńska, A. M. Trzeciak and P. Štěpnička, *Eur. J. Inorg. Chem.*, 2019, 4846–4854; (b) O. Bárta, I. Císařová, J. Schulz and P. Štěpnička, *New J. Chem.*, 2019, **43**, 11258–11262.

20 (a) P. Štěpnička and I. Císařová, *Dalton Trans.*, 2013, **42**, 3373–3389; (b) J. Schulz, P. Vosáhlo, F. Uhlík, I. Císařová and P. Štěpnička, *Organometallics*, 2017, **36**, 1828–1841; (c) T. Sasamori, H. Ueno and S. Morisako, *Inorganics*, 2022, **10**, 22; (d) J. Antala, J. Schulz, I. Císařová and P. Štěpnička, *New J. Chem.*, 2024, **48**, 5107–5119.

21 Selected examples: (a) D. T Hill, G. R. Girard, F. L. McCabe, R. K. Johnson, P. D. Stupik, J. H. Zhang, W. M. Reiff and D. S. Eggleston, *Inorg. Chem.*, 1989, **28**, 3529–3533; (b) J. E. Aguado, S. Canales, M. C. Gimeno, P. G. Jones, A. Laguna and M. D. Villacampa, *Dalton Trans.*, 2005, 3005–3015; (c) T. Rossler, T. Ruffer, B. Walfort, R. Packheiser, R. Holze, M. Zharnikov and H. Lang, *J. Organomet. Chem.*, 2007, **692**, 1530–1545; (d) U. Siemeling, T. Klemann, C. Bruhn, J. Schulz and P. Štěpnička, *Anorg. Allg. Chem.*, 2011, **637**, 1824–1833; (e) J. Schulz, J. Tauchman, I. Císařová, T. Riedel, P. J. Dyson and P. Štěpnička, *J. Organomet. Chem.*, 2014, **751**, 604–609; (f) K. Škoch, I. Císařová and P. Štěpnička, *Chem. Eur. J.*, 2015, **21**, 15998–16004; (g) K. Škoch, I. Císařová, J. Schulz, U. Siemeling and P. Štěpnička, *Dalton Trans.,* 2017, **46**, 10339–10354; (h) J. Antala, J. Schulz, I. Císařová and P. Štěpnička, *New J. Chem.*, 2024, **48**, 5107–5119.

22 B. Cordero, V. Gómez, A. E. Platero-Prats, M. Revés, J. Echeverría, E. Cremades, F. Barragán, S. Alvarez, *Dalton Trans.*, 2008, 2832–2838.

23 S. Alvarez, *Dalton Trans.*, 2013, **42**, 8617–8636.

24 C. Hansch, A. Leo and R. W. Taft, *Chem. Rev.*, **1991**, *91*, 165–195.

25 M. E. N. P. R. A. Silva, A. J. L. Pombeiro, J. J. R. Fraústo da Silva, R. Herrmann, N. Deus and R. E. Bozak, *J. Organomet. Chem.*, **1994**, *480*, 81–90,

26 K. Fujimoto and A. Osuka, *Chem. Sci.*, **2017**, *8*, 8231–8239.

27 R. M. Gomila and A. Frontera, *Dalton Trans.*, 2025, **54**, 3095–3105.

28 E. R. Johnson, S. Keinan, P. Mori-Sánchez, J. Contreras-García, A. J. Cohen and W. Yang, *J. Am. Chem. Soc.*, 2010, **132**, 6498–6506.

29 S. Scheiner, M. Michalczyk and W. Zierkiewicz, *Inorg. Chem.*, 2023, **62**, 20209–20218.

30 (a) R. Bianchi, G. Gervasio and D. Marabello, *Inorg. Chem.*, 2000, **39**, 2360–2366; (b) E. Espinosa, I. Alkorta, J. Elguero and E. Molins, *J. Chem. Phys.*, 2002, **117**, 5529–5542.

31 M. J. Frisch, M. J. Frisch, G. W. Trucks, H. B. Schlegel, G. E. Scuseria, M. A. Robb, J. R. Cheeseman, G. Scalmani, V. Barone, G. A. Petersson, H. Nakatsuji, X. Li, M. Caricato, A. V. Marenich, J. Bloino, B. G. Janesko, R. Gomperts, B. Mennucci, H. P. Hratchian, J. V. Ortiz, A. F. Izmaylov, J. L. Sonnenberg, D. Williams-Young, F. Ding, F. Lipparini, F. Egidi, J. Goings, B. Peng, A. Petrone, T. Henderson, D. Ranasinghe, V. G. Zakrzewski, J. Gao, N. Rega, G. Zheng, W. Liang, M. Hada, M. Ehara, K. Toyota, R. Fukuda, J. Hasegawa, M. Ishida, T. Nakajima, Y. Honda, O. Kitao, H. Nakai, T. Vreven, K. Throssell, J. A. Montgomery Jr, J. E. Peralta, F. Ogliaro, M. J. Bearpark, J. J. Heyd, E. N. Brothers, K. N. Kudin, V. N. Staroverov, T. A. Keith, R. Kobayashi, J. Normand, K. Raghavachari, A. P. Rendell, J. C. Burant, S. S. Iyengar, J. Tomasi, M. Cossi, J. M. Millam, M. Klene, C. Adamo, R. Cammi, J. W. Ochterski, R. L. Martin, K. Morokuma, O. Farkas, J. B. Foresman and D. J. Fox, *Gaussian 16 Revision C.01*, Gaussian Inc., Wallingford CT, 2016.

32 (a) J. P. Perdew, K. Burke and M. Ernzerhof, *Phys. Rev. Lett.*, 1996, **77**, 3865–3868; (b) J. P. Perdew, M. Ernzerhof and K. Burke, *J. Chem. Phys.*, 1996, **105**, 9982–9985; (c) M. Ernzerhof and G. E. Scuseria, *J. Chem. Phys.*, 1999, **110**, 5029–5036; (d) C. Adamo and V. Barone, *J. Chem. Phys.*, 1999, **110**, 6158–6170.

33 (a) F. Weigend, F. Furche and R. Ahlrichs, *J. Chem. Phys.*, 2003, **119**, 12753–12762; (b) F. Weigend and R. Ahlrichs, *Phys. Chem. Chem. Phys.*, 2005, **7**, 3297–3305.

34 (a) M. Dolg, U. Wedig, H. Stoll and H. Preuss, *J. Chem. Phys.*, 1987, **86**, 866–872; (b) A. Bergner, M. Dolg, W. Küchle, H. Stoll and H. Preuß, *Mol. Phys.*, 1993, **80**, 1431–1441; (c) G. Igel-Mann, H. Stoll and H. Preuss, *Mol. Phys.*, 1988, **65**, 1321–1328; (d) D. Andrae, U. Häußerman, M. Dolg, H. Stoll and H. Preuß, *Theor. Chim. Acta*, 1990, **77**, 123–141.

35 (a) A. D. Becke and E. R. Johnson, *J. Chem. Phys.* **2005**, *123*, 154101; (b) S. Grimme, J. Antony, S. Ehrlich and H. Krieg, *J. Chem. Phys.*, 2010, **132**, 154104; (c) S. Grimme, S. Ehrlich and L. Goerigk, *J. Comput. Chem.*, 2011, **32**, 1456–1465.

36 Lu, T.; Chen, F. MultiWFN: A Multifunctional Wavefunction Analyzer. *J. Comput. Chem.* **2012**, *33*, 580–592.

37 Knizia, G. http://www.iboview.org.